STUDIES OF STERICALLY CONTROLLED SOLVENT

INDUCED NMR CHEMICAL SHIFTS

A THESIS PRESENTED TO

THE UNIVERSITY OF ASTON IN BIRMINGHAM

FOR THE DEGREE OF

DOCTOR OF PHILOSOPHY

BY

HAFID KADIM AL-DAFFAEE B.Sc.

SUPERVISOR DR. J. HOMER D.Sc.,FRSC.

OCTOBER 1983

THE DEPARTMENT OF CHEMISTRY

THE UNIVERSITY OF ASTON IN BIRMINGHAM

ABSTRACT:

"Studies of sterically controlled solvent

induced NMR chemical shifts".

A Thesis Presented For The Degree Of Doctor Of Philosophy

By

HAFID KADIM AL-DAFFAEE

1983

Recently Homer and Percival have postulated that intermolecular van der Waals dispersion forces can be characterized by three mechanisms. The first arises via the mean square reaction field due to the transient dipole of a particular solute molecule that is considered situated in a cavity surrounded by solvent molecules; this was characterized by an extended Onsager approach. The second stems from the extra cavity mean square reaction field of the near neighbour solvent molecules. The third originates from square electric fields due to a newly characterized effect in which peripheral solute atoms are "buffeted" by the peripheral atoms of adjacent solvent molecules.

Extensive justification for the use of these terms in total has been provided elsewhere for simple isotropic molecular systems. The present work shows that the overall treatment is similarly successful when applied to the proton chemical shifts of more complex molecules, and it is suggested and demonstrated that the buffeting shifts may prove useful in elucidating features of molecular structure. More importantly the present work provides strong experimental evidence for the separate existence of the three individual contributions to dispersion forces.

In the course of this work a novel method of measuring volume magnetic susceptibility is proposed and evaluated. Additionally, the theoretical and practical implications of errors that may arise when measuring chemical shifts with Foriour Transform NMR Spectrometers that are field/frequency locked to signals arising from materials in various physical environments are evaluated.

Nuclear Magnetic Resonance.
Reaction Field/Continuum Model.
Solvent Induced Chemical Shifts.
NMR Lock Effects On σ_b.
NMR Method For Determining Volume Magnetic Susceptibility.

DEDICATION

TO MY WIFE WITH LOVE

TO MY PARENTS WITH FAITH

ACKNOWLEDGEMENTS

(v)

CHAPTER THREE   **THE VAN DER WAALS SCREENING CONSTANT σ_w**

CHAPTER FOUR   **ANALYSIS OF NMR INDUCED SOLVENT CHEMICAL SHIFTS TO STUDY THE STERIC CONFIGURATION OF COMPLEX SYSTEMS**

CHAPTER FIVE   **VOLUME MAGNETIC SUSCEPTIBILITY EFFECTS WHEN USING HETERONUCLEAR FIELD/FREQUENCY LOCK TO MEASURE NMR CHEMICAL SHIFTS**

CHAPTER SIX   A NEW METHOD FOR DETERMINING THE
                     VOLUME MAGNETIC SUSCEPTIBILITY OF
                     ORGANIC LIQUIDS

CHAPTER ONE

SOME THEORETICAL CONSIDERATIONS

OF NUCLEAR MAGNETIC RESONANCE

1.1   **INTRODUCTION:**

In 1924, Pauli[1] suggested that certain muclei possess
spin angular momentum and a related magnetic moment. He
proposed that such nuclei interact with the atomic orbital
electrons and modify certain properties of the latter. He was
led to this suggestion by the occurrence of hyperfine structure
in the electronic spectra of certain atoms observed when using
optical spectrographs with very high resolving power[2]. Stern
and Gerlach[3,4] subsequently showed that the measurable values
of a nuclear magnetic moment are discrete in nature. When a
nucleus is placed in an unhomogeneous magnetic field, the
allowed values of the magnetic moment correspond to space
quantisation of the nucleus. The magnetic moment of the

1

hydrogen nucleus was determined by directing a beam of hydrogen atoms through a static magnetic field which deflected the beam. This method was developed by using two, oppositely inclined, magnetic fields of similar gradients. The atomic beam was diffused by the first magnetic field, and focused by the second one onto a detector. The introduction of a radiofrequency signal between the two original fields, such that the oscillating magnetic component of the r.f signal was perpendicular to the main field, showed that the density of the atoms reaching the detector was reduced when the energy of the radiofrequency signal was equal to the energy required to induce transitions between the nuclear energy levels corresponding to quantisation of the nuclear magnetic moments[6].

In 1946, the first nuclear magnetic resonance (NMR) signals from bulk matter were observed independently by two teams led by Bloch[7] and Purcell[8]; they used samples of water and parafine wax respectively. In 1949, it was found that the energy of the nuclear levels are dependent on the compound in which the nucleus is found and on its position on that compound[9]. The determination of nuclear properties and molecular structure is thus possible from a knowledge of precise resonance frequencies[9,10,11]. For convenience the following discussion of the basic theory of nuclear magnetic resonance spectroscopy consider first on isolated nucleus in a magnetic field, the resonance conditions of this, and then

2

other factors relevant to resonance in bulk samples.

1.2   **MAGNETIC AND RELATED PROPERTIES OF NUCLEI:**

Nuclei of certain isotopes may be considered to behave as spinning spherical, or ellipsoidal, bodies possessing uniform charge distribution around at least one axis. Such a positively charged spinning nucleus produces a magnetic field with axis coincident with the axis of spin. The angular momentum and the magnetic moment behave as parallel vectors related by:

$$\mu = \quad \gamma \ \overrightarrow{I \hbar} \quad \ldots\ldots\ldots\ldots\ldots\ldots\ldots\ldots\ldots\ldots (1.1)$$

where γ is a characteristic constant of each nuclear species called the magnetogyric ratio or magnetogyric constant, μ is the magnetic moment of the nucleus, I is the nuclear spin quantum number and $\hbar$ is the reduced plank's constant ($h/2\pi$). Nuclear angular momentum is quantised and in magnetic fields the maximum measurable component of angular momentum (actually $\sqrt{I(I+1)} \ \hbar$) in the field direction is always an integral or half integral multiple of $\hbar$.

There are $2I + 1$ such values given by $[+ I, (+ I - 1),$ ..., 0, ... $(- I + 1)$, $- I]\ \hbar$. If $I = 0$; then $\mu = 0$ and no magnetic characteristics are observed, but if I is non-zero, μ has a finite value. It is obvious from equation (1.1) that the quantisation of the nuclear angular momentum parallels the

3

quantisation of the magnetic moment μ , which therefore possesses only discrete components corresponding to different orientations with respect to the reference axis of an applied magnetic field.

Therefore, when placed in a magnetic field a nucleus of spin I has available to it $2I + 1$ energy states. NMR spectrosiopy is concerned with observing nuclear transitions between the permitted energy states.

1.3 NUCLEI IN A MAGNETIC FIELD:

The different values of the components of the angular momentum are degenerate in the absence of a magnetic field. However, the application of an external magnetic field, B_O, causes the degeneracy to be lifted. The resulting energy levels correspond to different nuclear spin orientations relative to the reference (Z) direction of the applied static field. The energy of the nucleus is given classically by:

$$E = E_O - E_z \quad \dots\dots\dots\dots\dots\dots\dots\dots\dots\dots\dots\dots\dots\dots\dots \quad (1.2)$$

where E_O is the energy of the nucleus in the absence of a magnetic field, and $E_z = - \mu_z B_O$. Therefore the change in energy when the external field is applied is given by:

$$E_z = - \mu B_O \cos\theta \quad \dots\dots\dots\dots\dots\dots\dots\dots\dots\dots\dots\dots \quad (1.3)$$

When the magnetic moment, μ , is inclined at an angle θ to the static field direction (Fig 1.1), it is evident that $\cos \theta$ can be defined in terms of m, the magnetic quantum numbers, by m/I where m adopts the values I, I −1 ...... − I.

Consequently:

$$E_z = - \mu \; \frac{m}{I} \; B_0 \; \dotsm \; (1.4)$$

Therefore, the energies of the allowed levels, characterised by the associated values of m, are:

$$- \mu B_0, \; -\frac{(I - 1)}{I} \; \mu B_0, \; \dots, \; \frac{(I - 1)}{I} \; \mu B_0, \; \mu B_0$$

The transition selection rule is that transitions are permitted only between adjacent levels i.e. $\Delta m = \pm 1$[12].

It follows that energy difference between two adjacent levels is given by:

$$E = \frac{\mu B_0}{I} \; \dotsm \; (1.5)$$

Using the Bohr frequency condition $\Delta E = h \upsilon$, equation (1.5) may be rewritten as:

$$\upsilon = \mu \; \frac{B_0}{Ih} = \frac{\gamma B_0}{2\pi} \; \dotsm \; (1.6)$$
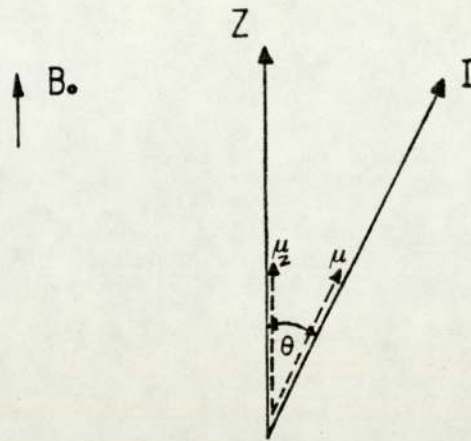
Figure 1.1   The relationship between the magnetic moment μ
and the spin angular momentum I .
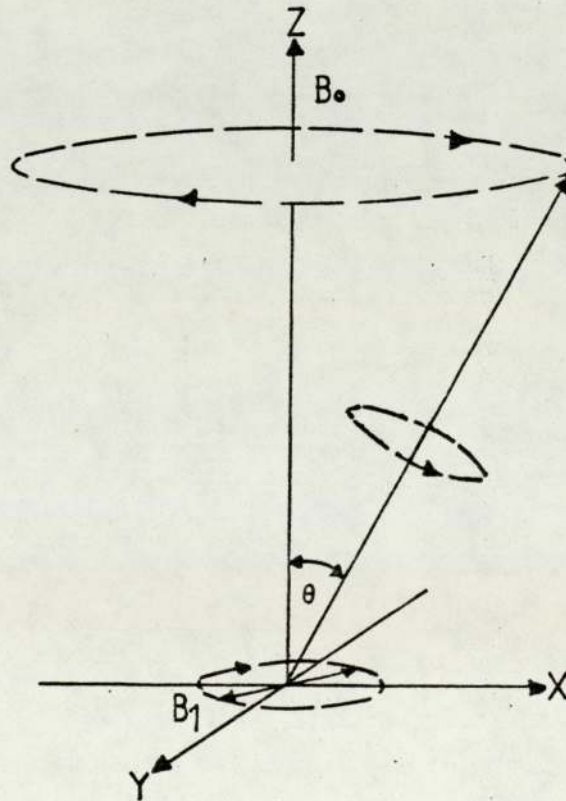
Figure 1.2   Victorial representation of the classical
Larmor precession.

6

which characterises the frequency in the electromagnetic
spectum at which nuclear transitions may be detected.

To appreciate the physical basis of equation (1.5), it is
convenient to consider the case of the simplest nucleus, that
of hydrogen. This consists of one proton, for which $I = 1/2$
and only two energy levels are permitted: these correspond to
$m = + 1/2$ and $m = - 1/2$. The situation for the proton can be
represented by:

$$- 1/2 \qquad + \mu\ Bo$$

$$E = 2\ \mu\ Bo$$

$$+ 1/2 \qquad - \mu\ Bo$$

No External Field   External Field   m   E
                          Applied = Bo
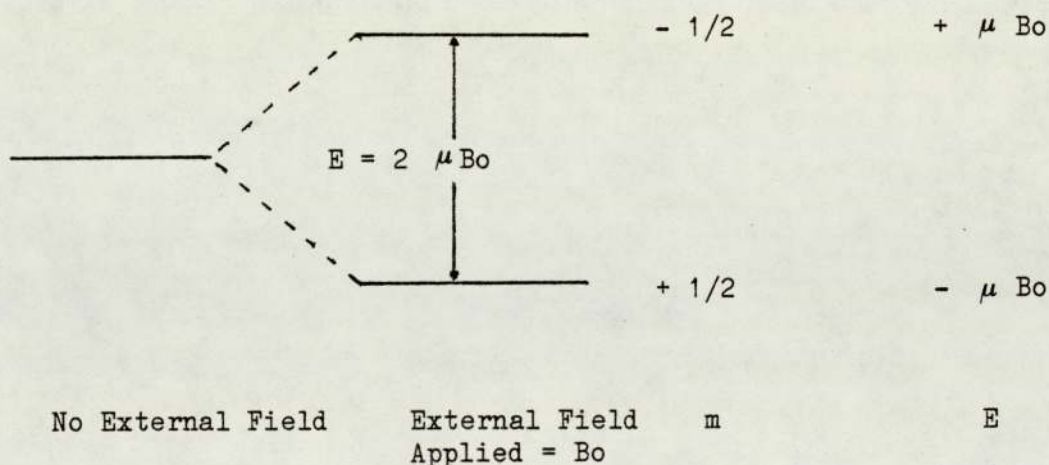
Because a particular nuclear species has constant values of
μ and I, υ depends directly on Bo, so the magnetic
resonance spectrum can occur under a variety of conditions. For
example, for proton three typical conditions where resonance
occurs are:-

Bo = 1.4092 Tesla; υ = 60.004 MHz

Bo = 2.03329 Tesla; υ = 89.56 MHz

Bo = 2.3490 Tesla; υ = 100.00 MHz

1.4   THE CONDITIONS AND CLASSICAL DESCRIBTION OF

NUCLEAR MAGNETIC RESONANCE:

An understanding of the mechanism of NMR can be approached
by a classical treatment of the nuclear dipole. If a spinning
charged particle, the nucleus, is placed in a magnetic field,
Bo, with its magnetic moment making an angle θ to the
direction of this field, it will experience a torque L to
constrain it parallel to the field, (Fig 1.2). Newton's Law of
motion states that the rate of change of angular momentum p
with the time is equal to the torque or

$$\frac{d\,p}{d\,t} = \vec{L} \quad \dots\dots\dots\dots\dots\dots\dots\dots\dots\dots \quad (1.7)$$

But according to magnetic theory:

$$\vec{L} = \vec{\mu} \; Bo \quad \dots\dots\dots\dots\dots\dots\dots\dots\dots \quad (1.8)$$

So

$$\frac{d\,p}{d\,t} = \vec{\mu}\,Bo = \gamma\,\vec{p}\,Bo \quad \dots\dots\dots\dots\dots\dots\dots \quad (1.9)$$

This equation describes the precession of the nuclear magnet
around Bo with an angular velocity ωo. The angular velocity
may be defined by:

$$\frac{d\,p}{d\,t} = p \; \omega o \quad \dots\dots\dots\dots\dots\dots\dots\dots\dots \quad (1.10)$$

8

Therefore

$$\omega_0 = \gamma B_0 \dots\dots\dots\dots\dots\dots\dots\dots\dots\dots\dots\dots (1.11)$$

Equation (1.11) is called the Larmor equation. It can be written in terms of frequency precession o by:

$$v_0 = \frac{\gamma B_0}{2\pi} \dots\dots\dots\dots\dots\dots\dots\dots\dots\dots\dots\dots (1.12)$$

If a low intensity magnetic field B_1 is applied that rotates in a plane at right angles to the main static field Bo, it is necessary, in order to exert the most torque on μ and change its orientation and thus the energy of the nucleus (Fig 1.2), for B_1 to rotate in synchronisation with the precession of μ about Bo, i.e, the rotation of B_1 must be in resonance with the Larmor precession about Bo.

The rotating B_1 for nucleus resonance can be obtained by applying an ac signal to a coil surrounding the sample. This produces a linearly oscillating field, and such a field can be regarded as a superimposition of two fields rotating in opposite directions. One field component will be rotating in the opposite direction of the nucleus and will have little effect on it, while the other component is in phase with and can perturb the precessional motion and thus induce energy changes when its frequency is equivalent to the Larmor frequency.

1.5   <u>THE DISTRIBUTION OF NUCLEI BETWEEN ALLOWED ENERGY LEVELS:</u>

This section considers the populations of the various accessible energy levels and the probabilities of transitions between them.

When a system of identical nuclei is at resonance, the probabilities P of transition occurring by absorption or stimulated emission of energy are equal; the effect of spontaneous emission of energy being negligable[13], i.e, there is an equal probability that Δm will be ± 1.

Normally there is a Boltzman distribution of nuclei between the various allowed energetically different nuclear levels. The probability of a given nucleus occupying a particular level, characterised by a magnetic quantum number m, is given by:

$$\frac{1}{2 I + 1} \quad \exp.\frac{m\, \mu\, Bo}{I\, k\, T} \quad \dots\dots\dots\dots\dots\dots\dots\dots\dots\dots \quad (1.13)$$

which approximates to:-

$$\frac{1}{2 I + 1} \left[1 + \frac{m\, \mu\, Bo}{I\, k\, T} \right] \quad \dots\dots\dots\dots\dots\dots\dots\dots\dots \quad (1.14)$$

Where k is Boltzman constant, and T is the temperature.

10

For a nucleus of spin $I = 1/2$, the occupations of the upper or lower energy states respectively are governed at thermal equilibrium by:

$$1/2 \left[1 - \frac{\mu B_0}{kT} \right]$$

and .... (1.15)

$$1/2 \left[1 + \frac{\mu B_0}{kT} \right]$$

There is, thus a distribution of nuclei favouring the lower energy state. The above equations also show that the normal excess of nuclei in the lower energy state enables NMR to be observed by the nett absorption of energy by the nuclear system.

If only two energy levels are considered, and N_1 and N_2 are the numbers of nuclei in the low and high energy levels respectively, the nett change in the system at resonance is given by:

$$P (N_1 - N_2) = P_n \text{ (excess)} \dots\dots\dots\dots\dots\dots (1.16)$$

Where P is the probability of a transition occurring, and n excess is the excess of nuclei in the lower relative to the higher state.

The above equations also, show that the absorption signal intensity increases with Bo. This should therefore be as high as possible; because the higher the field, the greater the sensitivity due to the increase in the excess population of nuclei in the lower energy state.

Nuclear magnetic resonance spectroscopy differs from optical spectroscopy[14,15] in the rate of return of an energetically perturbed system to equilibrium. In the case of optical spectroscopy, after the absorption of energy, a very rapid recovery to equilibrium from an excited state to the ground state after occurs. However, in nuclear magnetic resonance the recovery is relatively slow and signals can be weakened and eventually disappear with increasing intensity of radio-frequency field B_1 because the number of excess nuclei in the lower energy state tends to zero. This phenomena is known as saturation.

1.6   **SATURATION EFFECTS:**

As absorption of energy from the radiofrequency field B_1 reduces the excess population in the lower energy state with respect to the upper energy state. This results in a reduction in the nett number of nuclei that can absorb energy from the radiofrequency field B_1. This effect will increase as the amplitude of the oscillating field is increased.

Saturation is reflected primarly in a reduction in signal

intensity. Moreover it distorts the signal shape causing a broadening of the signal. If the spectrum includes several lines, the effect of saturation need not be the same for each absorption. This is because the absorptions may have different relaxation times T_1 and T_2 (see 1.7.1 and 1.7.2).

1.7   RELAXATION PROCESSES:

If the effects of saturation were not reversible, it would not be possible to reproduce the spectrum of a given sample.

However, a natural process known as relaxation removes the excess energy from a saturated system and allows it to reachieve the equilibrium Boltzman distribution of nuclei between the permitted levels.

There are two principle kinds of relaxation processes, namely the spin-lattice and spin-spin relaxation of these only the spin-lattice relaxation mechanism influences the nett population of energy levels.

1.7:1   Spin-Lattice Relaxation:

The term lattice refers to the molecular system as a whole which contains the nuclei being studied. All these molecules or their constituent particles in the lattice may have permanent or induced magnetic properties, and as they are undergoing transitional, rotational, and vibrational motions, a

variety of time dependent magnetic fields are present in the lattice. When the resultant lattice field has a component at the resonance frequency which is sychronous with the precessional frequency of a given nucleus, this field will preferentially induce either stimulated emission or absorption transitions. However the probability of emission is greater than that of absorption, and the overall energy will be transfered from the spin system to the surrounding lattice.

This is the mechanism of spin-lattice, or longitudinal, relaxation and is responsible for the achievement of the Boltzman population distribution of nuclear spin states when the molecule is initially placed in a magnetic field. The rate at which a system returns to equilibrium after being perturbed is characterized by the spin-lattice relaxation time and this is usually denoted by T_1.

The relation between the upward and the downward transition relaxation probabilities P_1 and P_2, follows from simple thermodynamics:

P_2 (upper to lower) $>$ P_1 (lower to upper). If a system is considered in which there are N_1 and N_2 nuclei in the lower and upper states respectively, then at equilibrium:

$$N_1 \, P_1 = N_2 \, P_2 \quad \dots\dots\dots\dots\dots\dots\dots\dots\dots\dots\dots (1.17)$$

The excess number of nuclei in the lower level is:

$$N \text{ excess} = N_1 - N_2 \quad \dots\dots\dots\dots\dots\dots\dots\dots\dots\dots\dots \quad (1.18)$$

The normal Boltzman distribution for two energy states is given by:[16]

$$\frac{N_1}{N_2} = \exp. \ (2 \ \mu \ Bo/kT) \quad \dots\dots\dots\dots\dots\dots\dots\dots\dots \quad (1.19)$$

$$= 1 + 2 \ \mu \ Bo/kT \quad \dots\dots\dots\dots\dots\dots\dots\dots\dots\dots \quad (1.20)$$

and therefore:

$$\frac{P_2}{P_1} = 1 + 2 \ \mu \ Bo/kT \quad \dots\dots\dots\dots\dots\dots\dots\dots\dots\dots \quad (1.21)$$

Hence, the rate of change of the number of excess nuclei, is given by:

$$\frac{d \ N \text{ excess}}{d \ t} = 2 \ N_2 \ P_2 - 2 \ N_1 \ P_2 \quad \dots\dots\dots\dots\dots\dots\dots \quad (1.22)$$

where the factor of two comes from the fact that an upward transition decreases and a downward transition increases N excess by two. So

$$\frac{d \ N \text{ excess}}{d \ t} = -2 \ P \ (N \text{ excess} - N \text{ equi.}) \quad \dots\dots\dots\dots\dots \quad (1.23)$$

where $P = (P_1 + P_2) / 2$.

and

15

$$N \text{ equi.} = \frac{\mu \ Bo}{k \ T} (N_1 + N_2)$$

N equi. is the number of excess nuclei in the lower state at equilibrum.

Integration of equation (1.23) gives:

$$(N \text{ excess} - N \text{ equi.}) = (No - N \text{ equi.}) \exp. (2Pt) \ \dots\dots (1.24)$$

where No is the initial value of N excess per unit volume.

The spin relaxation time T_1 is given by [16]:

$$T_1 = \frac{1}{2 \ P} \ \dots\dots\dots\dots\dots\dots\dots\dots\dots\dots\dots\dots (1.25)$$

Therefore from equations (1.24 and 1.25):

$$(N \text{ excess} - N \text{ equi.}) = (No - N \text{ equi.}) \exp. \frac{- t}{T_1} \ \dots\dots (1.26)$$

This equation shows that the rate by which the excess population reaches its equilibrium value is governed exponentially by the spin-lattice relaxation time T_1.

1.7:2   **Spin Spin Relaxation:**

Beside the mechanism which has been described in the previous section, the nuclei also interact among themselves. The actual magnetic field felt by the nucleus is not only due

to the steady magnetic field Bo, but it is this plus small magnetic fields produced locally by other surrounding nuclear magnets precessing about the direction of Bo. These fields may be thought to have oscillating and static components.

A nucleus producing a magnetic field oscillating at its Larmor-frequency, may induce a transition in a like neighbouring nucleus in a similar way to an applied alternatively magnetic field that is used to observe resonance. This will lead to an interchange of energy between the pair of spins, while the total energy of the pair is conserved. Thus there is no effect on the population distribution of the nuclear spins.

The process is known as spin-spin relaxation. The characteristic spin-spin relaxation time is denoted by T_2.

1.8   **NMR IN MACROSCOPIC SAMPLES:**

So far the discussion has considered the magnetic properties of isolated nuclei. In the treatment of the experimental observation of NMR for bulk systems, it is convenient to adopt the approach of Bloch[17,18,19] and consider the assembly of nuclei in macroscopic terms.

An assembly of nuclei in an applied field has their various spin states occupied to different extents, and this

gives the sample a magnetic moment per unit volume, M, according to:

$$M = Bo \; X_o \; \dotfill \; (1.27)$$

where X_o is the static magnetic susceptibility.

The bulk magnitisation is analogous to the nuclear moment μ, except for one important difference that in the absence of an applied radiofrequency field, M has only a z- component whereas μ has x, y and z - components (i.e: $Mx = \Sigma_i \; \mu_x = 0$, $M_y = \Sigma_i \; \mu_y = 0$ and $M_z = \Sigma_i \; \mu_z = M_o$ the sums are over i nuclei). The individual nuclei precess about z- axis with no phase coherence and so the x and y components average to zero in forming M_o.

When the assembly of nuclei is exposed to the rotating field B_1, then as this field approaches the value required for resonance, nuclei will start to precess in phase and give non-zero values to Mx and My (Fig 1.3).

The effect of B_1 will be to exert a torque on M tending to tip the moment toward the plane perpendicular to Bo; M will move away from the z-direction and precess about the effective field direction with the Larmor-frequency at resonance. The precession of M can be described by the following equations:

$$\frac{d \; Mx}{d \; t} = \gamma \left[M_y \; B_o - M_z \; (B_1)_y \right] \; \dotfill \; (1.28)$$

$$\frac{d M_y}{d t} = \gamma \left[M_x B_o - M_z (B_1)_x \right] \quad \dots\dots\dots\dots\dots\dots\dots\dots\dots\dots\dots \quad (1.29)$$

$$\frac{d M_z}{d t} = \gamma \left[M_x (B_1)_y - M_y (B_1)_x \right] \quad \dots\dots\dots\dots\dots\dots\dots\dots\dots \quad (1.30)$$

where $(B_1)_x$ and $(B_1)_y$ are the components of B_1 (rotating at angular frequency ω) along the x-y axes and are given by:

From Fig 1.4

$$(B_1)_x = B_1 \cos \omega t \quad \dots\dots\dots\dots\dots\dots\dots\dots\dots\dots\dots\dots\dots \quad (1.31)$$

$$(B_1)_y = -B_1 \sin \omega t \quad \dots\dots\dots\dots\dots\dots\dots\dots\dots\dots\dots\dots\dots \quad (1.32)$$

To proceed further the effect of relaxation processes must be taken into account. M_z does not remain constant, but after resonance approaches its equilibrium value M_o, at a rate governed by the spin relaxation time T_1, which in macroscopic systems is termed the longitudinal relaxation time. Additionally the effect of the transverse relaxation time T_2 must also be considered. The complete Block equations are therefore:

$$\frac{d M_x}{d t} = \gamma (M_y B_o + M_z B_1 \sin \omega t) - \frac{M_x}{T_2} \quad \dots\dots\dots\dots\dots\dots \quad (1.33)$$

$$\frac{d M_y}{d t} = \gamma (M_z B_1 \cos \omega t - M_x B_o) - \frac{M_y}{T_2} \quad \dots\dots\dots\dots\dots\dots \quad (1.34)$$

$$\frac{d M_z}{d t} = - \gamma (M_x B_1 \sin \omega t + M_y B_1 \cos \omega t) - \frac{M_z - M_o}{T_1} \quad \dots\dots \quad (1.35)$$
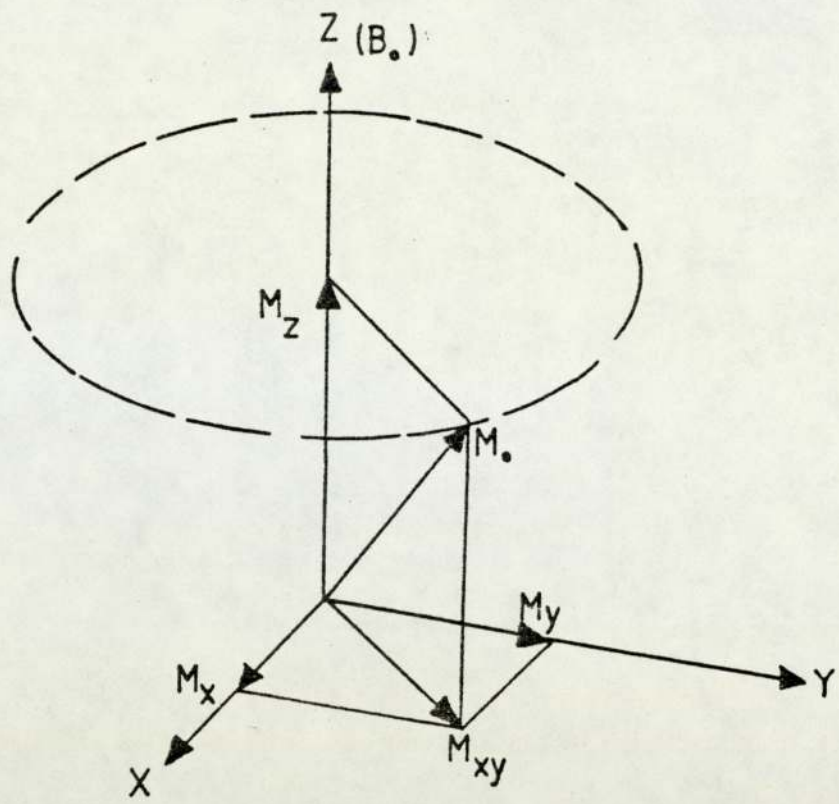
Figure 1.3   The resolving components of the magnetization vector.
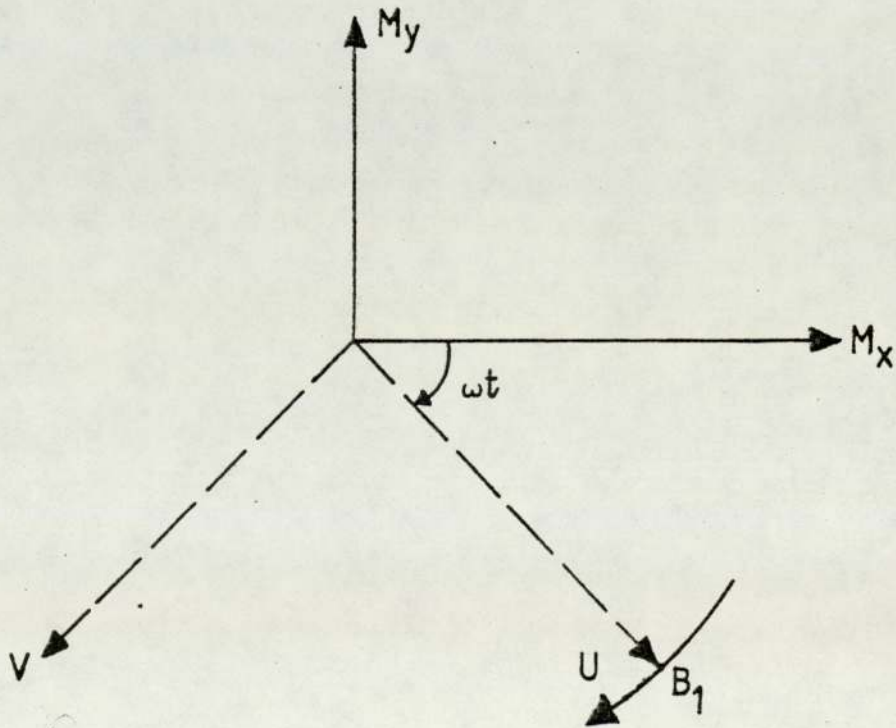
Figure 1.4   The transient components of the magnetization vector with respect to fixed and rotating axis.

Assuming that resonance is passed through slowly (the show passage approximation) the differentials with respect to time become zero and the solutions of equations (1.33, 1.34, and 1.35) are:

$$u = M_o \cdot \gamma B_1 T_2^2 (\omega_o - \omega) / D \dots\dots\dots\dots\dots\dots \quad (1.36)$$

$$v = M_o \cdot \gamma B_1 T_2 / D \dots\dots\dots\dots\dots\dots\dots\dots \quad (1.37)$$

$$M_z = M_o \cdot [1 + T_2^2 (\omega_o - \omega)^2] / D \dots\dots\dots\dots\dots \quad (1.38)$$

where

$$D = 1 + T_2^2 (\omega_o - \omega)^2 + \gamma^2 B_1 T_1 T_2 \dots\dots\dots\dots\dots \quad (1.39)$$

and M_o is the magnitude of the vector M in the absense of a radiofrequency magnetic field B_1, u is the component of M that rotates in phase with B_1, and v is the component of M that rotates 90° out of phase with B_1.

Depending on whether u or v is observed a dispersion (u – mode signal) or absorption curve respectively will be obtained (Fig 1.5). It should be noted that the equation for v is almost an expression of the Lorenzian curve[17,20] which is the generally accepted absorption signal.

The area under an absorption curve can be obtained by integration of the v term over all values of $(\omega_o - \omega)$. The area under each resonance is therefore a direct indication of the number of nuclei of a particular type undergoing resonance.
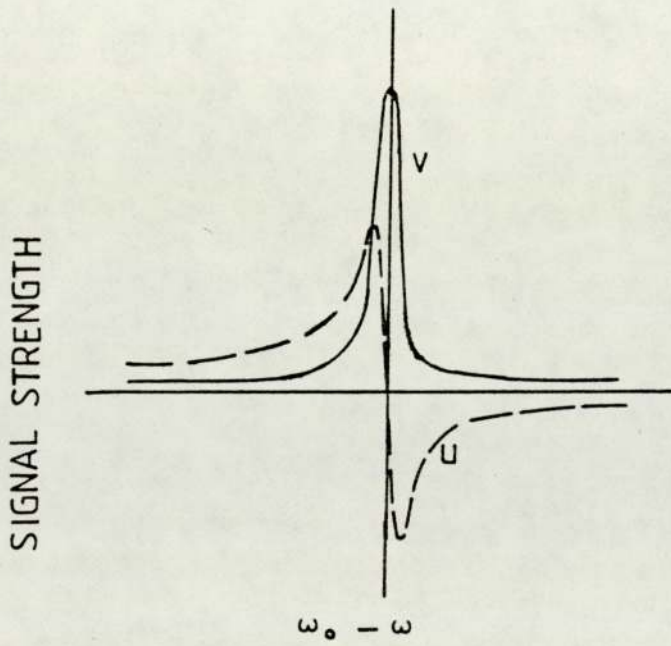
Figure 1.5   The absorption line shape (V-mode) and dispersion
              line shape (U-mode) of NMR signal.

1.9   FACTORS AFFECTING THE LINE-WIDTH:

Superficially, it might be accepted that the NMR signal should appear as a sharp absorption line, but in practice absorption occurs over a finite frequency range due to several line broadening factors. Usually the signal width is defined as its width at half hight expressed in terms of the applied field or frequency.

The various factors affecting the line shape will now be discussed.

1.9:1   Spin-Lattice Relaxation:

A nucleus may remain in a given energy state no longer than a factor of the spin-relaxation time T_1. There is therefore some uncertainty in the life time of that particular spin state that is characterized by the Heisenberg uncertainty principle which requires that:

$$\Delta E \cdot \Delta T \approx \frac{h}{2\pi} \quad \dots\dots\dots\dots\dots\dots\dots\dots\dots \quad (1.40)$$

Because energy and frequency are related by

$$\Delta E = h.\Delta v \quad \dots\dots\dots\dots\dots\dots\dots\dots\dots \quad (1.41)$$

Where Δv is the uncertainty in frequency of a particular resonance line, it follows from equations (1.40 and 1.41) that:

$$\Delta v = \frac{1}{2\pi \Delta T} \quad \dots\dots\dots\dots\dots\dots\dots\dots \quad (1.42)$$

23

and because $\Delta T = 2 T_1$ .... (1.43)

$$\Delta v \simeq \frac{1}{4 \pi T_1}$$ .... (1.44)

This shows that small values of T_1 leads to line broadening.

1.9:2 Spin-Spin Relaxation:

This relaxation process produces an uncertainty in the lifetime of any particular nuclear state in a similar manner to that of spin lattice relaxation and also leads to a broadened absorption signal.

1.9:3 Magnetic Dipole Interaction:

The magnetic environment of a nucleus may be modified by fields due to magnetic moments of neighbouring nuclei. In solids or viscous liquids a nucleus at distance r from the nucleus being considered produces a magnetic field at the nucleus of magnitude in the range of $+ 2 \mu/r^3$ to $- \mu/r^3$ where μ is the dipole moment of the nucleus. This means that the nuclei in a sample will experience a field spread over that range (derived from $\mu = (3 \cos^2 \theta - 1)/r^3$ where θ is the angle between r and Bo) and the absorption will be broadened[21].

In liquids and gases where the modecules are subject to rapid random motion, the magnetic field at any nucleus due to

neighbouring nuclei effectively averages to zero because $\cos^2 \theta$ = 1/3; this occurs because the molecular correllation time is less than the time required for the observation of a nuclear magnetic resonanse signal. Accordingly magnetic dipole broadening will be negligible in liquid and gas samples which are used for normal high resolution investigations.

1.9:4   Magnetic Field Inhomogeneity:

Inhomogeneity of the applied static magnetic field over the sample volume can cause line broadening due to the fact that absorption occurs over a range of resonance conditions corresponding to the range of field inhomogeneity. This effect can be reduced by applying correcting fields and by rapid spinning of the sample.

1.9:5   Saturation:

A large amplitude of the applied radiofrequency field may cause the excess number of nuclei in the lower energy state to be removed before the resonance line has been observed, if the effect of spin-lattice relaxation is inadequate to maintain a ground state excess. Therefore the nett radiofrequency energy absorbed will decrease. The decrease is greater at the absorption centre and the intensity of the signal will decrease while the effective line width increases. If sufficient radio-frequency power is applied the signal may disappear entirely.

1.9:6   **Miscellaneous Effects:**

As the presence of any paramagnetic species will significantly decrease T_1, the absorption line will be broadened, as mentioned before in section (1.9:1).

Finally a non-spherical nuclear charge distribution for nuclei of spin $I > 1/2$ confers to the nucleus a quadrapole moment q . Interaction of the quadrapole with environment electric field gradients promotes relaxation which gives uncertainty of the resonance position of the nuclear absorption line.

1.10   **THE CHEMICAL SHIFT AND NUCLEAR SCREENING:**

1.10:1   **Introduction To Chemical Shift:**

At an early stage in the history of NMR, it was found that the resonant frequencies for isotopically similar nuclei in the same molecule could be different when using the same applied magnetic field. The magnitude of this effect was shown[22, 23, 24] to be related to the chemical environments of the resonant nuclei, which cause them to be screened differently from the applied magnetic field.

If the applied magnetic field is Bo, the actual magnetic field experienced by the resonant nucleus is given by: $Bo(1-\sigma)$ where σ is the nuclear screening constant for the resonant

26

nucleus. This screening constant parameter can be introduced
to the resonance equation (1.12), so that:

$$v = \frac{\gamma}{2\pi} \text{Bo} (1-\sigma) \quad \dots\dots\dots\dots\dots\dots\dots\dots (1.45)$$

If σ, which is dimensionless and commonly positive,
reduces the effect of Bo will reduce the energy required for a
transition between the energy states will also be reduced. This
means that the resonance frequency will be lower.

Consequently, if two isotropically similar nuclei, in
different electronic environments i and j, have shielding
constants σ_i and σ_j respectively, the difference between the
two screening constants define the so-called "chemical shift
δ_{ij}"

$$\delta_{ij} = \sigma_i - \sigma_j \quad \dots\dots\dots\dots\dots\dots\dots\dots\dots (1.46)$$

For practical purposes the chemical shift can be expressed
in terms of the magnetic fields experienced by the two nuclei
during a constant frequency experiment, as:

$$v_{ij} \simeq \frac{\text{Bi} - \text{Bj}}{\text{Bj}} \quad \dots\dots\dots\dots\dots\dots\dots\dots (1.47)$$

Alternatively, for constant field experiments, the
chemical shifts may be written as:

$$\delta_{ij} = \frac{v_i - v_j}{v_{osc}} \quad \dots\dots\dots\dots\dots\dots\dots\dots\dots (1.48)$$

where ν osc is the radiofrequency of the signal applied to the irradiation coil to produce B_1. Chemical shifts expressed in this way are quoted in ppm.

Usually the chemical shift of a particular isotope is measured relative to the resonance of a suitable reference. The most commonly used reference for proton resonance is tetramethylsilane[25] (T.M.S.). This is often chosen because its resonance is a clear sharp line occuring to a high (shielding) field of most resonances of interest and it is soluble in most organic compounds while being chemically inert. Moreover, it has low boiling point (26.7°C), so it is easy to remove from the sample after the experiment has been concluded. The position of the resonance of TMS when it is at infinite dilution in Carbon tetra-chloride CCI4 is taken to be as $\delta = 0$. Signals to higher magnetic field, or greater screening, than TMS signal should have positive δ values, although common practice is to assign them (-) ve δ values. Another scale commonly used is the τ - scale[26], for which the TMS proton signal is taken as 10 τ . The two scales should be related by:

$$\tau = \delta + 10$$

As indicated above the δ and τ scales have been much abused and many of the quoted values of chemical shifts must be treated with caution[27,28].

1.10:2   <u>Some Details of Nuclear Screening:</u>

The nuclear screening parameter may be considered akin to many other observable physical properties. Consequently its composition can be examined by using the Virial expansion[29].

$$X = A + \frac{B}{Vm} + \frac{C}{Vm^2} + \ldots\ldots\ldots\ldots\ldots\ldots\ldots\ldots \quad (1.49)$$

where X is the observable molecular parameter, A is the perfect gas value of X, B represents the effect of the pairwise molecular interaction, C and higher terms represent the effects of multimolecular interactions; and Vm is the molar volume of the material studied.

Similarly, σ , the screening constant can be given in terms of a Virial expansion, as[29].

$$\sigma = \sigma_0 + \frac{\sigma_1}{V_m} + \frac{\sigma_2}{Vm^2} + \ldots\ldots\ldots\ldots\ldots\ldots\ldots \quad (1.50)$$

Where σ_0 is the screening in the isolated molecule, σ_1 represents the effect of pairwise molecular interaction on the screening, σ_2 and higher terms represent the effect of multimolecular interaction on the screening.

For particular reasons equation (1.50) is better rewritten to represent the chemical shift as:

$$\delta_{obs} = (\sigma - \sigma\,ref.) = (\sigma_0 - \sigma\,ref.) + \frac{\sigma_1}{V_m} + \frac{\sigma_2}{V_m^2} + \quad \ldots \ldots \quad (1.51)$$

Where $\sigma\,ref$ is the screening constant of the reference nucleus.

A significant observation was that the relationship between the chemical shift $\sigma - \sigma\,ref.$ and the bulk density of a gas is linear[30,31]. This relationship seems to extend into the liquid phase. The implication of this would lead to the conclusion that the only term additional to σ_0 in the Virial equation (1.51) is $\frac{\sigma}{V_m}$, and that the terms higher than first order can be ignored. This means that screening constant arises from two factors viz. the absolute screening constant (intramolecular) and the screening contribution from the bimolecular interaction (intermolecular) σ_{inter}. Therefore equation (1.50) may be reduced to

$$\sigma = \quad \sigma_0 \quad + \frac{\sigma_1}{V_m} \quad \ldots\ldots\ldots\ldots\ldots\ldots\ldots\ldots\ldots\ldots\ldots\ldots \quad (1.52)$$

or $\quad \sigma = \sigma_{intra} + \sigma_{inter} \ldots\ldots\ldots\ldots\ldots\ldots\ldots\ldots\ldots \quad (1.53)$

Studies of σ_{intra}[32,33] have been carried out using quantum mechanical treatments. For these it has been suggested that the screening constant of a nucleus A in an isolated

30

molecule is adequately represented by:

$$\sigma_{intra}^{A} = \sigma_{para}^{AA} + \sigma_{dia}^{AA} + \sum_{A \neq B}^{A} \sigma^{AB} + \sigma_{del}^{A} \cdots\cdots (1.54)$$

In equation (1.54) σ_{para}^{AA} is the screening contribution that comes from the mixing of ground and excited electronic states by the magnetic field and leads to induced paramagnetic current around A. σ_{dia}^{A} is due to the diamagnetic currents resulting from electronic motion about A. The induced currents in bonds or atoms rather than A provide the anisotopic contribution to the screening σ^{AB}, and σ_{del}^{A} comes from the induced electronic motion of delocalized electrons in the molecular structure surrounding A.

Considering the second part of the screening constant σ_{inter}, this arises from the interaction of the molecule, containing the nucleus being studied, and the solvent molecules. In other words σ_{inter} arises from solvent-solute interactions.

It was suggested by Buckingham in 1960[35, 29] that σ_{inter} may be generally formulated by:

$$\sigma_{inter} = \sigma_b + \sigma_w + \sigma_a + \sigma_E + \sigma_s \cdots\cdots\cdots\cdots\cdots (1.55)$$

The individual terms of this equation generally represent the total contribution for all components of a mixture to the screening of a nucleus in one molecule (solute) are as follows:

31

σ_b is due to the bulk magnitization of the sample. σ_w is due to the effect of van der Waals, but principally attractive dispersion, forces. σ_a is due to the secondary fields produced by magnitically anisotropic solvent molecules. σ_E is a composite term basically due to the effect on an electrically polar solute of the reaction field of the solvent which is induced by the solute, but includes the effects of electric fields due to permanent dipoles or quadrapoles in the solvent. σ_s is due to the contribution of any specific or binding interactions between the solute and the solvent molecules, e.g when hydrogen bonding or complex formation occurs.

It is obvious from what has been explained above that σ_{intra} depends on the structure of the molecule of interest and so is a parameter of particular interest to most chemists. In this thesis however, investigations of aspects of σ_{inter} rather than σ_{intra} are reported, although there is an underlying interest in the elucidation of molecular structure using σ_{inter}.

Many people have worked over the past three decades to establish theoretical models for the characterization of the components of σ_{inter}. Even so, the magnetic susceptibility screening parameter σ_b is the only parameter which can be considered adequately characterized (more details about this can be found in chapter six of this thesis). Dickenson showed that

$$\sigma_b = (\alpha - q - \frac{4\pi}{3}) \, X_v \dots\dots\dots\dots\dots\dots\dots \quad (1.56)$$

Where α is the sample shape factor, q is the magnetic field interaction factor, and X_v is the volume magnetic susceptibility of the matter under test. It was shown that q can be considered approximately zero. α the sample shape factor is taken to be 2π for a cylindrical sample with a length at least four times its diameter[37,38]. As all the sample tubes used throughout this work meet the above criteria, the parameter σ_b can be easily calculated.

Experimentally the chemical shift is taken with respect to a reference. The physical way in which this reference is used may effect the contribution of σ_b to the measured shift. A common method of referencing is by mixing the reference substance homogenously with the sample. This procedure is called the internal referencing procedure. In this method the molecule of interest and the reference are in the same medium and hence, both the sample and the reference experience the same magnetic susceptibility screening contribution. This eliminates the σ_b contribution to the chemical shift measurement[39].

Another common referencing procedure is that of external referencing which employs the reference material in a separate vessel surrounded by the subject compound. A common method of external referencing is to use two co-axial cylinders, so that

the reference material is in a capillary tube situated inside and co-axial with the main cylindrical sample tube. The theoretical implications of such arrangement have been considered by Frost and Hall[40] who extended Dickinson's approach. They deduced that the true chemical shift devoid of susceptibility effects of the sample of interest (A) relative to a reference material (B) is given by

$$\delta^{t}_{A-B} = \delta^{o}_{A-B} - \frac{2\pi}{3} (X_A - X_B) \quad \dots\dots\dots\dots\dots \quad (1.57)$$

Where δ^{t}_{A-B} is the true chemical shift of A from the reference B, δ^{o}_{A-B} is the corresponding observed shift, and X_A and X_B are the volume magnetic susceptibilities of A and B respectively.

The above equation applies for long perfectly cylindrical tubes. However, if the reference can be contained in a spherical vessel, the shape factor for which is $\alpha = 4\pi/3$, it emerges that $\Delta\sigma_b = 0$, which means that there is no need for any susceptibility correction. Unfortunately, the last technique is difficult to employ with precession.

The disadvantages of the external reference is that its correction depends on the volume magnetic susceptibility of the samples used and errors can arise from the uncertainty in these values, especially in the case of mixtures[41].

34

This thesis include in chapter 6 a novel suggestion for determining volume magnetic susceptibilities, X_v.

It is obvious now that the contribution of the volume magnetic susceptibility to chemical shifts can be estimated. Moreover, it is possible that significant contribution due to σ_S can be avoided by using very low concentration of the subject molecule, the solute (infinitely diluted) in an inert solvent. However, the relative importance of the remaining screening parameters, need to be assessed. It is probably fair to observe that σ_W, σ_a, and σ_E, which in this order represent the relative ease of their experimental accessibility, have not been characterized precisely.

The major part of this thesis is concerned with σ_W as the correct formulation of this may provide the key to the elucidation of σ_a and σ_E. Some intensive work on σ_W has already been carried out by Homer and Percival. The present work may be considered as extensing and further sustentation Homer's basic theory.

In order to isolate σ_W, it is necessary to measure the chemical shift of a solute molecule with respect to a suitable reference in two physically different situations. The first one is when the solute is in the gas phase (at zero pressure) to give ($\sigma_0 - \sigma_{ref.}$), and the second one is when the solute

molecule is at infinite dilution in a solvent to give ($\sigma -$ $\sigma_{ref.}$). When the solute and the solvent molecules are perfectly isotropic, the difference between the susceptibility corrected chemical shifts in the liquid phase relative to the gas phase will give only σ_w.

$$\delta \text{ liquid - gas } = \sigma_b + \sigma_w \dots\dots\dots\dots\dots\dots\dots (1.58)$$

$$\delta_{\text{liquid to gas (after susceptibility correction)}} = \sigma_w \dots (1.59)$$

There have been many ways proposed to calculate σ_w theoretically, but these have been considered to be incomplete by Homer. The past work with the not-recently proposed theory will be discussed in chaper 3.

1.11 NUCLEAR SPIN-SPIN COUPLING:

High resolution spectra may reveal that chemically shifted absorption bands are composed of several lines. This added multiplicity is attributed to the intra molecular interaction between magnetically non-equivalent nuclear magnetic moments[42,43]. The multiplicity comes from the coupling interaction between neighbouring nuclear spins. Important features are exibited by spin-spin interactions which distinguish them from the chemical shift. For example they are independent of B and temperature in most cases.

In the simplist case the spacings between these multiplet

36

lines are equal and the magnitude of this spliting is known as the compling or the spin-spin coupling constant. This is symboled by J for which the unit is H_z.

The effect can be explained naievly in terms of the fact that a nuclear spin tends to orient the spins of the nearest electrons which then orientatethe spins of the electrons and subsequently the spins of other nuclei. The electron spins mechanism may be considered the most important contribution to spin spin coupling.

In general the magnitude of the coupling constant decreases as the number of bonds separating the interacting nuclei increases, and increases with the atomic number of each nucleus.

The complexity of the spin patterns is largely dependent on the relative magnitude of the chemical shift differences and spin-spin coupling between the interacting nuclei. When the chemical shift of the two nuclei is of the same order of magnitude as the coupling constant (both in H_z), the nuclei are identified by closely positioned alphabetic letters A,B,C ... When the chemical shift is longer than the coupling constant between the nuclei ($\delta \gg J$) the latter are identified by letters widely spaced in the alphabet e.g A and X. Nuclei with the same chemical shifts are assigned the same letter and the number of such nuclei is indicated by the appropriate numerical subscript. Such nuclei are deemed either chemically

37

equivallent or magnetically equivalent. Chemical equivalent
nuclei only have the same chemical shift.

Magnetically equivalent nuclei do not show any
experimental evidence of any coupling between them, although in
fact such coupling does occur. Nuclei are said to be
magnetically equivalent when they have the same chemical shift
and couple equally to any other resonant nuclei in the
molecule.

The signal arising from one set of nuclei is termed an
absorption band, while constituent lines of such a band arising
from coupling are called peaks. The number of the latter can
be predicted simply for first order situation for which $\delta \gg J$.

For a set of n_A equivalent nuclei of type A and n_x
equivalent nuclei of type X, a first order coupling treatment
(Dixon 1972[44]) gives $(2n_x I_x + 1)$ peaks for A band and $(2n_A
I_A + 1)$ peaks for X band.

The relative intensities of the peaks comprising the
multiplit structure are given by the nth polynomial
coefficients. These rules are strictly valid only if $\delta \gg J$.
When $\delta - J$, the spectra should be treated as second order
spectra and the above simple spacing and intensity rules are no
longer valid.

The spin-spin coupling aspect of NMR spectroscopy has not encountered in this work and therefore will not be considered further.

CHAPTER TWO

NMR INSTRUMENTATION; C.W. AND F.T. SPECTROMETERS

2.1 INTRODUCTION:

Inspection of the basic nuclear resonance equation:

$$v_0 = \frac{\gamma}{2\pi} B_0 \ (1 - \sigma) \ \dots\dots\dots\dots\dots\dots\dots\dots\dots\dots\dots \ (2.1)$$

reveals the fundamental requirements for the observation of NMR
spectra. For chemically similar nuclei to be studied via a
continuous spectrum either B_0 or v_0 must be varied over a small
range, while the other parameter is maintained constant.

The early work of Block et al [17,45] showed that NMR in bulk
materials can be observed in several ways. For the slow passage
experiment the radiofrequency (r.f) experienced by the sample is
slowly swept with the magnetic field B_0 constant, or conversely

the magnetic field is slowly swept at a constant radiofrequency. Alternatively, spectra may be observed under adiabatic rapid passage conditions, which requires rapid sweep of either frequency or magnetic field between certain limits.

Both slow passage and rapid passage techniques are continuous wave (c.w) experiments, because the r.f is continuously applied during the spectrum observation.

Another technique which was suggested by Block [17], uses pulses of r.f power essentially at a discrete frequency. Detection of the NMR signal is made after turning the r.f off. This is basically the pulse method which has recently been developed to provide a routine method of observing NMR spectra.

Two types of spectrometers are now currently available for NMR experiments viz the continuous wave c.w and the Fourier transform F.T spectrometers. The main differences between the two types of spectrometers lie in the power and time dependence of the r.f wave and in the method of signal acquisition. Both types of spectrometers have been used for the work described herein. Consequently, the principles underlying each approach will be discussed before dealing with the specific spectrometers employed.

2.2 BASIC COMPONENTS OF C.W. NMR SPECTROMETERS

Inorder to produce high resolution NMR spectra, the instrument employed should contain the following basic components:

a - A magnet capable of producing a very strong homogeneous and highly stable magnetic field.

b - A sweep unit to vary the magnetic field and/or the radiofrequency over a small range.

c - A highly stable radiofrequency oscillator.

d - A probe which holds the sample and contains the r.f transmitter and receiver coils together with facilities for spinning the sample.

e - A radiofrequency receiver and amplifier with high gain and low noise.

f - An oscilloscope and/or pen recorder to present the spectra.

The basic requirements for the individual components of a high resolution nuclear magnetic resonance spectrometer will now be discussed.

2.2:1   **The Magnet:**

The sensitivity of the NMR signal is theoretically proportional to B^2_o and the chemical shift frequency separation between resonances depends on B_o. It is therefore advantageous to use very strong magnetic fields, which have to be highly

homogeneous.

Suitable magnetic fields may be provided by electromagnets, permanent magnets or superconducting magnets. The advantage of electromagnets is that, the field strength can be varied and controlled within the range of about 1.0 to 2.5 Tesla. In principle this allows all magnetic nuclei to be studied at more than one frequency, and thus is very useful in interpreting complex spectra. The disadvantage of the electromagnet is the high cost of the control equipment, its relatively short life-time and high running costs. The permanent magnet does not have the same flexibility of operation and also has a practical upper limit of field strength at about 2.5 Tesla. However, it does have the advantage of high field resolution stability and low running costs. Since the field strength cannot be varied by more than about 1%, different nuclei require different operating frequencies. The uniformity of the field obtainable by both types of magnets are comparable, both being capable of ultimately producing fields that are homogeneous to the order of 3 parts in 10^9.

Superconducting magnets are also employed in modern NMR spectrometers and can produce fields of the required homogenity at field strengths of the order of 5 Tesla. This type of magnet requires an elaborate control system to maintain the low temperature of the conducting wire within the required range. Usually the low temperature can be achieved using liquid helium

and this, of course, is costly. It is however claimed by some manufacturers that the running costs of both superconducting and electromagnets are now similar. No use of the former has been made here and so this type of magnet will not be discussed further.

The upper limits of the field strength mentioned above come from the need for field homogeneity over a sample volume of 0.5 cm^3 or even larger. The necessary homogeneity requires that the magnet pole faces are strictly parallel, free from machining marks and ideally optically flat [46]. The pole cap material must be metallurigically uniform and chromium plated to reduce any corrosion effects. Homogeneity can be further improved by using Golay or shim coils near to the pole faces; these carry currents to generate the required inhomogeneity correction fields. Final improvements to the field homogeneity at the sample may be achieved by spinning the sample tube about its longitudinal axis.

High field stability is important for the production of reproducible spectra and the accurate measurement of chemical shifts. In this connection early workers often prefered a permanent magnet because it is capable of maintaining a sufficiently constant field, when carefully thermostatted [47] and placed away from magnetic disturbance although the latter can be minimized by mu-metal screening or by correction using field sensing devices. The field stability of electromagnets additionally depends upon the stability of the currents passing

through their energizing coils. To achieve field stability with an electromagnet, a feedback system is required to stabilize the current passing through the magnets coils. This is often done by passing the magnet current through an appropriate resistance and the voltage compared with a reference voltage. The difference between these voltages is amplified and used as an error voltage for correction purposes.

High resolution NMR Spectrometers incorporating either a permanent magnet or an electromagnet usually employ flux "pick-up" coils [48] to detect any fluctuation in the flux across the poles gap. The voltage induced in these coils is integrated to provide correction signals that are then passed through componsating or "buck out" coils. The field produced by these coils eliminates the original flux change and restores the field to its original value and maintains it stable.

Field/frequency locking is also used to stabilize B_0. This is described later in Section 2.2:3.

2.2:2   **The Magnetic Field Sweep:**

As was mentioned at the beginning of this chapter, the strength of the main field B_0 (field sweep method) or the frequency of the r.f oscillator (frequency sweep method) may be varied inorder to reachieve resonance while maintaining the other parameter constant. One early experimental difficulty was to provide suitably stable and linear frequency sweep and this often

led to the use of the magnetic field sweep approach. Technically, this can be done by using a saw tooth generator which feeds two small Helmholtz coils placed close to the sample with their axes in the direction of that of the main magnetic field B_0. These are driven by the output of a sweep amplifier from which a tap is also fed to the x-plates of the oscilloscope. This produces a current sweep which facilitates rapid monitoring of a sweep on an oscilloscope. The region to be scanned may be selected by electrically shimming the magnetic field and so changing the intensity of the field and the magnitude of the sweep. Inorder to produce a permanent record of a spectrum, the sweep of the magnetic field (or frequency) is often controlled by a potentionmeter connected directly to the drive of the chart recorder.

When recording spectra, the correct sweep rate should be selected very carefully, because rapid passage of an absorption may produce ringing after the signal or alternatively a very slow sweep rate may produce saturation [49].

2.2:3   **Field Stabilizer - Field/Frequency Locking:**

NMR spectrometers, particularly those employing electromagnets, often have field/frequency lock devices to stabilize B_0.

For this a lock material, contained within the analytical

sample or as a separate sample, is used to produce a signal in the dispersion mode (Fig 1.5). The signal level at its centre is monitored and any change in this from zero, which indicates a drift in the resonance position, is used to operate an electronic feedback loop which restores the resonance to its original position.

When using a control sample, that is physically separate from the sample under test, changes in the two resonance conditions need not be exactly paralleled. This was the reason for devising the so-called internal locking system [52]. In this system two separate audiofrequency modulation of the driving r.f signal are used, one at the locking frequency and the other one at the observing frequency. Thus the NMR spectrum consists of a centre band spectrum and side band spectra to high and low fields from the centre bands that are shifted by the modulation frequencies. The magnetic field is then adjusted to a value that corresponds to one of the sidebands and a sharp resonance detected in the dispersion mode. This signal is passed through a phase sensitive detector operating at the frequency of the sideband being used for the lock signal. The output from the phase sensitive detector is rectified and the resulting signal operates a control loop to a flux stabilizer, the output of which maintains the necessary constant ratio of field strength to frequency.

Other resonances from the sample can now be observed by varying the observing audiofrequency through a suitable range and the spectral responses detected using a second phase sensitive

detector operating at the observing frequency. The output of this phase sensitive detector is then fed to the recorder and/or oscilloscope.

When the lock frequency is kept constant and the observing frequency varied, a true frequency sweep experiment is performed. When the observing frequency is held constant and the lock frequency varied, field sweep experiments are possible.

2.2:4   **The Radiofrequency Transmitter:**

As has been mentioned in section 2.2:1, the upper limit of the main magnetic field from permanent and electromagnets is in the region of 2.4 Tesla, and this requires that the highest radiofrequency for ^1H resonance is at about 100 MHz. The stability of the r.f transmitter must be the same as that of the main magnetic field namely 1 part in 10^8 to 10^9 per minute. The common method used for producing such radiofrequencies is to employ a high precission quartz oscillator source with automatic frequency control at the output stage. The output from this is amplified to the desired power level and after automatic gain control the output level is appropriately attenuated.

2.2:5   **The Probe And Detection System:**

The sample holder, the probe, essentially carries: the transmitter and the receiver coils mounted on a glass former in

which a sample tube is spun using an air turbine. In addition it may carry linear sweep and shunt coils and usually a preamplifier. The radiofrequency coils are usually constructed from a few turns of copper wire wound around or as saddle on the glass former that is mounted vertically and perpendicular to B_o. The probe position is often slightly variable to enable the best position for the polarizing field to be obtained.

The sample, in its cylindrical glass tube, is inserted down and inside the glass former and is usually supported at the top and bottom to facilitate spinning and improve field homogeneity.

There are two basic types of probes: the single coil probe [21], and the double or crossed coil probe [53]. With the single coil probe a bridge circuit is used to balance out the transmitter signal and to allow small absorption or dispersion signals to appear as an out of balance e.m.f. across the bridge. In high resolution NMR, a twin T-bridge is often used, which has the advantage of good stability and the facility to distinguish between U and V mode signals. The absorption U mode is selected by introducing a leakage of the transmitter signal out of phase with the dispersion signal.

The detection system with a crossed coil probe was used in the first successful nuclear induction experiment [7]. In the induction method, two orthogonal coils are used. The receiver coil surrounds the sample with its axis perpendicular to both axis of the transmitter coil and the direction of the main field B_o. In

this arrangement the signal experienced by the receiver coil is that corresponding to the absorption of energy by the sample nuclei. This signal is therefore isolated from the background r.f signal by the geometrical arrangement of the two coils. Any lack of orthoginality between the coils causes the transmitter to couple with the receiver coil and hence a leakage voltage can be induced in the latter. A small amount of leakage is desirable since it serves as a source of carrier signal. Control leakage of flux without moving the receiver coil is achieved by introducing semicircular sheets of metal placed at the end of the transmitter coil; these plates are called paddles. The paddles are used to control a finite leakage voltage that enables the detector to operate at an efficient level and also allow the desired mode of the NMR signal to be selected.

A schematic diagram of a c.w NMR spectrometer is presented in Fig (2.1).

2.3 THE C.W. SPECTROMETERS USED:

Two continuous wave spectrometers have been used during the work reported in this thesis. These were the Varian Associates HA 100 D NMR spectrometer, and Perkin-Elmer R12B NMR spectrometer. The former operates at 100 MHz and the latter at 60 MHz for ^{1}H resonances. Whilst many of the principles applicable to these two spectrometers, have been discussed, the salient features of each will now be reviewed.
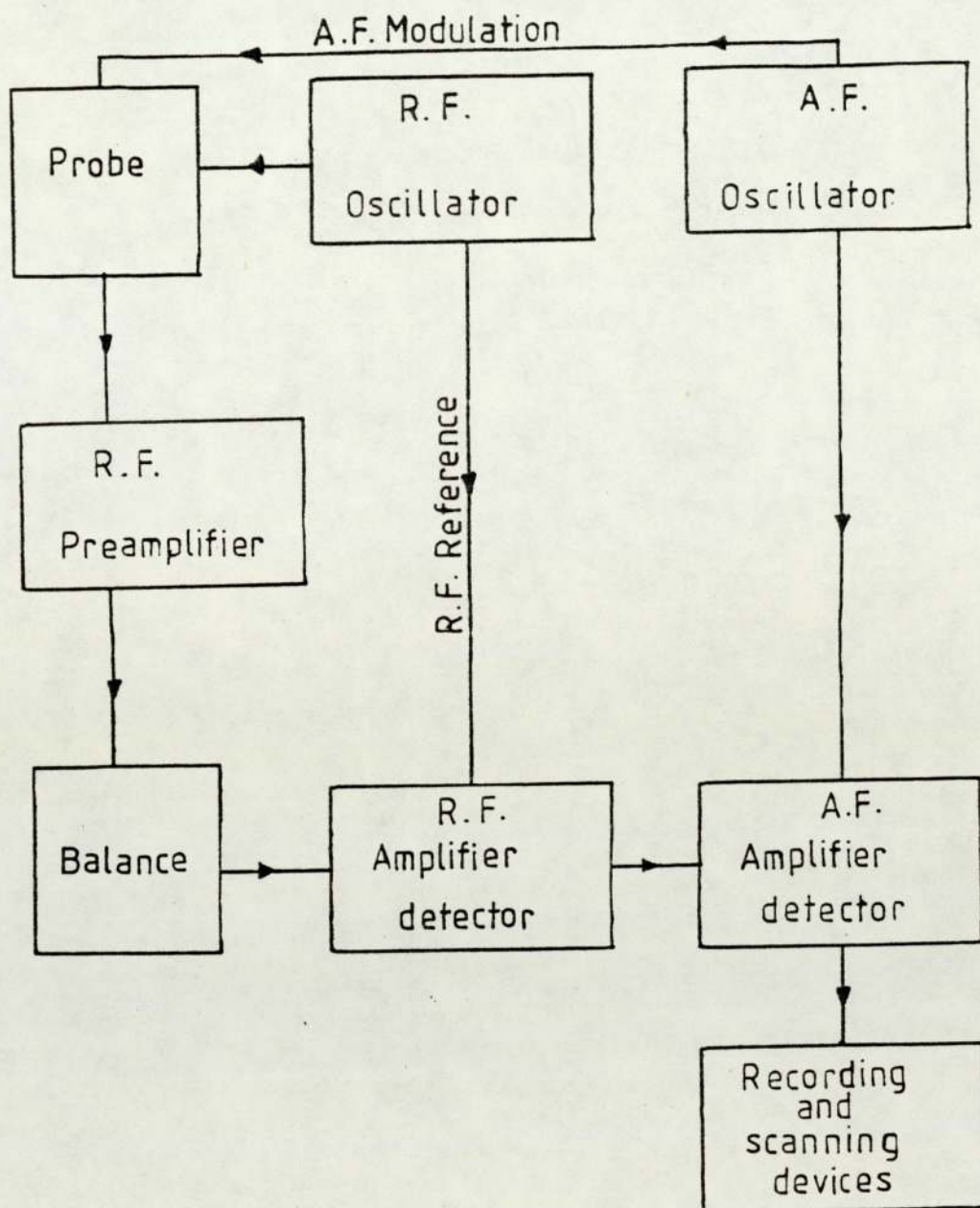
Figure 2.1   Schematic diagram of a typical c.w NMR
              spectrometer.

2.3:1   The Varian Associates HA 100 D NMR Spectrometer:

This spectrometer [54] possesses an electromagnet having a magnetic field strength of 2.349 Tesla, which permits hydrogen resonance spectra to be measured at 100 MHz. Spectra are detected by sidebands modulation at 2.5 KHz with field sweep being possible using the lower sideband, and frequency sweep (HA mode) using the upper sideband.

The low impedence coils of the magnet are fed from a three phase driven power supply, and cooled with thermostated water, maintaining the pole gap region at - 33°C. The magnet current is variable and a fine field trimmer is provided to compensate for day to day changes in magnetic field strength. Golay shim coils are mounted directly on the pole faces. The whole magnet is contained in an isolated housing to help maintain thermal stability.

The probe body is constructed from aluminium, and is designed to accommodate 5mm O.D NMR tubes carrying a turbine made of milled teflon. The turbine is fitted around the sample tube at a suitable position and driven by compressed air.

The probe contains coils for sweeping the polarizing magnetic field B_o, a transmitter coil for producing the rotating field B_1, a receiver coil for detecting the NMR signal and two sets of paddles for adjusting the leakage between the transmitter and receiver coils. The transmitter and the receiver coils are

52

orthoganal to each other; any small amount of coupling between the transmitter and receiver coils can be controlled effectively by paddles, which are equivalent to inductors, coupled to both the transmitter and the receiver. A controlled leakage introduced in phase with the absorption signal effectively supresses the dispersion mode.

A linear sweep unit allows variable sweep times and widths to be provided by a sawtooth waveform derived from a phantastron oscillator. In this the sawtooth voltage modulates a 50 KHz signal applied from separate oscillator circuit. This modulated 50 KHz signal is amplified in two stages and then mixed with an unmodulated 50 KHz signal which is π out of phase. This provides a stable linear direct current sweep connected to the D.C modulation coils on the probe so that B_o can be modified.

The Varian Associates HA 100 D spectrometer is suitable for use in two basic modes viz, the HA mode, which uses the field/frequency lock system; and the HR mode, which has an unstabilized repetitive field sweep facility. The operational bases of these two modes are shown schematically in Figures (2.2 and 2.3).

The way this spectrometer was used for the work reported here utilizes only the HA mode of operation. For this a reference material has to be added to the sample under study, so the references and the sample are subject to the same conditions. The
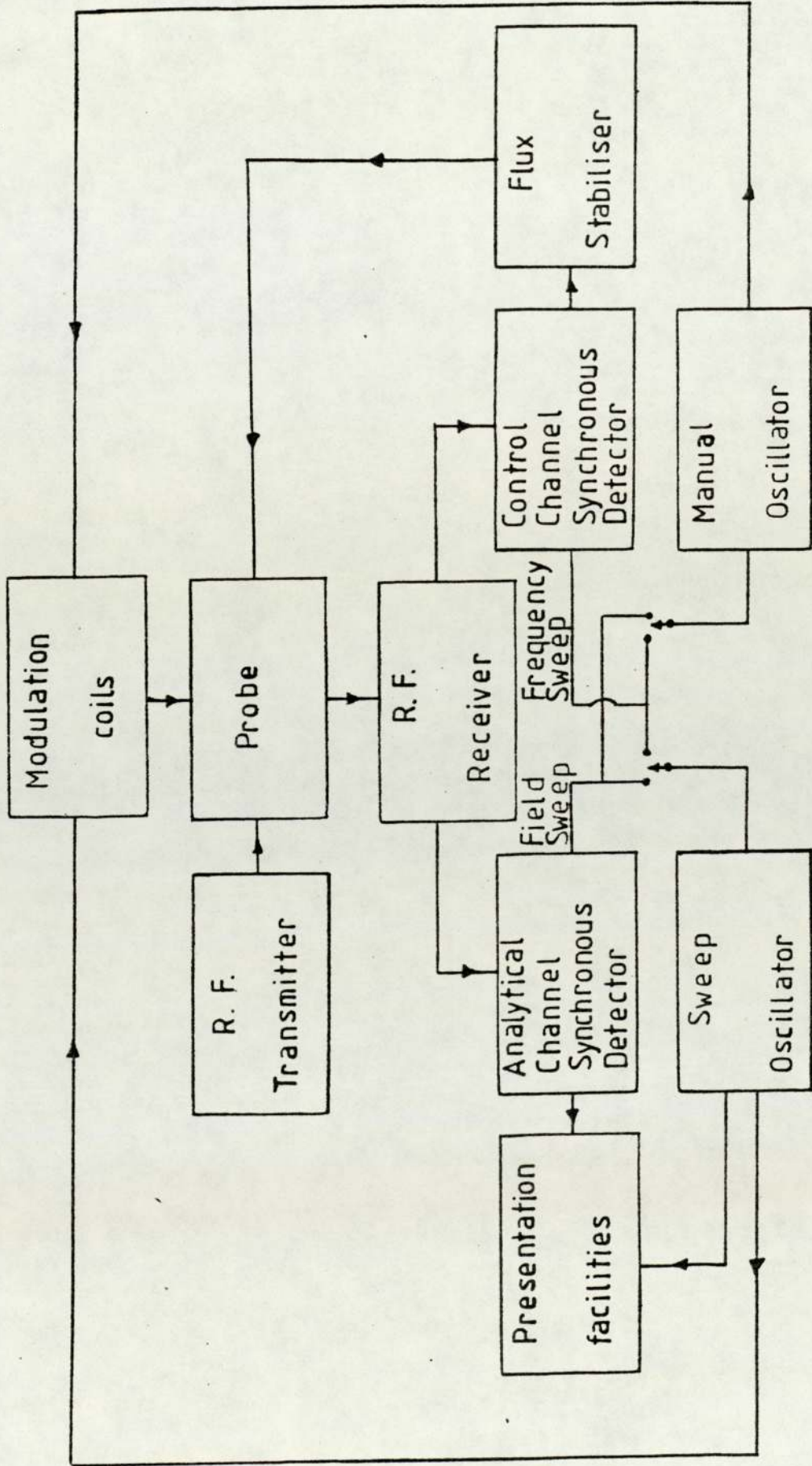
Figure 2.2   A schematic representation of the internal field/frequency lock system of Varian Associates HA 100 D NMR spectrometer.

54

Integrator /Oscillator

2.5 KHz

Probe

Linear sweep

R. F. Attenuator

Flux Stabilizer

Preampli_fier

R. F. Oscillator

Slow sweep

R. F. Amplifier

Mixer

95 MHz

95 MHz Oscillator

95 MHz

Mixer

5.0025MHz NMR Signal

I. F. Amplifier

Receiver gain

I. F. Amplifier

5 MHz

5.0025 MHz NMR Signal

R. F. Detector

Recorder

Leakage level

2.5 KHz NMR Signal

Audio Amplifier

NMR Signal

Oscilloscope
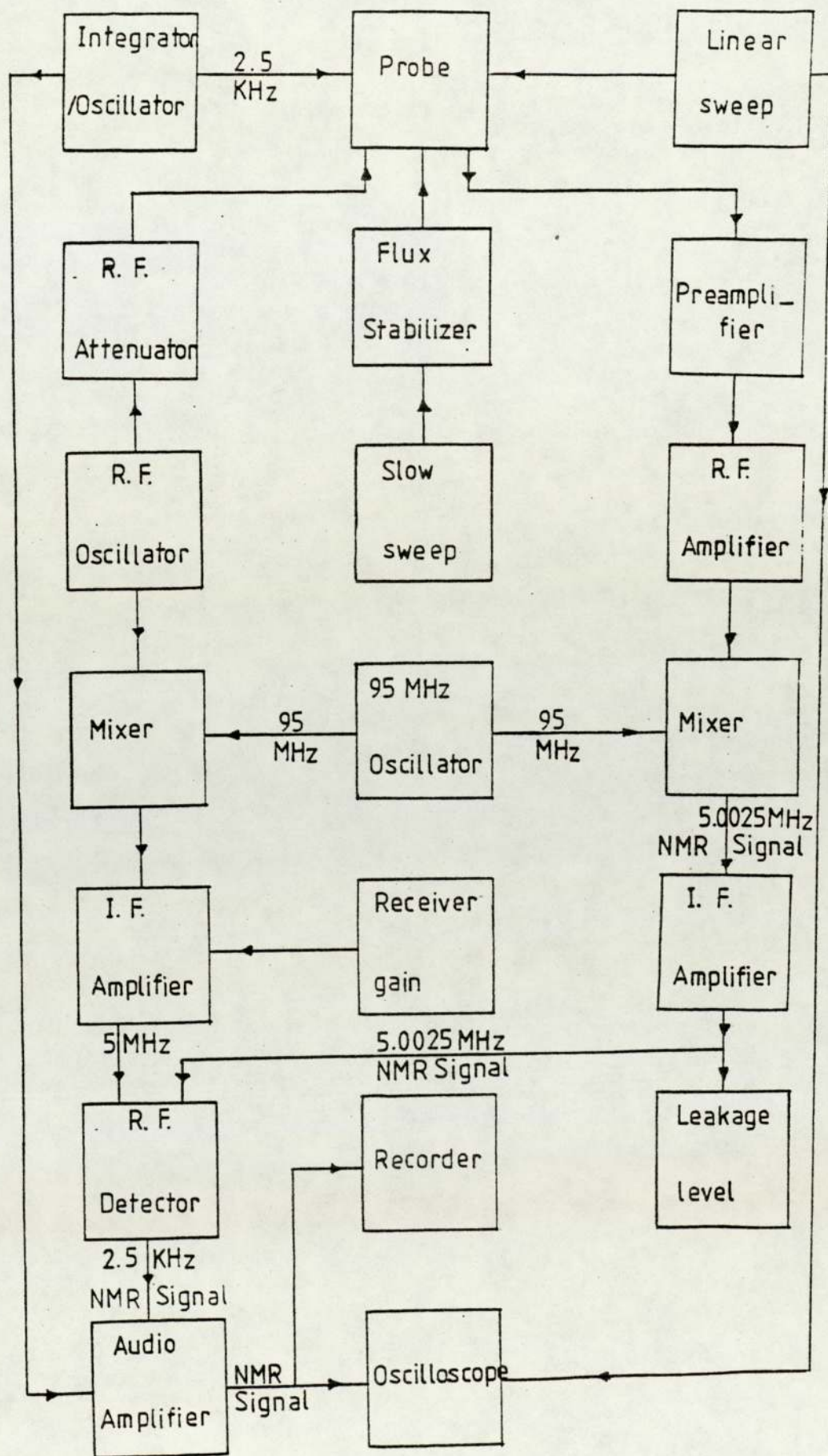
Figure 2.3   A schematic representation of the Varian Associates
HA 100 D NMR spectrometer operating in the HR mode.

NMR signal from the reference is detected in a control channel at the centre of the dispersion mode so that any movement of the signal yields a finite voltage in the detector. The signal is amplified and applied to the field compensator and the output of this enables the instability to be corrected. The sample signals are processed separately in the analytical channel and are ultimately passed to the recorder. A schematic representation of the lock system for the HA mode is given in Figure 2.2.

The HA mode of operation is controlled, apart from the display facilities, by the R.F.Unit and the internal reference stabilization unit. The latter adjusts the main field to allow for minor variation in field or frequency to keep these two parameters in constant proportion. The field compensator and presentation facilities unit houses the A.F and phase detection circuitry for both analytical and control channels and is linked to the R.F Unit.

The transmitter section comprises two A.F oscillators, the sweep oscillator, variable from 3500 Hz to 2500 Hz, and the manual oscillator, variable from 1500 Hz to 3500 Hz. The frequency of the former is controlled by the movement of the recorder along its x-axis. The frequency of the manual oscillator is controlled by potentiometers which vary the position of the lock signal on the recorder. The oscillator circuits are identical modified Wien bridge sine wave generators, and are tuned for 50, 100, 250, 500 and 1000 Hz sweep ranges; those can be operated by sweep rates of 25, 50, 100, 250, 500, 1000, 2500 and 5000 sec. within the ranges

of 1500 - 2500 and 2500 - 3500 Hz. A switch on the front panel of the unit enables the selection of either the lock signal, the sweep or the manual oscillators, an external signal, or the difference of the two oscillator frequencies to be presented to the oscilloscope or the Varian 4315A frequency counter.

The two frequencies are applied to the AC coils in the probe after suitable amplification and filtering, and independently modulate the 100 MHz carrier. The detected NMR signals are processed by the receiver in the R.F Unit, then they are reduced to A.F signals which are modulated with the NMR information. These resultant signals are amplified and filtered and then split into their analytical and control components by phase sensitive detectors.

The control signal is applied through the "lock on" switch to the stabilization filter which removes the extra noise, and passes the DC signal to the flux stabilizer to complete the loop. The NMR signal in the analytical channel is similarly detected and passed to the integrator/decoupler where it is amplified, filtered and, if required, integrated before being applied to the recorder y-axis circuits to be presented.

2.3:2   **The Perkin-Elmer R 12 B NMR Spectrometer:**

This spectrometer [55] has a permanent magnet giving a magnetic field strength of 1.492 Tesla, for ^1H resonance at 60

MHz. The magnet is of a rigid barrel construction that protects it from any distortion of the pole pieces. The field stability is maintained principally by keeping the magnet at constant temperature by passing heated air around the magnet, and by use of U-metal screening. The field homogeneity is improved by means of Golay coils mounted near the pole tips. The sample is spun about its longitudinal axis using a plastic turbine fitted to the sample tube.

Sweep and shift coils are wound on a former on the magnet pole pieces. The magnetic field can be swept through a small range by passing a sawtooth current through the sweep coils. The sweep range may be varied by changing the amplitude of the sawtooth. In addition, the sweep current may be derived from a potentiometer driven by the pen recorder and this enables the spectrum to be observed on a recorder in addition to the oscilloscope.

Regions of the spectrum may be selected for expansion or study by field shift and width controls; the adjustment of which changes the current passing through the appropriate coils.

The operational basis of the spectrometer is shown schematically in Fig (2.4).

The irradiation field (60 MHz) B_1 is derived from a highly stable crystal-controlled oscillator kept in a thermally regulated oven. The frequency stability of the oscillator is of the order
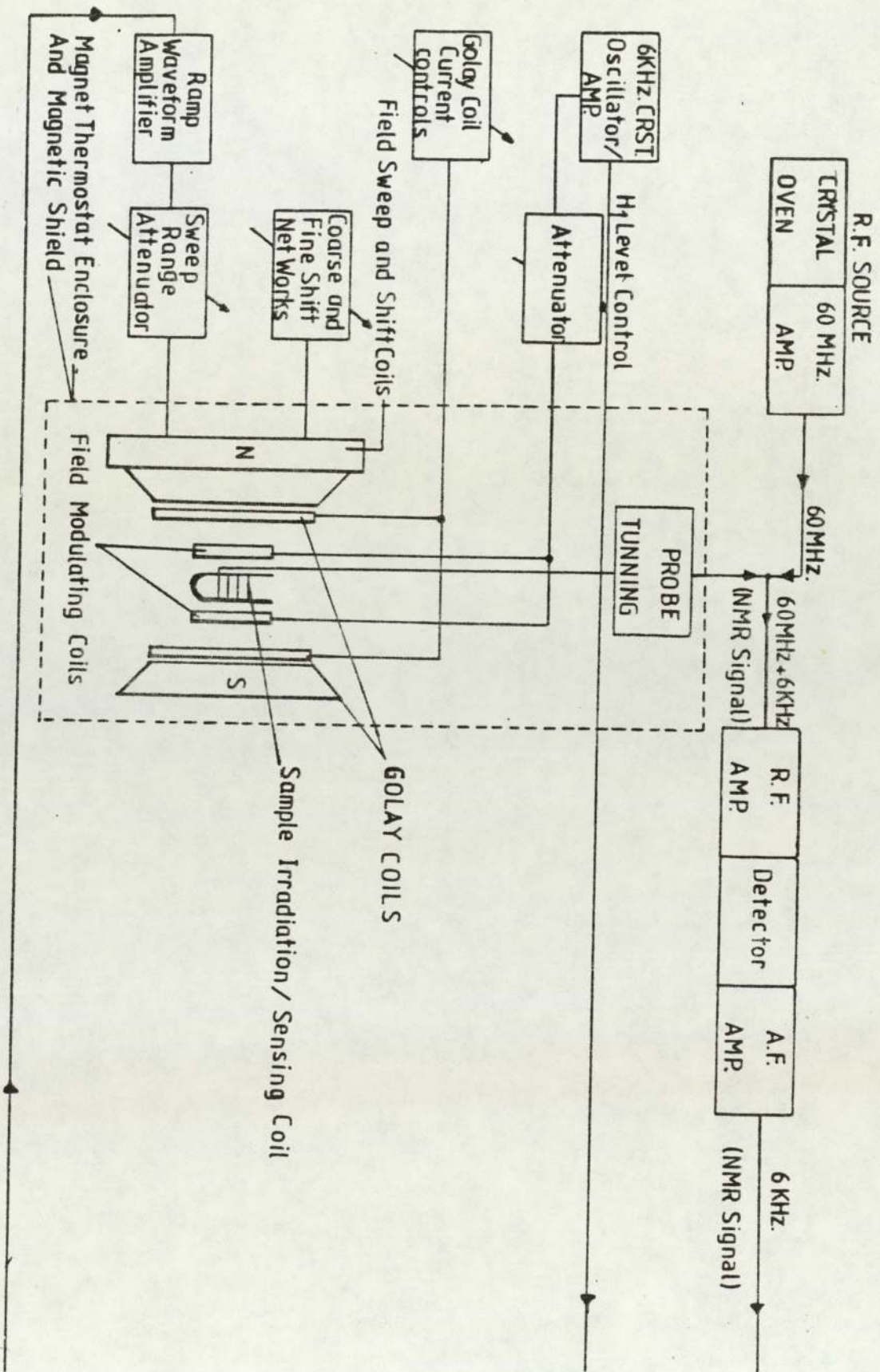
Figure 2.4   A Perkin-Elmer R 12 B NMR Spectrometer Block Diagram.
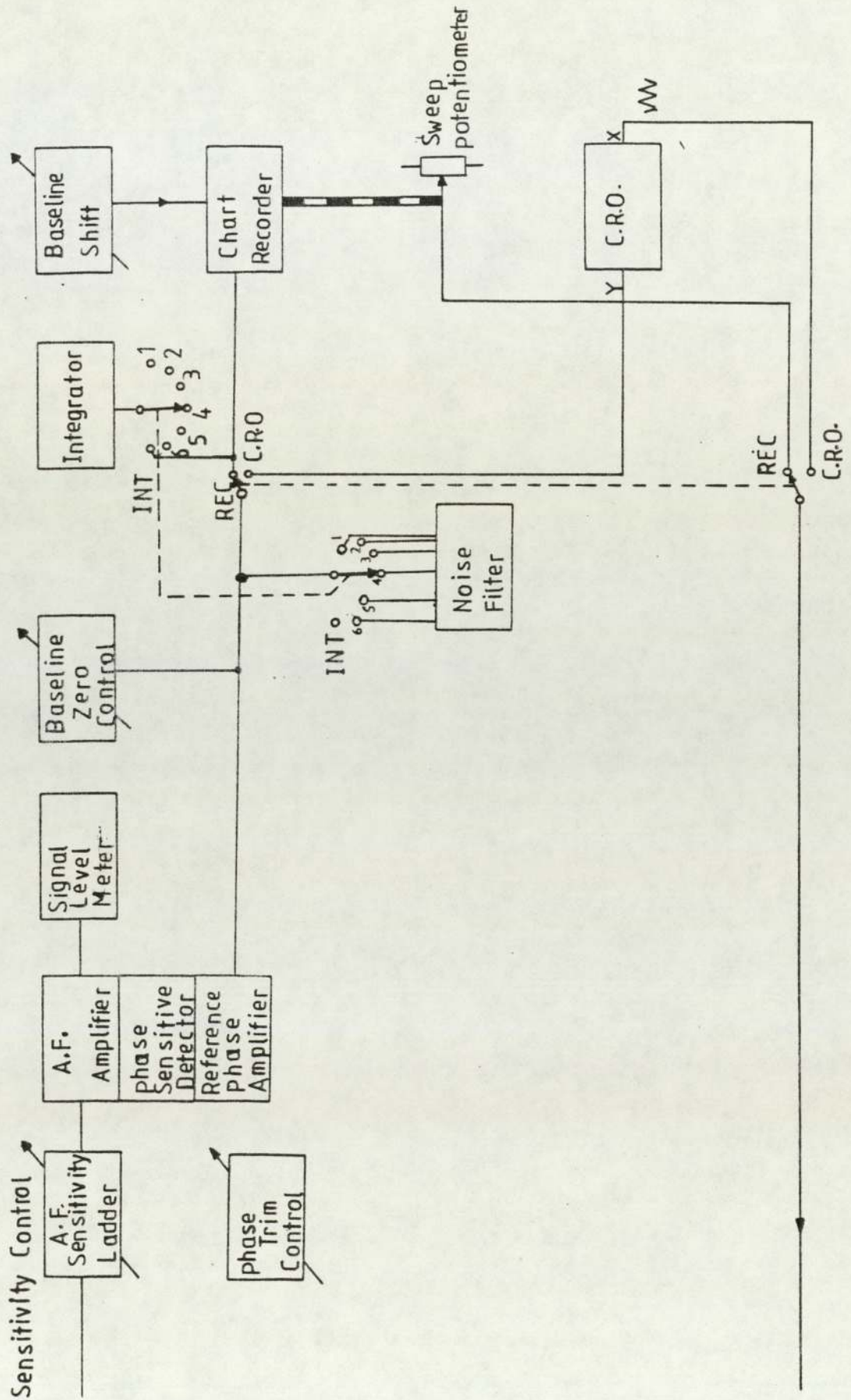
of 2 parts in 10^9 per hour. A 6 KHz signal, also derived from a crystal-controlled oscillator, is applied to coils orthogonally located relative to the probe radiofrequency coil and aligned with the magnet axis, so that the magnetic field in the sample region is audiofrequency modulated.

At resonance the sample acts as a mixing device, and NMR sidebands are produced at field strengths corresponding to 59.994 and 60.006 MHz. Each sideband, when stimulated, induces in the probe a 60 MHz radiofrequency response, amplitude-modulated at 6 KHz, the modulation containing information about the NMR signal. The probe output is applied to a radiofrequency amplifier, located in the double resonance accessary, when fitted, the output of which is detected to obtain the 6 KHz signal. This signal is amplified and compared with a reference signal of adjustable phase, so the V-mode or U-mode component of the 60.006 MHz sideband may be selected as required for observation or recording. The NMR signal may be filtered, integrated if necessary, and then presented.

2.4 **F.T. NMR SPECTROSCOPY**:

2.4:1   **Introduction**:

Pulse F.T. spectrometers are characterized by their ability to provide information in a much shorter time than c.w spectrometers.

Basically, if a radiofrequency signal produces a field B_1 by pulsing for a very short time, tp. The equilibrium magnetization of the sample, M_O, is rotated from the direction of B_O by an angle θ radians according to:

$$\theta = \gamma \ B_1 \ tp \ \dots\dots\dots\dots\dots\dots\dots\dots\dots\dots\dots\dots \ (2.2)$$

The pulse time tp is usually of the order of microseconds.

The radiofrequency pulse envelope may be described as a square wave (Fig 2.5c) with many components covering a relatively wide range of frequency Δv . This allows all nuclei with their Larmore frequencies within Δv to be stimulated and resonate. Essentially, therefore, the short r.f pulse is equivalent to all of the frequencies that would have to be produced by many transmitters producing frequencies distributed over the spectral range required.

If a $\frac{\pi}{2}$ pulse is applied along the x-axis in the frame rotating at the r.f (Fig 2.5a), M, lies entirely along the y-axis. Since the detector coil is usually arranged to detect signals in the (xy) plane, the magnitude of Mxy determines the strength of the observed signal. The nuclear signal is detected after the pulse is switched off as the free induction signal (FID), so-called because the nuclei process freely and lose phase coherence without the applied r.f (Fig 2.5 b and d).

The decay component of the perturbed magnetization in the xy
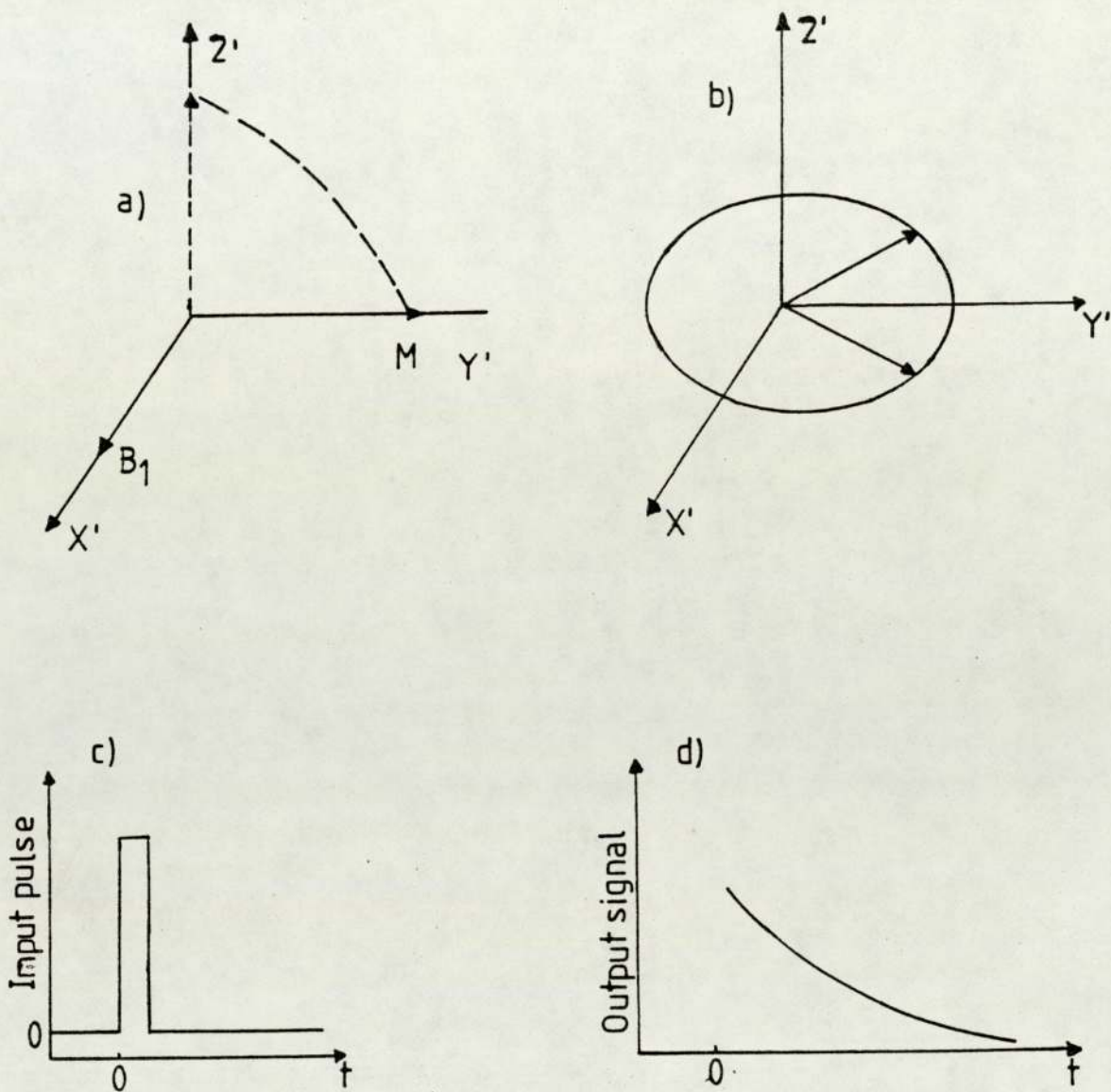
Figure 2.5   A representation of the FID.

a) 90° pulse along x' rotates M to the y' axis.
b) Mxy decreases.
c) Input r.f pulse.
d) Free induction decay signal FID corresponding
    to b).

plane, is thus detected as the FID. The latter is sampled for a characteristic time and stored in the computer required for FT NMR. Successive FID's may be added to the computer to improve the signal to noise ratio and finally the resultant FID is subjected to Fourier Transformation to produce a conversional frequency domain spectrum. Ideally pulse sequences should not be repeated within less that $5T$, after the last sequence, so that the nuclei can return to equilibrium before the next pulse.

If a $\frac{\pi}{2}$ pulse is applied and B_o is perfectly homogeneous, the magnetization should decay with a time constant T_2 (Fig 2.5 d). Infact,.however, Mxy decays in a time T_2^* because of field inhomogeneity, that causes nuclei in different part of the field to precess at slightly different frequencies, due to their different chemical shifts and/or spin-spin coupling. T_2^* is given by:

$$\frac{1}{T_2^*} = \frac{1}{T_2} + \frac{\gamma}{2} \Delta B_o \quad \dots\dots\dots\dots\dots\dots\dots (2.3)$$

where ΔB_o is the field inhomogeneity.

For a sample with nuclei equivalent chemically and magnetically a simple FID is obtained which after transformation yield a single absorption line. When the sample contains magnetically distinct nuclei, a more complex FID is obtained that may appear as a regular beat pattern. The Fourier Transform of the latter gives an NMR spectrum composed of several lines.

2.4:2   The Basic Components Of F.T NMR Spectrometers:

Although C.W and F.T spectrometers have similarities, they do have characteristic differences.   Figure 2.6 is a schematic representation of the basic components of an F.T spectrometer.

The short powerful r.f pulse, needed for an F.T spectrometer, necessitates a high power transmitter to produce B_1 in the range of 0.01 - 0.04 Tesla at the sample, thus can stimulate the whole resonance spectrum.   Consequently, the pulse NMR receiver must be able to handle larger voltages and recover very quickly, inorder to detect the FID signal without interference.

Beside the requirements referred to above, Fourier transform spectrometers have essentially similar basic units to those in C.W spectrometers; the main differences being that the transmitter and receiver circuits are adopted for pulsed operation.   In addition, there are several supplementary units such as a pulse programmer and a system for acquiring and processing the data.

The basic components of F.T spectrometer (Fig 2.6) will be discussed now:-

2.4:2.1   The Pulse Programmer:

The pulse programmer controls when, for how long and for which channel the r.f gate will be opened.   The output of the r.f transmitter is interrupted by a sequence of pulses.   If it is a
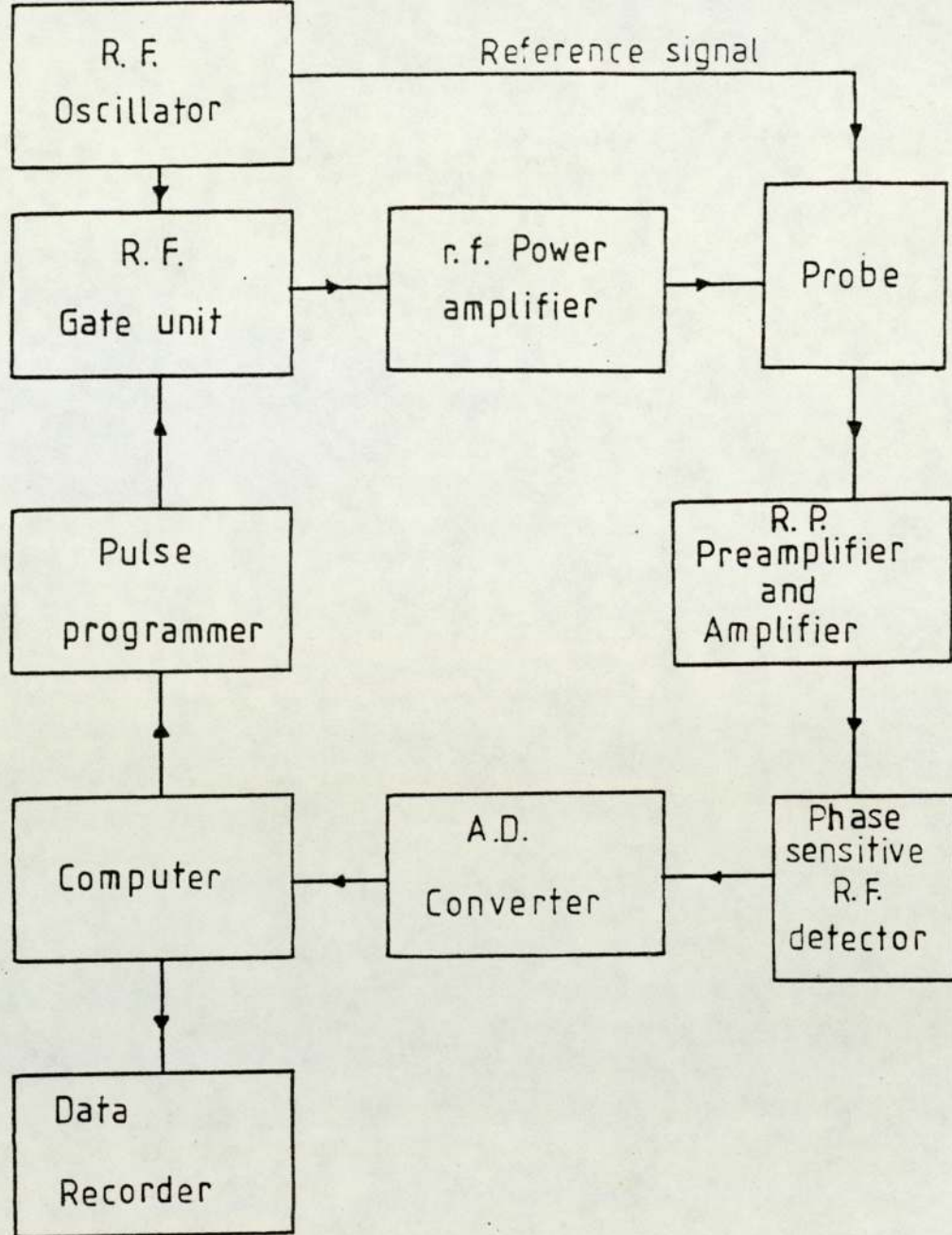
Figure 2.6   Basic components of FT NMR spectrometer.

periodic single pulse of width tp, it can be compared to the sweep field in order to detect the absorption signal in C.W NMR operations. More complex sequences of two or more pulses are used for getting more information, for example in order to measure relaxation times.

2.4:2.2   **The R.F. Gate Unit:**

The r.f output channel is provided with a gating device, which can be switched on and off, so that the r.f is applied to the probe in pulses. The timing of the pulse generator is determined by digital programming. The r.f gate is used to drive the transmitter which contains a very stable quartz crystal oscillator and usually the r.f switch which is "on" in the presence of a dc pulse signal from the pulse programmer and in the "off" position otherwise [56].

2.4:2.3   **The R.F Power Amplifier:**

The value of the r.f magnetic field B_1 used with F.T spectrometers has to be high inorder to ensure sufficiently uniform distribution of r.f power across the spectrum.

The r.f power required for pulse spectroscopy is higher that needed for c.w NMR spectroscopy; typically 100 watts is needed for F.T NMR compared with 1 watt for a c.w instrument. After the pulse less than 10^{-9} of the output power is radiated, so that the

67

interferogram can be obtained by the receiver without perturbation.

2.4:2.4   **The Probe**

Beside the requirements for the probe used in the c.w spectrometer, F.T technique necessates that the probe has the following characteristics:

1 - It must be able to handle the large r.f voltage present while the pulse is on.

2 - It must recover rapidly from the powerful pulse.

3 - It should quickly receive and process the weak nuclear signals following the pulses.

4 - In addition, in some cases, it must continuously deliver noise modulated or coherent decoupling power to the sample at a second r.f frequency without interfering with the processing of the FID signal.

5 - It must have facilities for essentially locking the magnetic field strength to the pulsed NMR frequency. This is usually achieved using a separate c.w r.f signal that enables locking to a heteronucleus.

6 - Moreover, the probe should have spinning facilities and

68

a temperature detector necessary for conducting variable temperature studies.

2.4:2.5   **The Receiver**

The main two characteristics of the receiver within an F.T spectrometer are; first, that it should recover very quickly from any overloads generated by the application of the r.f pulse. Second, the receiver and the transmitter should be well isolated from one another in order to achieve minimum overload conditions and the fastest recovery time [58].

The receiver follows a preamplifier. The preamplifier should have a low noise figure, a fast recovery time from overloads and a modest gain. Both preamplifier and receiver should have linear response over a wide range [59].

The nuclear signal enters the receiver (r.f detector) as a band of radiofrequencies near the basic transmitter frequency, during the free precession period after the pulse. Passing the signal through a phase detector results in a series of audiofrequencies which are filtered by being fed through a low pass filter with a band width usually just equal to the chosen spectral width. The r.f carrier has to be positioned so that all the audiofrequencies have the same sign, because the signal phase detection does not allow distinction between positive and negative frequencies. If the r.f carrier is placed at the end of the

spectrum and the set spectral width is larger than the chemical shift range, the frequencies can be digitized unambiguously. However, if the spectral width is set to a value smaller than the chemical shift range, some of the frequencies corresponding to lines at the one end of the spectrum can be folded. This effect is avoided by using an experimental technique called quadrature detection. This employs two phase sensitive detectors to distinguish between high and low field frequencies; for this the r.f carrier frequency should be placed in the middle of the spectrum.

2.4:2.6   **The Analogue To Digital Converter (A.D.C.)**

The detected FID is an analogue signal and because this has to be stored and processed by the spectrometer computer, it is necessary to digitize the signal. An analogue to digital converter is used for this purpose. This analogue to digital converter samples the face induction decay at regular time intervals and converts each voltage measured to a binary number that can be stored in the corresponding memory location of the computer.

The rate at which a spectrum of width ΔF must be collected by the A.D.C. is twice the spectral width $2\Delta F$. Inorder to avoid line shape distortions, the FID should be sampled until its amplitude has fallen off to zero. As long as the signal is sampled over a period of time T seconds, this defines a total of $2\Delta FT$ sampling points. Since each point is stored, a memory of N

70

words is needed ($N = 2 \Delta FT$) where T is the acquisition time and is related to the digital resolution of the instrument.

The dynamic range of the signals that are to be digitized is a critical parameter when weak signals have to be detected in the presence of strong signals. When the interferogram is displayed on the screen of the oscilloscope, the minicomputer represents the maximum peak to peak amplitude by a number close to 2^{12}. Then if the largest signal detected has the intensity Hs, the smallest signal which can be recorded will have an intensity, Hw such that:

$$\frac{Hs}{Hw} = 2^{12}$$

This ratio is called the dynamic range of spectrum.

For an A.D.C. of 12 bytes is normally measured in steps of $10 /(2^{12} - 1) = 2.44$ mV, if the voltage range is $\pm$ 10 volts. This means that all signals which correspond to a potential lower than 2.44 mV will not be read by the converter.

2.4:2.7 **The Computer:**

The mathematical requirements of F.T NMR necessitate the resistance of a computer. The computer is generally used for three types of mathematical manipulations of data:

1 - Data acquisition and coherent addition of repeated
signals to improve the signal to noise ratio.

2 - To carry out the Fourier transformation.

3 - During the whole process between the above mentioned
steps, or after them many other types of data processing
have to be carried out by the computer eg. setting of
frequencies display conditions etc.

A computer usually consists of input and output units,
control, storage and arithmetic units. It controls the
transmitter and receiver functions, stores and processes the FID
and transfers the results to display units viz oscilloscope or the
recorder. The minicomputer is characterized by two essential
parameters that define its storage capacity. These are the number
of memory location and the word length. Memory locations are
counted in multiples of K; which stands for $2^{10} = 1024$.

According to the requirements of F.T spectrometer, a computer
with 12K memory is the minimum requirement for pulsed NMR. The
word length determines the amount of data or their magnitude that
can be stored in each memory location. The information is stored
in binary form. In general, for n bytes the largest possible
decimal number that can be represented is 2^{n-1}. Therefore, it is
very important to have large values of n, eg. n = 12 inorder to
detect small signals.

When collecting the FID, each pulse has the same characteristics. Any change in the field homogeneity will cause observed peak shapes to change on different passes, damaging the final spectrum. This problem can be overcome by the computer. In one approach, the height of an absorption peak of the reference compound (lock signal) is monitored. With field homogeneity optimized, the peaks show a maximum height. Any change from the optimal condition is detected. The error signal is then used to control the shim current and return the field to the optimum value.

2.4:3   **The JEOL FX 90 Q F.T NMR Spectrometer:**

A JEOL FX 90 Q F.T NMR spectrometer was one of the instruments used in carrying out the work reported in this thesis. The spectrometer can be used to detect all NMR active nuclei in five different ranges of frequencies [60]. This pulsed F.T NMR spectrometer permits the observation of proton resonance at a frequency of 89.6 MHz and ^{13}C at 22.5 MHz.

The instrument uses a tunable 10mm probe that is optimized for the observation of ^{13}C resonances for which the instrument specifications are quoted. When studying ^{1}H the performance is not guaranteed unless a dedicated $^{13}C - ^{1}H$ probe is employed. This was not available for the present work.

This system has unique facilities in the form of, digital

73

quadrature detection (D.Q.D.), light pen control system (L.P.C.S.) and autostacking software. Also the system has a computer having a memory of 24K words where 8K words are used for the programme and 16K words for the data.

Fig 2.7 shows the basic units in the FX 90 Q spectrometer. The specific components will be discussed now.

2.4:3.1 **The Magnet System:**

The instrument is provided with an electromagnet, fed by a voltage and current regulated power supply system, that produces a magnetic field of 2.11 Tesla. The magnet is accommodated in a compact console to help maintain it at constant temperature. The magnetic field homogeneity is controlled conventionally using Golay shim coils mounted on the probe between the pole pieces. The instrument is capable of producing a ^{13}C line width of less than 0.3 Hz. In the long term this may degrade and result in line broadening, although the magnetic field stability is 0.1 Hz per hour. This degradation may be corrected particularly by using an autoshim unit which corrects small field drifts in the y-direction.

It should be noted that during the early stages of this work, significant problems were encountered with maintaining resolution over a period of time exceeding 15 minutes. This was particularly evident when conducting ^{1}H studies. The fault was attributed in the author's laboratory to very low lock loop gain which resulted
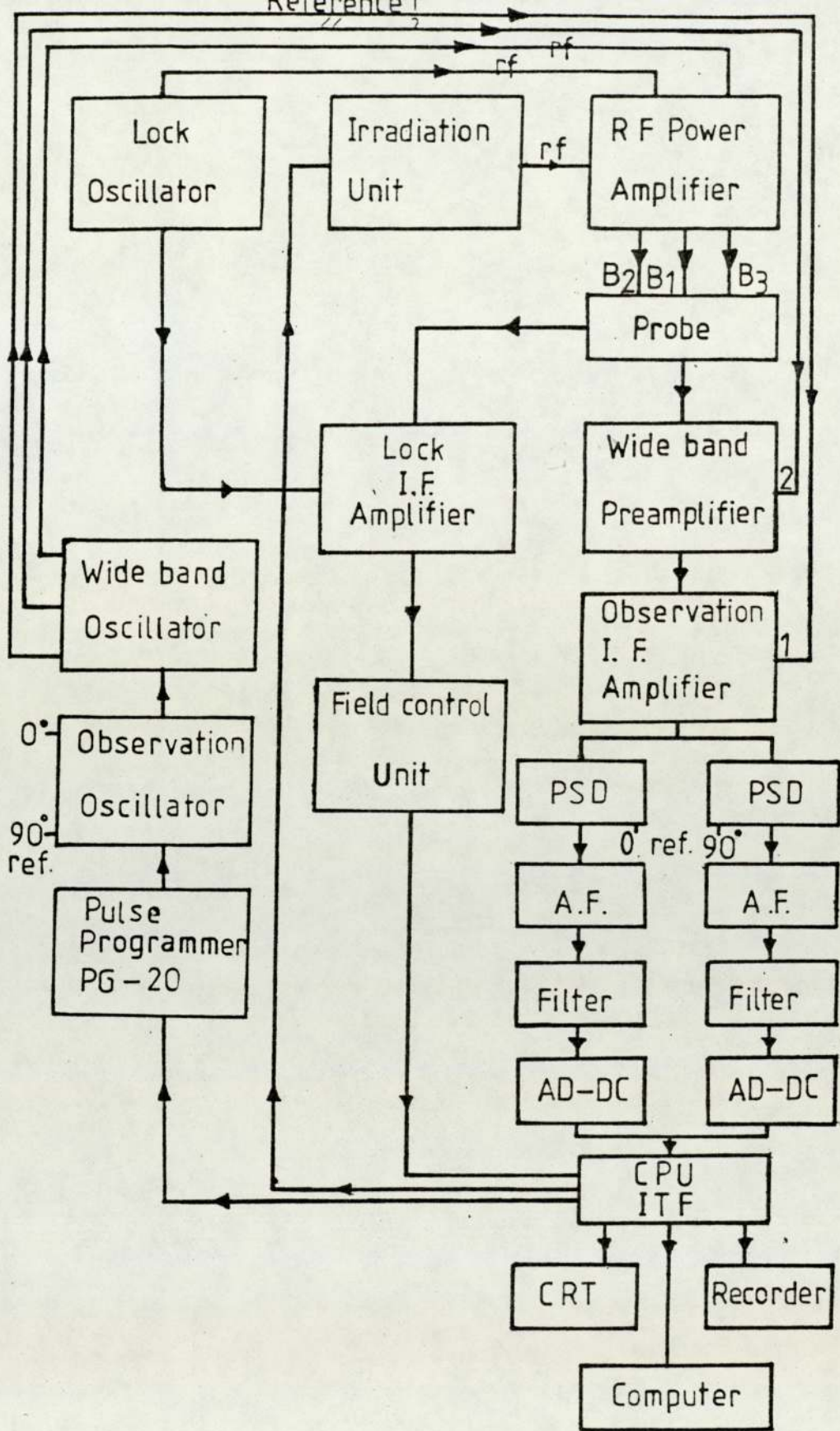
Figure 2.7   Schematic representation of the basic units in the
              JEOL FX 90 Q spectrometer.

in superimposition of shifted spectra that appeared to result in poor resolultion. The manufacturers ignored this suggestion and replaced the magnet with no significant improvement. Ultimately, they improved the lock loop and the "resolution" was satisfactory. This process took considerable time and consequently the experimental work presented herein was subject to appreciable delay.

2.4:3.2 **Transmitter, Receiver And Data System:**

The transmitter system has three channels manifest in observation, irradiation and lock oscillator units which have a reference frequency of 44 MHz supplied by a master clock unit. The observation oscillator has a 4-phase generator which is used to generate the OFFSET components of the OBS RF output. A PG 20 pulse programmer operates the gate of the oscillator, generating the desired R.F pulse sequence up to 2 pulses only. Two I.F reference signals at 0 and $\pi/2$ out of phase are passed to the OBSIF amplifier unit to be used in the D.Q.D. system. The frequency signal is then adjusted to the selected nucleus at the wide band local oscillator unit. Then the R.F is amplified in the R.F power amplifier unit. When the R.F signal reaches the probe, the sample absorbs most of the energy generated at the transmitter coil.

The F.I.D., occuring after the R.F pulse, is detected by the receiver coil and amplified in a wideband preamplified unit, where

a reference signal from the wideband local oscillator unit is used to reduce the signal level when they are mixed. Another amplification and frequency reduction occurs at the OBSIF amplifier where further 0 and $\pi/2$ reference signals from the OBS OSC unit are used to get the audiofrequencies 0 and $\pi/2$ out of phase. It is obvious now that the detection system has two phase sensitive detectors (P.S.D.) rather than one; these are required in the digital quadrature detection D.Q.D. technique.

The D.Q.D. system allows the F.T measurements to be carried out with the excitation pulse placed in the centre of the observation width. This reduces the observation band width to only half that required for signal phase detection (S.P.D.) resulting in $\sqrt{2}$ fold improvement of the signal to noise ratio. Consequently, as long as the r.f pulse is delivered at the centre of the spectrum, the efficiency of the r.f power is enhanced 4 times compared with the S.P.D., which helps to obtain more accurate information.

The AD-DA Unit receives filtered analogue signals which are converted to digital form. Then they are transferred via C.P.U. (controller) to the computer where the information is stored. When it is required, the FID is transferred to get the spectrum signal in digital form. The DA Unit changes the information to analogue signals which can be recorded or displayed on the oscilloscope screen.

The operator can deal with the FX 90 Q instrument and the computer using the light pen unit. By pointing to a particular function or command on the screen, the order is transferred to establish a link between the computer and the spectrometer units controlling its operations.

The lock in the FX 90 Q spectrometer can be obtained as in any c.w spectrometer. The LOCK oscillator unit produces an r.f signal at the appropriate resonance frequency which is amplified in the R.F power amplifier. The field control unit produces a sawtooth signal which modulates the magnetic field and allows the observation of the lock resonance signal and this is phase sensitive detected at the LOCK I.F. amplifier unit, which receives a reference signal from the LOCK OSC Unit. Beside being used for lock the signal is also used for rapid resolution adjustment ^{2}D and ^{7}Li be used for locking purpose and selected by simple switching.

For double irradiation purposes the r.f irradiation oscillator units can be selected according to the experiment: noise irradiation and coherent R.F power. For both cases the irradiation r.f is amplified, but at different levels that are controlled by the irradiation selector unit which is linked to the R.F power amplifier.

The noise irradiation modulation width can be selected to be 0.5, 1, 2.5 and 5 KHz. For ^{13}C detection on irradiation of 1 KHz is used normally for proton irradiation.

2.4:3.3 **The Probe**

The probe placed between the pole pieces of the magnet, has several modules:

1. The permabody which is fixed. It accommodates replaceable modules eg. the insert, which are housed in a double wall dewar for variable temperature experiments. On the permabody probe, irradiation coils and thermocouples are mounted. Spinning photosenser facilities are placed on the top to detect the spinning rate. Current shim broads are attached on both sides of the permabody.

2. The r.f tunable module which facilitates the selection of the nuclei. It has five ranges of frequencies, corresponding to five channels, and a five tuner for optimizing the sensitivity for a given nucleus.

3. The irradiation module which enables the tuning of the irradiation circuit to use most of the energy in the irradiation coil and produce maximum field.

4. The sample insert which is exchangeable for different sample tube sizes and holds the sample coil and LOCK coil wound around the glass tube.

2.4:3.4   **Autostacking Program:**

The computer JEC - 980B, in the JEOL 90 Q spectrometer, has a memory of 24K words. The program is stored in 8K words memory, the other 16K words of memory are used for the data. The different operations that can be done by the computer are stored in the autostacking program.

The autostacking program contains the following programs:

1 - Normal Program

2 - Stacking Program

3 - Analysis Program.

Throughout the work reported in this thesis, the normal program was the only one used and the basic facilities of this only will now be described.

The Normal Program is used for routine measurement. The light pen is used to select any of the several command pattern included in it. The basic operation requires the setting of the pulse width, pulse mode, pulse repetition, frequency range, observation frequency, irradiation mode, irradiation frequency and OBSET which has to be placed at the centre of the spectrum. The number of scans necessary to obtain good spectra can also be selected.

Following the accumalation of the FID, various mathematical parameters are selected to produce the final spectra. Finally the required data can be obtained in printed form from the computer or from a conversional spectrum.

THE VAN DER WAALS SCREENING CONSTANT σ_W

3.1 INTRODUCTION:

Recently Homer and Percival have developed a new reaction field treatment of gas-to-liquid shifts for isotropic molecules i.e. of σ_W. Their theory has three component parts. The first is based on an improved Onsager approach. The second part recognizes the deficiencies in the Onsager model that stem from ignoring the effects of near neighbour molecules. The third is a newly characterized "buffeting" contribution that arises only when solvent approaches to a solute resonant nucleus are stericaly hindered. The major emphasis of the present work are to find direct experimental justification of the second contribution and to develop the third contribution to permit the elucidation of molecular structure through studies in the liquid phase.

Before detailing the results of the present investigations it is important to review the work which has been already done in characterizing the van der Waals screening constant.

3.2 MODELS CHARACTERIZING σ_w:

Essentially there have been three models proposed to characterize σ_w viz:

1. The Gas Phase Model
2. The Cage Model
3. The Continuum Model.

3.2:1 The Gas Phase Model:

The gas theory [30, 61] basically depends on the characterization of bimolecular interactions and the calculation of two centre potential energies. Whilst it is tempting to extend this approach to liquids, it is unrealistic to consider that such a basis could be applicable to the liquid phase, because of the relatively small molecular separations involved that must result in simultaneous interactions between several molecules. Obviously multimolecular interactions would have to be considered. From an energetic standpoint, this could be done by considering these as an average sum of several nonequivalent biomolecular interactions. Nevertheless, the potential difficulties with such an approach suggest that it would be unprofitable.

3.2:2   **The Cage Model:**

This model [62] considers only the first solvent shell around a given solute molecule. The average effect of one solvent molecule on the nuclear screening of the solute has to be characterized and summed over a number of solvent molecules around the solute molecule in the first shell. Again it is possible to anticipate difficulties with this approach although some workers eg. Homer and Redhead[106] have achieved some success with it when calculating σa.

Both the gas phase and the Cage models were developed significantly by Rummens [61], but undoubtedly underestimate the extensive properties of the solvent molecules in the bulk liquid.

3.2:3   **The Continuum Model:**

This model [62,63] which has certain appeal, treats the solute molecule as being a single point species at the centre of a cavity surrounded by a continuum representing the solvent. This approach probably affords a better representation of the liquid phase than the two models previously described, although it is demonstratably inadequate in accounting for σ_w.

Homer and Percival have used it as the basis for the most recent attempt to characterize physical properties of matter that depend entirely on inter-molecular van der Waals forces.

84

3.3 THE CONTINUUM MODEL APPLIED TO σ_w;
ITS DEVELOPMENT AND EXTENSION:

Following Onsager [62], any treatment of σ_w on a continuum basis requires that one solute molecule is singled out and treated as being a point species at the centre of a cavity surrounded by a homogeneous continuum representing the solvent medium. In his work on electric dipole moments of molecules in liquids, Onsager specifically treated polar molecules but implied that there should be no real difference between this approach and that of non-polar molecules; the approach should therefore be suitable for the characterization of van der Waals forces. Following Onsager many workers have attempted to characterize σ_w on a continuum basis [35,65,66,67] eg. Haward and Linder, used the generally accepted equation for σ_w:

$$\sigma_w = -B \langle R^2_1 \rangle \quad\dots\dots\dots\dots\dots\dots\dots\dots\dots\dots\dots \quad (3.1)$$

where $\langle R^2_1 \rangle$ is the mean square reaction field in the solute cavity, and B is the screening coefficient. Other workers [68,69] e.g. Lumbroso and Fontaine, have used the continuum theory to correct observed shifts in polar systems and obtain information about linear electric field effects on nuclear screening.

Equation 3.1 provides a test of the validity of different equations proposed for calculating σ_w. Using equation 1.59, which shows that susceptibility corrected gas-to-solution chemical

shifts give the van der Waals dispersion force contribution to the screening constant, a plot of gas-to-solution chemical shifts against $< R^2_1 >$ (which may generally be defined in terms of refractive indicies as $f(n_1, n_2)$) should produce a straight line passing through the origin. Indeed the general trend of plots of this type produced by many workers do show a straight line regression with slopes generally similar to expected values of B but they do not pass through the origin [29]. This indicates that the formulaes used for calculating $< R^2 >$ are not correct, and/or there could be a term missing from equation 3.1 that would account for the y-intercepts.

The most consistent explanation of the variation of σ_w for a given solute with solvent properties was published by De Montgolfier [70,71,72,73]. He concluded that σ_w can be characterized by the following equation:

$$\sigma_w = -6 \left[\frac{(n_2^2 - 1)}{(2n_2^2 + 1)(n_2^2 + 2)} \right]_{\text{solution}} \left[\frac{k_1 \ B \ \Delta E_1}{\alpha_1} \right]_{\text{solute}} \ldots\ldots\ldots (3.2)$$

where n_2 is the refractive index of the solvent, ΔE_1 is a complex transition energy of the solute molecule, α_1 is the mean polarizibility of the solute molecule, and k_1 is a site factor depends on the geometry of the solute molecule.

De Montgolfier ideas were reconsidered by Rummens [74,75,76,77], who rejected the site factor k_1 as having no place

in the continuum model. Nevertheless, Rummens later reintroduced another site factor and formulated the following quite widely accepted continuum equation:

$$\sigma_W = \frac{-6\ k_1\ B\ \alpha_1\ I_1}{a_1^6} \cdot \frac{n_2^2 - 1}{(2n_2^2 + 1)^2}\ S \quad \dots\dots\dots\dots\dots\dots\dots (3.3)$$

where S is the Rummens site factor that he introduced to account for the intercept found in the regression of σ_W against $f(n_1, n_2)$, I_1 is the ionization energy of the solute molecules, a_1 is the solute cavity radius and K is the reaction field solute factor constant.

Rummens took the correctly defined site factor for a pair of molecules in the gas phase, S pair [78,79] and transposed this to the liquid phase. The site factor for a pair of molecules is given by:

$$S\ pair\ =\ \frac{1 + q^2}{(1 - q^2)^4} \quad \dots\dots\dots\dots\dots\dots\dots\dots\dots\dots\dots (3.4)$$

where $q = d/r$, with d being the distance of the resonant nucleus from the centre of mass of the solute molecule, and r the distance between the centres of masses of the solute and solvent molecules.

Rummens derivation of his site factor has been critized by

Homer and Percival [64] who also demonstrated that it did not, in fact, improve the regression of σ_w on $f(n_1, n_2)$, i.e. an intercept remained. They have reformulated the site factor, which they in fact also think irrelevant, as:

$$S \text{ cont.} = \frac{5}{6} \left[\frac{1 + q^2}{(1 - q^2)^3} + \frac{(3 - 2q^2)}{3q^4 (1 - q^2)} \right]$$

$$+ \frac{5}{8q^5} \quad \text{In} \quad \left[\frac{1 - q}{1 + q} \right] \quad \dots\dots\dots\dots\dots\dots\dots\dots\dots\dots (3.5)$$

As might be expected they demonstrated that this improved site factor was unable to complete the characterization of σ_w; nevertheless, Homer's site factor did improve the correlation of σ_w against $f(n_1, n_2)$ as shown in Table 3.1 for group IV B tetramethyl systems. Albeit this correlation still gave a straight line with finite intercept.

Earlier than his improvement on the site factor, Homer [29] had concluded, from the literature and his own extensive work concerning chemical shifts due to intermolecular interactions, that there are major inadequacies in calculating σ_w. In a major review he noted:

"Superficially, it appears that little more than quantitative agreement between predicted and observed shifts is obtained. Indeed the general trend in the plots (of calculated parameters against the appropriate gas-to-solution shifts

88

SOLUTE*	CORRELATION COEFFICIENT	INTERCEPT/ppm
CMe_4	0.885	0.100
$SiME_4$	0.923	0.135
$GeMe_4$	0.918	0.134
$SnMe_4$	0.930	0.148
$PbMe_4$	0.936	0.152

* at infinite dilution in all five group IVB tetramethyl solvents

Regression Analyses of $-\sigma_W$ (expt) at $30^{\circ}C_{DM}(n_2^2 - 1)^2 / (2n_2^2 + 1)^2$

For The Group IVB Tetramethyl Systems.

Table 3.1

together with a theoretical line of slope B = 1 x 10^{-18} esu) away from the origin might be taken to indicate shortcoming in the general approach".

Homer has suggested that the reason for the inadequacies in existing theories might lie with facts alluded to by Buckingham:

" . . . . . dispersion screenings, because these may be considered to arise from two separate effects. The first effect is due to the interaction between the solute and the solvent, in its equilibrium configuration, which causes the distortion of the electronic environment of the nucleus in the solute. The second is due to changes in the solvent equilibrium configuration, which leads to a "buffeting" of the solute and hence to a time dependent distortion of the electronic structure".

Essentially, this was the basis for Homer's recent theory for characterizing σ_w. This will be dealt with in the following sections.

3.4 <u>HOMER'S THEORY FOR CHARACTERIZING σ_w</u>:

Homer's intention was to complete the characterization of the van der Waals screening constant, which he saw to arise mainly from two sources. The first stems from interactions between solute and solvent molecules in their equilibrium situation. In

order to deal with this, Onsager-based reaction field theory was improved and extended. Even so, the results of this approach did not show complete characterization of σ_W and this led to the recognition of a second part. The second contribution comes from solvent-solute interactions in their non-equilibrium (continuum) situation. This was considered to arise from the unique effects of discrete pair-wise solvent-solute encounters. Homer characterized this by a buffeting interaction between the resonant nucleus in the solute molecule and the peripheral atoms of the solvent molecule.

Because van der Waals dispersion forces are additive, Homer has defined σ_W by:

$$\sigma_W = \sigma_{R.F} + \sigma_{BI} \dots\dots\dots\dots (3.6)$$

where $\sigma_{R.F}$ and σ_{BI} are the reaction field and the buffeting contributions to the screening, respectively.

3.4:1   **Improvement And Extension Of Reaction Field Theory:**

As Onsager's model and its improvements appeared to be inadequate, Homer and Percival's initial work was to extend the continuum approach. They considered the reaction field for transient dipoles in isotropic systems to be made up of two parts. The first is the classical reaction field or the primary reaction field that has been recognised before. The second arises from a further field stemming from the extra cavity reaction field of the

nearest neighbour solvent molecules. Both parts were dealt with on continuum basis. Therefore, the total mean square reaction field $< R^2_T >$ experienced by the solute molecule in a solvent will come from the sum of the primary reaction field contribution and the contribution of the extra cavity fields arising from the solvent molecules surrounding the solute.

The following sections will describe the two parts of $< R^2_T >$.

3.4:1.1   The Primary Reaction Field R_1:

The basic equation for calculating R_1 using Onsager's model (Fig 3.1) is represented by [62]:

$$R_1 = \frac{2 \ (\epsilon_2 - \epsilon_1)}{2 \cdot \epsilon_2 + \epsilon_1} \ \frac{\mu_1}{a_1^{\,3}} \quad \dots\dots\dots\dots\dots\dots\dots\dots\dots\dots \quad (3.7)$$

where ϵ_1 and ϵ_2 are the dielectric constants of the solute and the solvent respectively, μ_1 is the dipole moment of the solute and a_1 is the radius of the Onsager cavity.

The cavity, in Onsager's model, was treated as being evacuated, so that $\epsilon_1 = 1$ and equation 3.7 for R_1 becomes:
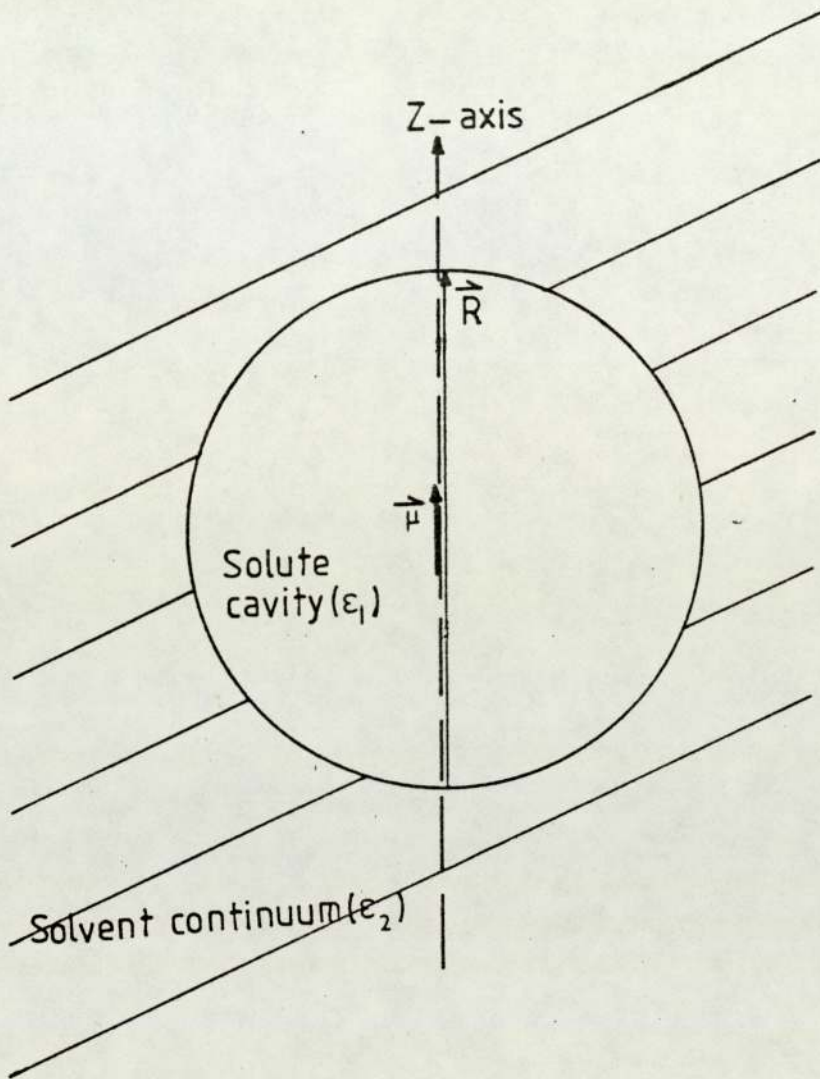
Figure 3.1   A representation of a solute cavity in the solvent
              continuum (Onsager type treatment).

$$R_1 = \frac{2(\epsilon_2 - 1)}{(2\epsilon_2 + 1)} \frac{\mu}{a^3} \quad \dots\dots\dots\dots\dots\dots\dots\dots\dots\dots\dots \quad (3.8)$$

where

$$g = \frac{2(\epsilon_2 - 1)}{(2\epsilon_2 + 1) a^3} \quad \dots\dots\dots\dots\dots\dots\dots\dots\dots\dots\dots \quad (3.9)$$

g is the reaction field factor

Therefore $R_1 = g\mu$ $\quad \dots\dots\dots\dots\dots\dots\dots\dots\dots\dots\dots\dots \quad (3.10)$

But, this reaction field, originating from the dipole moment μ, will induce further electric moments in the cavity that are proportional to the primary reaction field. Therefore, the true reaction field must be given by [64]:

$$R_1 = g\mu (1 - \alpha_1 g)^{-1} \quad \dots\dots\dots\dots\dots\dots\dots\dots\dots\dots \quad (3.11)$$

where α_1 is the solute molecule polarizibility. It was assumed that, although the above equation is strictly for a permanent dipole moment, it applied also to transient dipole moments; subsequently this has been shown theoretically by Sultan Mohammadi [99].

Since σ_w is related to the mean square reaction field $\langle R^2_1 \rangle$, the latter was given by:

$$\langle R^2_1 \rangle = g^2 (1 - \alpha g)^{-2} \mu^2 \quad \dots\dots\dots\dots\dots\dots\dots\dots \quad (3.12)$$

By substituting for g in the above equation and following the approximation that $\epsilon_2 = n^2_2$ for isotropic solvents, and employing

the expression [62]:

$$\frac{n_1^2 - 1}{n_1^2 + 2} = \frac{\alpha}{a^3} \quad \dots\dots\dots\dots\dots\dots\dots\dots\dots\dots \quad (3.13)$$

the mean square reaction field of a polarizable dipole was shown to be given by:

$$\langle R_1^2 \rangle = \left[\frac{8 \pi L}{9 V_m} \right]^2 \frac{(n_1^2 + 2)^2 (n_2^2 - 1)^2}{(2n_2^2 + n_1^2)^2} \mu_1^2 \quad \dots\dots\dots\dots \quad (3.14)$$

Where L is Avogadro's Number and Vm is the molar volume of the solute.

The derivation of that equation is necessarily based on an oversimplified model because in reality a molecule is not a point as assumed, and there is no such thing as a microscopically indivisible continuum; also no account was taken of fields produced by higher electric moments of the solute molecule.

Homer demonstrated that equation 3.14 did not account completely for the reaction field and this led him to recognize the so-called extra cavity reaction field.

3.4:1.2   **The Extra Cavity, Secondary Reaction Field Of The Solvent R_2:**

Homer and Percival [64] treated the nearest neighbour solvent molecules by accounting for the effect of their reaction fields, recognized as R_2. With R_1 this makes up the total reaction field effecting the solute molecule in Onsager's cavity.

The primary reaction field R_1 produces a uniform polarization of the cavity through the potential arising from the charge distribution on the cavity wall. The reaction field is continuous in the solvent medium, but its effect decreases rapidly with the separation from the cavity centre.

Homer and Percival's method for calculating $< R^2_2 >$ depends on considering two cavities 1 and 2 (Figure 3.2) in the continuum. When the two cavities are well separated from each other, R_1 does not effect cavity 2 and R_2 does not effect cavity 1. However, when the two cavities are close to each other, the reaction field of each molecule will effect the other one.

In the case of an infinitely dilute solute 1 in solvent 2, the central solute molecule 1 will always be surrounded by solvent molecules 2. Consequently, the solute molecule will experience the reaction field arising from its own transient dipole, and additionally the sum of the extra cavity reaction fields due to the surrounding solvent molecules.

It was assumed that the number of the solvent molecules that
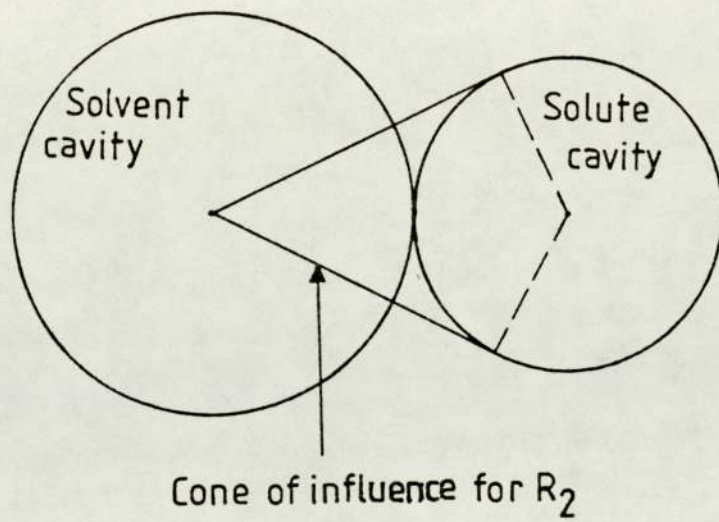
Figure 3.2   Cone of influence for R_2 with a solute and
              solvent cavities in contact.

can surround the solute molecule is Z_2, and the number of the solute molecules that may surround the solvent molecule is Z_1.

Homer has shown that the additional secondary mean square field experienced by the solute molecule is $2 (Z_2/Z_1) < R^2_2 >$.

The total mean square reaction field experienced by the solute molecule is thus:

$$< R^2_T > = < R^2_1 > + 2 \left(\frac{Z_2}{Z_1} \right) < R^2_2 > \quad \dots\dots\dots\dots\dots\dots\dots \quad (3.15)$$

Using the formula for the close packing of sphere, Z can be presented by:

$$Z_1 = \frac{(r_1 + r_2)^2}{r_1^2} \pi \quad \dots\dots\dots\dots\dots\dots\dots\dots\dots\dots\dots \quad (3.16)$$

where r_1 and r_2 are the radii of the solute and the solvent molecules, respectively. Consequently, equation 3.15 can be rewritten as:

$$< R^2_T > = < R^2_1 > + 2 \left(\frac{r_1}{r_2} \right)^2 R^2_2 \quad \dots\dots\dots\dots\dots\dots\dots\dots \quad (3.17)$$

$< R^2_2 >$ was formulated by an approach analogue to that for $< R^2_1 >$. The final equation for the total mean square reaction field is:

98

$$\langle R_T^2 \rangle = \left(\frac{8\pi}{9}\right)^2 \frac{\mu_1}{V_1^2} \frac{(n_1^2 + 2)^2 (n_2^2 - 1)^2}{(2n_2^2 + n_1^2)^2} +$$

$$2\left(\frac{r_1}{r_2}\right)^2 \frac{\mu_2^2}{V_2^2} \frac{(n_2^2 + 2)^2 (n_2^2 - 1)^2}{9n_2^4} \quad \ldots\ldots\ldots\ldots\ldots (3.18)$$

Based on London's [85,86] treatment of a quantum mechanical oscillator, the required dipole moments can be expressed by:

$$\mu = 3 \alpha I \quad \ldots\ldots\ldots\ldots\ldots\ldots\ldots\ldots\ldots\ldots\ldots\ldots\ldots\ldots (3.19)$$

where α is the polarizibility of the molecule and I is the ionization potential.

The reaction field contribution to the nuclear screening constant $\sigma_{R.F}$ can now be expressed as:

$$\sigma_{R.F} = - B \langle R_T^2 \rangle \quad \ldots\ldots\ldots\ldots\ldots\ldots\ldots\ldots\ldots\ldots\ldots\ldots (3.20)$$

where B is the nuclear screening coefficient which depends on the nature of the nucleus and the chemical bonds to it.

Homer and Percival tested the validity of equation 3.18 by correlating the gas-to-solution chemical shifts for protons in the group IV B tetramethyls (as solute and solvent) against the calculated $\langle R_T^2 \rangle$ for each system using equation 3.18. The regressions were linear with correlation coefficients close to

unity and slopes in good agreement with the theoretical value of B (Table 3.2). However, it can be seen from Table 3.2 that all the straight lines did not pass through the origin. This was taken to mean that equation 3.18 presents an incomplete description of van der Waals forces effecting the molecules. This fact led Homer to recognize his buffeting theory which will be dealt with in the following section.

3.4:2   **Buffeting Theory:**

Homer and Percival [64] characterized and recognized the buffeting interaction between the solute and the solvent molecules as analogous to the non-equilibrium situation first mentioned by Buckingham. The buffeting interaction was considered on the basis of a perturbation of the peripheral solute atoms by electric fields originating from atoms at the periphery of the solvent molecule. This was treated on the basis of pair-wise encounters. The reference for such encounters was a right hand triple taking the solute resonant nucleus at the origin with its bond to the other atom in the molecule colinear with the z-axis (Figure 3.3).

The electric field $\vec{E}$ produced at the solute atom containing the resonant nucleus of interest by a moment $\vec{m}$ in a solvent peripheral atom and separated from the solute nucleus by distance r, is given by [80]:

SOLUTE*	CORRELATION COEFFICIENT	GRADIENT $= 10^{18}$ B/esu	INTERCEPT /ppm
CMe_4	0.933	0.81	0.128
$SiMe_4$	0.953	0.87	0.169
$GeMe_4$	0.950	0.87	0.170
$SnMe_4$	0.960	0.92	0.185
$PbMe_4$	0.966	0.88	0.190

* solute at infinite dilution in all five groups IVB tetramethyls as solvents

Table 3.2   Linear Regression Analyses Of $- \sigma_W$ (expt) at $30^{o}C$ on R_T^2

For The Group IVB Tetramethyl Systems.
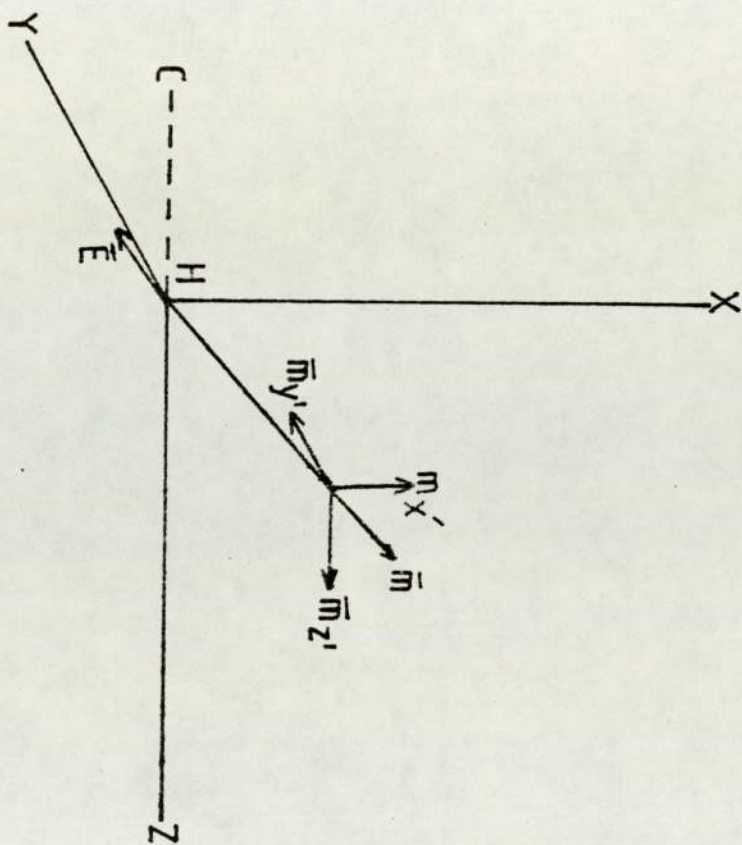
Fig 3.3

Space average situation of a solvent molecule average electric moment.

102

$$\vec{E} = 3 \, (\vec{m} \cdot r) \, \frac{r}{r^5} \quad - \quad \frac{\vec{m}}{r^3} \quad \dots\dots\dots\dots\dots\dots\dots\dots\dots\dots\dots \quad (3.21)$$

Assuming that there is no restruction on the approach of the solvent molecule to the solute atom, the time average of the electric field over all space will be zero. However, the mean square value may still be finite. Therefore, Homer evaluated the square of the instantaneous electric field at the resonant nucleus. This instantaneous value of the time average electric field was deduced by considering the situation in one octant about the solute resonating nucleus. On time average the appropriate solvent atom can be considered to lie on an axis at an angle of $54^\circ \, 44'$ ($\cos^{-1} 1/\sqrt{3}$) to each of the three coordinate axes based on the solute nucleus. The solvent moment $\vec{m}$ was characterized by considering the solvent electron moment in one octant about the solvent atom.

The electric fields at the solute resonant nucleus that are parallel and perpendicular to the bond containing the resonant nucleus are given by:

$$\vec{E}_x = \frac{2\vec{m}_x{}'}{r^3} - \frac{\vec{m}_y{}'}{r^3} - \frac{\vec{m}_z{}'}{r^3} \quad \dots\dots\dots\dots\dots\dots\dots\dots\dots\dots \quad (3.22)$$

$$\vec{E}_y = \frac{2\vec{m}_y{}'}{r^3} - \frac{\vec{m}_x{}'}{r^3} - \frac{\vec{m}_z{}'}{r^3} \quad \dots\dots\dots\dots\dots\dots\dots\dots\dots\dots \quad (3.23)$$

$$\vec{E} = \frac{2\vec{m}_z{}'}{r^3} - \frac{\vec{m}_x{}'}{r^3} - \frac{\vec{m}_y{}'}{r^3} \quad \dots\dots\dots\dots\dots\dots\dots\dots\dots\dots \quad (3.24)$$

103

that are illustrated in Figure 3.4. It was accepted that because the accessibility of the solvent atom to the solute resonant nucleus is anisotropic, $\vec{E}_z$, $\vec{E}_y$ and $\vec{E}_x$ are modulated by weighting factors which are considered to be a measure of the anisotropy of relative approach, accessibility or steric hindrance of the solvent molecule to the solute resonant nucleus. Solute-solvent encounters parallel to the bond are restricted by $0 \leqslant \beta \leqslant 1$, and those perpendicular to the bond are defined by $0 \leqslant \alpha \leqslant 1$ and $0 \leqslant \alpha' \leqslant 1$. It is assumed also, for the axially symmetric bond around z-axis (as in the case of C-H or C-F bonds) that $\alpha = \alpha'$ and $2\alpha = \xi$. By taking the sum over four octants the final deriviation of the mean square dispersion field was given by the simplified equation:

$$E^2 = - \frac{K}{r^6} (2\beta - \xi)^2 \quad \dots\dots\dots\dots\dots\dots\dots\dots\dots\dots (3.25)$$

where K is a constant depending on the electron displacement around the peripheral solvent atom.

Therefore, the contribution of the buffeting interaction to the nuclear screening constant is characterized by:

$$\sigma_{BI} = - \frac{B K}{r^6} (2\beta - \xi)^2 \quad \dots\dots\dots\dots\dots\dots\dots\dots (3.26)$$

where r is the interatomic distance between the resonant nucleus and the atom on the periphery of the solvent molecule (taken as the sum of van der Waals radii of the atoms considered), β and ξ describe the total effective accessibility of a solute atom to the solvent atom as a result of pair-wise encounters, they are

$$\bar{E}_{xx'} = 2\bar{m}\hat{x}'/r^3$$

$$\bar{E}_{xy'} = -\bar{m}\hat{y}'/r^3$$

$$\bar{E}_{xz'} = -\bar{m}\hat{z}'/r^3$$

$$\bar{E}_{yx'} = -\bar{m}\hat{x}'/r^3$$

$$\bar{E}_{yy'} = 2\bar{m}\hat{y}'/r^3$$

$$\bar{E}_{yz'} = -\bar{m}\hat{z}'/r^3$$

$$\bar{E}_{zx'} = -\bar{m}\hat{x}'/r^3$$

$$\bar{E}_{zy'} = -\bar{m}\hat{y}'/r^3$$

$$\bar{E}_{zz'} = 2\bar{m}\hat{z}'/r^3$$
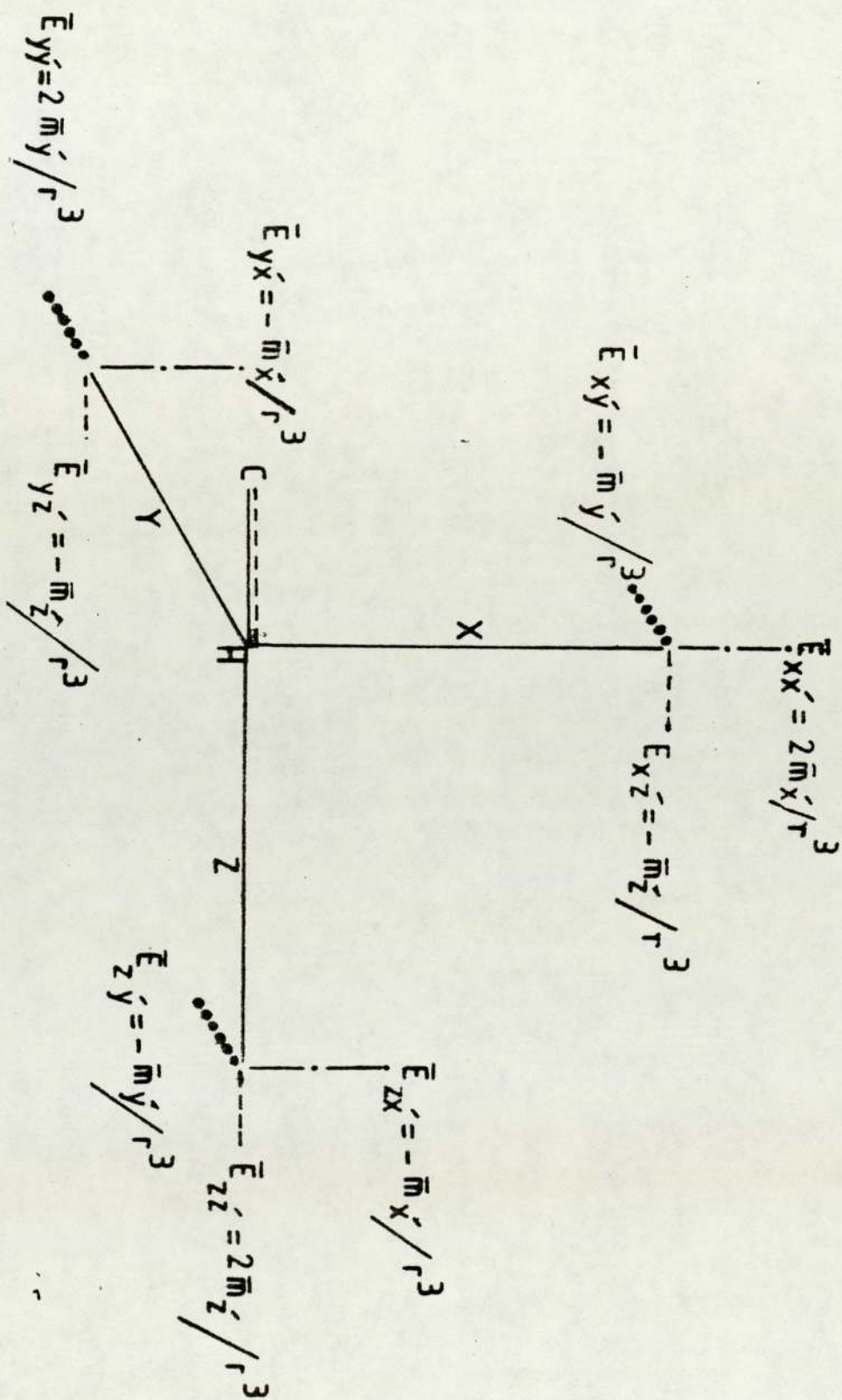
Fig 3.4

Time average electric fields with respect to directions parallel and perpendicular to the axis of the C-H bond.

105

based on a geometrical accessibility where the encountering species are rigid and passive (there will be more description detailing the measurement of these parameters in Chapter 4).

The above discourse merely summarizes the salient features of the evidently complex arguments leading to the derivation of σ_{BI} subject of an earlier thesis [64]. The full details of the approach and of that leading to $< R^2_2 >$ are contained in a lengthy paper now accepted for publication in "J Chem Soc" Faraday II.

The application of buffeting theory was not limited just to the NMR field, but to other aspects of chemistry and physics. For example, Fig 3.5 shows the relationship between calculated van der Waals a-values, and those obtained from either data. The correlation which is in quite satisfactory and appears to be significant with the expected slope of unity and zero intercept.

3.5 CONCLUSION

The overwhelming success obtained by the extensive tests of Homer and Percival's theory is beyond the realism of chance. Consequently, despite the acknowledged simplicity of Homer and Percival's approach it would appear that they have proved a working theory that can be used to accurately predict observable properties of matter that stem from van der Waals forces.
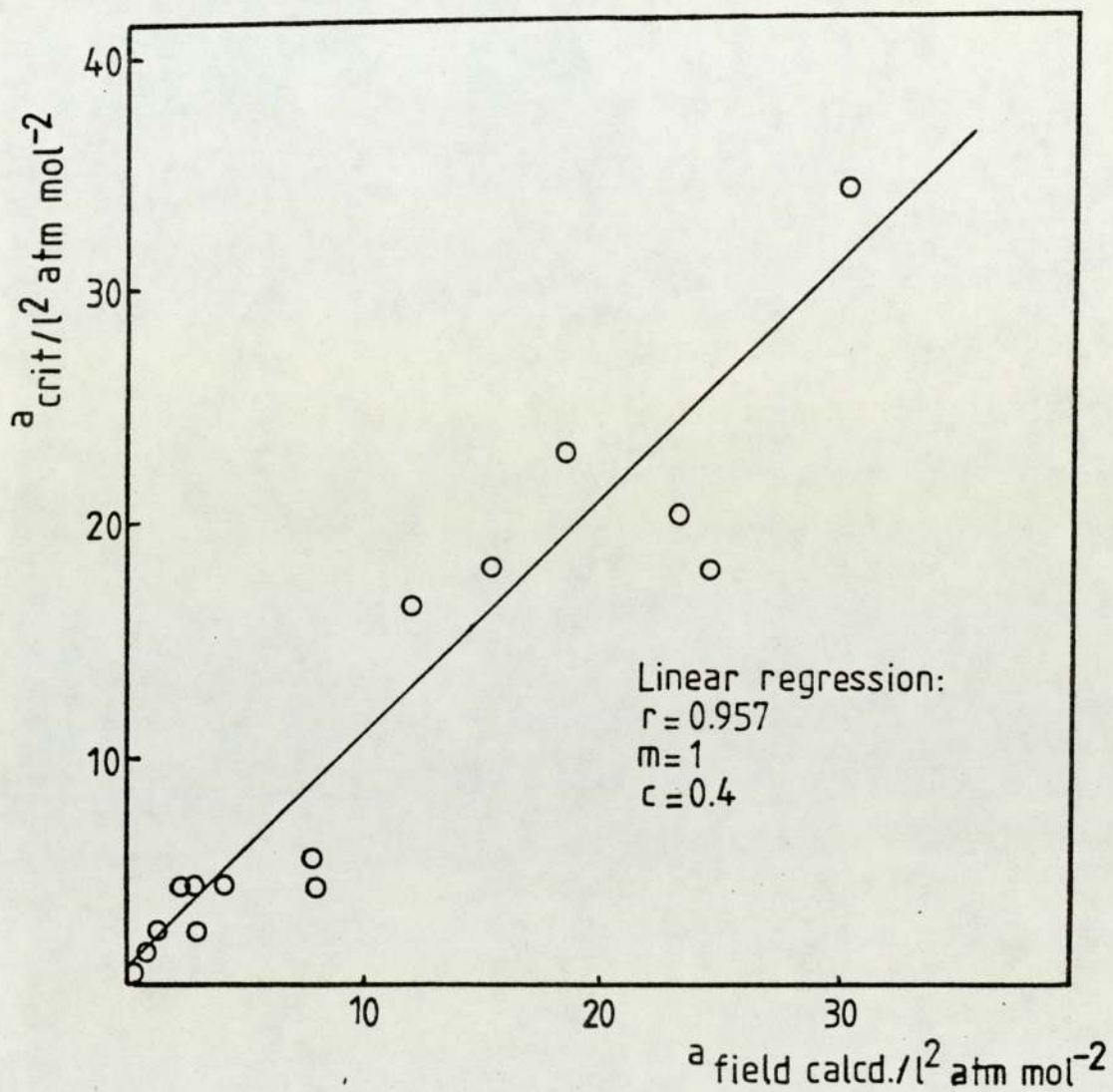
Figure 3.5   Relationship between critical and field calculated
              van der Waals a-values (Reprinted from ref. 64).

The work reported in Chapter 4 of this thesis will demonstrate a direct application of Homer's theory and will also provide more supporting evidence to it.

AN APPRAISAL OF THE APPLICABILITY OF REACTION FIELD
AND BUFFETING THEORY TO THE ANALYSIS OF SOLVENT INDUCED
SHIFTS FOR COMPLEX MOLECULES IN THE LIQUID PHASE - A
POSSIBLE ROUTE TO MOLECULAR STRUCTURE

4.1 INTRODUCTION:

This chapter will demonstrate that the solvent chemical shift
induced in quite complex molecules in the liquid phase can be
explained by the reaction field and buffeting theory described in
the previous chapter and that the approach may be used to study
steric aspects of those quite complex molecules. For this work no
gas-to-solution chemical shifts were needed to analyse the solvent
buffeting effect. This development was achieved by using two
different solvents have different buffeting Q values with the same
solute. This enables the elimination of the necessity of
measuring the gas-to-solution chemical shift which is difficult or
in some cases impossible and in any event may be subject to
significant errors.

Basically the experimental work of this chapter has been undertaken to provide chemical shifts from which the buffeting interaction contribution to the nuclear screening, σ_{BI}, can be isolated by subtracting the calculated effect of the reaction field part of the van der Waals screening. The isolated σ_{BI} was tested against the existing Homer theory.

4.2 ISOLATION OF σ_w FROM THE EXPERIMENTAL CHEMICAL SHIFTS FOR MOLECULES IN THE LIQUID PHASE:

The screening constant of an isotropic solute in an isotropic solvent is

$$\overset{i}{\sigma}_s = \overset{i}{\sigma}_o + \overset{i}{\sigma}_w \quad \dots\dots\dots\dots\dots\dots\dots\dots\dots\dots\dots\dots\dots \quad (4.1)$$

where $\overset{i}{\sigma}_s$ is the screening constant of nucleus i in the solute contained in solution s, $\overset{i}{\sigma}_o$ is the absolute screening constant of nucleus i in the gas phase under zero pressure, and $\overset{i}{\sigma}_w$ is the contribution of van der Waals dispersion forces to the screening of nucleus i.

From equation (3.6):

$$\overset{i}{\sigma}_w = \overset{i}{\sigma}_{RF} + \overset{i}{\sigma}_{BI} \quad \dots\dots\dots\dots\dots\dots\dots\dots\dots\dots\dots\dots \quad (4.2)$$

therefore,

$$\overset{i}{\underset{s}{\sigma}} = \overset{i}{\sigma}_o + \overset{i}{\sigma}_{RF} + \overset{i}{\sigma}_{BI} \quad \dots\dots\dots\dots\dots\dots\dots\dots\dots\dots\dots \quad (4.3)$$

where σ_{RF} and σ_{BI} are the reaction field and the buffeting interaction effects on the screening of constant of i.

Usually the chemical shift of each resonating nucleus is measured from a reference, which is one of the components in the solution when using the internal reference technique; this is the case adopted throughout the work reported in this chapter. Consequently, the reference will experience the same environment as the solute, and its chemical shift is, therefore, given by:

$$\sigma_s^r = \sigma_0^r + \sigma_w^r \quad\dots\dots\dots\dots\dots\dots\dots\dots\dots\dots\dots\dots \quad (4.4)$$

where the superscript r in the above equation identifies the reference. Following equation (1.46) the chemical shift is defined by:

$$\delta_s^i = \sigma_s^i - \sigma_r^i \quad\dots\dots\dots\dots\dots\dots\dots\dots\dots\dots\dots\dots \quad (4.5)$$

Therefore using equations (4.1 and 4.4) the above equation may be written as:

$$\delta_s^i = (\sigma_0^i - \sigma_0^r) + (\sigma_w^i - \sigma_w^r) \quad\dots\dots\dots\dots\dots\dots\dots\dots \quad (4.6)$$

Since the term $(\sigma_0^i - \sigma_0^r)$ represents the difference between the single molecule or the absolute screening constants of nucleus i and that of the reference r, this term is constant whereas the other term $(\sigma_w^i - \sigma_w^r)$ depends on the properties of the solvent. The difficulty of obtaining the absolute screening difference in

111

the above equation may be avoided by finding the appropriate chemical shifts in two different solvents, so that the difference between these two chemical shifts for a given solute using the same reference will eliminate the term ($^i\sigma_0 - {}^r\sigma_0$) as explained below:

The chemical shift of the resonant nucleus i contained in an isotropic solute at infinite dilution in an isotropic solvent A is represented by:

$$\delta^{i/A} = (\,^i\sigma_0 - {}^r\sigma_0) + (\,^{i/A}\sigma_W - {}^{r/A}\sigma_W) \dots\dots\dots\dots\dots (4.7)$$

and similarly the chemical shift of i using another isotropic solvent B is given by:

$$\delta^{i/B} = (\,^i\sigma_0 - {}^r\sigma_0) + (\,^{i/B}\sigma_W - {}^{r/B}\sigma_W) \dots\dots\dots\dots\dots (4.8)$$

By subtracting equation 4.7 from 4.8, the difference of the chemical shifts of i on changing from solvent A to solvent B, is given by:

$$(\,\delta^{i/B} - \delta^{i/A}) = (\,^{i/B}\sigma_W - {}^{i/A}\sigma_W) - (\,^{r/B}\sigma_W - {}^{r/A}\sigma_W) \dots\dots (4.9)$$

which may be rewritten as follows by using equation 4.2 with rearrangement:

$$(\delta^{i/B} - \delta^{i/A}) = (\,^{i/B}\sigma_{RF} - {}^{i/A}\sigma_{RF}) + (\,^{i/B}\sigma_{BI} - {}^{i/A}\sigma_{BI})$$
$$- (\,^{r/B}\sigma_W - {}^{r/A}\sigma_W) \dots\dots\dots\dots\dots\dots\dots\dots\dots (4.10)$$

112

For simplicity it will be assumed that there is no solute -
reference interaction since both of the components are considered
to be infinitly dilute. Therefore, in equation (4.10) the term
representing the difference of van der Waals dispersion forces
screening of the reference should be a constant value independent
of the solute, provided the same solvents A and B are used.

It is convenient, therefore, to isolate the required
difference in buffeting contribution to the nuclear screening
constant, by rearranging equation 4.10 as:

$$(\delta^{i/B} - \delta^{i/A}) - (\,^{i/B}\sigma_{RF} - \,^{i/A}\sigma_{RF}) = (\,^{i/B}\sigma_{BI} - \,^{i/A}\sigma_{BI})$$
$$- (\,^{r/B}\sigma_W - \,^{r/A}\sigma_W) \dots\dots\dots\dots\dots\dots\dots\dots\dots\dots\dots (4.11)$$

It will be shown that the above equation enables the
isolation of the difference in the buffeting interaction
contribution to the screening, together with a constant factor on
the right hand side. The left hand side of the equation contains
the difference of the experimentally measured chemical shifts
together with the difference of the reaction field contribution to
the screening that can be calculated using the established
equation (3.18).

Equation (4.11) will be used to carry out the task of this
chapter.

113

<u>Characterizing σ_{BI} In Different Solvents:</u>

The intention now, is to measure chemical shifts giving ($\delta^{i/B} - \delta^{i/A}$), subtract from these the calculated value of ($^{i/B}\sigma_{RF} - {}^{i/A}\sigma_{RF}$) and correlate the resultant of these with suitable functions of the buffeting term ($^{i/B}\sigma_{BI} - {}^{i/A}\sigma_{BI}$).

The solvents chosen for this work were TMS and CCl_4 (representing A and B respectively). The use of the latter requires that the basic buffeting equation (3.26) has to be modified to account for the increased number of electrons in the chlorine atom in CCl_4. Homer and Percival[64] have done this by reference to the work of Yamamoto[82] who in another context has used an analogue Hartree-Fock based scaling factor, Q, which is equal to unity for hydrogen atom and is replaced by:

$$Q = \frac{\langle \Sigma_i x^2_i \rangle}{a^2_o}$$

for other atoms such as the halogens. The experimentally based value of Q deduced by Homer and Percival correlate well with these of Yamamoto. Consequently, the appropriate values of Q can be inserted reliably into equation (3.26) to obtain the effect of buffeting for non-hydrogen buffeting atom X. It should be noted that because of the different van der Waals radii of hydrogen and other atoms, the Q values of the latter must be distance modulated. Accordingly, equation (3.26) may be rewritten as follows:

$$\sigma_{BI} = \left(\frac{-BK^H}{r^6_{HH}}\right) \ Q^x \ \left(\frac{r_{HH}}{r_{HX}}\right)^6 \ (2\beta - \xi)^2 \ \ldots\ldots\ldots\ldots \ (4.12)$$

where X refers to the interacting solvent atom.

This general form of the buffeting equation can be used to analyse the buffeting difference term in equation (4.11). Assuming that the two solvents are such that the buffeting atom in A is hydrogen and that in B a halogen X, the difference term is:

$$(\ {}^{i/B}\sigma_{BI} - \ {}^{i/A}\sigma_{BI}) = \left[\frac{-BK_H}{r^6_{HH}} \left(\frac{r_{HH}}{r_{HCl}}\right)^6 Q^{Cl} (2\beta' - \xi')^2\right] -$$

$$\left[\frac{-BK_H}{r^6_{HH}} (2\beta - \xi)^2\right] \ldots\ldots\ldots\ldots\ldots\ldots\ldots \ (4.13)$$

where β', ξ' and β, ξ are the solute peripheral atom buffeting parameters when buffeted by solvents B and A respectively.

Equation 4.13 can be rewritten as:

$$(\ {}^{i/B}\sigma_{BI} - \ {}^{i/A}\sigma_{BI}) = \frac{-BK_H}{r^6_{HH}} \left[\Delta(2\beta' - \xi')^2 - (2\beta - \xi)^2\right] \ldots\ldots \ (4.14)$$

where

$$\Delta = \left[\frac{r_{HH}}{r_{HX}}\right]^6 \ Q^x \ \ldots\ldots\ldots\ldots\ldots\ldots\ldots\ldots\ldots\ldots\ldots\ldots\ldots \ (4.15)$$

Equation 4.14 represents the buffeting effect on the screening constant based on Homer theory, while equation 4.11 contains the experimentally isolated buffeting effect difference. Therefore, equations 4.11 and 4.14 can be used to carry out the aim of this chapter.

It is important before preceeding any further, to discuss the method used in this thesis for obtaining the values of the buffeting parameters β and ξ for complex molecules. The following section will deal with this point.

4.2:2 <u>Measurement Of The Buffeting Parameters β And ξ :</u>

The geometrical buffeting parameters β and ξ represent the effective accessibility of the solvent peripheral atom to the solute resonant nucleus, as a result of pair-wise encounters in their non-equilibrium situation. In order to imagine this buffeting, the solvent molecule containing the peripheral atom is assumed to be spherical because of its rotational motion. Both solute and solvent molecules are taken to be rigid and passive. On these bases, Figure (4.1) shows the approach that is assumed to represent pair-wise encounters from a geometrical point of view. It shows that the solvent molecule is buffeting the solute atom under interest with a distance r between the centres of the resonant nucleus and the peripheral atom on the solvent. The figure shows a hypothetical two-dimensional encounter situation.

116
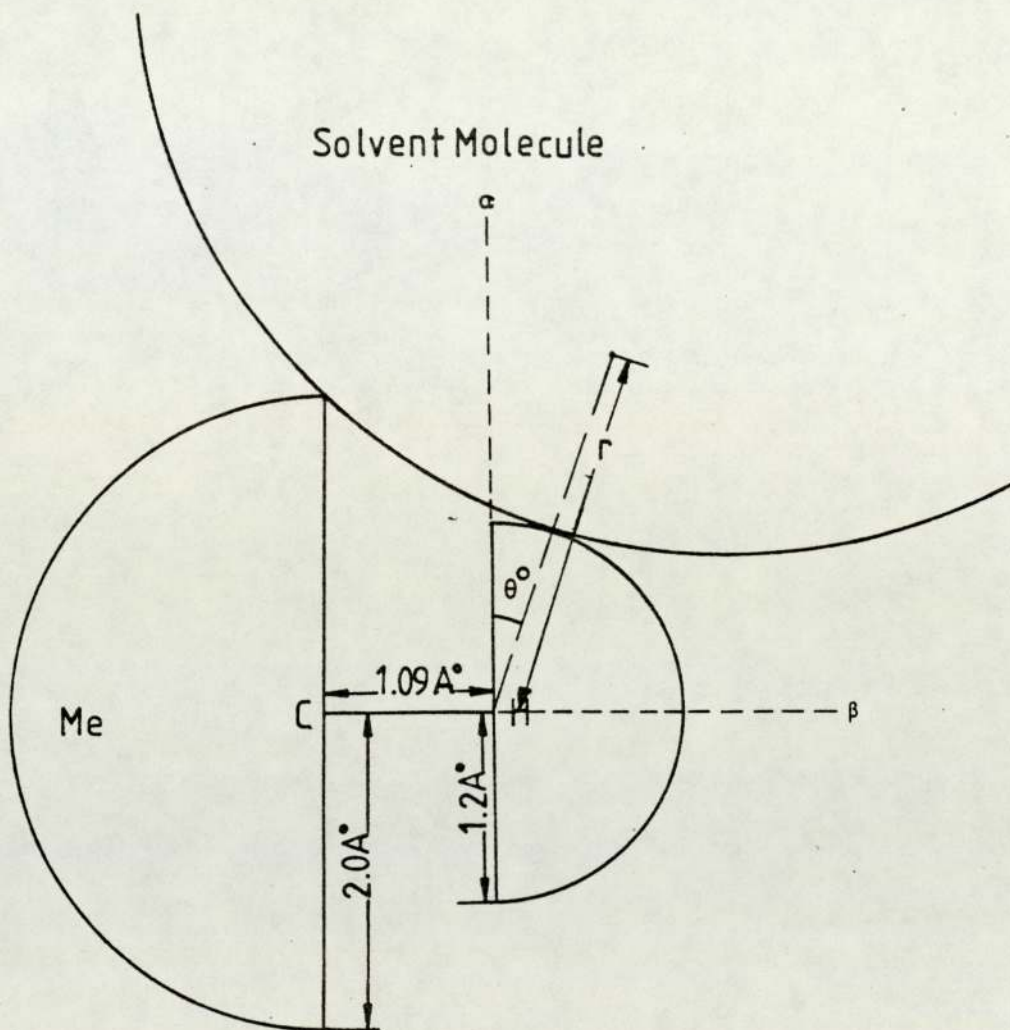
Figure 4.1   Two-dimensional representation of a methane molecule
             (Hydrogen H and methyl group Me) encountered by
             an isotropic solvent molecule.

If in figure (4.1) the centre of the peripheral solvent atom can adopt all positions on an arc of radius r_c from the centre of the solute atom throughout the octant of interest, then $\beta = 1$ and $\alpha = 1$ ($\xi = 2$) and there will be no buffeting screening. If the contact distance r_c is sterically precluded within the octant, β and α will be less than unity. If the two dimensional angle θ is the angle between the radius vector and the so-called α-axis which defines the limit where r_c no longer applies (i.e. $r > r_c$) the following equations are applicable:

$$\text{If } \theta \leqslant 45 ; \quad \beta_c = 1 , \quad \alpha_c = \frac{45 - \theta}{45} \quad \ldots\ldots\ldots\ldots\ldots\ldots (4.16)$$

$$\text{If } \theta \geqslant 45 ; \quad \alpha_c = 0 , \quad \beta_c = \frac{90 - \theta}{45} \quad \ldots\ldots\ldots\ldots\ldots\ldots (4.17)$$

The above equations enable the contact geometrical buffeting parameters β_c and ξ_c to be deduced when the solvent peripheral atom is in contact with the solute atom. The remaining parts of β and α, $(1 - \beta_c)$ and $(1 - \alpha_c)$, may be deduced by distance modulation. The modulation is based on the inverse sixth power of distance, because of the distance dependence of van der Waals dispersion forces. If r' is the distance between the centres of the solute atom - solvent atom at the α-axis, viz the extreme point of the octant of interest where direct atom-atom contact is prevented by steric hendirance, r_c is the distance between the centres of the solute-atom solvent-atom at contact, and assuming a continuous change in distance from r_c to r', the average inverse power of the distance used for the modulation of $(1 - \beta_c)$ and

118

$(1 - \alpha_c)$ is $< r^{-6} >$ where:

$$< r^{-6} > = \frac{\int_{r_c}^{r'} r^{-6} dr}{\int_{r_c}^{r'} dr} = \frac{r^{-5}_c - r'^{-5}}{5 (r' - r_c)} \quad \ldots\ldots\ (4.18)$$

The total values of β and ξ are given by:

$$\beta_T = \beta_c + (1 - \beta_c)\ r^6_c\ < r^{-6} > \quad \ldots\ldots\ldots\ldots\ldots\ldots\ldots (4.19)$$

$$\alpha_T = \alpha_c + (1 - \alpha_c)\ r^6_c\ < r^{-6} > \quad \ldots\ldots\ldots\ldots\ldots\ldots\ldots (4.20)$$

or $\quad \xi_T = \xi_c + (2 - \xi_c)\ r^6_c\ < r^{-6} > \quad \ldots\ldots\ldots\ldots\ldots\ldots\ldots (4.21)$

for the appropriate situations.

It is worth pointing out that totally independent calculations of β_T and ξ_T for given systems by this author and by Percival produce insignificant differences between the independent sets of β_T and ξ_T.

4.3 EXPERIMENTAL REQUIREMENTS:

The contribution of the buffeting interaction to the solvent induced nuclear screening represents only a small part of the total chemical shift; in some systems it is just few Hertz at 100 MHz. The

isolation of such effects from the experimental shifts therefore requires high accuracy in the measurements of the latter. The factors that effect the chemical shift measurements e.g. the sample preparation and the concentration of the solute under interest will be discussed now.

4.3:1   **Measurements of Accurate Chemical Shifts:**

The chemical shifts measurements reported in this chapter, were performed using a Perkin-Elmer R 12 B 60 MHz NMR spectrometer during the first stage of the work, but the main results were obtained using a Varian Associates HA 100 D NMR spectrometer. With the latter instrument the absorptions are recorded on a calibrated chart and chemical shift are shown on the instrument frequency counter display. The shifts are measured by placing the pen on the top of the peak of interest and measuring the a.f modulation frequency. The error in the frequency display is $\pm$ 0.1 Hz, but the total error in measuring the absorption frequency is $\pm$ 0.2 Hz due to the uncertainty in locating the pen at the top of the absorption. Maintaining only this error in the measurement necessitates careful control of conditions such as using the same sweep rate and filter to minimize random errors. All the spectra were drawn out in expanded form i.e. maximum spectral width, and the measurements made several times to average any variations. Internal lock was used throughout to avoid any possible signal drifting.

For the few measurements made using the Perkin-Elmer R 12 B instrument for which there is no frequency counter, the chart was precalibrated, and the chemical shifts found by averaging several measurements for the same sample.

The temperature was kept constant throughout all the chemical shift measurements at $33^{\circ}C$ to eliminate the effect of temperature variations.

4.3:2   **Preparation of Samples:**

All the samples investigated were prepared at effectively infinite dilution (see section 4.3:3) to eliminate any concentration effect.   New 5mm O.D NMR tubes for each sample were used throughout.

To ensure that there was negligible dissolved oxygen that could contribute to the shifts, the samples were prepared under vacuum.   The transference of solutions to NMR tube under vacuum was effected using special glassware designed[83] for this purpose.   Figure (4.2) shows the vacuum manifold and syphoning apparatus used.

Initially, the three-way tap and the rotaflow taps were adjusted so that the flask was isolated from the rest of the apparatus.   All parts of the manifold were then evacuated, except for the flask.   Meanwhile the flask was cooled using liquid nitrogen.   About 2.5ml of the prepared solution was quickly

Figure 4.2 The manifold and the syphoning apparatus used together in samples preparation.
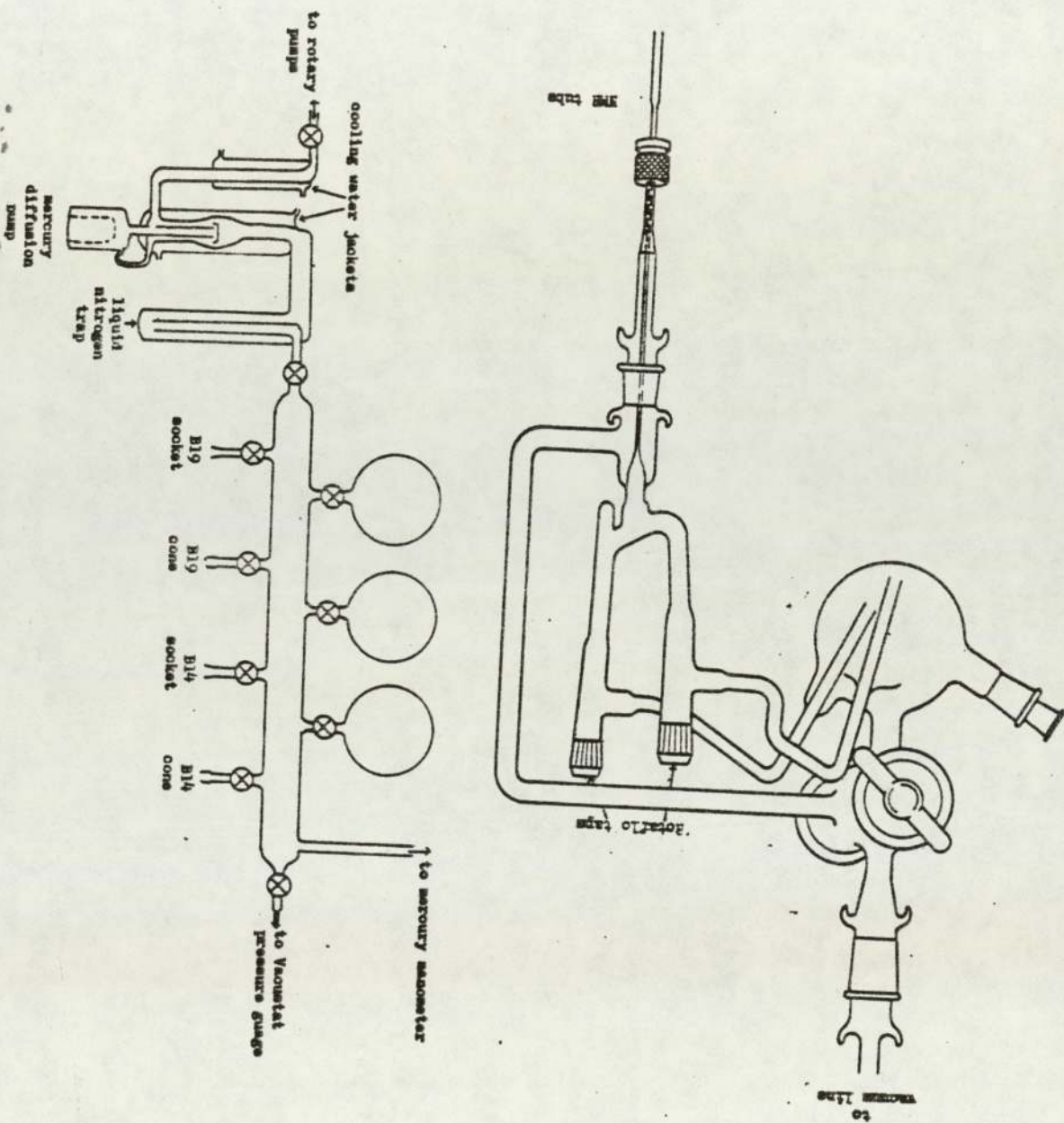
inserted in the flask. Then the solution inside the flask was frozen by liquid nitrogen. At this stage the flask was opened to the evacuated manifold while the solution was frozen. Vacuum was achieved using conventional rotary pump techniques and the pressure assessed using a mercury manometer connected to the manifold. The vacuum at this point was checked using the manometer for a pressure of 10^{-3} Torr or less. Subsequently the flask was isolated from the vacuum system by the three-way tap and allowed to warm up.

The NMR tubes were connected to the manifold using a special glass-to-metal joint with an o-ring seal. Each tube was evacuated and checked for any leakage. The NMR tube was warmed gently to remove any oxygen adhering to the wall. Then the vacuum manifold was isolated from the pump and the taps leading to the sample tube and the flask were opened. By cooling the NMR tube the sample was distilled over; during this procedure the NMR tube was cooled and the flask containing the sample warmed while controlling the taps until enough sample in the NMR tube has been transferred and collected. At this stage the sample tube was frozen and the manifold re-evacuated. Finally the NMR tube was sealed under vacuum. In order to improve the sealing, the NMR tubes were prepared before use by flame heating around a point about 2cm from the open end prior to the installation on the vacuum system. This caused a restriction and thickening of the tube at the appropriate point. Subsequently, a very good seal was obtained by touching the narrow part of the tube with the flame. Then the sealed tube

was kept under a glass beaker for at least two hours after the solution inside it had melted so that the effects of explosure or implosion could be monitored.

4.3:3   **Effects of Concentration on NMR Chemical Shifts:**

Chemical shifts studies relating to the Homer and Percival theories ideally require the use of infinitly dilute solutions. Consequently it was important to establish the limit of concentration which could be considered to behave as an infinitly dilute solution.

This was done by investigating the dependence of an appropriate chemical shift on the solute concentration.   The system chosen for this purpose was a typical system, in which the reference was an external reference (TMS) contained in a capillary inserted co-axially inside the 5mm O.D NMR tube.   The solution in the annulus between the tubes was composed of TMS in CCl_4. The proton chemical shift of TMS (in the solution) was measured with respect to the reference (pure TMS in the capillary).   Different concentrations of TMS in CCl_4 were prepared starting with 10% molar and then halved each time to (5, 2.5, 1.25, 0.613 and 0.31)% molar.   The chemical shift was measured for each concentration, using a field/frequency locked Varian Associates HA 100 D spectrometer.   Table 4.1 presents the resultant chemical shifts. A plot of these against concentration is shown in Figure 4.3; the y-intercept represents the chemical shift of the sample at zero concentration viz: the infinite dilution chemical shift.   Whilst

124

Concentration of TMS in CCl_4		TMS/in CCl_4 δ_o
	(Molar)	
X	10%	-43.5
1/2 X	5%	-45.2
1/4 X	2.5%	-45.9
1/8 X	1.25%	-46.2
1/16 X	0.625%	-46.2
1/32 X	0.313%	-46.2

Table 4.1   Dependence of chemical shift of TMS in CCl_4 from external TMS using verian HA100 D spectrometer at t = 33°C.
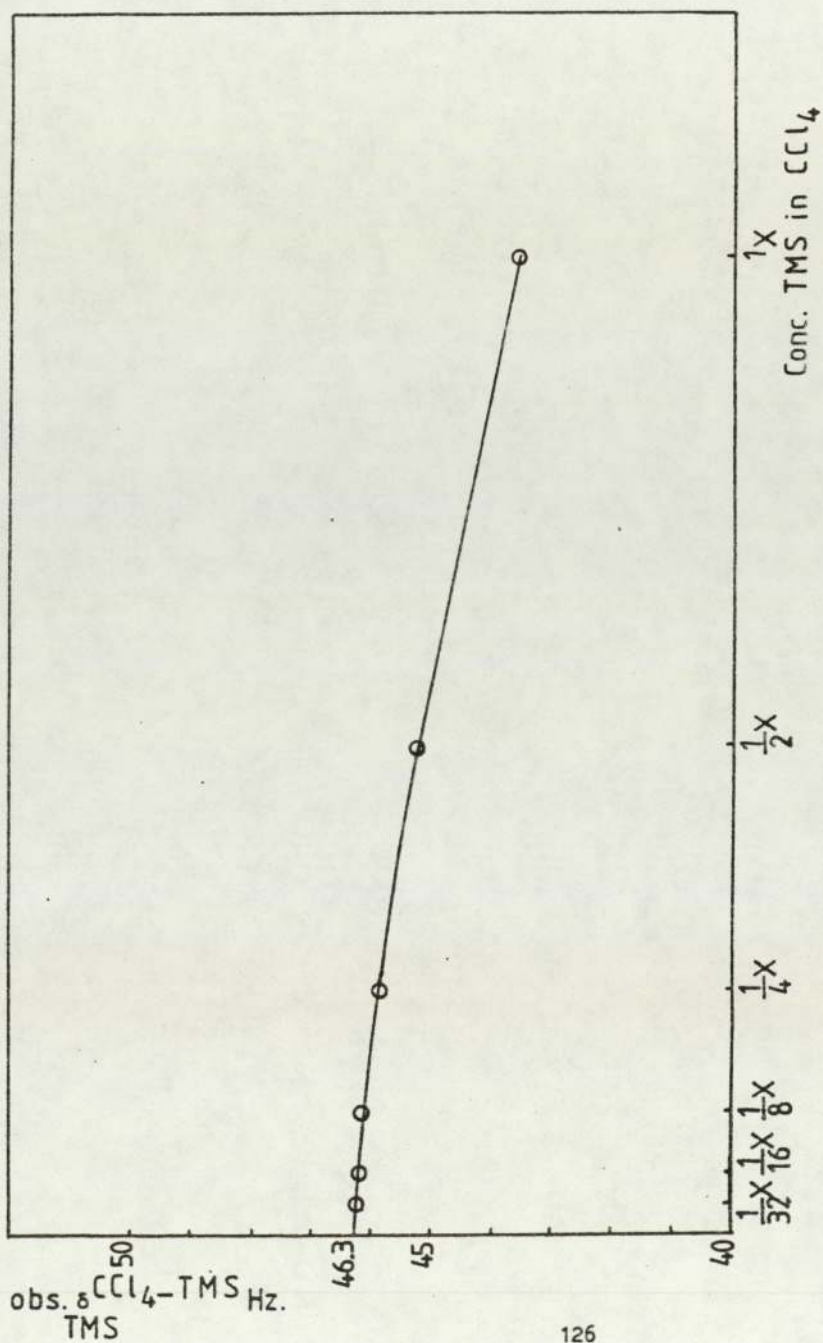
Figure 4.3   The dependence of ^1H shifts (Hz) of TMS on the concentration. Measurements were made employing Varian Associates HA 100 D instrument operating at 33^oC, from internal reference TMS.

these shifts are not susceptibility corrected, it can be seen that below a concentration of 1.25% molar the shifts are almost constant. Therefore, in practice a solution of 1% molar can be assumed to be infinitly diluted.

All of the samples used throughout this work were prepared at 1% molar; this avoids any unwanted interaction that may occur between the solute and the solvent at higher concentrations.

4.4 σ_w For The Reference TMS:

If some correlation between the term on the left hand side of equation 4.11 and the first term of the right hand side can be demonstrated a further test of the validity of this equation may be made by analysing the value obtained from the second term of the right hand side i.e. ($r/\sigma_w^B - r/\sigma_w^A$). Consequently, the next stage of the work was to deduce, by an independent method, a value of this term for the reference. This term should be constant and can in fact be estimated separately. The experiment that was described in section (4.3:3) can be adopted for this purpose.

From equations (4.1 and 4.5), the chemical shift of TMS in the solvents CCl_4 and TMS can be represented respectively by:

$$\delta_{TMS}^{CCl_4} = \sigma_o + \sigma'_b + \sigma'_w \dots\dots\dots\dots\dots\dots (4.22)$$

127

$$\overset{TMS}{\delta}{}_{TMS} = \sigma_o + \sigma_b + \sigma_w \dots\dots\dots\dots\dots\dots\dots\dots\dots\dots \quad (4.23)$$

Therefore,

$$\overset{CCl_4}{\underset{TMS}{\delta}} - \overset{TMS}{\underset{TMS}{\delta}} = (\sigma'_b - \sigma_b) + (\sigma'_w - \sigma_w)\dots (4.24)$$

In the above equation the term representing the screening effect of magnetic susceptibilities can be calculated using equation (1.57), where the volume magnetic susceptibilities are -0.536×10^{-6} for TMS[61] and -0.689×10^{-6} for CCl_4[84]. This would give $(\sigma'_b - \sigma_b) = -0.32$ ppm.

Using the value deduc ed in section (4.3:3) for the experimental difference in the chemical shifts of TMS on changing from CCl_4 to TMS as solvent (for infinitly dilute solutions) given the term ($\overset{CCl_4}{\delta_{TMS}} - \overset{TMS}{\delta_{TMS}}$) as -46.3 Hz at 100 MHz (From Table 4.1 and Figúre 4.3). Therefore, substituting these values in equation (4.24) would give the difference in van der Waals screening for the reference ($\sigma'_w - \sigma_w$) equal to -14.3 Hz. This value is in exact agreement with the value deduced by Homer[87] using a novel referencing system for the same purpose. He obtained -8.6 Hz at 60 MHz which is equivalent to -14.3 Hz at 100 MHz.

Figure 4.4 illustrates the above method schematically.
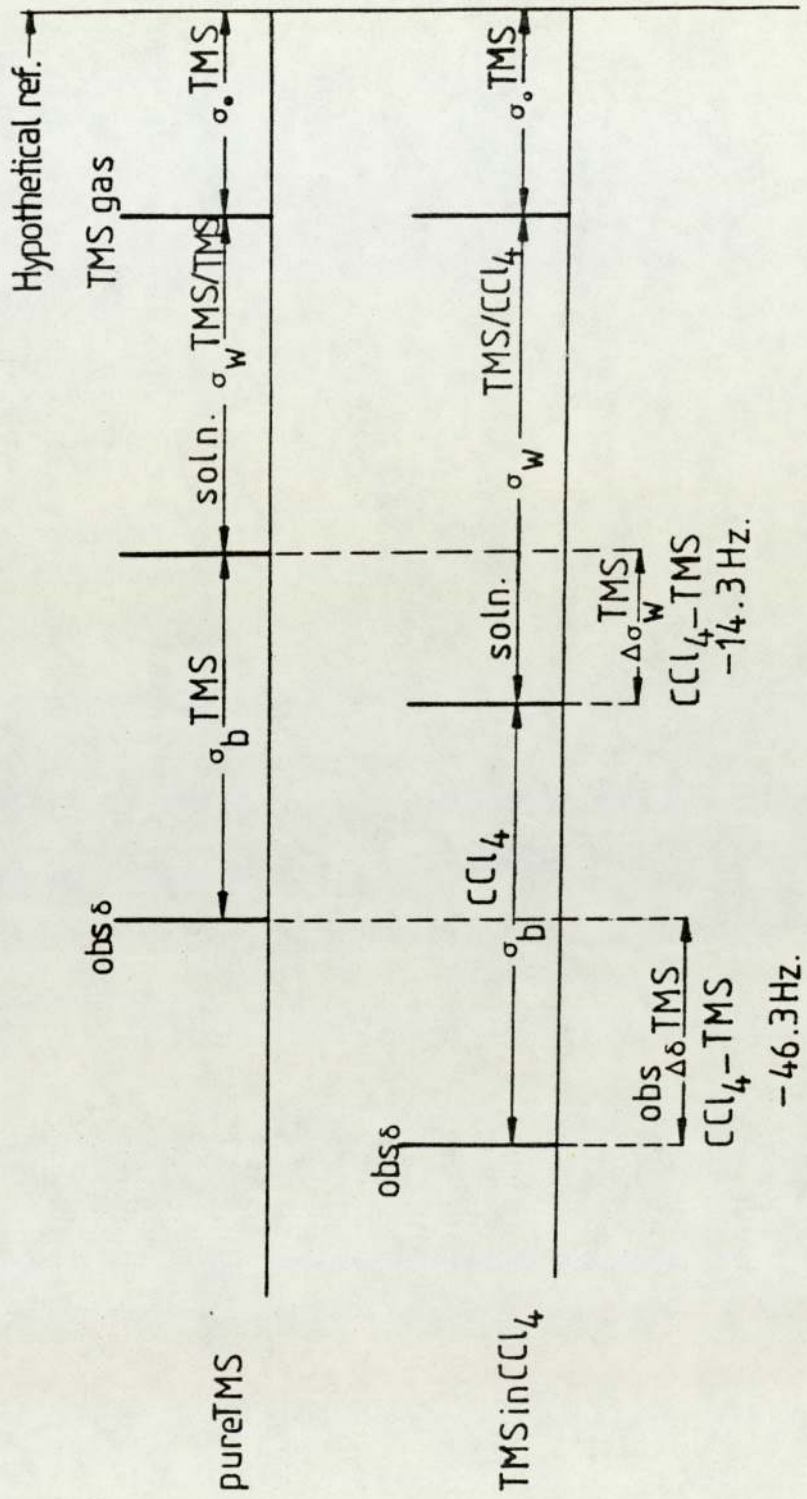
Figure 4.4   Schematic representation of evaluation of σ_w of TMS on changing from TMS in CCl_4 to pure TMS.

129

4.5   APPLICATION OF BUFFETING THEORY TO THE METHYL GROUPS
       IN DIFFERENT STERIC POSITIONS:

       The next stage of the work was to measure chemical shifts
from which σ_{BI} can be isolated and tested against Homer's theory.
The general approach for this has been explained in section (4.2).

       It was proposed that the methyl groups in a selection of
organic molecules were suitable objects of study since they are
expected to be in different steric positions.   The molecules
studied were: Camphor, Pinene, Fenchone, Menthol, P-Cymene,
Paraldehyde, Durene, Mesitylene, P-Xylene and Toluene.

       Initially, it was necessary to investigate the dependence of
the proton chemical shifts of the methyl groups of the above
mentioned samples on the concentration of the solute.   If
significant dependence was found, it was considered necessary to
determine the shifts at infinite dilution.   Experiments
demonstrated that there is no appreciable concentration dependence
for the proton shifts when using any concentration around 1%
molar. Thus it was possible to use this order of concentration to
represent an effectively infinite dilution solution.

       All of the above mentioned samples were prepared in the two
solvents TMS and CCl_4 at concentration of 1% molar. These were
transferred to 5mm O.D sealed NMR tubes under vacuum (section
4.3:2). TMS was used as an internal reference in all cases. The
chemical shifts of the methyl groups in each sample were measured

130

relative to the proton resonance in the reference TMS. The Varian Associates HA 100 D NMR spectrometer was employed for these measurements under lock conditions and at a temperature of 33°C. The experimental chemical shifts are given in Table 4.2, and the change in the chemical shifts of each methyl group on changing from CCl_4 to TMS as solvents ($\delta\ CCl_4 - \delta\ TMS$) are tabulated also. The assignment of the methyl groups chemical shifts are either based on the literature[100] or by correlation to the structural environment and the electronic effect on the deshielding of the resonant nuclei. However, there was uncertainty in the assignment of the methyl groups b and c in Camphor, but this seems to have no effect on the subsequent correlation.

It was necessary to calculate the contribution to the screening due to the reaction field for each solute in each solvent. Table 4.3 shows the data required for the reaction field calculations for all systems. Table 4.4 gives the calculated total mean square reaction field $< R^2_T >$ and its contribution to the screening constant σ_{RF} in each solvent using the deduced B value[64] of 0.87×10^{-18} e.s.u. Also the difference in the reaction field contribution to the screening constant on changing from CCl_4 to TMS as solvent $\Delta^{C-T}\sigma_{RF}$ is tabulated.

In order to isolate the term representing the true difference in the buffeting interaction to the nuclear screening, equation (4.11) was used. The relevant data are given in Table (4.5).

SOLUTE	CH_3 Position	δ_o^C in CCl_4 H_z	δ_o^T in TMS H_z	$\delta^C - \delta^T$ Expr. H_z
Camphor	a	-94.5	-93.0	-1.5
	b	-85.5	-86.1	+0.6
	c	-82.8	-80.8	-2.6
Pinene	a	-162.6	-162.4	-0.2
	b	-81.3	-85.2	+3.9
	c	-125.4	-126.4	+1.0
Fenchone	a	-99.6	-97.3	-2.3
	b	-99.6	-97.3	-2.3
	c	-108.9	-108.2	-0.7
Menthol	a	-91.15	-91.65	+0.5
	b	-90.9	-90.65	-0.25
	c	-79.15	-80.5	+1.35
P-Cymene	a	-228.5	-224.5	-4.d
	b	-122.2	-121.4	-0.8
Paroldehyde		-128.5	-128.0	-0.5
Durene		-214.8	-212.8	-2.0
Mesitylene		-222.0	-216.6	-5.4
P-Xylene		-227.1	-223.2	-3.9
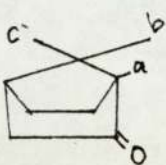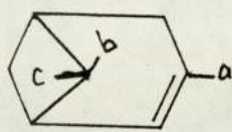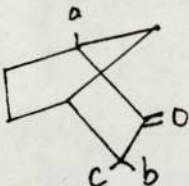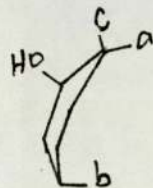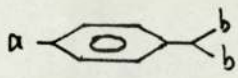
P.T.θ →

Toluene   -234.0   -230.0   -4.0

Table 4.2   The 100 MHz chemical shifts at 33°C of the methyl groups of selected molecules from internal TMS at infinite dilution in CCl_4 δ^c and TMS δ^T, and the difference between them ($\delta^c-\delta^T$). Locking was on the ^1H in TMS.

133

Sample	r A$^\circ$	α cm$^3/10^{-23}$	I erg$/10^{-12}$	Vm cm$^3/10^{-22}$	n_D^2
Camphor $C_{10}H_{16}O$	3.948	1.778	13.46	2.1	2.3907
Pinene $C_{10}H_{16}O$	4.261	1.77	12.93	2.64	2.1486
Menthol	4.381	1.983	13.458	2.87	2.1316
P-Cymene	4.239	1.725	12.02	2.60	2.2278
Paralolehyde	4.016	1.343	14.4	2.21	1.9737
Durene	4.266	1.725	12.9	2.65	2.2849
Mesitylene	4.074	1.551	13.46	2.307	2.2482
P-Xylene	3.916	1.3775	14.04	2.05	2.2374
Toluene	3.726	1.204	14.74	1.765	2.2383
TMS	4.079	1.19	15.7	2.316	1.8266
CCl_4	3.613	1.05	18.3	1.61	2.1144

Table 4.3 Data of the selected samples used
for reaction field calculations. Collected
from ref (61, 84, 29, 101, 102)

r   Molecular Radius

α Polarizibility

I   Ionization Potential

n_D Refractive Index

Solute	$<R_T^2>/10^{11}$ e.s.u. in solvent		$<R_T^2> - <R_T^2>/10^{11}$ e.s.u. CCl_4 TMS	$(\overset{C}{\delta}R.F - \overset{T}{\delta}R.F)$ Hz 100 MHz
	CCl_4	TMS		
Camphor	2.823	0.9667	1.856	-16.15
Pinene	2.925	0.8608	2.064	-17.95
Fenehone	2.952	0.8712	2.081	-18.1
Menthol	3.062	0.8905	2.172	-18.89
P-Cymene	2.876	0.8411	2.035	-17.71
Paraldehyde	2.662	0.8421	1.820	-15.84
Durene	2.925	0.8578	2.067	-17.98
Mesitylene	2.795	0.8667	1.928	-16.77
P-Xylene	2.703	0.8819	1.821	-15.84
Toluene	2.638	0.9243	1.714	-14.91
TMS	2.714	0.8145	1.899	-16.52

Table 4.4   Reaction fields calculated for various solutes in CCl_4 and TMS, and the reaction field screening difference on changing from these two solvents taking B for the methyl C-H bond as 0.87 x 10^{-18} e.s.u (from Homer and Percival). The last column in Hz (100 MHz).

SOLUTE	CH$_3$	$\delta^C - \delta^T$ 100 HHz Exp	$\sigma_{R.F}^{C-T}$ Hz	$\delta_{Exp}^{C-T} - \sigma_{R.F}^{C-T}$ / Hz
	a	−1.5		14.65
	b	+0.6	−16.15	16.75
	c	−2.6		13.55
	a	−0.2		17.75
	b	+3.9	−17.95	21.85
	c			18.95
	a	−2.3		15.8
	b	−2.3	−18.1	15.8
	c	−0.7		17.4
	a	+0.5		19.39
	b	−0.25	−18.89	18.69
	c	+1.35		20.24
	a	−4.0	−17.71	13.71
	b	−0.8		16.91
Paraldehyde		−0.5	−17.84	11.94
Durene		−2.0	−17.98	15.98
Mesitylene		−5.4	−16.77	11.37
P.Xylen		−3.9	−15.84	11.94
Toluene		−4.0	−14.91	10.91
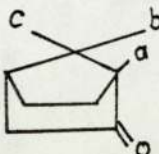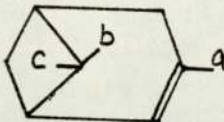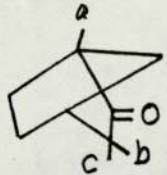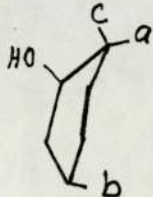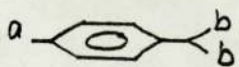
<u>Table 4.5</u> The isolated buffeting screening differece for selected solutes from being in CCl$_4$ to TMS solvents.

Therefore, the effect of the buffeting interaction on nuclear screening in a solute on changing between two solvents may be analysed using equation (4.11). Consequently, the validity of this theory may be checked by ploting the term representing $f(\beta, \xi)$, the first term of the right hand side of equation (4.11) given by equation (4.14), against the left hand side of equation (4.11). This requires the evaluation of the geometrical buffeting parameters. The way this was done is as follows:

The β and ξ values for each methyl group were estimated using "Courtauld Atomic Models" to represent the solute molecules and spheres of appropriate sizes[84] for the encountering solvent molecules. The β and ξ values estimated in this way are probably reasonably accurate, because independent checks with Percival's values proved satisfactory.

The method described in section (4.2:2) was followed. For accuracy, the parameters were obtained for four octants based on each proton in the methyl group and the twelve values were averaged overall. The intention of this was to take into consideration the freedom of rotation of the methyl groups in the molecule. All the parameters were distance modulated using equations (4.19 to 4.21). Table (4.6) gives the values of β'_T and ξ'_T for all the methyl groups when they are buffeted by CCl_4 as solvent, and β_T and ξ_T when they are buffeted by TMS as solvent.

	CH₃	CCl₄ (Buffeting molucule-solvent) TMS					
Solute	Position	β'_T	ξ'_T	$(2\beta' - \xi')^2$	β_T	ξ_T	$(2\beta - \xi)^2$
a	a	0.715	0.708	0.521	0.738	0.654	0.676
	b	0.754	0.738	0.592	0.716	0.665	0.588
Camphore	c	0.754	0.738	0.592	0.716	0.665	0.588
	a	0.843	0.868	0.669	0.778	0.815	0.549
	b	0.665	1.042	~ 0.085	0.667	0.98	0.125
Pinene	c	0.743	0.757	0.531	0.738	0.651	0.681
	a	0.801	0.95	0.425	0.768	0.773	0.426
	b	0.718	0.972	0.215	0.706	0.883	0.28
Fenchone	c	0.674	0.85	0.248	0.631	0.815	0.2
	a	0.66	0.9	0.176	0.66	0.81	0.057
	b	0.645	0.85	0.194	0.642	0.815	0.22
Menthol	c	0.583	0.93	0.056	0.583	0.075	0.085
	a	0.862	0.85	0.764	0.8	0.815	0.616
	b	0.718	0.716	0.518	0.665	0.623	0.5
P.Cymene							
Paraldehyde		0.962	0.885	1.08	0.917	0.815	1.038
Durene		0.743	0.85	0.404	0.7	0.815	0.342
Mesitylene		0.862	0.85	0.764	0.8	0.815	0.616
P.Xylene		0.862	0.85	0.764	0.8	0.815	0.616
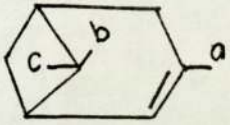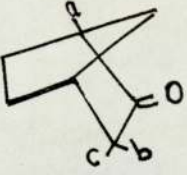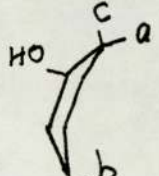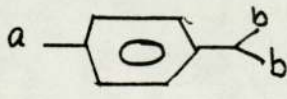
Toluene   0.88   0.85   0.828   0.83   0.815   0.714

Table 4.6   The buffeting geometrical pamometers for selection of complex molecules using two different buffeting molecules (solvents) CCl_4 and TMS.

139

Equation 4.14 can be applied to find the difference in the buffeting due to using CCl_4 and TMS as solvents, and this is given by:

$$\left(\sigma_{BI}^{CCl_4} - \sigma_{BI}^{TMS} \right) = \frac{-BK^H}{r^6_{HH}} \left[\Delta(2\beta' - \xi')^2 - (2\beta - \xi)^2 \right] \cdot (4.25)$$

where,

$$\Delta = \left(\frac{r_{HH}}{r_{HCl}} \right)^6 Q^{Cl}$$

The values of the left hand side of equation 4.11, $(\Delta\delta^{c-T}_{exp} - \Delta {}^{c-T}_{\sigma}{}_{RF})$ can now be correlated with the function of the geometrical buffeting parameters from equation 4.22, $\left[\Delta(2\beta' - \xi')^2 - (2\beta - \xi)^2 \right]$. Theoretically this plot should give a straight line of slope equal to $(-100\ BK^H)/r^6_{HH}$ and y-intercept equivalent to $- ({}^{CCl4}_{\sigma}{}_{w} - {}^{TMS}_{\sigma}{}_{w})$ for the reference, in equation 4.11.

Accordingly, the correlations were carried out trying different values of Δ, and the linear regressions for each value was tested. The correlated data and the analysis of the regressions are shown in Table 4.7, which demonstrates that the best regression is found when using $\Delta = 1.2$ with correlation coefficient of 0.7, slope of -17.08 and y-intercept of 18.1 Hz or $\Delta = 1.0$, y-intercept of 16.4, slope = -14.91 and correlation coefficient of -0.44, overall the former is probably the best

$$\Delta(2\beta' - \zeta') - (2\beta - \zeta)^2$$
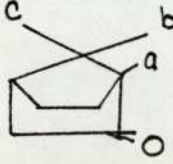
Solute	CH_3	$\Delta = .7$	$\Delta = .8$	$\Delta = .9$	$\Delta = 1.0$	$\Delta = 1.1$
Camphor	a_1	-0.311	-0.259	-0.207	-0.155	-0.103
	b_2	-0.174	-0.114	-0.055	+0.004	+0.063
	c_3	-0.174	-0.114	-0.055	+0.004	+0.063
Pinene	a_4	-0.081	-0.014	+0.053	+0.12	+0.187
	b_5	-0.066	-0.057	-0.049	-0.04	-0.032
	c_6	-0.309	-0.256	-0.203	-0.15	-0.097
Fenchone	a_7	-0.129	-0.086	-0.044	-0.001	+0.042
	b_8	-0.13	-0.108	-0.087	-0.065	-0.044
	c_9	-0.026	-0.002	+0.023	+0.048	+0.073
Menthol	a_{10}	+0.066	+0.084	+0.101	+0.119	+0.137
	b_{11}	-0.084	-0.065	-0.045	-0.026	-0.007
	c_{12}	-0.046	-0.04	-0.045	-0.029	-0.023
P-Cymene	a_{13}	-0.081	-0.005	+0.0716	+0.148	+0.224
	b_{14}	-0.137	-0.086	-0.034	+0.018	+0.07
Paralolehyde	15	-0.282	-0.174	-0.066	+0.042	+0.15
Durene	16	-0.059	-0.019	+0.022	+0.062	+0.102
Mesitylene	17	-0.081	-0.005	+0.0716	+0.148	+0.224
P-Xylene	18	-0.081	-0.005	+0.0716	+0.148	+0.224
Tolnene	19	-0.134	-0.052	+0.031	+0.114	+0.197
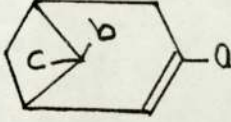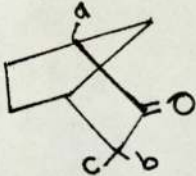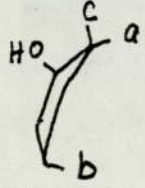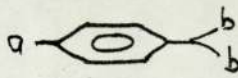
141

$$\Delta \cdot (2\beta' - \zeta)^2 - (2\beta - \zeta)^2$$

Solute	CH_3	$\Delta = .7$	$\Delta = .8$	$\Delta = .9$	$\Delta = 1.0$	$\Delta = 1.1$
Correlation Coefficient		0.31	0.1	-0.21	-0.44	-0.6
Slope		10.06	2.4	-7.54	-14.91	-17.4
Y-intercept		17.2	16.15	15.8	16.4	17.3
B Value$/_{10}18$		-0.14	-0.034	0.11	0.21	0.24

$\Delta = 1.2$	$\Delta = 1.3$	$\Delta = 1.4$	$\Delta = 1.5$	$\Delta = 1.6$	$\Delta = 1.7$	$\dfrac{(\delta^C - \delta^T)_{\text{Exp}}}{\left(\sigma_{RF}^C - \sigma_{RF}^T\right)_{\text{Cal.}}}$
−0.051	+0.001	+0.053	+0.106	+0.1576	+0.21	14.65
+0.122	+0.182	+0.241	+0.3	+0.359	+0.418	16.75
+0.122	+0.182	+0.241	+0.3	+0.359	+0.418	13.55
+0.254	+0.321	+0.388	+0.455	+0.521	+0.588	17.75
−0.023	−0.015	−0.006	+0.003	+0.011	+0.02	21.85
−0.044	+0.009	+0.062	+0.116	+0.169	+0.222	18.95
+0.084	+0.127	+0.169	+0.212	+0.254	+0.297	15.8
−0.022	0	+0.021	+0.043	+0.064	+0.086	15.8
+0.098	+0.122	+0.147	+0.172	+0.197	+0.222	17.4
+0.154	+0.172	+0.189	+0.207	+0.225	+0.242	19.39
+0.013	+0.032	+0.052	+0.071	+0.09	+0.11	19.69
+0.01	+0.005	−0.001	−0.007	−0.012	−0.018	20.24
+0.301	+0.377	+0.454	+0.53	++0.606	+0.683	13.71
+0.1216	+0.173	+0.225	+0.277	+0.329	+0.381	
+0.258	+0.366	+0.474	0.582	+0.69	+0.798	11.94
+0.143	+0.183	+0.224	+0.264	+0.304	+0.345	15.98
+0.301	+0.377	+0.454	+0.53	+0.606	+0.683	11.37
+0.301	+0.377	+0.454	+0.53	+0.606	+0.683	11.94
+0.24	+0.362	+0.445	+0.528	+0.611	+0.694	10.91

P.T.D →

$\Delta = 1.2 \quad \Delta = 1.3 \quad \Delta = 1.4 \quad \Delta = 1.5 \quad \Delta = 1.6 \quad \Delta = 1.7$

r	-0.69	-0.74	-0.77	-0.79	-0.81	0.81
m	-17.08	-15.7	-14.1	-12.6	-11.4	-10.28
c	18.1	18.7	19.2	19.46	19.7	19.8
$\dfrac{B/-18}{10}$ e.s.u	0.24	0.22	0.2	0.18	0.16	0.14

<u>Table 4.7</u>: Analysis of the regression of $(\overset{C}{\delta} - \delta^T)_{exp} - (\sigma_{RF}^C - \sigma_{RF}^T)_{Cal}$ on $\Delta(2\beta' - \xi')^2 - (2\beta - \xi)^2$

144

correlation and Figure 4.5 shows this regression together with the theoretical line (broken). The regression of using $\Delta = 1.2$ enables a B value of 0.24×10^{-18} e.s.u. to be deduced from the slope which is in reasonable agreement with theoretical value of Homer and Percival of 0.87×10^{-18} e.s.u.; and also it gives from the y-intercept a value of -18.1 Hz for $(\sigma_W^C - \sigma_W^T)^{TMS}$ which is in good agreement with the experimental value of -14.3 Hz obtained in section 4.4. The value of 1.2 for Δ implies, because of the definition of the latter, that, using $r_{HH} = 2.4 \times 10^{-8} cm^{(84)}$ and $r_{HCl} = 3.0 \times 10^{-8} cm^{(84)}$, the Hartree Fock scaling factor Q for Chlorine is 3.2. The value obtained by Homer and Percival is $6.5^{(64)}$.

The above results may be taken as encouraging because of the non-spherical nature of the systems used in this investigation. In fact the solutes used were complicated molecules and their chemical shifts may be affected by, for example, σ_E for which no allowance has been made.
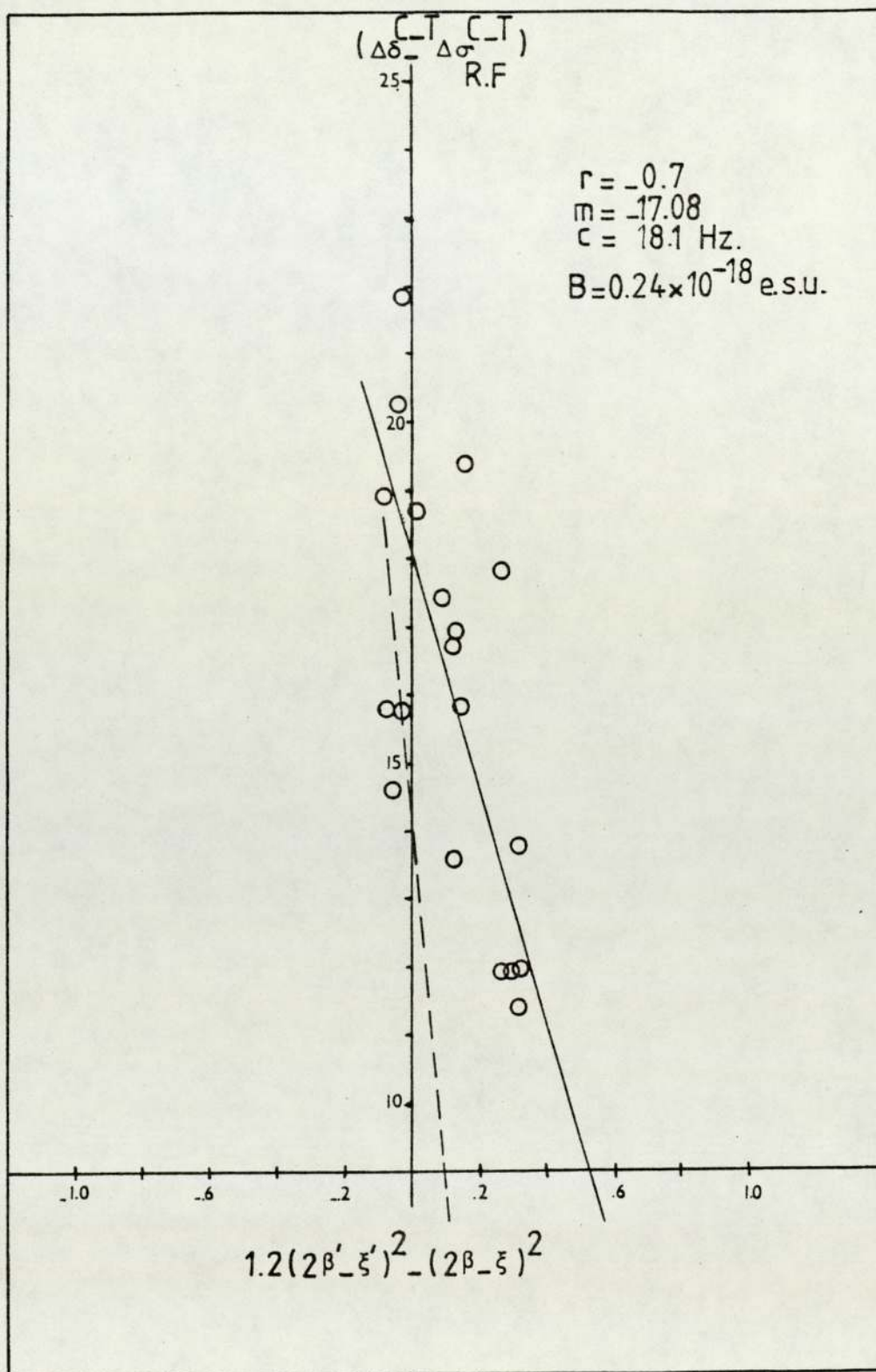
Figure 4.5   Regression of $1.2 \, (2\beta' - \xi')^2 - (2\beta - \xi)^2$ on
$(\delta^c - \delta^T) - (\sigma^c_{RF} - \sigma^T_{RF})$ for the methyl protons.

146

4.6 <u>APPLICATION OF BUFFETING THEORY TO ARYL PROTON</u>

<u>SOLVENT INDUCED CHEMICAL SHIFTS:</u>

As a further test of buffeting theory the solvent induced ^{1}H shifts of aryl protons in different steric positions were investigated.

This study was made for two reasons. First because the B values of these protons are expected to be different from the B values for the methyl protons studied earlier and the magnitude of the buffeting effect may be different. Second because the aromatic molecules have high electron density on the ring and this may influence the solvent interaction and hence the buffeting parameters i.e. collisions may be favoured with the π system (to form transient molecular complexes) rather than with the peripheral atoms or vice versa.

The aromatic molecules selected for study were Benzene, Toluene, P-Xylene, Mesitylene and Durene. The same overall approach was used as described in section (4.2). Each of the solutes were dissolved in the two solvents CCl_4 and TMS at a concentration of 1 mol %. The solutions were transferred to 5mm OD NMR tubes and sealed under vacuum as described in section (4.3:2). Employing the Varian Associates HA 100 D NMR spectrometer, the chemical shifts from the internal lock TMS were measured for each aryl proton in each sample in the two solvents. These chemical shifts are given in Table (4.8), together with the differences in the chemical shifts on changing from CCl_4 to TMS as

147

Solute	δ^{CCl_4}	δ^{TMS} Hz	$(\delta^C - \delta^T)$	$<R_T^{2C}> - <R_T^{2T}> / 10^{12}$ e.s.u.
Benzene	−725.4	−721.6	−3.8	0.16156
Tolnene	−707.65	−705.8	−1.85	0.17138
P−Xylene	−693.1	−692.4	−0.7	0.1821
Mesitylene	−665.1	−665.9	+0.8	0.1928
Durene	−673.9	−675.6	+1.7	0.2067

Table (4.8)   The chemical shifts of the aryl protons in methyl
substituted benzenes in CCl_4 and TMS. Shifts are
in Hz at 100 MHz from TMS as internal reference;
the solutes were at offective infinite dilution.
The measurements were made at $33^{\circ}C$ using a Varian
Associates HA 100 D NMR spectrometer.

solvents. The appropriate differences between the total reaction fields ($< R^2_T >_C - < R^2_T >_T$) are given in Table (4.8) also. Table 4.9 shows the relevant data for Benzene. Following the approach described in section (4.4) the values of the total buffeting parameters were deduced in both CCl_4 and TMS as buffeting molecules. These are given in Table (4.10).

Because the value of B for aryl protons is not known with certainty, the reaction field screenings were deduced using different values of B, around the value estimated by Homer and Percival (0.66 x 10^{-18} e.s.u.). Table 4.11 shows the values of ($\delta^C - \delta^T$) - ($\sigma^C_{RF} - \sigma^T_{RF}$) (see equation (4.11)) using B equal to (0.4, 0.5, 0.6, 0.7, 0.8) x 10^{-18} e.s.u. for the aryl protons. The values of $\Delta(2\beta' - \xi') - (2\beta - \xi)^2$ are given in Table 4.12, where Δ is set equal to 0.8, 0.9, 1.0, 1.1, 1.2, 1.3, 1.4 and 1.5, 1.6, 1.7. A matrix set of regressions of ($\delta^C - \delta^T$) - ($\sigma^C_{RF} - \sigma^T_{RF}$) on $\Delta(2\beta' - \xi') - (\beta - \xi)^2$ was carried out, and Table 4.13 gives the values of the term - ($\sigma^C_W - \sigma^T_W$) so deduced for the reference TMS (from the y-intercept), together with the B values extracted from the slopes of the regressions. It is evident from the results of these regressions that are given in Table 4.13 that no satisfactory correlation was obtained. This may not be too surprising because it has been mentioned in the literature that specific interaction between the aryl protons in substituted Benzene and the solvents may occur [88,89,90]. These interactions modify the effective σ_W for the aryl protons. It is now proposed that this type of effect operates in the present solutions and

Molecular radius r 3.51×10^{-8} cm

Polarizibility α 1.0302×10^{-23} cm^{-3}

Molecular Volume Vm 1.467×10^{-22} cm^3

Ionization Potential I 15.0595×10^{-12} erg

(Refractive Index)^2 n_C^2 2.2533

$< R_T^2 >$ in CCl$_4$ 0.262×10^{-12} e.s.u.

$< R_T^2 >$ in TMS 0.1005×10^{-12} e.s.u.

$(< R_T^{2^T} > - < R_T^{2^T} >)/_{10}12$ 0.16156 e.s.u.

Table (4.9)   The relevant data for benzene (84, 101, 102).

150

Solute	CCl$_4$ Buffeting Molecule			TMS Buffeting Molecule		
	β_T'	ξ_T'	$(2\beta' - \xi')^2$	β_T	ξ_T	$(2\beta - \xi)^2$
Benzene	0.95	1.04	0.74	0.92	0.755	1.178
Toluene	0.95	1.04	0.74	0.92	0.755	1.178
P-Xylene	0.88	0.95	0.656	0.83	0.74	0.846
Mesitylene	0.76	0.8	0.518	0.68	0.705	0.429
Durene	0.76	0.8	0.518	0.68	0.705	0.429

Table (4.10   The geometrical buffeting parameters for several methyl substituted benzene.

Solute	$\langle R^2_C T\rangle - \langle R^2_T T\rangle$ $/10^{12}$ e.s.u.	$\delta^C - \delta^T$ $/10^{-18}$ e.s.u.	$(\delta^C - \delta^T) - \left[-B(\langle R^2_C T\rangle - \langle R^2_T T\rangle)\right]$ Hz/100 MHz				
			B = 0.4	B = 0.5	B = 0.6	B = 0.7	B = 0.8
Benzene	0.16156	-3.8	2.66	4.28	5.89	7.51	9.12
Toluene	0.17138	-1.85	5.01	6.72	8.43	10.15	11.86
P-Xylene	0.1821	-9.7	6.58	8.41	10.23	12.05	13.87
Mesitylene	0.1928	+0.8	8.51	10.44	12.37	14.3	16.22
Durene	0.2067	+1.7	9.97	12.04	14.10	16.17	18.24

Table (4.11)   The values of $(\delta^C - \delta^T) - (\sigma^C_{RF} - \sigma^T_{RF})$ using different values of B, for the aryl protons in various methylated benzenes.

for $\Delta(2\beta' - \xi')^2 - (2\beta - \xi)^2$

Solute	Δ = 0.8	Δ = 0.9	Δ = 1.0	Δ=1.1	Δ = 1.2	Δ = 1.3	Δ = 1.4	Δ = 1.5	Δ = 1.6	Δ = 1.7
Benzene	-0.59	-0.51	-0.44	-0.364	-0.29	-0.22	-0.14	-0.07	+0.004	+0.08
Toluene	-0.54	-0.51	-0.44	-0.364	-0.29	-0.22	-0.14	-0.07	+0.004	+0.08
P-Xylene	-0.321	-0.256	-0.19	-0.124	-0.059	+0.007	+0.072	+0.138	+0.203	+0.27
Mesitylene	-0.015	+0.037	+0.089	+0.141	+0.193	+0.244	+0.296	+0.348	+0.4	+0.45
Durene	-0.015	+0.037	+0.089	+0.141	+0.193	+0.244	+0.296	+0.348	+0.4	+0.45

Table (4.12) The difference between the buffeting parameter $(2\beta - \xi)^2$ for methyl benzenes on changing from CCl_4 to TMS as solvent.

$$\Delta (2\beta - \xi)^2 - (2\beta - \xi)^2$$

$B/_{10}{-}18$		Δ 0.8	0.9	1.0	1.1	1.2	1.3	1.4	1.5
0.4	c	9.42	8.92	8.37	7.77	7.11	6.42	5.59	4.75
	m	9.39	9.87	10.21	10.7	11.18	11.64	12.39	12.93
	r	0.94	0.94	0.94	0.94	0.94	0.94	0.94	0.94
0.5	c	11.43	10.91	10.31	9.67	8.98	8.2	7.37	6.47
	m	0.97	10.48	10.84	11.36	11.8	12.37	13.16	13.37
	r	0.94	0.94	0.94	0.94	0.94	0.94	0.94	0.94
0.6	c	13.44	12.87	12.25	11.57	10.84	10.06	9.13	8.15
	m	10.56	11.09	11.48	12.02	12.57	13.09	13.93	12.71
	r	0.94	0.94	0.94	0.94	0.94	0.94	0.94	0.94

$B/10^{-18}$		Δ	0.8	0.9	1.0	1.1	1.2	1.3	1.4	1.5
0.7	c		15.44	14.85	14.19	13.48	12.7	11.88	10.91	9.91
	m		11.13	11.7	12.1	12.68	13.26	13.8	14.69	15.32
	r		0.94	0.94	0.94	0.94	0.94	0.94	0.94	0.94
0.8	c		17.4	16.8	16.1	15.38	14.57	13.7	12.67	11.62
	m		11.71	12.31	12.73	13.3	13.95	14.5	15.46	16.12
	r		0.94	0.94	0.94	0.94	0.94	0.94	0.94	0.94

Table 4.13 Linear regression analysis of $f(\beta, \xi)$ on the isolated buffeting screening for the aryl protons.

that the complex experimental shifts may be unravelled by the use of buffeting theory.

The approach adopted was based on the idea that the present solvent-solute interactions are essentially between the π electrons of the Benzene ring of the solute system and the solvent molecule. Because of the distances involved, it is proposed that this interaction will have its major effect on the aryl protons, with negligible effect on the substituted methyl groups. The approach was to estimate the effect of this type of interaction on the buffeting parameters of the aryl protons, since they are the factors most likely to be affected. The previous analysis involved trying to correlate the term $\Delta (2 \beta' - \xi')^2 - (2\beta - \xi)^2$ with the corresponding isolated difference in buffeting screening. It now is assumed that the former term should be modified due to specific solute-solvent interactions. If equation 4.11 is rearranged and rewritten in the following form:

$$(\delta^C - \delta^T) - \left[- B_H (< R^2_T >^C - < R^2_T >^T) \right] + (\sigma_w^C - \sigma_w^T)^r = - B_H K/r^6 E \left[\Delta(2 \beta' - \xi') - (2\beta - \xi)^2 \right] \dots\dots\dots\dots\dots\dots (4.26)$$

where E represents an effect of the interaction on the term representing the buffeting.

It was demonstrated before in this section that there is no satisfactory correlation when the above equation used without E. The intention now is to use equation 4.26 to calculate E values for the aryl protons. This was carried out by finding the values

156

of the right hand side of equation 4.26 using the same range of B values as before. These are given in Table 4.14. The term $(\ _{\sigma_w}^C - \ _{\sigma_w}^T)^{TMS}$ represents the difference between the van der Waals screening of the reference TMS in changing from CCl_4 to TMS as solvent; this term was taken to be $- 14.3$ Hz as deduced earlier in this chapter (section 4.4). The values recorded in Table 4.14 were then divided by $(- BK^H/r^6_{HH})$ for the appropriate B values, these terms are also given in Table (4.14), in order to find an "experimental" value for the modulated term $E \left[\Delta (2 \beta' - \xi')^2 - (2\beta - \xi)^2 \right]$. The values of the latter term are shown in Table 4.15.

The values in Table 4.15 were correlated with the number of methyl groups substituted in the Benzene ring; the results of the regression analyses are given in Table 4.16. These regressions show a perfectly linear dependence on the number of methyl groups substituted on the Benzene ring. Therefore $E_{C/T}$ can be represented as a linear function of N, the number of methyl groups.

Accordingly, the effect of interaction arising from interactions with CCl_4 may be represented by:

$$E'_C = m' N + C' \dots\dots\dots\dots\dots\dots\dots\dots\dots\dots\dots\dots \quad (4.27)$$

and similarly the effect of the interaction arising from the effect of TMS is:

157

Solute	$(\delta^C - \delta^T) - \left[- B (<R_T^{2C}> - <R_T^{2T}>)\right] + (\sigma_w^C - \sigma_w^T)\,^{TMS}$				
$B/10^{-18}$	0.4	0.5	0.6	0.7	0.8
Benzene	-11.64	-10.02	-8.41	-6.79	-5.18
Toluene	-9.29	-7.58	-5.87	-4.15	-2.44
P-Xylene	-7.72	-5.89	-4.07	-2.25	-0.43
Mesitylene	-5.79	-3.86	-1.93	0	+1.92
Durene	-4.33	-2.26	-0.2	+1.87	+3.94
$-BK/r^6$ (Hz)	-28.43	-35.67	-42.8	-49.93	-57.06

Table (4.14)   The experimentally isolated buffeting difference with
the reference van der Waals screening differce on
changing from CCl_4 to TMS solvents, for the benzene
methylated system.

158

Values of $E\left[\Delta(2\beta' - \xi')^2 - (2\beta - \xi)^2\right]$

Solute

$B/10^{-18}$ e.s.u.	0.4	0.5	0.6	0.7	0.8
Benzene	+0.409	+0.281	+0.196	+0.136	+0.091
Toluene	+0.327	+0.213	+0.137	+0.083	+0.043
P-Xylene	+0.272	+0.165	+0.095	+0.045	+0.008
Mesitylene	+0.204	+0.108	+0.045	0	-0.034
Durene	+0.152	+0.063	+0.005	-0.037	-0.069

Table (4.15)   The experimentally isolated $E\left[\Delta(2\beta' - \xi')^2 - (2\beta - \xi)^2\right]$ using different B values.

Regression analysis	B value $/10^{-18}$ e.s.u.				
	0.4	0.5	0.6	0.7	0.8
Correlation	1	1	1	1	1
Slope	-0.0637	-0.0541	-0.0474	-0.042	-0.0397
Y-intercept	0.4002	0.2732	0.1904	0.132	0.0872

Table (4.16)   Analysis of the linear regression of E f (β, ξ) on the number of methyl groups substituted on the benzene ring.

$$E_T = m \, N + C \; \ldots\ldots\ldots\ldots\ldots\ldots\ldots\ldots\ldots\ldots\ldots\ldots\ldots\ldots\ldots\ldots\ldots\ldots \; (4.28)$$

where the m, m' and C, C' are the slopes and the y-intercepts of the linear dependence of E and E' on the number of methyl groups N in the case of TMS and CCl_4 as solvents respectively. This is not unexpected because for analogues interactions with methyl Benzenes ΔG^{o} for complex formation is thought to vary systematically with the number of methyl substituents [107]. E in equation 4.26 is evidently a complex parameter that includes a combination of the difference of the interaction effects of TMS and CCl_4 with the π electrons in the Benzene ring. Therefore the experimentally obtained values in Table 4.15 can be represented as a combination of a difference of two linear functions, and having the following form:

$$E \left[\Delta (2\beta' - \xi')^2 - (2\beta - \xi)^2 \right]_{exp} =$$

$$(m' \, N + C') \left[\Delta (2\beta' - \xi')^2 \right] - (m \, N + C) \left[(2\beta - \xi)^2 \right] \; \ldots\ldots \; (4.29)$$

For simplicity it will be assumed that m = m' and C = C'; there is, however, no reason why they should be equal and indeed there is no basis for such an assumption because it has been demonstrated that $E_C \neq E'_T$. Nevertheless, accepting this assumption, that would provide for the most analytical conditions, equation 4.29 can be rewritten as:

$$E \left[\Delta (2 \beta' - \xi')^2 - (2\beta - \xi)^2 \right]_{exp} =$$

$$(m N + C) \left[\Delta (2 \beta' - \xi') - (2\beta - \xi)^2 \right] \quad \ldots\ldots\ldots\ldots\ldots\ldots\ldots (4.30)$$

This can be rearranged to show a linear dependence of E on N as follows:

$$E \left[\Delta (2 \beta' - \xi')^2 - (2\beta - \xi)^2 \right]_{exp} =$$

$$Nm \left[\Delta (2 \beta' - \xi')^2 - (2\beta - \xi)^2 \right] + C \left[\Delta (2 \beta' - \xi')^2 - (2\beta - \xi)^2 \right]$$

$$(4.31)$$

If the above equation is valid there can be no linear dependence of the left hand side of the above equation on the value of N because $\Delta (2 \beta' - \xi')^2 - (2\beta - \xi)^2$ is a variable. In fact the regressions observed are linear.

The only interpretation of this in terms of an equation of the form of 4.31 is that both $m \left[\Delta (2 \beta' - \xi')^2 - (2\beta - \xi)^2 \right]$ and $C \left[\Delta (2 \beta' - \xi')^2 - (2\beta - \xi)^2 \right]$ are in fact constant. This would be consistent with them both being representative of the situation in Benzene with the variation among the methylated Benzene being dependent on the operation of N on the former term only. The y-intercept would then represent the value when N = 0 i.e. for Benzene.

In order to be consistent with the observed data, equation 4.31 has to be rewritten as:

$$E \left[\Delta (2\beta' - \xi')^2 - (2\beta - \xi)^2 \right]_{exp} = Nk \left[\Delta (2\beta' - \xi')^2 - \right.$$

$$\left. (2\beta - \xi)^2 \right]_{\phi} - C \left[\Delta (2\beta' - \xi')^2 - (2\beta - \xi)^2 \right]_{\phi} \dots\dots\dots (4.32)$$

and this can be arranged as:

$$E \left[\Delta(2\beta' - \xi')^2 - (2\beta - \xi)^2 \right]_{exp} =$$

$$(Nk - C) \left[\Delta (2\beta' - \xi')^2 - (2\beta - \xi)^2 \right]_{\phi} \dots\dots\dots\dots\dots (4.33)$$

It can be seen from the above equation that there are three unknowns Δ, C and k that makes it impossible to solve with the available data. This conclusion warns that the use of σ_{BI} to elucidate molecular structure may be difficult when the solute of interest interacts specifically with the buffeting solvents.

4.7 CONCLUSION

This chapter demonstrates that the induced solvent shifts due to molecular encounters may, by inverting the analyses employed here, be used to elucidate local features of molecular structure in quite complicated molecules in a liquid phase.

No gas-to-solution chemical shifts were needed to analyse solvent buffeting effects. This was achieved by using two

163

different solvents for the same solute under test.

One further additional point may be deduced and this is that the implicit assumption in the work throughout this chapter that σ_E is unimportant to the proton shifts is satisfactory. This is not altogether unexpected because the corresponding intermolecular linear electric field effect is generally considered negligible for proton screening.

VOLUME MAGNETIC SUSCEPTIBILITY EFFECTS WHEN
USING HETERONUCLEAR FIELD/FREQUENCY LOCK TO
MEASURE NMR CHEMICAL SHIFTS

5.1   **INTRODUCTION**

When evaluating chemical shift differences it is of
paramount importance to effect appropriate corrections for
screening differences arising from the volume magnetic
susceptibilities of the materials used.   This is not so
straightforward as may appear at the first sight when using
modern NMR spectrometers that utilize heteronuclear
field/frequencey lock.

During this work it became evident that the use of the
different locking techniques available when operating the
JEOL FX 90 Q NMR spectrometer, could produce significant
differences between spectral measurements that might not be

widely appreciated. The origin of these differences which are important when using an internal lock compound are independent of the magnetic properties of the observed nucleus, and dependent only on the magnetic properties of the locking nucleus and its environment.

Essentially, this chapter attempts to firmly base the necessary corrections to the bulk volume magnetic susceptibility screening that have to be considered for most common methods of obtaining stabilized NMR spectra using hetero-nuclear field/frequency lock.

5.2   <u>**THE EFFECTS OF LOCKING TECHNIQUES ON VOLUME MAGNETIC**</u>
        <u>**SUSCEPTIBILITY CORRECTION:**</u>

In order to study screening constants other than σ_b, it is necessary to account for the changes in the latter which contribute to the measured chemical shifts. The way this is done depends on the referencing procedure adopted for the determination of the shifts.

For the purpose of the study undertaken in this chapter, both the referencing procedures and the locking systems employed are important. In order to simplify the discussion centred on these two points, a general system will be assured for which it is desired to measure the shifts of the resonance of a particular nucleus x in a compound X at very low

concentration in a solvent A relative to the same nucleus x in X at the same concentration in solvent B. The instrument will be considered field/frequency locked to a heteronucleus c in a compound C and operating under conventional pulsed FT conditions.

The intention here is to deal with the main referencing methods that may be employed when using both iron magnet and superconducting solenoid spectrometers, accordingly three general cases will be considered and the implication of these on volume magnetic susceptibility correction to the measured shifts will be discussed in the following sections:

5.2:1 CASE 1: Field/Frequency Lock Using a Separate Locking Sample in a Second Probe:

Some NMR spectrometers are provided with two separate probes, where one of these probes contains a locking compound while the second one contains the sample of interest. The advantage of this arrangement is that it should avoid any possible interaction between the sample under observation and the reference material or the locking compound used.

In this situation it is possible to measure the chemical shift for x by a substitution method in which X in a solvent A (labelled A) is first investigated in a particular sample tube, and then X in another solvent B (labelled B) is substituted and investigated under the same conditions; identical tubes are

167

best used. The relative positions of the resonances of x and c
are illustrated schematicaly in Figure 5.1a. It is assumed
that the tubes containing, C, the lock material and the samples
referred to above have the same perfect shapes, and have the
same orientation to the static magnetic field.

The volume magnetic susceptibility can be found
classically for each sample separately with no interference
between either of them. Therefore the relationship between the
volume susceptibility corrected shifts, δ^{True}, and the
observed shifts are given by the following equations:

$$\delta^{True \perp}_{A-B} = \delta^{obs. \perp}_{A-B} + \frac{2\pi}{3} (X_B - X_A) \ldots\ldots\ldots (5.1)$$

$$\delta^{True \parallel}_{A-B} = \delta^{obs. \parallel}_{A-B} + \frac{4\pi}{3} (X_A - X_B) \ldots\ldots\ldots (5.2)$$

where equations 5.1 and 5.2 are applicable respectively to the
situations where the axes of the sample tubes are perpendicular
($\perp$)[36,40] and parallel ($\parallel$)[91,29] to the direction of the
magnetic field. In the above equations X_A and X_B are the
volume magnetic susceptibilities of compounds A and B
respectively.
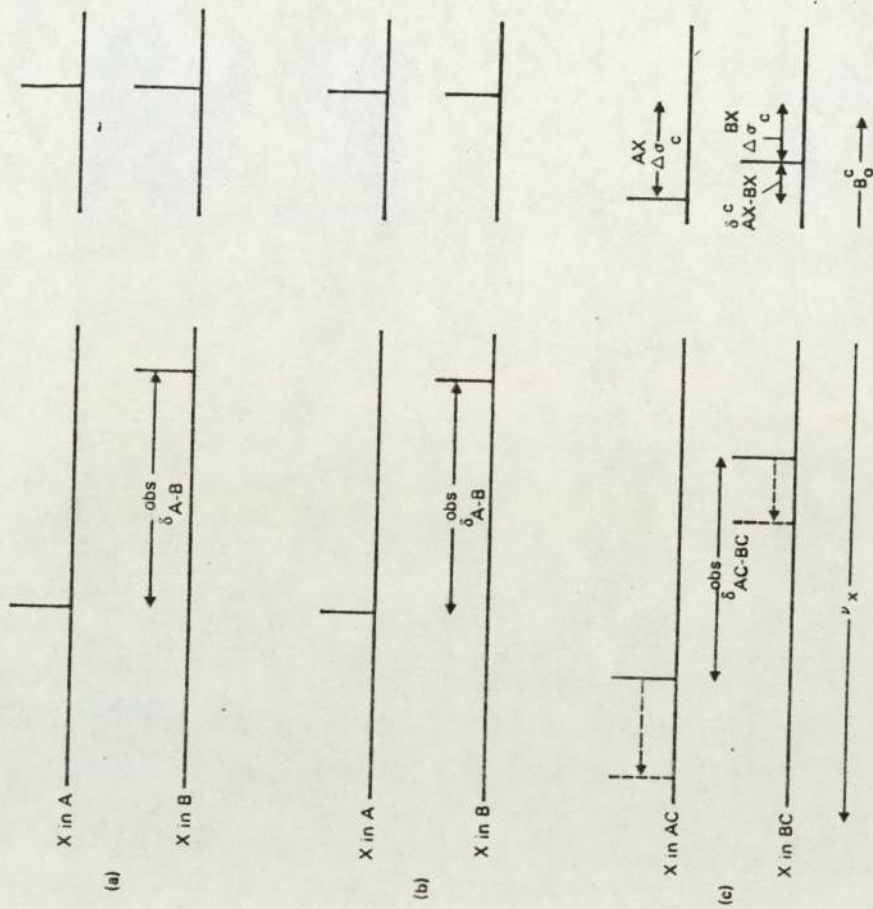
Figure 5.1

Schematic representation of the x and c sprectra of compounds X and C measured (a) with X dissolved in A or B and C in a separate lock probe, (b) with X as in (a) surrounding a co-axial capillary containing C and (c) with X dissolved in mixtures of A and C or B and C.

5.2:2   CASE 2:   <u>Field/Frequency Lock Using a Separate Locking</u>
<u>Sample in a Co-axial Cylindrical Tube:</u>

In this case, the reference material (or the locking material) is kept physically separated from the sample under observation, in a simpler way than the previous case. Usually the sample of interest is placed in a conventional NMR tube, and the locking material (or the reference) is placed in a separate cylindrical tube co-axially with the original NMR tube.

By keeping the material C constant in the inner reference vessel, the shift between x in A and x in B can be measured in two separate experiments that determine the resonance conditions of x in the two solvents.

Inspection Fig 5.1b reveals that the simple situation relevant to the previous case (section 5.2:2) applies to the present situation also, and equations 5.1 and 5.2 again hold. This arises because the samples containing the resonant nuclei are again physically separated and experience the effect of their relevant susceptibility screening constants appropriately given by:

$$\sigma^{||} = -\frac{4\pi}{3} X \quad \dots\dots\dots\dots\dots\dots\dots\dots\dots\dots\dots\dots\dots (5.3)$$

$$\overset{\perp}{\sigma} = + \frac{2\pi}{3} X \quad \dots\dots\dots\dots\dots\dots\dots\dots\dots\dots \quad (5.4)$$

where $\sigma^{||}$ and $\sigma^{\perp}$ are the respective screening constants for the situations when the axes of the sample tubes are parallel($||$)[91,29] and perpendicular($\perp$)[36,40] to the direction of the static magnetic field.

Therefore, provided the lock frequency is the same as in the previous case, there should be no changes in the absolute resonance conditions of c, unlike the case described in the following section.

5.2:3   **CASE 3**   <u>**Field/Frequency Lock Using The Locking Sample**</u>

<u>**Homogeneously Mixed with The Sample Studied**</u>

<u>**(Internal Referencing Procedure)**</u>

The most common method of field/frequency locking is when the locking material (or/and the reference material) are mixed homogeneously with the sample under observation. In this case all the materials are in the same enviroment, so that the relative effects on the screening of the different components will be different to that when they are physically separated as described in sections 5.2:1 and 5.2:2.

When the reference component C is mixed together with the samples to be studied, several changes in the screenings occur relative to those encountered in the previous cases. The

171

nucleus c will suffer the following changes, when used to measure the shift of x in two different samples:

1. Since the material C is mixed homageneously with the solvent and the sample under interest, the properties of the media containing C will be different when using different solvents. Therefore, C may experience different values of, σ_b, bulk susceptibility screening in different samples.

2. In addition to the change in, σ_b, there will be other effects that contribute to the change in the screening of c, <u>viz</u>: σ_w, σ_a, σ_E and σ_s [29, 35]. In the previous case, these could arise from C/C interaction only, while in the current situation these effects additionally arises from X/C and A/C interactions in one sample and due to X/C and B/C in the other sample.

Maintaining the resonance frequencies and the other conditions the same as in the previous cases, the nucleus c will resonate at new values of the applied magnetic field due to the above changes in the screening constant. This is illustrated in Figure 5.1c. The following section will demonstrate the theorectical implication of these effects.

5.3   **NMR LOCK EFFECTS ON CHEMICAL SHIFTS WHEN USING AN**
        INTERNAL REFERENCE:

Following the conclusion of the last section and inspecting Fig 5.1, the difference between the screening of c on changing from an external reference (sections 5.2:1 and 5.2:2) to an internal reference (section 5.2:3) is defined in Figure 5.1 as $\Delta \sigma_c$, and this can be written generally as:

$$\Delta \sigma_c = \Delta \sigma_b + \Delta \sigma_m \quad \dots\dots\dots\dots\dots\dots\dots\dots\dots\dots\dots\dots \quad (5.3)$$

where $\Delta \sigma_b$ is the contribution arises from the difference in the bulk magnetic susceptibility correction, and $\Delta \sigma_m$ represents the contributions due to all the solvent effects mentioned earlier except the volume magnetic susceptibility.

The sign and magnitude of $\Delta \sigma_c$ depends on the components of the samples used and the nature of the locking material. Therefore it is important to appreciate the practical consequences of the factors contributing to $\Delta \sigma_c$ in equation 5.3. Suppose that $\Delta \sigma_c$ amounts to a deshielding of c (This assumption is considered in Fig 5.1c), in order to establish the lock at the original constant frequency it is necessary to reduce the magnitude of the applied field.

Provided that the observed nucleus x is subjected to the same effects, then, whatever the new screening of x may be, as governed by an equation of the same form as 5.3, the absolute

173

reduction in the applied field will demand that its observation frequency (illustrated in full lines in Fig 5.1c) is reduced also. But the extent of this particular change will be different using different solvents. In other words the new screening of x will be different for X in A and C and for X in B and C. The significance of this is that this effect depends only on the magnetic properties of the locking nucleus c and not on those of nucleus x. The practicle outcome of this is that in both samples the nucleus x will appear to be more screened than it really is.

Consequently, before susceptibility correction can be made using equations such as 5.1 and 5.2, the observed resonance frequencies of x must be corrected (to broken lines in Fig 5.1c) by amounts equivalent to the corresponding changes in the screening of c that have to be accommodated when establishing the lock. If the changes in the screening of c, defined by equation 5.3 as $\Delta \sigma_c$, due to changes from pure C to (A and X) and to (B and X) are $\Delta \sigma_c^{AX}$ and $\Delta \sigma_c^{BX}$ respectively, the difference between these can be equated to the required correction δ_{AX-BX}^{c} ppm.

5.4   **MODIFICATION OF THE CLASSICAL VOLUME MAGNETIC SUSCEPTIBILITY CORRECTION EQUATIONS FOR USE WITH FIELD/FREQUENCY INTERNALLY LOCKED REFERENCE SYSTEMS:**

In order to place the quantitative proposals discussed in

section 5.3 on a firmer theoretical base, it is convenient to imagine that the chemical shift between the resonances of the nucleus x in solvents A and B are to be determined using a lock nuclide c in the same samples.

If c resonates at a fixed frequency v^c, the lock signals will be achieved at two different fields B_A and B_B. Consequently, when observing the spectra of x, the fundamental resonance equations that apply are:

$$v_A^x = \frac{\gamma^x}{2\pi} B_A (1 - \sigma A^x) \dots\dots\dots\dots\dots\dots\dots (5.4)$$

and

$$v_B^x = \frac{\gamma^x}{2\pi} B_B (1 - \sigma B^x) \dots\dots\dots\dots\dots\dots\dots (5.5)$$

It follows from these equations that:

$$\frac{v_A^x - v_B^x}{v_B^x} \simeq \frac{B_A - B_B}{B_B} + \sigma B^x - \sigma A^x \dots\dots\dots\dots\dots (5.6)$$

The first term on the right hand side of equation 5.6 can only be assessed in chemical shift terms by measurements at fixed frequency. For these, reference can be made to the resonance equations for the c NMR signals of A and B. If these occur at some field B(constant field) determined by

175

establishing lock on a third nucleus in a separate lock system, the relevant equations are:

$$v_A^c = \frac{\gamma^c}{2\pi} \; B \, (1 - \sigma_A^c) \;\; \dots\dots\dots\dots\dots\dots\dots\dots\dots\dots\dots \;\; (5.7)$$

$$v_B^c = \frac{\gamma^c}{2\pi} \; B \, (1 - \sigma_B^c) \;\; \dots\dots\dots\dots\dots\dots\dots\dots\dots\dots\dots \;\; (5.8)$$

But, considering the alternative case where the resonance would occur at some constant frequency v^c and the appropriate fields B_A and B_B, the applicable equations are:

$$v^c = \frac{\gamma^c}{2\pi} \; B_A \, (1 - \sigma_A^c) \;\; \dots\dots\dots\dots\dots\dots\dots\dots\dots\dots \;\; (5.9)$$

$$v^c = \frac{\gamma^c}{2\pi} \; B_B \, (1 - \sigma_A^c) \;\; \dots\dots\dots\dots\dots\dots\dots\dots\dots\dots \;\; (5.10)$$

From equations 5.7 to 5.10, it emerges that:

$$\frac{B^A - B^B}{B_\mathbf{A}} \; \simeq \; \frac{v_B^c - v_A^c}{v_B^c} \; \simeq \; \delta_{A-B}^c \;\; \dots\dots\dots\dots\dots\dots\dots \;\; (5.11)$$

and equation 5.6 can now be rewritten as:

$$\delta_{A-B}^{x \; corr.} = \delta_{A-B}^c + \delta_{A-B}^{x \; obs.} \;\; \dots\dots\dots\dots\dots\dots\dots \;\; (5.12)$$

where $\delta_{A-B}^{\text{x corr.}}$ corresponds to the observed shifts in equations 5.1 and 5.2. Since $\delta^c{}_{A-B}$ is equal to $\delta^c{}_{AX-BX}$, which was earlier defined as the correction arising from the use of lock nucleus with different screening constants due to its different chemical environments. It follows that equations 5.1 and 5.2 have to be rewritten in general forms, considering the above conclusion from equation 5.12, as follows:

$$\delta^{\text{True }\perp}_{AC-BC} = \delta^{\text{obs.}\perp}_{AC-BC} + \delta^{c\,\perp}_{Ax-Bx} + \frac{2\pi}{3}(X_{BC} - X_{AC}) \cdot\cdot \ (5.13)$$

$$\delta^{\text{True }\parallel}_{AC-BC} = \delta^{\text{obs.}\parallel}_{AC-BC} + \delta^{c\,\parallel}_{AX-BX} + \frac{4\pi}{3}(X_{AC} - X_{BC}) \cdot\cdot \ (5.14)$$

where all the parameters in equations 5.13 and 5.14 have been defined earlier. It is essential when using the above two equations to devote special care to the absolute signs of each of the measured shifts. In other words, if the absorption that is chosen as the reference is more shielded, the chemical shift is negative. To emphasise this point, the shifts differences indicated in Fig 5.1c are all negative while the experimental results, later on, will show both signs.

5.5   **APPLICATION TO SELECTED SYSTEMS;**

RESULTS AND DISCUSSION:

At this stage it would appear prudent to assess the magnitude of the practical problem arising from the effects

alluted earlier. Because ^2D is frequently used as the lock nucleus, it would not be unreasonable to select this nucleus to represent c. In an attempt to approach practical reality it was assumed that A = C = $CDCl_3$ and B = $(CH_3)_2$ CO, so that the spectra of a solute X in both samples could be stabilized by locking to the ^2D resonance of $CDCl_3$. Even neglecting $\Delta\sigma_m$ in equation 5.3 $\delta^c AX$ - BX can, taking the volume magnetic susceptibility of $CHCl_3$ as -0.740×10^{-6} and of $(CH_3)_2$ CO as -0.460×10^{-6} at $20^\circ c^{(84)}$, with $\sigma_b = (2\pi/3)X$, be deduced to be -0.5865 ppm. If A = C = D_2O and B = $(CH_3)_2$ CO the corresponding shift is 0.5425 ppm, taking X of D_2O = -0.719×10^{-6}. These values of shift contributing to the chemical shift of x are independent of the magnetic properties of that nucleus and arise only from the nature of the locking nucleus c. The two values quoted above for $\delta^c AX$ - BX are by no means insignificant. Moreover it should be noted that if there are significant contributions from $\Delta\sigma_m$ in equation 5.3, the overall effects may be even larger, as it will be shown by the following experimental results.

Although it is difficult to test the present contention experimentally for the general case presented earlier, it is possible to investigate a specific case. For this purpose, X is studied in A alone, and then as pure X; with X containing both the resonant nucleus of interest x, and the locking nucleus c. Now, if some other material D containing a second heteronucleus d, is introduced to a coaxial cylindrical tube inside both main sample tubes, this can be used as invarient

178

lock. This enables the spectra of c in the two samples to be measured to obtain $\Delta \sigma_c$ or δ_{AX}^c - XX experimentally and so avoid the difficulties in calculating $\Delta \sigma_m$. This method also enables the measurement of the shift of x. When the lock is changed to c another value of the observed shifts of x may be obtained that should differ from the previous value by the amount δ_{AX}^c - XX.

In order to test the approach outlined immediately above, the following systems were selected for study:

1. X is represented by $(CH_3)_2O$, and A by H_2O
2. X is represented by $CDCl_3$, and A by $(CH_3)_2 CO$
3. X is represented by $DMSO(d_6)$, and A by $CDCl_3$
4. X is represented by C_6D_6, and A by CCl_4
5. X is represented by a mixture of 1:1 H_2O/D_2O
   and A by $(CH_3)_2 CO$

Each sample was studied in the same 10 mm OD NMR tube having coaxial inside it a 5 mm OD NMR tube containing a saturated solution of Li_2SO_4 in water representing material D. It is evident that ^2D represents c and ^7Li represents d. Using a JEOL FX 90 Q NMR spectrometer, the appropriate shifts of each system were obtained with a reproducibility of $\pm$ 0.2 Hz. These shifts are represented in Tables 5.1 to 5.5. All the measurements were carried out at 30^oC, and the precise irradiation conditions were kept constant

System	Lock nuclei	Observed nuclei	δ/Hz
$(CD_3)_2$ CO pure	^2D	^{13}C	20.75
$(CD_3)_2$ CO pure	$^7\underline{Li}$	^{13}C	117.43
$(CD_3)_2$ CO pure	$^7\underline{Li}$	^2D	10.16
$(CD_3)_2$ CO in H_2O	^2D	^{13}C	7.81
$(CD_3)_2$ CO in H_2O	^7Li	^{13}C	88.62
$(CD_3)_2$ CO in H_2O	$^7\underline{Li}$	^2D	0.00

$+ \quad v_o \ ^{13}C = 22.5$ MHz $+ 31.7$ KHz $= 22.5317$ MHz

$\# \quad v_o \ ^2D = 13.7$ MHz $+ 57.9$ KHz $= 13.7579$ MHz

Table 5.1 $^{13}C^+$ and $^2H^\#$ shifts using both ^2H = c and ^7Li = d lock in the system with A = H_2O and X = $(CD_3)_2$ CO

System	Lock nucleus	Observed nucleus	δ/Hz
$CDCl_3$ pure	^2D	^{13}C	-45.41
$CDCl_3$ pure	^7Li	^{13}C	-82.52
$CDCl_3$ pure	^7Li	^2D	-1.39
$CDCl_3$ in Aceton	^2D	^{13}C	-54.44
$CDCl_3$ in Aceton	^7Li	^{13}C	-93.75
$CDCl_3$ in Aceton	^7Li	^2D	-2.59

$$v_o \,^{13}C = 22.5 \text{ MHz} + 32.6 \text{ K Hz} = 22.5326 \text{ MHz}$$

$$v_o \,^2D = 13.7 \text{ MHz} + 58.56 \text{ K Hz} = 13.75856 \text{ MHz}$$

<u>Table 5.2</u> $^{13}C^+$ and $^2H^{\#}$ shifts using both $^2H = c$ and $^7Li = d$ lock

in the system with A = Aceton and X = $CDCl_3$

System	Lock nucleus	Observed nucleus	δ/Hz
DMSO pure	^{2}D	^{13}C	81.30
DMSO pure	^{7}Li	^{13}C	154.54
DMSO pure	^{7}Li	^{2}D	5.93
DMSO in DCCl$_3$	^{2}D	^{13}D	78.61
DMSO in CDCl$_3$	^{7}Li	^{13}C	148.44
DMSO in CDCl$_3$	^{7}Li	^{2}D	4.27

$$\nu_o \, ^{13}C = 22.5 \text{ MHz} + 32.00 \text{ KHz} = 22.532 \text{ MHz}$$

$$\nu_o \, ^2D = 13.7 \text{ MHz} + 54.8 \text{ KHz} = 13.7548 \text{ MHz}$$

Table 5.3 $^{13}C^+$ and $^2H^\#$ shifts using both ^2H = c and ^7Li = d lock in the system with A = CDCl$_3$ and X = DMSO

182

System	Lock nuclei	Observed nuclei	δ/Hz
C_6D_6 pure	^2D	^{13}C	10.86
C_6D_6 pure	^7Li	^{13}C	-8.54
C_6D_6 pure	^7Li	^2D	-0.39
C_6D_6 in CCl_4	^2D	^{13}C	13.67
C_6D_6 in CCl_4	^7Li	^{13}C	-17.82
C_6D_6 in CCl_4	^7Li	^2D	-7.91

$$v_o \; ^{13}C = 22.5 \text{ MHz} + 33.8 \text{ KHz} = 22.5338 \text{ MHz}$$

$$v_o \; ^2D = 13.7 \text{ MHz} + 54.85 \text{ KHz} = 13.75485 \text{ MHz}$$

<u>Table 5.4</u> $^{13}C^+$ and $^2H^\#$ shifts using both $^2H = c$ and $^7Li = d$ lock in the system with $A = CCl_4$ and $X = C_6D_6$

System	Lock nucleus	Observed nucleus	Relative $\delta/_{Hz}$
(D_2O/H_2D) pure	^2D	^1H	-16.24
(D_2O/H_2O) pure	^7Li	^1H	65.43
(D_2O/H_2O) pure	^7Li	^2D	-26.27
(D_2O/H_2O) in Aceton	^2D	^1H	-14.26
(D_2O/H_2O) in Aceton	^7Li	^1H	156.84
(D_2O/H_2O) in Aceton	^7Li	^2D	-12.30

$$\nu_o\ ^2D = 13.7\ MHz + 54.8\ KHz = 13.7548\ MHz$$

$$\nu_o\ ^1H = 89.56\ MHz + 44.5\ KHz = 89.6045\ MHz$$

<u>Table 5.5</u> $^{13}C^+$ and $^2H^{\#}$ shifts using both $^2H = c$ and $^7Li = d$ lock

in the system with A = Aceton and X = system of (D_2O/H_2O)

1:1 in volumes

184

for each set of spectra as shown in the tables.

Table 5.6 shows all the relative shifts of the systems studied arranged together in a way that compares these results. It can be seen from columns 7 and 8 that a particular chemical shift measured using ^{7}Li external lock is larger than that measured using an internal ^{2}D lock. The difference between these shifts corresponds to $\delta_{AX}^{c\ \perp} - XX$ (column 9), and this agrees, within the experimental errors, with the frequency scaled value represented in column 10, that is deduced from the directly measured values of $\delta_{AX}^{c\ \perp} - XX$ given in column 6. The general agreement between the corresponding values in columns 9 and 10 provides adequate support for the proposals made earlier. Specific attention is drawn to the magnitude of $\delta_{AX}^{c\ \perp} - XX$ for the mixture of H_2O/D_2O in $(CH_3)_2\ CO$. It is interesting to note that although $\delta_{AX}^{c} - XX$ may be of either sign, depending on the relative field shifts necessary to establish lock for the internal lock materials, it is apparent that the first four systems referred to tables 5.1 to 5.4 and also in table 5.6 correspond to the situation depicted in Figure 5.1c.

5.5 CONCLUSION:

It has been demonstrated that equations 5.13 and 5.14 present significant practical difficulties. The main reason for this is that whilst the $\Delta\sigma_b$ component of $\delta_{AX}^{c} - XX$, implicit in equation 5.3, can be estimated, the other

Table: Shift^C/Hz relative to selected pulse frequency for

Sample	XX[b]	1 $^2H(^7Li)$	2 $^{13}C(^2H)$	3 $^{13}C(^2H)$	4 $^1H(^7Li)$	5 $^1H(^2H)$	6 1AX-1XX	7 3/5AX-3/5XX	8 2/4AX-2/4XX	9 diff 2-3 / 8-7	10 6. $^v/_v\,^2H$
$(CD_3)_2$ CO in H_2O		0.00	88.62	7.81							
	$(CD_3)_2CO$ 10.16		117.43	20.75			-10.16	-12.94	-28.81	-15.87	-16.64[d]
CD_3 in $(CH_3)_2$ CO	$CDCl_3$	-2.59	-93.75	-54.44							
		-1.39	-82.52	-45.41			-1.20	-9.03	-11.23	-2.20	-1.97[e]
DMSO-d_6 in $CDCl_3$	DMSO-d_6	4.25	148.44	78.61							
		5.93	154.54	81.30			-1.66	-2.69	-6.10	-3.51	-2.72
C_6D_6 in CCl_4		-7.91	-17.82	13.67			-7.52	2.81	-9.28	-12.09	-12.31[H]
H_2O/D_2O in $(CH_3)_2CO$		-12.30			156.84	-14.26					
	H_2O/D_2O	-26.27			65.43	-16.24	13.97	1.98	91.41	89.43	91.00[g]

186

P.T.O →

a 5% v/v A in X

b Pure X

c Lock signal in parentheses

d ^{13}C = 22.5317 MHz ; ^{2}H = 13.7579 MHz

e ^{13}C = 22.5326 MHz ; ^{2}H = 13.75846 MHz

f ^{13}C = 22.5320 MHz ; ^{2}H = 13.7548 MHz

g ^{1}H = 89.6045 MHz ; ^{2}H = 13.7548 MHz

H ^{13}C = 22.5338 MHz ; ^{2}H = 13.75485 MHz

Table (5.6) ^{1}H, ^{2}H and ^{13}C relative shifts in Hz at 89.6045 MHz, 13.76 MHz and 22.53 MHz respectively obtained for several solvent

mixtures using ^{2}H and ^{7}Li field/frequency lock

187

contribution $\Delta \sigma_m$ can not. It is evident, therefore, that the popular method of using heteronuclear internal reference compounds for field/frequency locking and subsequently measuring shifts in different samples for comparison purposes can be misleading. This would be particularly true if solvent effects were studied, as in the type of work described in chapters 4 and 7 of this thesis. The implicit ambiguities could occur even though precautions may be taken to use the same lock material with the different samples, and the conventional equations 5.1 and 5.2 applied to correct the observed shifts.

In order to illustrate the danger of attempting to correlate the shifts of solutes dissolved in different materials that are frequently used both as solvents and internal lock compounds, the relative ^2D shifts of several compounds are presented in Table 5.7. Even after allowing for volume magnetic susceptibility corrections estimated at the frequency of the lock nuclei, it is evident that large shifts remain, that can contribute to δ_{AX}^c - XX. The values of the latter can be much larger than the corresponding values referred to in Table 5.6, because with the pure solvents there are contributions to δ_{AX}^c - XX from differences in intra as well as intermolecular screening.

With such potentially large effects due to δ_{AX}^c - XX, it is essential to arrange for its impact to be minimal. The only

Compound	Shift Hz	$\frac{(2\pi X \upsilon)}{Hz}^{2}D/3$ *
$CDCl_3$	-61.28	-21.32
D_2O	-26.18	-20.72
$(CD_3)_2 CO$	20.26	-13.25
C_6D_6	-50.42	-17.60

Table 5.7   Relative ^2D shifts at 13.7548 MHz for some common
             deutrated solvents.

* X_v for the compounds taken from:-

   J.W. Emsley, J.Feeney & L.H. Sutcliffe

   High Resolution N.M.R. Spectroscopy. Pergman, Oxford 1965, Vol 1.

safe way is to always use an additional inert homonuclear
reference because if this is used internally it will experience
precisely the same effect of δ_{AX}^c - XX as will the solute
studied. If this is impractical, it is desirable to ensure
that either A=B with C at same concentration in each sample, or
better that A=B=C, so that the same material is used as solvent
and locking compound. Fortunately relative intramolecular
shifts will be unaffected by the choice of the heteronucleus
used for lock.

As a result of the work presented in this chapter it was
decided to measure, where practicable, chemical shifts from
spectra stabilized by field/frequency locking to a
heteronucleus in a compound contained in a separate cylindrical
tube coaxial with the main NMR tube.

A NEW NMR METHOD FOR DETERMINING THE VOLUME
MAGNETIC SUSCEPTIBILITY OF ORGANIC LIQUIDS

6.1 INTRODUCTION:

Volume magnetic susceptibilities are not only essential for the correction of NMR chemical shifts determined using external reference compound [29], but can in their own right, provide valuable chemical information.

In the content of the work reported in this thesis, it has proved necessary to correct for $\Delta\sigma_b$, to obtain the true shifts of the various compounds being used to investigate aspects of reaction field and buffeting theory when applying Homer's theory. Because X_v for one key compound, $C(CH_2 CH_3)_4$, is not well documented, it became necessary to determine this. Initially it was intended to use one of the existing NMR methods for this purpose· However, the introduction of a novel shift referencing technique in the author's laboratory[87] stimulated the evaluation

of a new NMR method of determining X_v. In this chapter the new method is explained and tested and also used to determine X_v for $C(CH_2 CH_3)_4$.

6.2 PREVIOUS NMR METHODS FOR DETERMINING THE VOLUME MAGNETIC SUSCEPTIBILITY X_v OF ORGANIC LIQUIDS

In order to provide an alternative to the classical methods of [92] determining volume magnetic susceptibilities, several NMR procedures have been described [93,94,95]. Whilst these methods are acceptably accurate, they do have certain disadvantages or difficulties.

The approach described by Reilly et al [93] depends on susceptibility induced shifts of resonance arising from a compound contained in the annular region of a cell having ($\alpha = 2\pi$) a cylindrical reference vessel precisely co-axial with the main tube.

The second approach by Frei and Bernstein [94] made simultaneous use of spherical and cylindrical reference vessel, each containing the same material, and both being surrounded by a second compound. Both the above methods involve the careful calibration of cells employed.

The approach developed by Homer and Whitney [95] made use of the differences in the shifts of a subject compound in different solvents situated separately in co-axial cylinders, and the

dependence of these differenc es, when measured using iron magnet and superconducting solenoid based spectrometers.

Any reliable NMR method for determining the magnetic susceptibilities that depends on the influence of this property on chemical shifts must avoid other solvent effects. Therefore, because the susceptibility screening constant, σ_b, depends on the shape of the vessels containing the materials studied, it has proved convenient to derive magnetic susceptibility data from appropriate shifts arising, from materials located in differently shaped cells. This, of course, is the principle underlying the method of Frei and Bernstein [94] who measured the shift difference for a particular compound contained in cylindrical and spherical cells.

6.3 A NEW NMR METHOD FOR DETERMINING X_v OF ORGANIC LIQUIDS

The intention now is to present a simple NMR method that largely avoids problems associated with cell calibration and which relies only on the use of an iron magnetic spectrometer.

It is intended to demonstrate that NMR chemical shift measurements for organic liquids contained first in their pure state in conventional NMR sample tubes, and then dispersed homogeneously in a reference material in the same tube, to enable the determination of their volume magnetic susceptibilities.

The method reported here is essentially an adaptation of that due to Frei and Bernstein.

Because of the difficulty of constructing perfectly spherical glass cells, it is proposed that the heterogeneous dispersion of a subject material in a suitable immiscible reference liquid will achieve the same ends as the method due to Frei and Bernstein. The forces at the interface of a droplet and the reference liquid, coupled with its motional characteristics should ensure that the material of interest can be considered to be in the form of a self-contained sphere. Additionally, provided the size of the droplet is much larger than the molecular dimensions, the compound within it should exhibit the same properties that it has in the natural bulk state. Consequently, nuclear screening must be the same in the pure and dispersed states except that the bulk susceptibility effect σ_b in the two situations will differ due to the effects of the differing peripheral shapes; i.e. cylindrical in an NMR tube and spherical in the droplet.

Figure (6.1a) schematically represents the situation in which some compound A, for which a value of its volume magnetic susceptibility X_v is required, is located in a cylindrical glass NMR sample tube.

Figure (6.1b) represents the case when compound A is dispersed in a reference liquid B in the same NMR sample tube. In both cases the axis of the sample tube is perpendicular to the direction of the polarizing magnetic field. The various shape

194
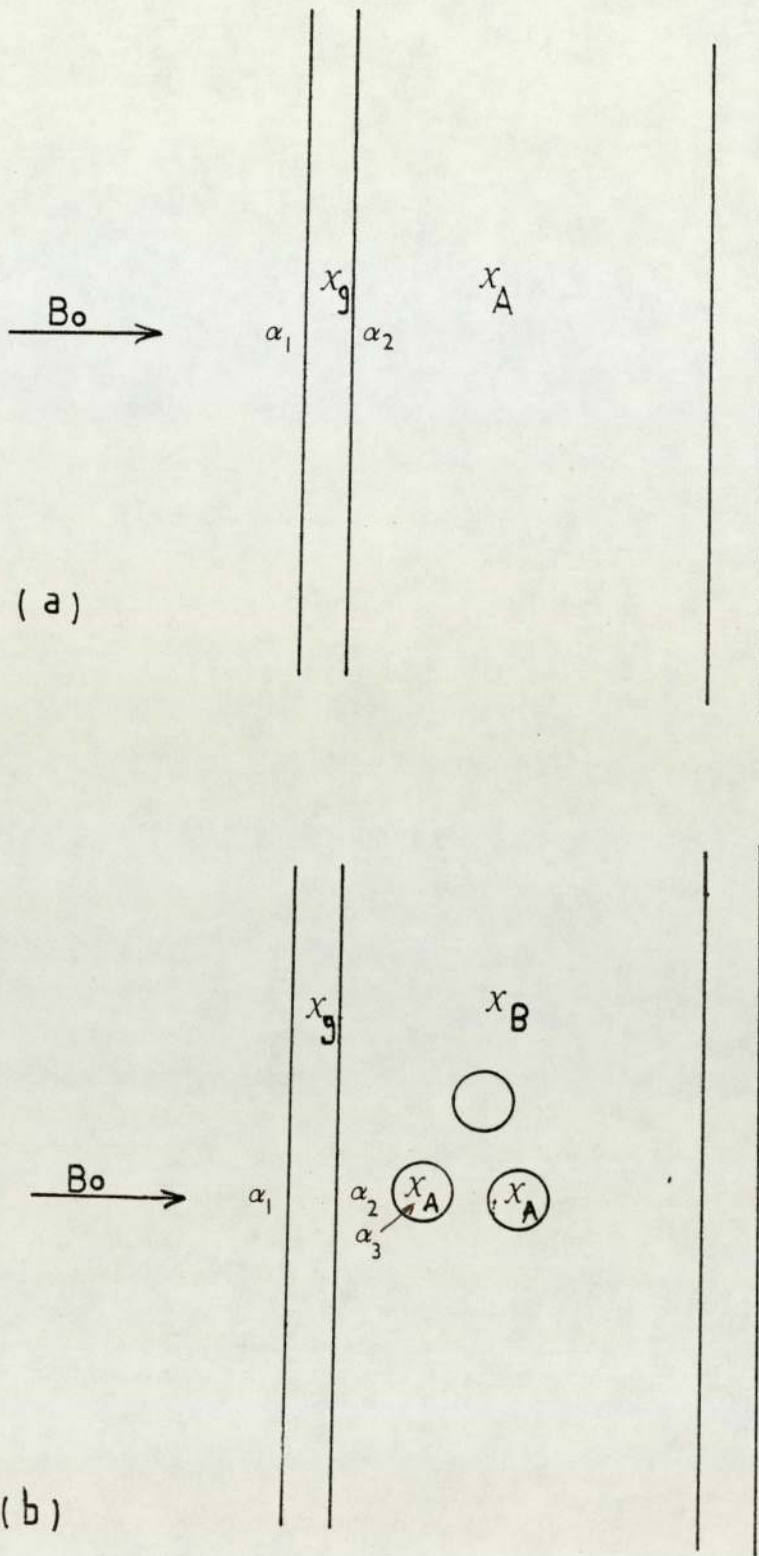
Figure 6.1

Schematic representation of a conventional NMR sample tube containing
(a) a pure compound A and (b) A dispersed heterogeneously in a
liquid B.

195

factors and the volume magnetic susceptibilities are identified by α and X respectively in the figure.

Following the approach of Frost and Hall [96], based on that of Dickinson [36], the magnetic fields, B^T_{Aa} and B^T_{Ab}, actually experienced by A when it resonates at the applied fields B^O_{Aa} and B^O_{Ab}, in a fixed frequency experiment, corresponding to the situations a and b of Figure 6.1, are given by the following equations 6.1 and 6.2 respectively:

$$B^T_{Aa} = B^O_{Aa} \; (1 - \alpha_1 \, X_g + \alpha_2 \, X_g - \alpha_2 \, X_A + \frac{4\pi}{3} \, X_A) \quad \ldots\ldots\ldots\ldots \; (6.1)$$

$$B^T_{Ab} = B^O_{Ab} \Bigl[1 - \alpha_1 \, X_g + \alpha_2 \, X_g - \alpha_2 \, X_B + \alpha_3 \, X_B$$

$$(- \alpha_3 \, X_A + \alpha_3 \, X_A - \alpha_3 \, X_B + \alpha_3 \, X_B)_n$$

$$- \alpha_3 \, X_A + \frac{4\pi}{3} \, X_A \Bigr] \quad \ldots\ldots\ldots\ldots\ldots\ldots\ldots\ldots \; (6.2)$$

where B^T_{Aa} and B^T_{Ab} are the true magnetic fields experienced by A in situations a and b respectively. B^O_{Aa} and B^O_{Ab} are the actual applied magnetic fields in cases a and b respectively. X_g, X_A and X_B are the volume magnetic susceptibilities of the glass of the tube and of the material A and B respectively. It should be noted that the term between brackets in (equation 6.2) which is repeated n times, represents the presence of n droplets across the tube. Because $\alpha_1 = \alpha_2 = 2\pi$ for a perfect cylinder and $\alpha_3 = \frac{4\pi}{3}$ for a perfect sphere [96] (the droplet), equations 6.1 and 6.2 can be ideally reduced to equations 6.3 and 6.4 respectively:

$$B_{Aa}^{T} = B_{Aa}^{o} \left[1 - \frac{2\pi}{3} X_A \right] \quad \dots\dots\dots\dots\dots\dots\dots\dots\dots\dots\dots\dots \quad (6.3)$$

$$B_{Ab}^{T} = B_{Ab}^{o} \left[1 - \frac{2\pi}{3} X_B \right] \quad \dots\dots\dots\dots\dots\dots\dots\dots\dots\dots\dots\dots \quad (6.4)$$

The true chemical shift difference between the resonances of A in the two cases a and b, therefore, should be zero, if it is devoid of susceptibility effects. Therefore, the observed chemical shift difference δ^{o}_{b-a} should be referred to the susceptibility effects and given by

$$\delta^{o}_{b-a} = \frac{2\pi}{3} (X_B - X_A) \quad \dots\dots\dots\dots\dots\dots\dots\dots\dots\dots\dots \quad (6.5)$$

Equation 6.5 enables the calculation of the volume magnetic susceptibility of unknown samples by using the method described in this chapter. The experimental results in the following sections show the validity of equation 6.5.

6.4 EXPERIMENTAL TECHNIQUES

Water was chosen as a reference compound A for two main reasons, first because its volume magnetic susceptibility is taken to be a standard and reliable value; and second because water is immiscible with many organic liquids.

Various liquids that are essentially immiscible with water were chosen to represent B. The samples were contained in a 10mm O.D NMR tube that had co-axial with it a 5mm O.D NMR tube containing D_2O which was used for field/frequency stabilization. Using a JEOL FX 90 Q multinuclear NMR spectrometer, the samples

were studied at a temperature of 20°C, unless otherwise stated. The absolute ^{1}H resonance frequencies of the pure organic compound were measured first. A small quantity, a drop ($\simeq$ 0.05ml), of B was then dispersed ultrasonically in water ($\simeq$ 10ml) and its resonance frequency again measured. In order to reduce the relative intensity of the ^{1}H water absorption resonance, either the classical $180 - \tau - 90$ double pulses technique was used or selective saturation of the H_2O resonance was employed, depending on the shift of the sample resonance from that of water.

Because of the small quantities of B used it was necessary to acquire as many FID's as possible within the relatively short time 20-30 minutes that the dispersion of B was maintained.

Also   same compounds were studied by reversing the roles of the reference and the subject compounds. For this the shift of the pure reference compound, water, is measured first and then its shift obtained when it is dispersed in the compound under study. Pure distilled water was used for the reference compound, and either ANALAR or BDH spectroscopic grade organic compounds were used depending on their availability in the laboratory.

All the compounds studied are documented as insoluble in water [97], therefore, there should be no solubility problems which might effect the absorption frequency or the volumatic volume susceptibility of the reference. In no case was a second absorption observed due to dissolved material in the support

compound used to contain the suspension.

The estimated experimental error in the chemical shifts measurements is $\pm$ 0.1 Hz.

6.5 **RESULTS AND DISCUSSION:**

The proton resonance frequencies for all compounds representing B in the pure state $\delta^o pB$, and for B dispersed in water $\delta^o dB$, are listed in Table 6.1. Where several absorptions occurred the highest intensity absorption was usually selected for measurement, i.e. CH_2 in n-Hexadecane, CH_3 in Mesitylene, CH_2 in n-Heptane, CH_3 in P-Cymene and CH_2 in n-Decane. The difference between ^1H chemical shift, δ^o_{b-a}, from the pure sample of interest and that of the same material dispersed in water (the reference) together with the selected observing frequency, are presented for all compounds in table 6.1. δ^o_{a-b} with the volume magnetic susceptibility of water, were used to evaluate X_v by employing equation 6.5. The values so obtained are given in table 6.2 together with the corresponding literature values. It can be seen from the percentage deviation between the two values for each sample that the agreement between the experimental values based on equation 6.5 and the literature values is reasonably good.

The Wilconxon pair-T-test[98] is a statistical method to prove the correlation between any set of experimentally obtained data with their theoretical values. Table 6.3 shows that this test gives a probability of significant difference less than 1%,

Compound A	$\overset{o}{\delta}_p B$ Hz	$\overset{o}{\delta}_d B$ Hz	$\overset{o}{\delta} B$ (a-b)	v_o* MHz	$\overset{o}{\delta} B$ ppm (a-b)
n-Hexade-cane	305.92	287.35	-18.57	89.6045	-0.207
Mesitylene	256.63	252.20	-13.43	89.6045	-0.1499
n-Heptane	322.75	294.92	-27.83	89.6045	-0.3105
O-Dichlo-robenzene	-202.88	-198.73	+4.15	89.6045	+0.0463
P-Cymene	252.20	240.72	-11.48	89.6045	-0.12812
Cychohexane	326.90	310.30	-16.6	89.604518	-0.1853
Benzene	-171.63	-187.01	-15.38	89.6045	-0.1716
Chloroform	-230.46	-225.59	4.87	89.60425	+0.0544
n-Decane	72.51	52.25	20.26	89.60425	+0.2261

* v_o is the observing frequencey.

Table (6.1) The observed ^{1}H shifts for a set of compounds (representing compound B) in their pure state, and dispersed in water. All measurements were carried out using a JEOL FX 90 Q NMR at 20°C utilizing [2]D external lock. The difference between the shifts for the pure and dispersed samples are tabulated in Hz and ppm.

Compound A	δ_B ppm. (d-p)	$-X_v /10^{-6}$ measured	$-X_v /10^{-6}$ [*] Literature Value	Deviation %
n-Hexadecane	-0.2072	0.62	0.6421	-3.4
Mesitylene	-0.1499	0.647	0.665	-2.7
n-Heptane	-0.3105	0.570	0.5817	+1.89
O-dichlor-abenzene	+0.0463	0.741	0.748	+0.94
P-Cymene	-0.1281	0.658	0.656	+0.3
Cyclohexane	-0.1853	0.63	0.627	+0.48
Benzene	-0.1716	0.637	0.611	+4.2
Chloroform	+0.0544	0.745	0.740	+0.68
n-Decane	+0.2261	0.611	0.6143	+0.54

[*] (All X_v from the literature are at 20°C).

Table (6.2)   Experimentally measured volume magnetic susceptibilities with the corresponding literature values and the percentage deviation.

Sample	$-X_v/\text{x}10^{-6}$ Literature Value	$-X_v/\text{x}10^{-6}$ Experimental Value	Difference	Rank $\pm$
n-Hexadecane	0.6421	0.62	0.0221	+ 8
Mesitylene	0.665	0.647	0.0180	+ 7
n-Heptane	0.5817	0.57	0.0117	+ 6
$O\text{-}C_6 H_4 Cl_2$	0.748	0.741	0.0070	+ 5
P-Cymene	0.656	0.658	-0.0020	- 1
$C_6 H_{12}$	0.627	0.63	-0.0030	- 2
$C_6 H_6$	0.611	0.637	-0.0026	- 9
$CHCl_3$	0.740	0.745	-0.0050	- 4
n-Decane	0.6143	0.611	0.0033	+ 3

$n = 9$ Ps.d $<$ 1%

Table (6.3) Data for a Pair-T-Test (Wilconxon Test) for experimental and theoretical significant correllation of X_v measurements.

i.e. significant difference is not proved. Therefore, statistically the experimental values are in good correlation with the literature values, which means that the method described in this chapter for obtaining X_v is a reliable method.

Table 6.4 represents the results when the roles of the reference compound (water) and the samples of interest were reversed. In this case the proton chemical shifts differences, δ^o_{b-a}, is between pure water and water dispersed in the sample under interest. The X_v results represents in Table 6.2 can be seen to be in reasonable agreement with those deduced from the shifts differences of the compounds B, themselves, and with the literature values.

In order to assess the influence of the shape of the main NMR sample tube on the values of the measured X_v using the method reported in this chapter, the system of water and P-cymene was studied using six different 10mm O.D NMR tubes. The results of the six experiments carried out for the six tubes for the same system are shown in Table 6.5. It indicates that the shape factors of the precision 10mm O.D tubes in common use vary insignificantly. That would imply negligible effect average of -0.2% on the previous measurements. Sample tube number 1 shows no shape effect on the measurement, therefore it was the one used throughtout the measurements carried out in this chapter.

Compound B	water δ_d Hz in B	water δ_{d-p} Hz	water δ_{d-p} ppm	$-\chi_v/\times 10^{-6}$ Experimental	$-\chi_v/\times 10^{-6}$ Literature	Deviation %
n–Heptane	14.4	32.47	0.3624	0.546	0.5817	6.1
ortho $0-C_6H_4Cl_2$	-16.6	-1.47	-0.0164	0.727	0.748	2.8
Benzene	0.0	18.07	0.2017	0.622	0.611	1.8

δ_{pure}^{water} = 18.07 Hz

v_o observing frequency = 89.6045 MHz

All measurement at 2o^{o}C

Table (6.4) Measured Chemical shift differences, $\delta_{b-a}^{0\ ref.}$ for water (A), and water dispersed in various compounds together with derived volume magnetic susceptibilities of the subject compound.

Sample Tube Number	$\delta \frac{CH_3}{d-p} H_3$ p-Cymene	$-X_v / 10^{-6}$ Measured	Deviation %
1	-11.8	0.656	0
2	-11.51	0.658	+ 0.3
3	-12.45	0.653	-0.45
4	-14.89	0.64	-2.44
5	-11.97	0.655	-0.15
6	-10.01	0.665	+1.52

* Average Deviation due to the tube used is -0.2%

* The Sample Tube used for the previous measurements is No. 1.

Table (6.5) Measured ^1H chemical shifts differences for the CH_3 groups in the P-cymene $\delta \frac{CH_3}{b-a}$, using different sample tubes to show the effect of these on the measured X_v. The observing frequency for all measurements is 89.6044 MHz.

6.6 MEASUREMENT OF X_v OF TETRAETHYLMETHANE

Tetraethylmethane (or 3,3 diethylpentane), $C(CH_2 CH_3)_4$ is an excellent compound with which to test Homer's theory, in terms of aspects of both the reaction field and the buffeting components. The value of its volume magnetic susceptibility needed to carry out this study is not documented. Therefore, the presently proposed method of obtaining X_v was used for this compound. Table 6.6 presents the data obtained by averaging several measurements of variation of $\pm$ 0.1 Hz. Used with equation 6.5 these yield a value of - 0.6657 $X10^{-6}$ for the volume magnetic susceptibility of this compound at a temperature of 30°C.

Table 6.6 The methyl proton resonance frequencies of the tetraethylmethane $C(C_2H_5)_4$ obtained using a JEOL FX 90 Q NMR Spectrometer at 30°C; ^2D lock, was established with D_2O in a central 5mm OD tube co-axial with the main 10mm OD tube.

δ^o pure	- 167.480 Hz
δ^o dispersed in water	- 157.471 Hz
δ^o_{a-b}	- 10.009 Hz
Observing frequency is 89.604 MHz.	
X_v $C(C_2H_5)_4$	= - 0.6657 x 10^{-6}

6.7 **CONCLUSION**

It is evident, now, that the potential difficulties [29] associated with the Frei and Bernstein [94] method of obtaining volume magnetic susceptibilities can be avoided by measuring the absolute resonance frequencies of nuclei in a subject compound, first in its pure state and then dispersed in an immiscible reference compound, or by corresponding measurements on the reference compound dispersed in the subject compound.

It is interesting to speculate that equation 6.5, on which the present method depends, may be used with materials A and B of known susceptibilities to rapidly assess how closely NMR tubes approximate to perfect cylinders.

AN INVESTIGATION OF THE CONTRIBUTIONS
CHARACTERIZING VAN DER WAALS FORCES

7.1 INTRODUCTION:

The original work of Homer and Percival[64] suggested that van der Waals dispersion forces can be characterized by three discrete effects. Justification for these three effects emerge from the self-consistency of their composite analysis of a vast range of experimental data. Similarly the work presented earlier in this thesis has revealed that the use of the primary and secondary mean square reaction fields together with the buffeting square electric field i.e. $< R^2_1 > + < R^2_2 > + E^2_{BI}$ can be used in a satisfactory self-consistent way to analyse the chemical shifts in a range of complex molecules. However, at no time has there been conclusive experimental proof that each of the three contributing terms exist separately.

The purpose of this chapter is to demonstrate that $\langle R^2{}_1 \rangle$, $\langle R^2{}_2 \rangle$ and $E^2{}_{BI}$ have been adequately characterized and act separately.

7.2 **THEORETICAL**

The derivation of $\langle R^2{}_1 \rangle$ from an Onsager type treatment indicates that all points in the hypothetical cavity will experience the full value of $\langle R^2{}_1 \rangle$. The original derivation of $\langle R^2{}_2 \rangle$, however, yields an equation slightly different to that presented earlier in this thesis. In essence the correct formulation of $\langle R^2{}_2 \rangle$ would be given by[64]:

$$\langle R^2_2 \rangle = \left(\frac{8\pi}{9}\right)^2 \; 2\left(\frac{r_1}{r_2}\right)^2 \; \frac{\langle \mu_2^2 \rangle}{v_2^2} \; \frac{(n_2^2 + 2)^2 (n_2^2 - 1)^2}{9 n_2^4} \; \left(\frac{r}{a}\right)^6 \;\; \cdots \; (7.1)$$

from which it can be seen that $(r/a)^6$ is included; where r is the solvent molecule radius and $a = r + d$ where d is the distance between the centre of the resonant nucleus and the periphery of the solute molecule. To all intents and purposes when considering regions at the periphery of the solute, $(r/a)^6$ may be taken as unity as assumed by Homer and Percival. If however, the screening of the nuclei within the solute molecule cavity is considered, the value of $(r/a)^6$ should be evaluated and used in equation (7.1). In a similar way when considering the buffeting square electric field $E^2{}_{BI}$, this was also derived for position at the periphery of the

solute molecule. However, considering the screening of nuclei within a molecule, it is evident that E^2_{BI} may be reduced or indeed zero.

The above principles that are implicit in the derivation of these three terms contributing to dispersion forces can be tested by investigating the screening of nuclei at different locations within a molecule. To this end the ^{1}H and ^{13}C of tetraethylmethane C $(CH_2CH_3)_4$ have been studied as well as ^{1}H, ^{13}C and ^{29}Si of tetramethylsilane Si $(CH_3)_4$.

The procedure adopted was to measure the appropriate shifts in the somewhat limited range of readily available and suitable solvents. These are TMS, CCl_4, C_6H_{12}, CEt_4 and C_6H_6 for TMS; and TMS, CCl_4, C_6H_{12} and CEt_4 for CEt_4. The measurements were carried out at 30°C, using a JEOL FX 90 Q NMR spectrometer locked to the ^{2}H resonance of D_2O contained in a 5mm OD NMR tube co-axial with the main 10mm OD NMR tube so that the system of interest was contained in the annulus. For each particular nuclide the irradiation frequency was kept constant and the shifts measured relative to the irradiating frequency that are mentioned in the appropriate tables. Because of the difference in the volume magnetic susceptibilities of the solvents used (see Table 7.1), each shift was corrected for the appropriate susceptibility of the solution; this was deduced by the solution volume fraction weighting of the susceptibilities of the pure materials.

210

Where feasible ^1H and ^{13}C gas phase shifts of TMS were also measured. Their gas phase shifts were measured at various gas pressures and extrapolated to zero pressure. The gas samples were prepared by the same procedure described in Chapter 4.

Compound	$-X_v/10^6$ at 30°C
$C\ (CH_2CH_3)_4$	0.6657
$Si\ (CH_3)_4$	0.536
C_6H_{12}	0.627
CCl_4	0.681
C_6H_6	0.611
D_2O	0.708

Table 7.1 The volume magnetic susceptibilities of the solvents used; all at 30°C.[84,106].

7.3 STUDIES OF TETRAETHYLMETHANE $C(CH_2CH_3)_4$:

The observed ^1H and ^{13}C shifts together with the volume
magnetic susceptibility corrected shifts for $C(CH_2CH_3)_4$ in
various solvents are recorded in Tables 7.2 and 7.3 respectively.

The present object is to ascertain whether the definitions of
$< R^2_1 >$, $< R^2_2 >$ and E^2_{BI} as given in Chapter 4 and also by Homer
and Percival for peripheral nuclei are adequate or whether it is
necessary to modify the latter two terms consistent with the
principles implicit in their derivation. Concurrently, it is
hoped to obtain experimental evidence for their separate
existance.

Using the data provided in Table 7.4, the appropriate values
of $< R^2_1 >$, $< R^2_2 >$ and $< R^2_T >$ are calculated and recorded in
Table 7.5. Additionally, the values of the buffeting
parameters β_T and ξ_T were deduced for the methyl and methylene
protons, and these together with $(2\beta_T - \xi_T)^2$ and E^2_{BI} are given
in Table 7.6 and 7.7 respectively. For the calculations of the
buffeting effects of CCl_4 the value of 6.5 for Q deduced by Homer
and Percival[64] for chlorine atom was used.

7.3.1 Analysis Of Proton Shifts Of $C(CH_2CH_3)_4$:

In the case of the methyl group $- CH_3$ in the
tetraethylmethane, Figure 7.1 shows the regression of
$(< R^2_T > + E^2_{BI})$ on the susceptibility corrected shifts. This

Solvent	^{1}H group	^{1}H δobs Hz	Hδobs ppm	$\frac{-2\pi}{3} \chi_v$ ppm	^{1}H δ true ppm	^{1}H δ true Hz
	CH$_2$	-7.42	-0.083		+1.04	93.17
SiMe$_4$				1.1226		
	CH$_3$	+30.86	+0.3444		+1.467	131.45
	CH$_2$	-31.25	-0.3488		+1.045	93.68
CEt$_4$				1.3942		
	CH$_3$	+6.25	+0.0698		+1.464	131.18
	CH$_2$	-23.24	-0.2594		+1.054	94.43
C$_6$H$_{12}$				1.3132		
	CH$_3$	+14.26	+0.1591		+1.4723	131.92
	CH$_2$	-39.83	-0.4445		+0.9818	87.97
CCl$_4$				1.4263		
	CH$_3$	-3.7	-0.0413		+1.385	124.10

Table (7.2) ^{1}H observed and susceptibility corrected shifts from ^{2}H, of CEt$_4$ in various solvents. Measurements were made employing a JEOL FX 90 Q NMR spectrometer at 30°C, with irradiation frequency of 89.60415 MHz.

Solvent	^{13}C	$_{o}.\delta$ H_z	δ^{obs}_{ppm}	$-2\pi/_{3}$ X_v ppm	δ^{t}_{ppm}
	C	1213.38	53.85		54.97
TMS	CH_2	1440.43	63.93	1.12	65.05
	CH_3	1887.20	83.75		84.87
	C	1208.50	53.63		55.02
CEt_4	CH_2	141.88	63.55	1.39	64.94
	CH_3	1881.10	83.48		84.87
	C	1210.94	53.74		55.05
C_6H_{12}	CH_2	1435.54	63.71	1.31	65.02
	CH_3	1887.20	83.75		85.06
	C	1198.73	53.20		54.63
CCl_4	CH_2	1425.78	63.28	1.43	64.71
	CH_3	1865.23	82.78		84.21

Table (7.3) ^{13}C observed and susceptibility corrected shifts, from 2H, of $C(CH_2CH_3)_4$ in different solvents. The measurements were made using a JEOL FX 90 Q NMR spectrometer operating at $30^{o}C$ with an irradiating frequency of 22.533. MHz.

Compound	r A°	$\alpha / 10^{-23}$ cm^3	I $/10^{-12}$ erg	Vm $/10^{-22}$ cm^3	n^2_D
$C\ (C_2H_5)_4$	4.358	1.64928	16.5	2.8258	2.0181
$Si\ (CH_3)_4$	4.079	1.19	15.7	2.316	1.8266
CCl_4	3.613	1.05	18.3	1.61	2.1144
C_6H_{12}	3.746	1.04	15.7162	1.7937	2.035

Table (7.4) Collected data required for reaction field calculations.

r Molecular radius

α Polarizibility

I Ionization Potential

n_D Refractive Index

Solvent	$<R_1^2>/10^{11}$ (esu)	$<R_2^2>/10^{11}$ (esu)	$<R_T^2>/10^{11}$ (esu)
Si $(CH_3)_4$	0.27345	0.61983	0.89328
C $(C_2H_5)_4$	0.36400	0.72801	1.09201
C_6H_{12}	0.37202	1.50833	1.88036
CCl_4	0.40964	2.63664	3. 04629

Table (7.5) The calculated mean square reaction fields $<R_1^2>$, $<R_2^2>$ and $<R_T^2>$ for CEt_4 in different solvents.

Buffeting molecule	β_c	ξ_c	$\dfrac{<r^{-6}>}{r^6}$	β_T	ξ_T	$\dfrac{(2\beta - \xi)}{}$	E^2_{BI} /10^{11} e.s.u.
TMS	0.51	0.87	0.21	0.61	1.11	0.11	0.086
CEt$_4$	0.53	0.86	0.27	0.66	1.16	0.16	0.183
C$_6$H$_{12}$	0.59	0.05	0.31	0.72	1.3	0.14	0.14
CCl$_4$	0.61	0.98	0.38	0.8	1.4	0.24	0.5

$$E^2_{BI} = K/_r{}^6 \, (2\beta - \xi)^2$$

$$K^H/_{r6_{HH}} = 0.7133 \times 10^{12} \quad \text{e.s.u.}$$

$$K^{Cl}/_{r_{HCl}} = 1.2715 \times 10^{12} \quad \text{e.s.u.}$$

$$Q = 6.5$$

$$r_{HH} = 2.4 \, A^o; \quad r_{HCl} = 3.0 \, A$$

Table 7.6   The geometrical parameter and the square buffeting electric field for the methyl protons CH$_3$ in CEt$_4$.

Buffeting Molecule	β_c	ξ_c	$<r^{-6}>r^6$	β_T	ξ_T	$(2\beta-\xi)^2$	E^2_{BI} /10^{11} e.s.u.
TMS	0.73	0.84	0.12	0.74	0.98	0.25	1.783
CEt_4	0.67	0.79	0.15	0.72	0.97	0.221	1.576
C_6H_{12}	0.61	0.73	0.16	0.67	0.93	0.168	1.198
CCl_4	0.55	0.6	0.22	0.65	0.91	0.152	1.933

Table (7.7)   The buffeting parameter for the methylene protons of CH_2 in CEt_4 together with the buffeting field $E^2_{BI} = K/_r6\ (2\beta - \xi\ )^2$.
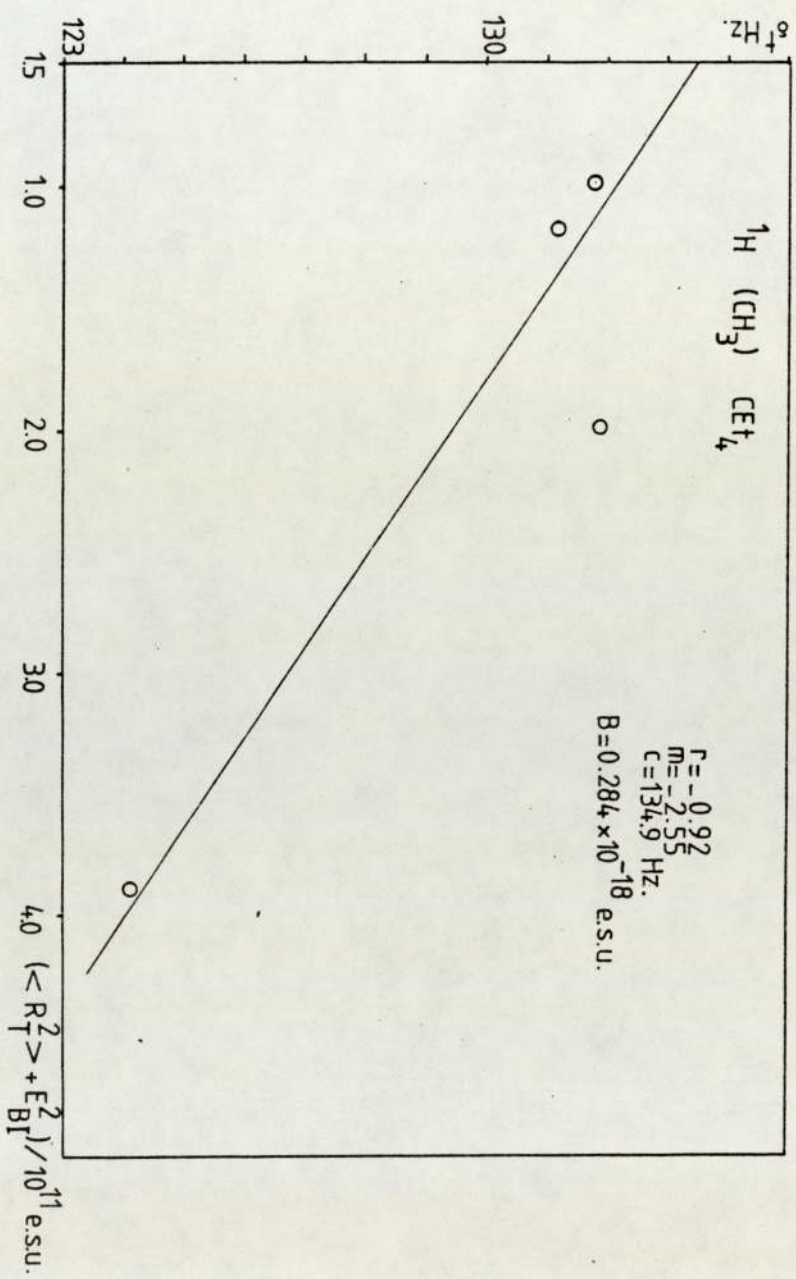
Figure 7.1 Regression of $(<R_T^2> + <E_{BI}^2>)$ on methyl proton shifts of CEt$_4$.

yields a B value of 0.284×10^{-18} e.s.u. which is evidently too small correspond with Homer and Percival average value of 0.87×10^{-18} e.s.u. Figure 7.2 shows the regression with the square buffeting field E^2_{BI} eliminated and this again gives a low value for B of 0.32×10^{-18} e.s.u. At the other extreme the regression of $< R^2_1 >$ on the corrected shifts (Figure 7.3) gives an unacceptably high value for B of 4.44×10^{-18} e.s.u.

Evidently the best value of B will be obtained from the appropriate regression that lies somewhere between $< R^2_1 >$ and $(< R^2_T > + E^2_{BI})$ on the corrected shifts.

Figure 7.4 presents a two-dimensional representation of $C(CH_2CH_3)_4$ molecule, from which the appropriate value for the $(r/a)^6$ modification implicit in the equation 7.1 can be estimated. For the two extremes for the methyl protons indicated in Figure 7.4 values of $d = 1.0$ A^o and $d = 2.25$ A^o. The average of these together with the possible positions at the periphery resulting from the rotation of the methyl group gives a total d value of 0.8 A^o. This was used to calculate the values of $< R^2_2 > (r/a)^6$ that are given in Table (7.8) together with other immediately relevant data.

The regression of $< R^2_1 > + < R^2_2 > (r/a)^6 + K/r^6 (2\beta - \xi)^2$ is shown in Figure 7.5. From this a value of 0.783×10^{-18} e.s.u. for B is deduced. If the regression is only for $< R^2_1 > + < R^2_2 > (r/a)^6$ on the corrected shifts a value of 1.13×10^{-18} e.s.u. for

δ†Hz.

123

130.

0.0

1.0

2.0

3.0

4.0

^1H (CH$_3$) CEt$_4$

r=-0.9
m=-2.875
c=134.93
B=0.32 ×10^{-18} e.s.u.

$<R_T^2>/10^{11}$ e.s.u.
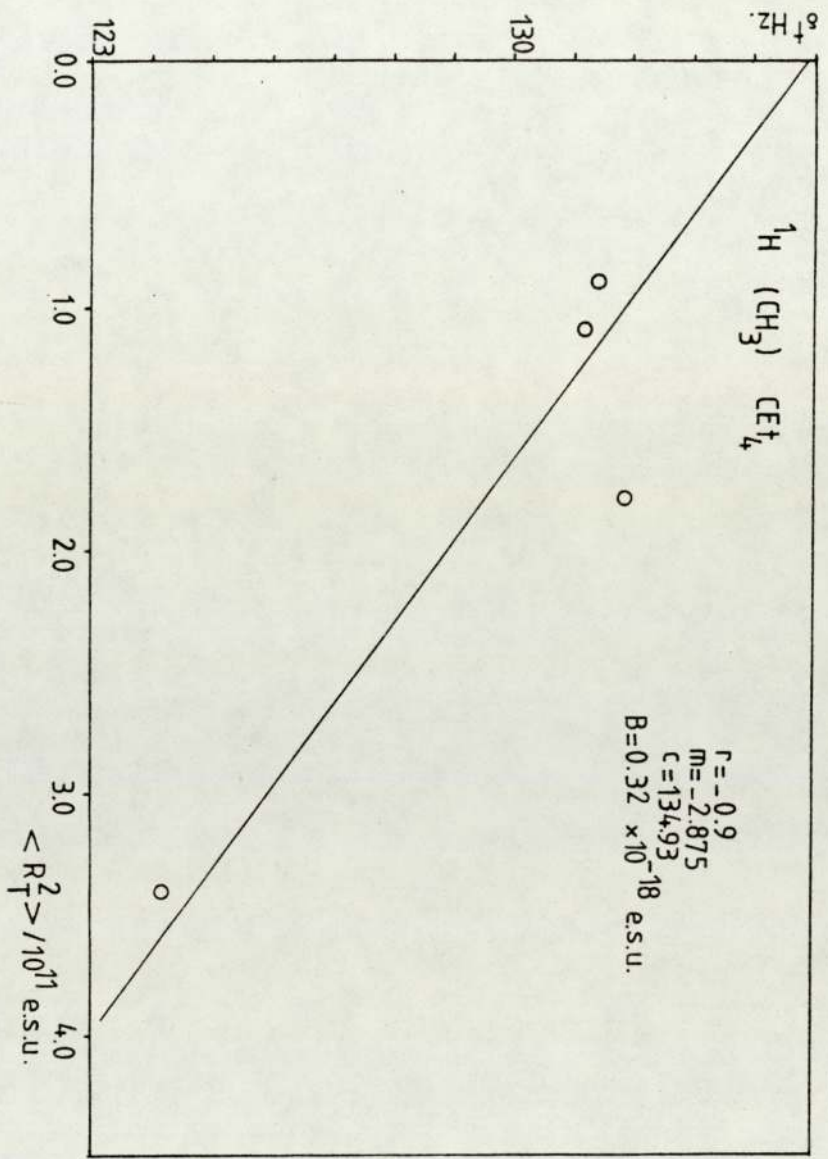
Figure 7.2 Regression of $<R_T^2>$ on methyl proton shifts of CEt$_4$.

2.21
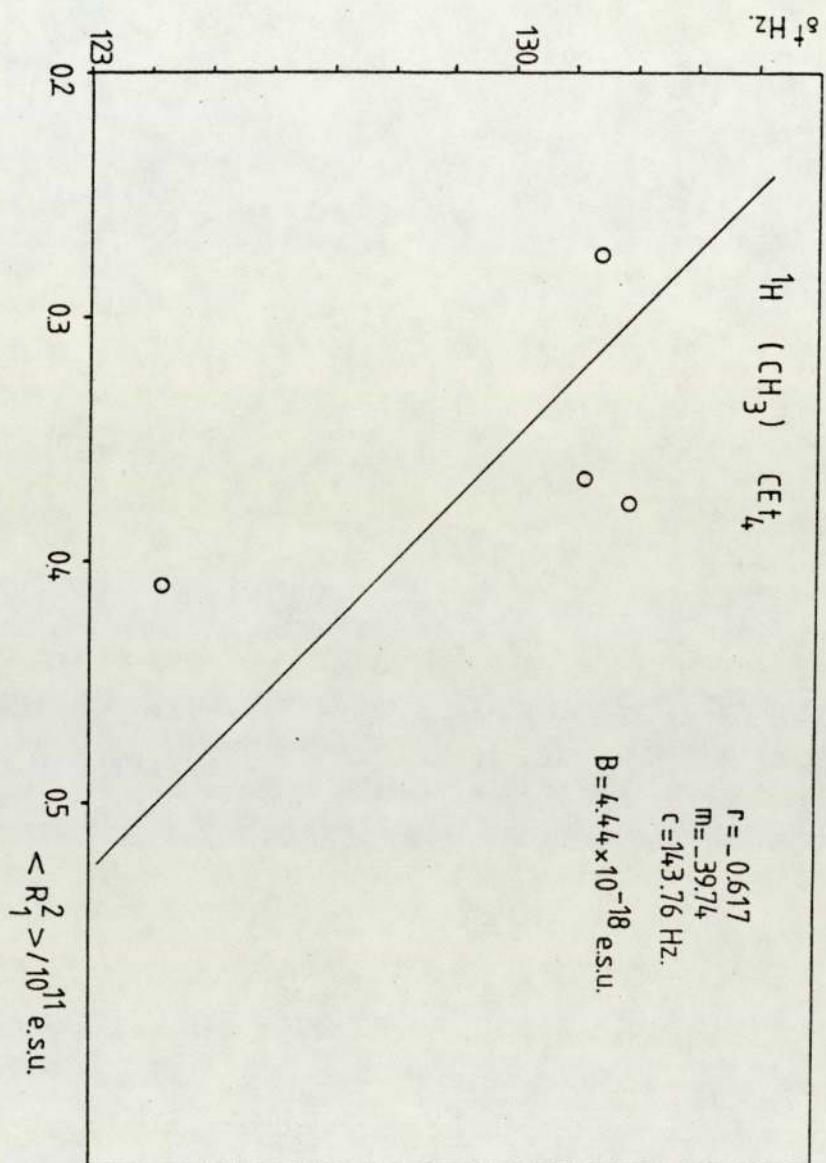
Figure 7.3   Regression of $\langle R_1^2 \rangle$ on methyl proton shift of
CEt_4.

$\delta /$ Hz.

123
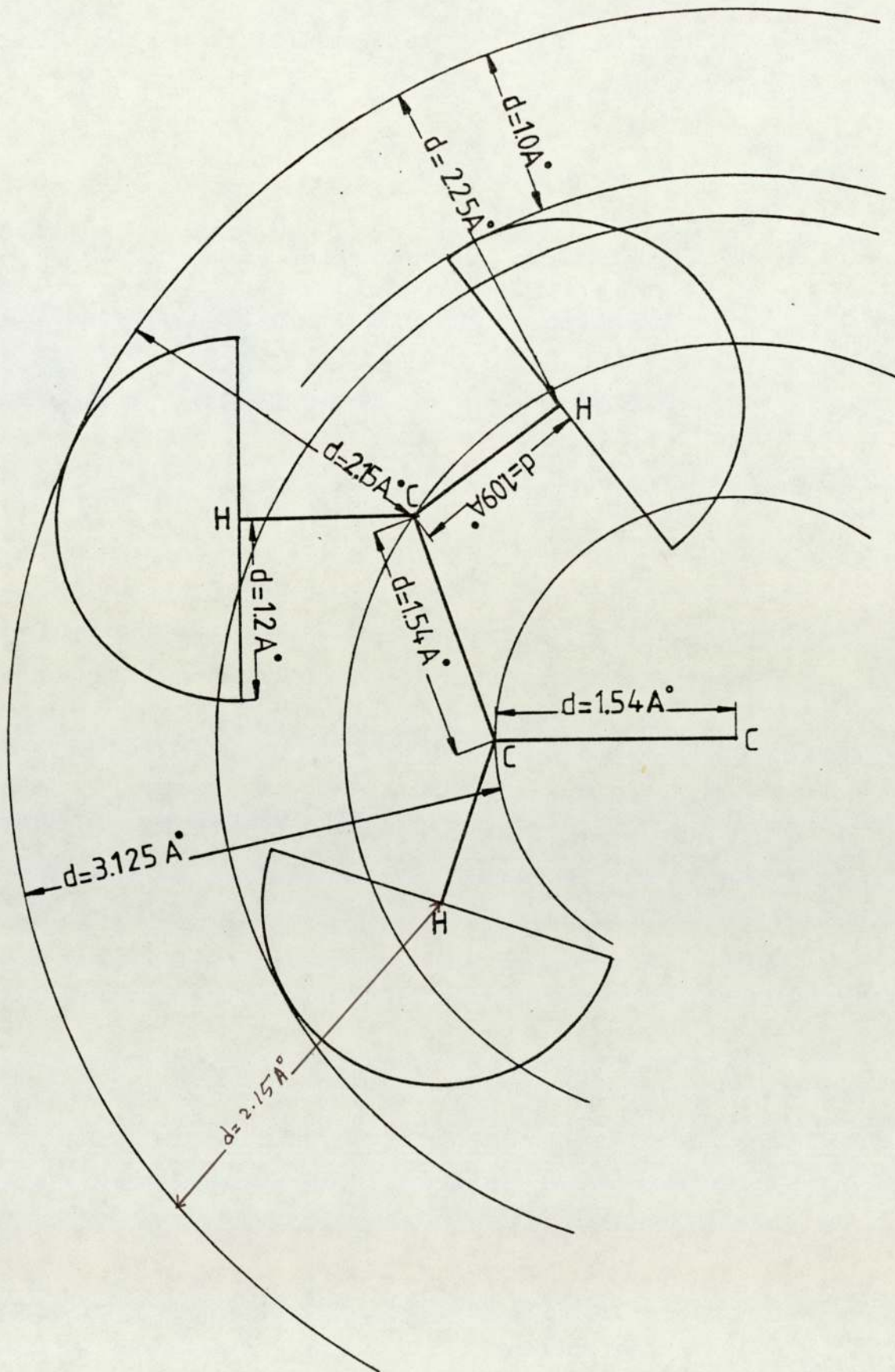
130

^1H (CH_3) CEt_4

$r = -0.617$
$m = -39.74$
$c = 143.76$ Hz.

$B = 4.44 \times 10^{-18}$ e.s.u.

$\langle R_1^2 \rangle / 10^{11}$ e.s.u.

0.2   0.3   0.4   0.5

Figure 7.4

Two-dimensional representation of CEt₄ molecule.

^1H (CH$_3$) CEt$_4$ d = 0.8 A°; a = r$_2$ + d

	$(r/r+d)^6$	$\langle R_1^2 \rangle /_{10}$	$\langle R_2^2 \rangle /_{10}$	$\langle R_2^2 \rangle (r/a)^6 /_{10}$	$\langle R_T^2 \rangle /_{10}$	$E_{BI}^2 /_{10}$	$(\langle R_T^2 \rangle + E_{BI}^2)/_{10}$	$\dfrac{\langle R_1^2 \rangle + \langle R_2^2 \rangle}{(r/a)^6 + E_{BI}} /_{10}$ $\delta^{'H}_{H_2}$
TMS	0.341	0.27345	0.61983	0.2114	0.89328	0.086	0.979	0.571 131.45
CEt$_4$	0.364	0.364	0.728	0.265	1.09201	0.183	1.275	0.812 131.18
C$_6$H$_{12}$	0.313	0.37202	1.50833	0.472	1.88036	0.14	2.020	0.984 131.92
CCl$_4$	0.301	0.40954	2.63664	0.79	3.0426	0.5	3.543	1.703 124.10

Table (7.8)   The mean square reaction fields $\langle R_1^2 \rangle$, $\langle R_2^2 \rangle$, $\langle R_T^2 \rangle$ with the modulated term $\langle R_2^2 \rangle > (\frac{r}{a})^6$ together with E_{BI}^2, for the methyl protons of CEt$_4$, where a = r$_2$ + 0.8 A°
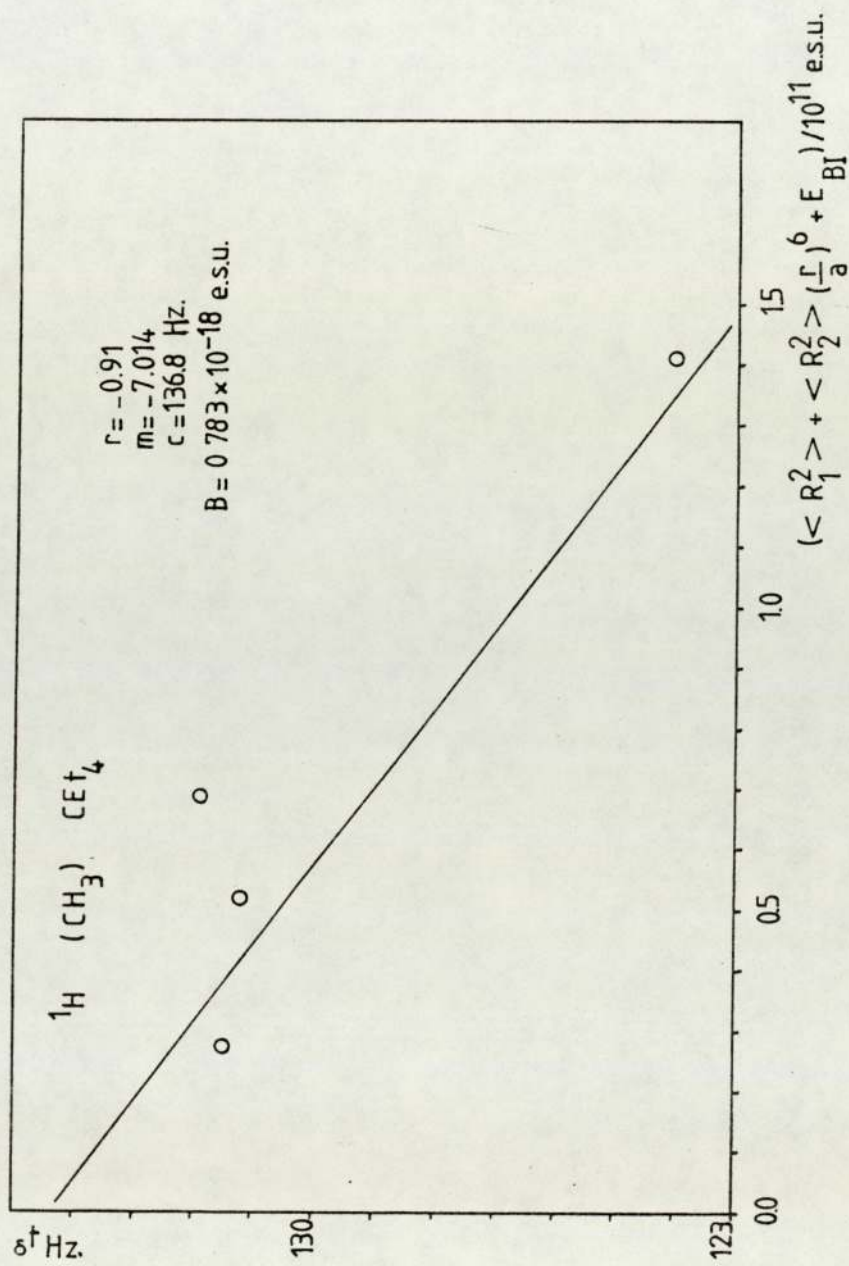
Figure 7.5   Regression of $(\ \langle R_1^2 \rangle\ +\ \langle R_2^2 \rangle\ (r/a)^6\ +\ E_{BI}^2)$ on methyl proton shifts of CEt_4.

$^1H\ \ (CH_3)\ \ CEt_4$

$r = -0.91$
$m = -7.014$
$c = 136.8$ Hz.
$B = 0\ 783 \times 10^{-18}$ e.s.u.

$(\langle R_1^2 \rangle + \langle R_2^2 \rangle\ (\frac{r}{a})^6 + E_{BI})/10^{11}$ e.s.u.

B is obtained.   Table (7.9) shows the collective B values obtained.

It is evident that the value of 0.783×10^{-18} e.s.u. is in most satisfactory agreement with that of 0.87×10^{-18} e.s.u. established before.

This gives an initial indication that $< R^2_1 >$ is induced uniformly through the cavity, and that $< R^2_2 >$ decreases with the distance from the centre of the solvent molecule, and that the buffeting is effective at the peripheral of the methyl protons.

For the case of the methylene protons, Table (7.7) shows the deduced values of the buffeting parameters together with $(2\beta - \xi)^2$ and E^2_{BI}. Then the values were calculated for $< R^2_1 >$, $< R^2_2 >$ $(r/a)^6$ and for the buffeting contribution. These are given in Table (7.10) with the d values deduced for the methylene protons from Figure 7.4 for the distance modulation calculations. The same approach as before was used in that the various regression applied to the case of the methyl protons were used for methylene protons also. These are shown in Figures (7.6, 7.7, 7.8 and 7.9). The values of B obtained therefore are summarized in Table (7.11). From the various values obtained for B, it can be seen that there is a little to chose between these obtained from the regressions including $< R^2_1 > + E^2_{BI}$ and $< R^2_1 > + < R^2_2 > + E^2_{BI}$. The reason for this is that the distance modulation for the methylene protons essentially eliminates $< R^2_2 >$. This is a particularly important result because it is to be expected that $< R^2_2 >$ for nuclei not at

Regression of	B value/10^{-18} e.s.u.
$< R_1^2 >$	4.44
$< R_T^2 >$	0.32
$< R_T^2 > + E_{BI}^2$	0.284
$<R_1^2> + <R_2^2>\left(\frac{r}{a}\right)^6 + E_{BI}^2$	0.783
$<R_1^2> + <R_2^2>\left(\frac{r}{a}\right)^6$	1.13

Table (7.9) Collected B values from the different regressions for the methyl protons in CEt_4.

^1H CH_2 CEt_4, d = 2.51 A°

$a = r_2' + d$

	$(r/r+d)^6$	$\langle R_1^2 \rangle /_{1b}''$	$\langle R_2^2 \rangle /_{1b}'$	$\langle R_2^2 \rangle (r/a)^6 /_{1b}''$	$\langle R_T^2 \rangle /_{1b}''$	$E_{BI}^2 /_{1b}''$	$\langle R_T^2 \rangle + E_{BI}^2$	$\dfrac{\langle R_1^2 \rangle + \langle R_2^2 \rangle}{(r/a)^6 + E_{BI}^2} /_{1b}''$	δ'_H Hz
TMS	0.0563	0.27345	0.61983	0.0349	0.89328	1.783	2.056	2.091	93.17
CEt_4	0.0653	0.364	0.728	0.0475	1.09201	1.576	1.94	1.9875	93.68
C_6H_{12}	0.0461	0.37202	1.50833	0.0695	1.88036	1.198	1.57	1.64	94.43
CCl_4	0.0422	0.40964	2.63664	0.1113	3.0426	1.933	2.343	2.454	87.97

Table (7.10) The mean square reaction fields $\langle R_2^2 \rangle \left(\frac{r}{a}\right)^6$ together with E_{BI}^2 for the methylene protons of CEt_4, where $a = r_2 + 2.51 A^\circ$.
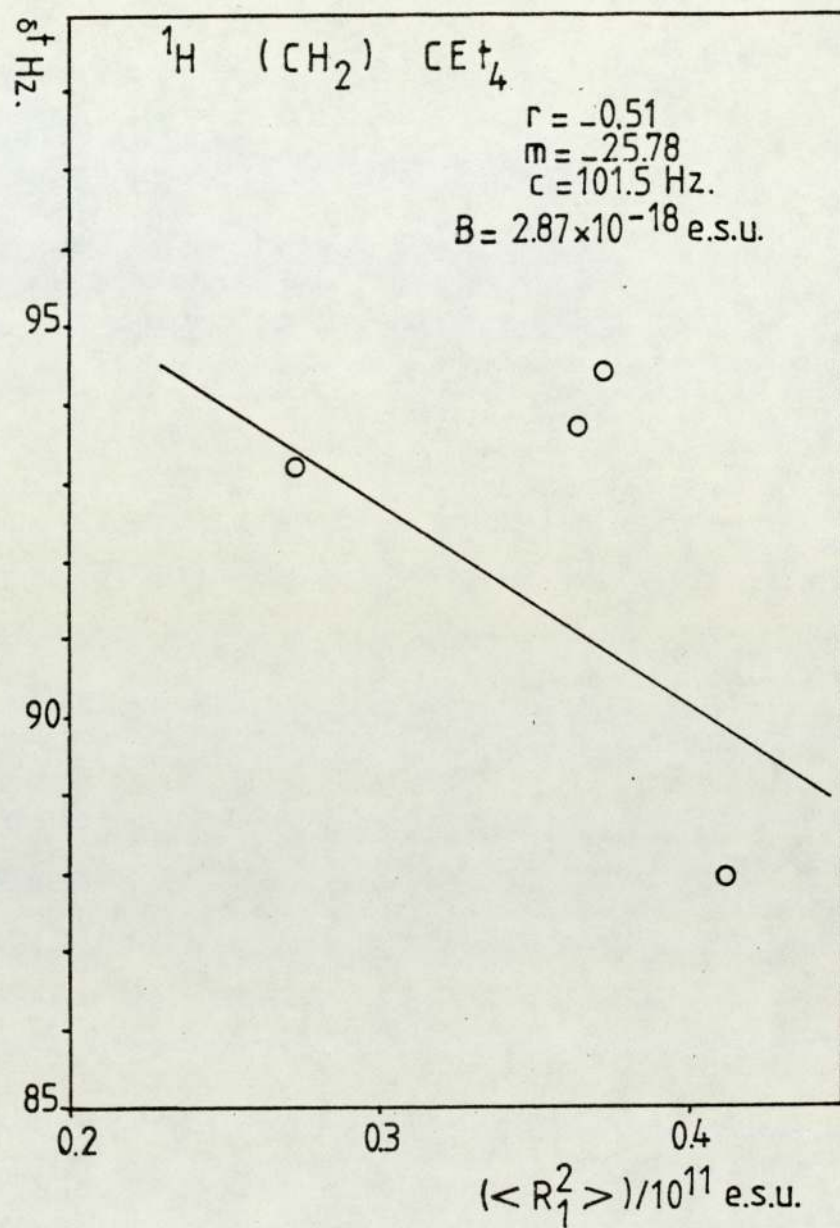
Figure 7.6   Regression of ($< R^2_1 >$) on methylene
proton shifts of CEt_4.

Figure 7.7   Regression of ($<R_1^2>$ + $<R_2^2>$) on methylene
proton shifts of CEt$_4$.

Figure 7.8   Regression of $(<R^2_1> + E^2_{BI})$ on
               methylene proton shifts of CEt_4.

$\delta^\dagger$ Hz.

^1H (CH_2) CEt_4

$r = -0.9$
$m = -7.94$
$c = 108.5$ Hz.
$B = 0.886 \times 10^{-18}$ e.s.u.

95

90

85

1.0   2.0   3.0

$(<R_1^2> + <R_2^2>(\frac{r}{a})^6 + E^2_{BI})/10^{11}$ e.s.u.
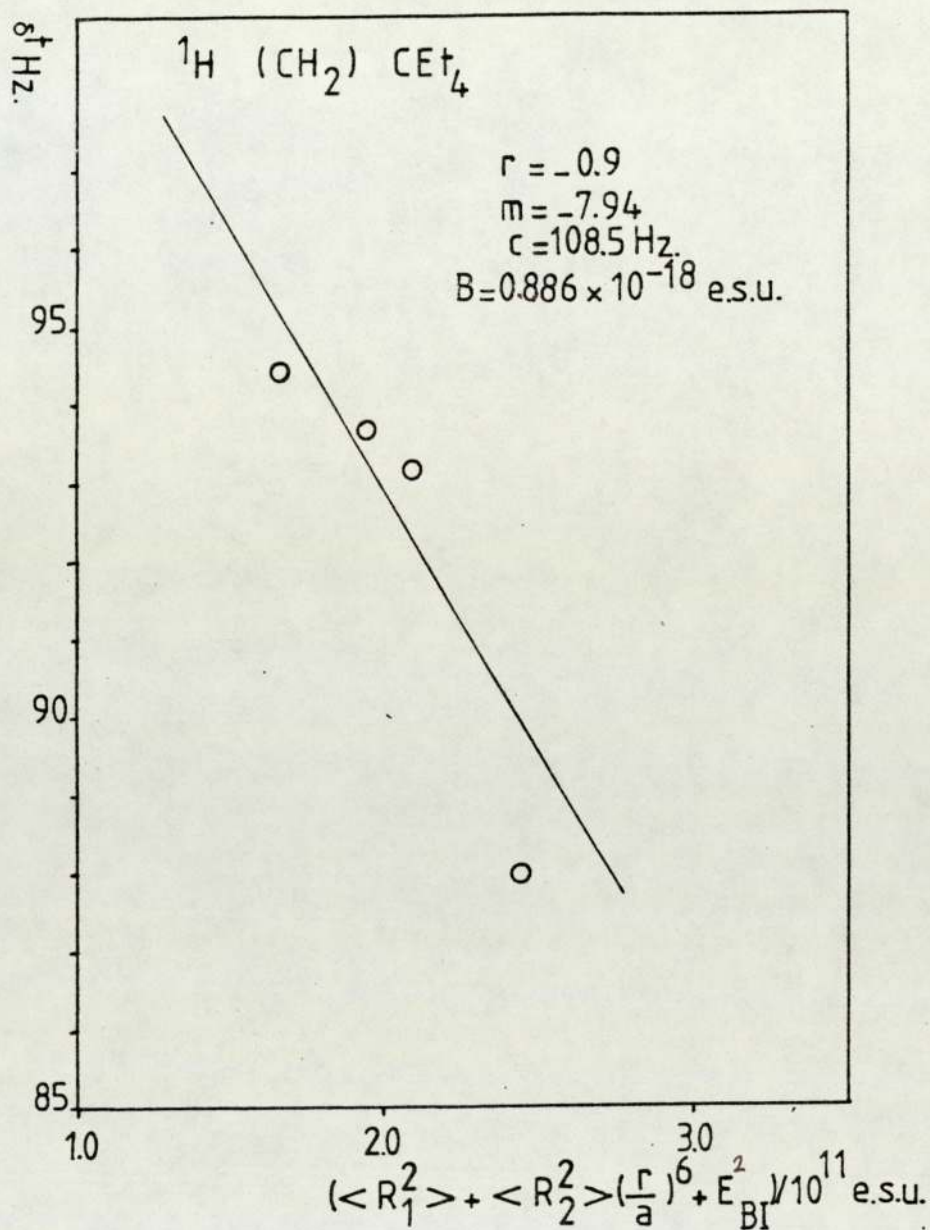
Figure 7.9   Regression of ($<R^2_1>$ + $<R^2_2>$ $(r/a)^6$ + E^2_{BI}) on methylene proton shifts of CEt_4.

232

^1H CH_2

Regression of	B value/10^{-18} e.s.u.
$\langle R_1^2 \rangle$	2.87
$\langle R_T^2 \rangle$	0.272
$\langle R_1^2 \rangle + \langle R_2^2 \rangle \left(\frac{r}{a}\right)^6 + E_{BI}^2$	0.886
$\langle R_1^2 \rangle + E_{BI}^2$	0.884

Table (7.11)   Collected B values from the different regressions for the methylene CH_2 protons in CEt_4.

the periphery of the molecule will be attenuated very rapidly with the distance of the resonant site from the centre of the solvent molecule.

In reaching the above conclusion the similarity between the values of B deduced with that obtained by Homer and Percival of 0.87×10^{-18} e.s.u.[64] has been used as the criterion for assessing the contributions of $< R^2_1 >$, $< R^2_2 >$ and E^2_{BI} to the intermolecular forces. This would appear reasonable because for a proton sp^3 bound to carbon, it is to be expected that they will always have similar B values. However, while in general, the B values for some nucleus X bonded to an atom Y may well be of similar magnitude for different Y, their precise values are expected to depend on the nature of Y [29,105]. This situation will probably occur for the three distinct ^{13}C nuclei in tetraethylmethane, because for the central, methylene and methyl carbons, each has different bonded atoms. This situation will now be discussed.

7.3.2 Analysis Of ^{13}C Shifts of $C(CH_2CH_3)_4$:

The observed and susceptibility corrected shifts of ^{13}C for $C(CH_2CH_3)_4$ are recorded in Table (7.3).

Even the methyl carbon in CEt_4 can be considered to be protected by the bonded protons from buffeting by the solvent molecule. It is reasonable, therefore, to assume that there is no

buffeting contribution to any of these ^{13}C shifts. Accordingly, only values of $\langle R^2_1 \rangle$, $\langle R^2_2 \rangle$ and $(r/a)^6 \langle R^2_2 \rangle$ were calculated for the methyl ^{13}C and these are recorded in Table (7.12). Figures (7.10, 7.11 and 7.12) show the regressions of $\langle R^2_1 \rangle$, $\langle R^2_T \rangle$ and $\langle R^2_1 \rangle + \langle R^2_2 \rangle (r/a)^6$ on the methyl ^{13}C shifts, respectively. These regressions yield B values of 44.78 x 10^{-18}, 2.94 x 10^{-18} and 24.07 x 10^{-18} e.s.u. respectively, these values are collected in Table 7.13.

For the methylene carbon in CEt_4, Table (7.14) shows the calculated $\langle R^2_1 \rangle$, $\langle R^2_T \rangle$ and $\langle R^2_2 \rangle (r/a)^6$. Figures (7.13, 7.14 and 7.15) show the regressions of $\langle R^2_1 \rangle$, $\langle R^2_T \rangle$ and $\langle R^2_1 \rangle + \langle R^2_2 \rangle (r/a)^6$ on the methylene ^{13}C shifts. Those gave B values are summarized in Table (7.15).

Since the central carbon is at the centre of the molecule, Figures (7.16 and 7.17) show the regressions of $\langle R^2_1 \rangle$ and $\langle R^2_T \rangle$ on the shifts; the data is given in Table 7.16. These gave values for B of 16.8 x 10^{-18} and 1.63 x 10^{-18} e.s.u. It seems for the sets of B values obtained in Tables 7.13, 7.15 and 7.16, that the values of 24.07 x 10^{-18}, 16.79 x 10^{-18} and 16.8 x 10^{-18} are for the methyl, methylene and central carbons respectively are immently reasonable, are consistant and the procedure by which they are obtained suggests again that $\langle R^2_1 \rangle$ is uniform through the cavity and that $\langle R^2_2 \rangle$ is modulated by the distance parameter. If in fact the values of B for the three carbons should be the same it would appear that the methyl carbon nucleus may be subject to buffeting to some small extent.

$^{13}C (CH_3) CEt_4$

$d = 2.15\,\text{Å}$ $a = r_2 + 2.15\,\text{Å}$

Solvent	$\left(\dfrac{r_2}{r_2+d}\right)^6$	$\langle R_1^2\rangle$	$\langle R_2^2\rangle$	$\langle R_2^2\rangle\left(\dfrac{r}{a}\right)^6$	$\langle R_T^2\rangle$	$\langle R_1^2\rangle + \langle R_2^2\rangle\left(\dfrac{r}{a}\right)^6$	^{13}C δ_{CH_3} ppm
TMS	0.079	0.27345	0.61983	0.04887	0.89328	0.3223	84.87
CEt_4	0.09	0.364	0.728	0.0656	1.09201	0.43	84.87
C_6H_{12}	0.066	0.37202	1.50833	0.0992	1.88036	0.47123	85.06
CCl_4	0.0607	0.40964	2.63664	0.1601	3.0426	0.5697	84.21

Table (7.12) The mean square reaction fields $\langle R_1^2\rangle$, $\langle R_2^2\rangle$, $\langle R_T^2\rangle$ and the modulated term $\langle R_2^2\rangle\left(\dfrac{r}{a}\right)^6$ for the methyl ^{13}C of CEt_4 where $a = r_2 + 2.15\,A^°$.
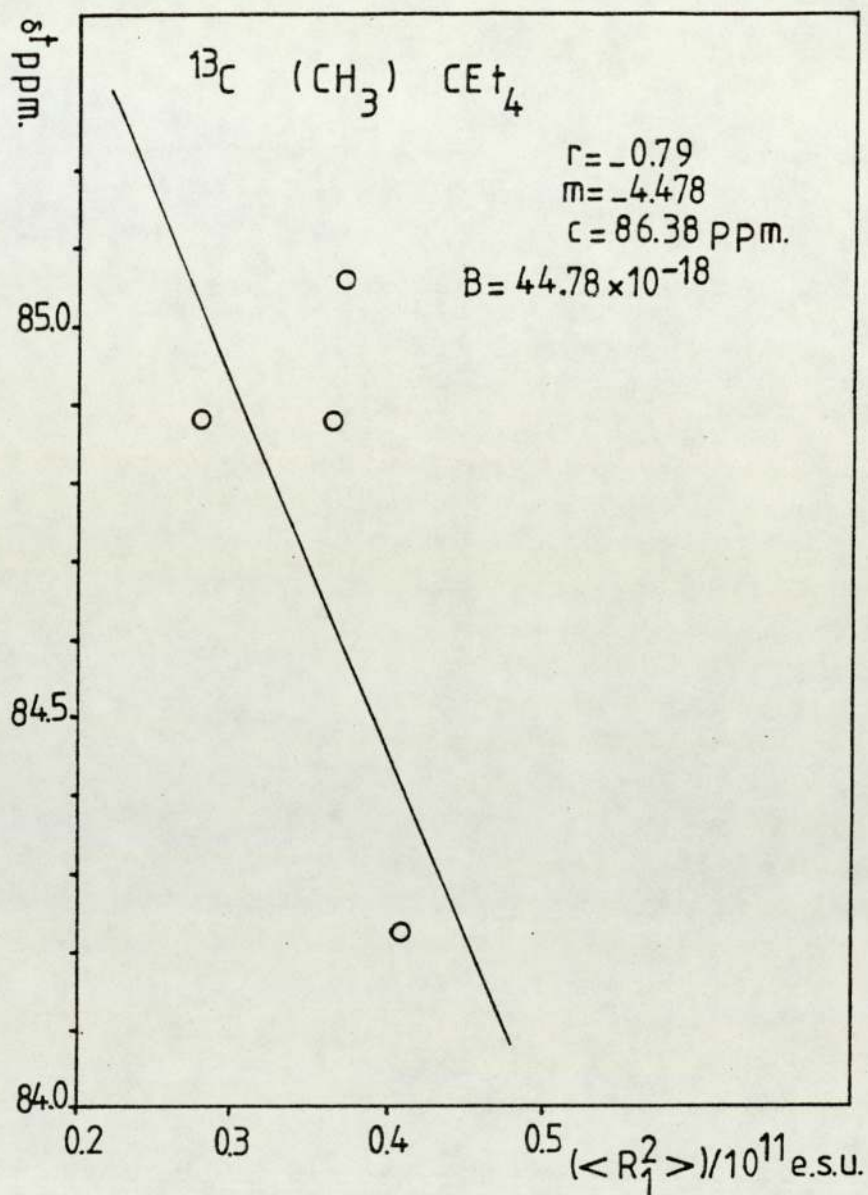
Figure 7.10   Regression of ($<R^2_1>$) on ^{13}C methyl shifts of CEt$_4$.

237
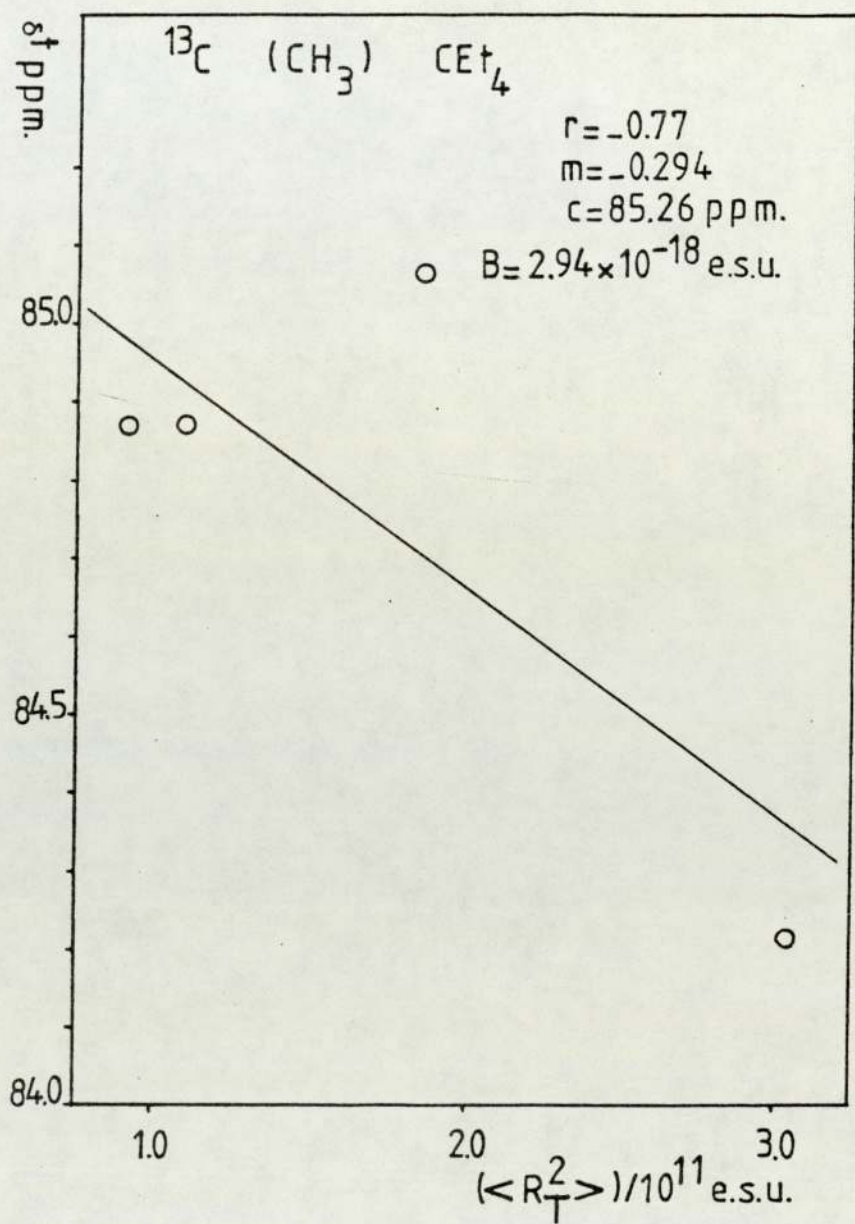
Figure 7.11   Regression of ($< R^2_T >$) on ^{13}C methyl shifts of CEt_4.

238
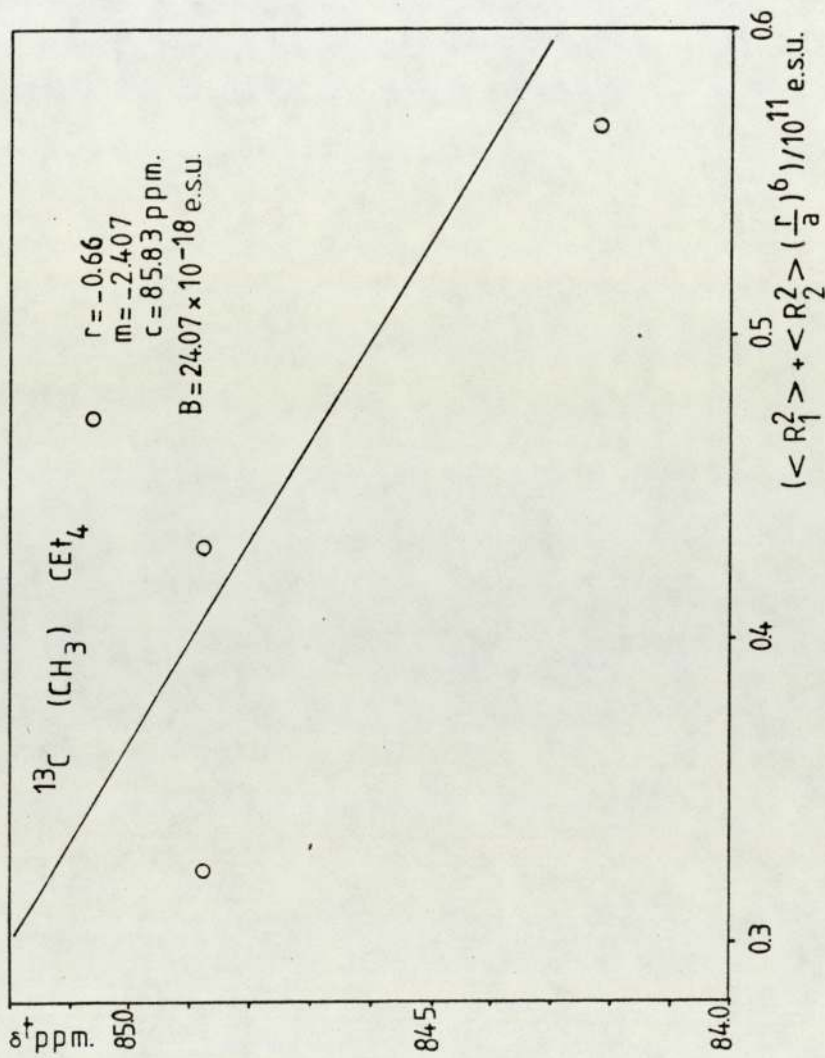
Figure 7.12 Regression of $(<R_1^2> + <R_2^2>) \; (r/a)^6)$ on ^{13}C methyl shifts of CEt_4.

239

^{13}C (CH_3) CEt_4

Regression of	B value/$_{10}-18$
$< R_1^2 >$	44.78
$< R_T^2 >$	2.94
$<R_1^2> + <R_2^2> \left(\frac{r}{a}\right)^6$	24.07

Table (7.13) Collected B values for various regression on the ^{13}C methyl of CEt_4.

^{13}C (CH_2) CEt_4

$d = 3.125$ A° $a = r_2 \, d$

Solvent	$\left(\dfrac{r_2}{r_2+d}\right)^6$	$\langle R_1^2\rangle/10^{11}$ e.s.u.	$\langle R_2^2\rangle/10^{11}$ e.s.u.	$\langle R_2^2\rangle\left(\dfrac{r}{a}\right)^6$ e.s.u. /10^{11}	$\langle R_T^2\rangle/10^{11}$ e.s.u.	$\langle R_1^2\rangle+\langle R_2^2\rangle\left(\dfrac{r}{a}\right)^6/10^{11}$ e.s.u.	^{13}C δ C CH_2 ppm
TMS	0.033	0.27345	0.61983	0.02425	0.89328	0.2939	65.05
CEt_4	0.039	0.364	0.728	0.0284	1.09201	0.3924	64.94
C_6H_{12}	0.0263	0.37202	1.50833	0.0396	1.88036	0.412	65.02
CCl_4	0.0238	0.40964	2.63664	0.0627	3.0426	0.472	64.71
B/10^{-18} e.s.u.			20.17		1.34	16.79	

Table (7.14) The reaction fields $\langle R_1^2\rangle$, $\langle R_2^2\rangle$, $\langle R_2^2\rangle$ and the modulated term $\langle R_2^2\rangle\left(\dfrac{r}{a}\right)^6$ for the methylene ^{13}C of CEt_4, where $a = r_2 + 3.125$ A°.

241
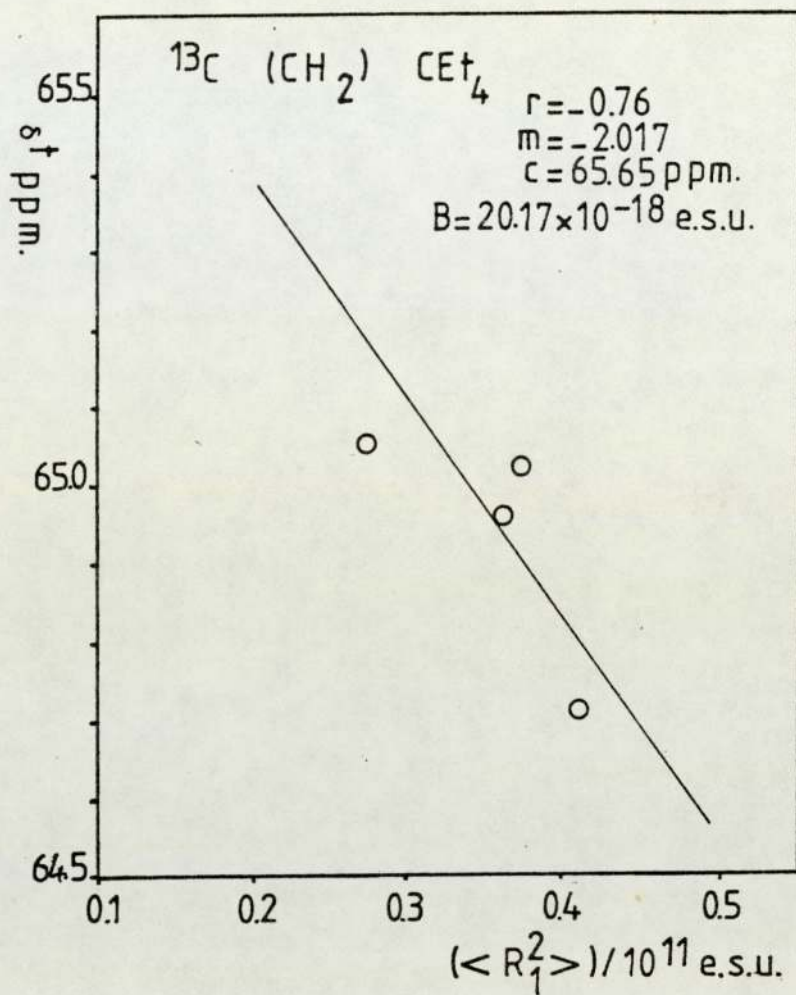
Figure 7.13   Regression of ($<R^2_1>$) on ^{13}C methylene shifts of CEt_4.
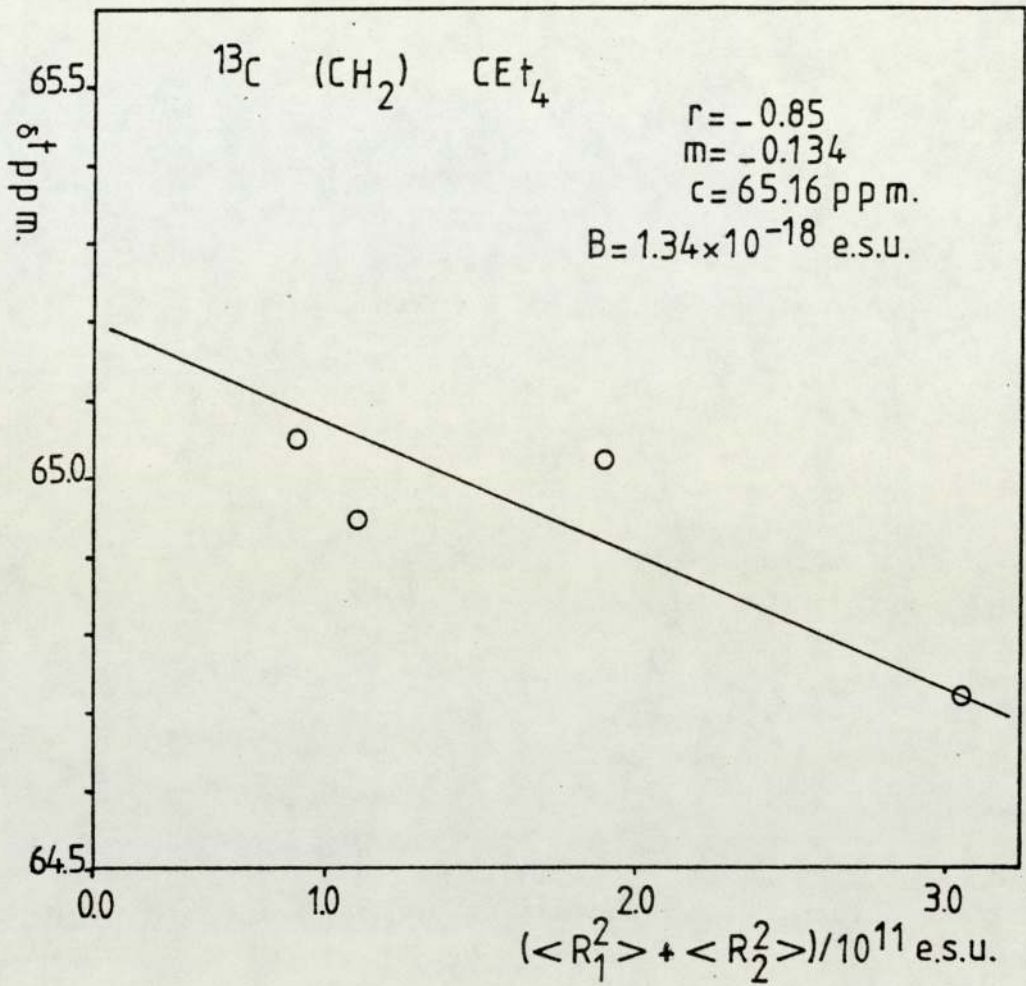
Figure 7.14   Regression of $(<R^2_1> + <R^2_2>)$ on ^{13}C methylene shift of CEt_4.
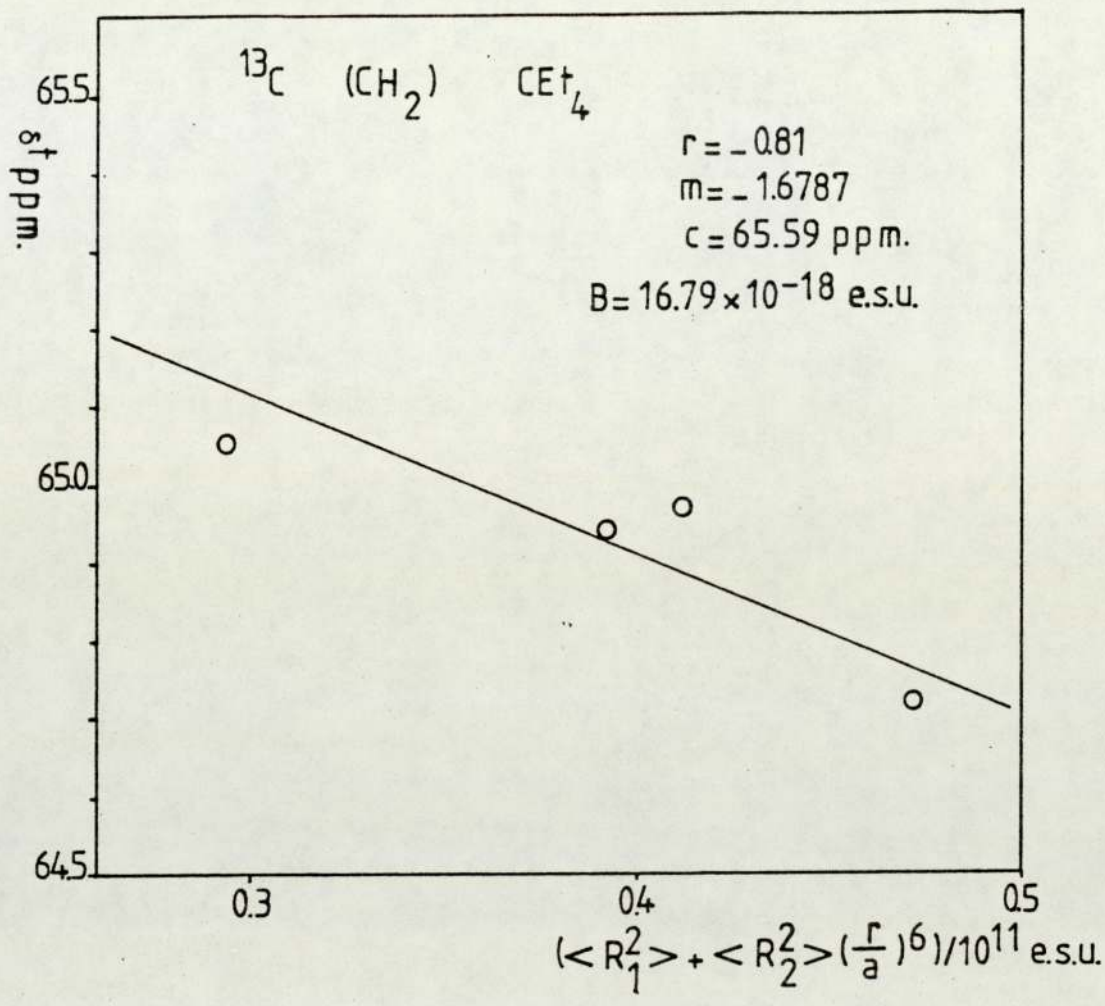
Figure 7.15   Regression of $(<R^2_1> + <R^2_2> (r/a)^6)$ on ^{13}C methylene shift of CEt_4.

244

Regression of	B value/10^{-18}
	e.s.u.
$\langle R_1^2 \rangle$	20.17
$\langle R_T^2 \rangle$	1.34
$\langle R_1^2 \rangle + \langle R_2^2 \rangle \left(\dfrac{r}{a}\right)^6$	16.79

Table (7.15)   Collected B values from various regression of the methylene ^{13}C in CEt_4.
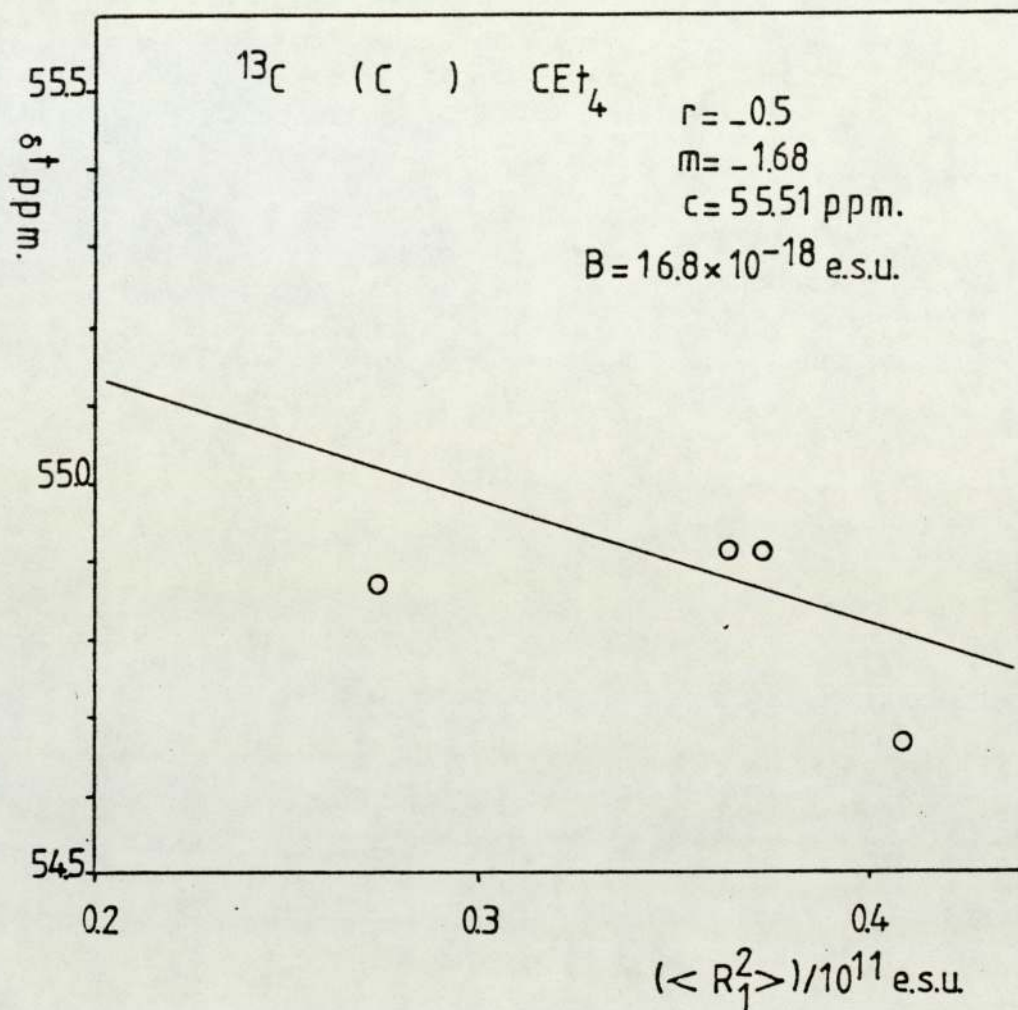
Figure 7.16   Regression of $(\langle R^2_1 \rangle)$ on central ^{13}C shifts of CEt_4.
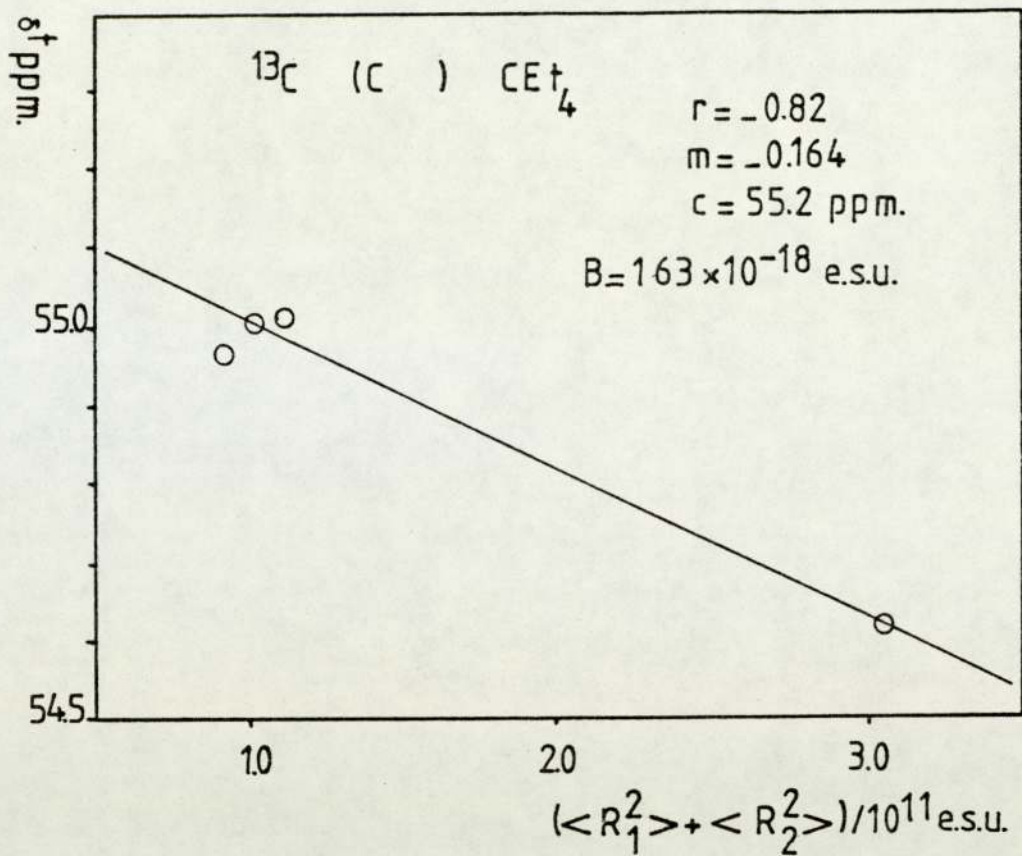
Figure 7.17   Regression of ($<R^2_1>$ + $<R^2_2>$) on central ^{13}C shifts of CEt$_4$.

Solvent	$<R_1^2>$	$<R_T^2>$	$\begin{matrix} ^{13}c \\ \delta \\ ppm \end{matrix}$
TMS	0.27345	0.89328	54.97
CEt_4	0.364	1.09201	55.02
C_6H_{12}	0.37202	1,88036	55.05
CCl_4	0.40964	3.0426	54.63
$B/_{10}-18$ e.s.u.	16.8	1.63	

Table (7.16)   The mean square reaction fields $<R_1^2>$, $<R_T^2>$ together with the 13_c shifts of the central carbon atom of $C(CH_2 CH_3)_4$.

7.4 **STUDIES OF TETRAMETHYLSILANE Si $(CH_3)_4$:**

In view of the encouraging analysis of the ^1H and ^{13}C shifts of CEt_4 just discussed, similar analysis for the ^1H, ^{13}C and ^{29}Si of TMS were undertaken.

The gas phase shifts of ^1H and ^{13}C of TMS were measured at various pressures and are given in Tables (7.17 **A and B**) respectively. The latter were extrapolated as shown in Figures (7.18 and 7.19) respectively to zero pressure and the values obtained are given in Table 7.18. These values were used in the subsequent analysis. The gas samples were prepared in the same manner to that described in Chapter 4 (section 4.3.2). Although not immediately relevant to the present investigation, the zero pressure ^1H and ^{13}C shifts together with the corresponding shifts in pure TMS Table 7.18 enable the appropriate gas-to-liquid shifts to be deduced, these are also given in Table 7.18.

7.4.1 **Analysis Of ^1H Shifts Of Si $(CH_3)_4$:**

The observed and susceptibility corrected shifts of the methyl protons of TMS in various solvents are given in Table (7.19). Using data collected earlier in Tables (7.4 and 4.9), the values of the square fields $< R^2_1 >$, $< R^2_2 >$ and $< R^2_T >$ are calculated and given in Table (7.20).

TMS Sample	^{1}H shift Hz
Gas P = 16cm Hg	125.49
Gas P = 24 cm Hg	124.51
Gas P = 33 cm Hg	124.51
Gas P = 47 cm Hg	123.78

Table (7.17)A   Proton gas shifts of $SiMe_4$ at different pressures. Measurements were made using a JEOL FX 90 Q NMR spectrometer locked onto ^{2}H of D_2O, at 30^oC operating at irradiator frequency of 89.60405 MHz.

TMS Sample	^{13}C shift Hz
Gas P = 24 cm Hg	173.34
Gas P = 33 cm Hg	173.34
Gas P = 47 cm Hg	172.12
Gas P = 60 cm Hg	172.12

✶ Table (7.17) B ^{13}C gas shifts of $SiMe_4$ at different pressures. Measurement were made using a JEOL FX 90 Q NMR spectrometer locked onto ^2H of D_2O at $30^{\circ}C$, operating at irradiation frequency of 22.531 MHz.

* See Table 7.18
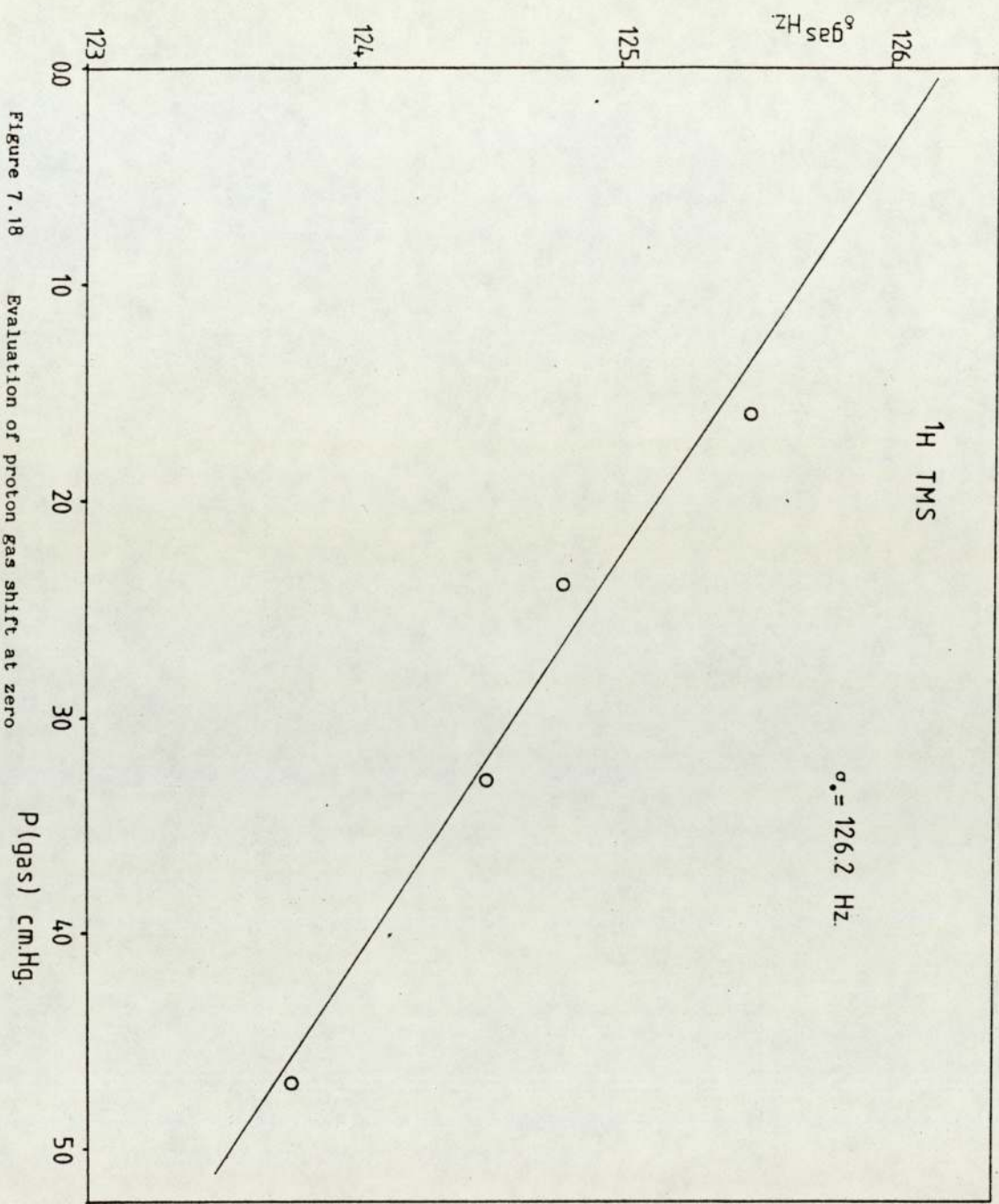
Figure 7.18   Evaluation of proton gas shift at zero pressure of TMS.

P(gas) cm.Hg.

δ_{gas} Hz.

^{1}H TMS

σ_o = 126.2 Hz.

The graph axes read:

σ_{o} gas Hz.

174, 173, 172, 171 (vertical axis)

^{13}C TMS

$\sigma_{o} = 174.4$ Hz.

P(gas) cm.Hg.

0.0, 10, 20, 30, 40, 50, 60 (horizontal axis)
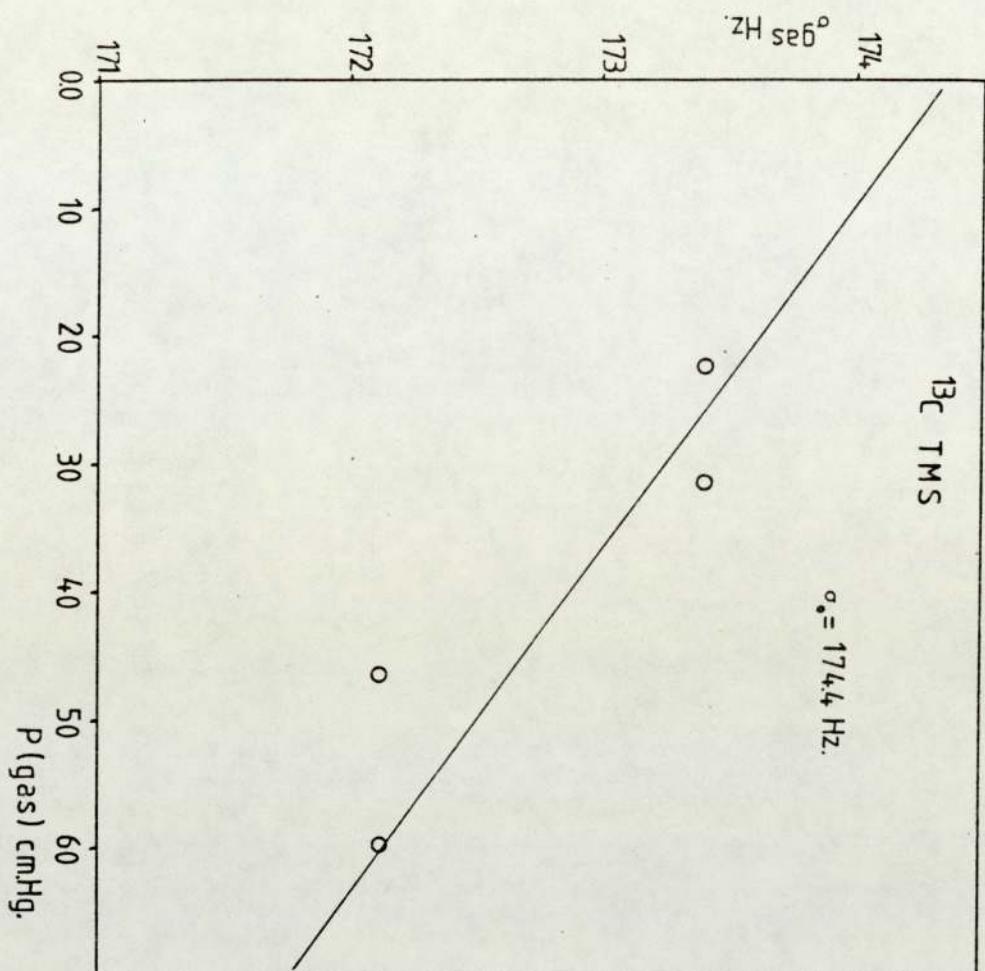
* Figure 7.19   Evaluation of ^{13}C gas shift at zero pressure of TMS.

* See Table (7.18)

	^1H	^{13}C
$\sigma_0 =$ gas (P = 0) (H_z)	126.2	174.4 *
obs δ liquid (H_z)	0.98	57.37
$-2\pi/3$ X_v (H_z)	100.59	25.29
true δ liquid (H_z)	101.57	82.66
δgas-to-liquid (H_z)	-24.63	-91.74
δgas-to-liquid (ppm)	-0.275	-4.07

Table (7.18) Gas-to-liquid chemical shifts for ^1H and ^{13}C in TMS. These shifts were measured with an irradiation frequency of 89.60405 MHz for ^1H and 22.531 MHz for ^{13}C.

* Subsequent consideration of this value indicates that an instrumental artifact may have resulted in this gas-phase shift being in error. This in no-way effects the conclusions of the ensuing analyses.

254

^{1}H in TMS

Solvent	obs $\delta\,^1$H Hz	obs $\delta\,^1$H ppm	$-2\pi/_3\,X_v$	true $\delta\,^1$H ppm
None gas (P=0)	326.16	3.640	0	3.640
TMS	200.00	2.232	1.123	3.355
CCl_4	164.31	1.834	1.442	3.276
C_6H_{12}	184.08	2.054	1.327	3.381
CEt_4	175.98	1.964	1.403	3.367
C_6H_6	217.29	2.425	1.296	3.721

Table (7.19)   The observed and susceptibility corrected proton shifts os $SiMe_4$ in different solvents obtained by using a JEOL FX 90 Q NMR spectrometer locked at ^{2}H of D_2O, operating at 30°C and an irradiation frequency of 89.60425 MHz.

Solvent	$\langle R_1^2 \rangle / 10^{11}$ esu	$\langle R_2^2 \rangle / 10^{11}$ esu	$\langle R_T^2 \rangle / 10^{11}$ esu
TMS	0.2715	0.543	0.8145
CCl_4	0.40412	2.3097	2.7138
C_6H_{12}	0.3676	1.3214	1.689
CEt_4	0.3598	0.6377	0.9975
C_6H_6	0.4671	2.7815	3.2486

Table (7.20)   The calculated mean square reaction fields $\langle R_1^2 \rangle$, $\langle R_2^2 \rangle$ and $\langle R_T^2 \rangle$ for TMS in various solvents.

By reference to Figure (7.20) which shows a two-dimensional representation of the $Si(CH_3)_4$ molecule, the values of the relevant distance modulation can be calculated, and these provided with the relevant tables, that including the modulated reaction field. Table (7.21) shows the modulated square reaction field with $< R^2_1 >$, $< R^2_2 >$ and $< R^2_T >$ together with E^2_{BI} for the protons in TMS. Figures (7.21, 7.22, 7.23 and 7.24) show the regressions of $< R^2_T >$, $< R^2_1 > + < R^2_2 > (r/a)^6$, $< R^2_1 > + < R^2_2 > + E^2_{BI}$ and $< R^2_1 > + < R^2_2 > (r/a)^6 + E^2_{BI}$ on the corrected proton shifts.

The gas phase shift was not initially used in the regressions but as a criterion additional to the B values, so that the best overall fit could be highlighted.

The values of B obtained from the various regressions on the protons of TMS, mentioned above, are shown in Table (7.22), which demonstrates again that the regression of $< R^2_1 > + < R^2_2 > (r/a)^6 + E^2_{BI}$ yields the most realistic value for B of 0.91×10^{-18} e.s.u. This indicates again that $< R^2_2 >$ is distance modulated and the buffeting contribution exist on the periphery.

Additionally, this regression has the intercept of 3.44 ppm, that is most consistent with the gas phase shift of 3.64 ppm, experimentally obtained earlier.

The data where benzene as a solvent was not included in the regressions, because of the contribution of σ_a. However from

257
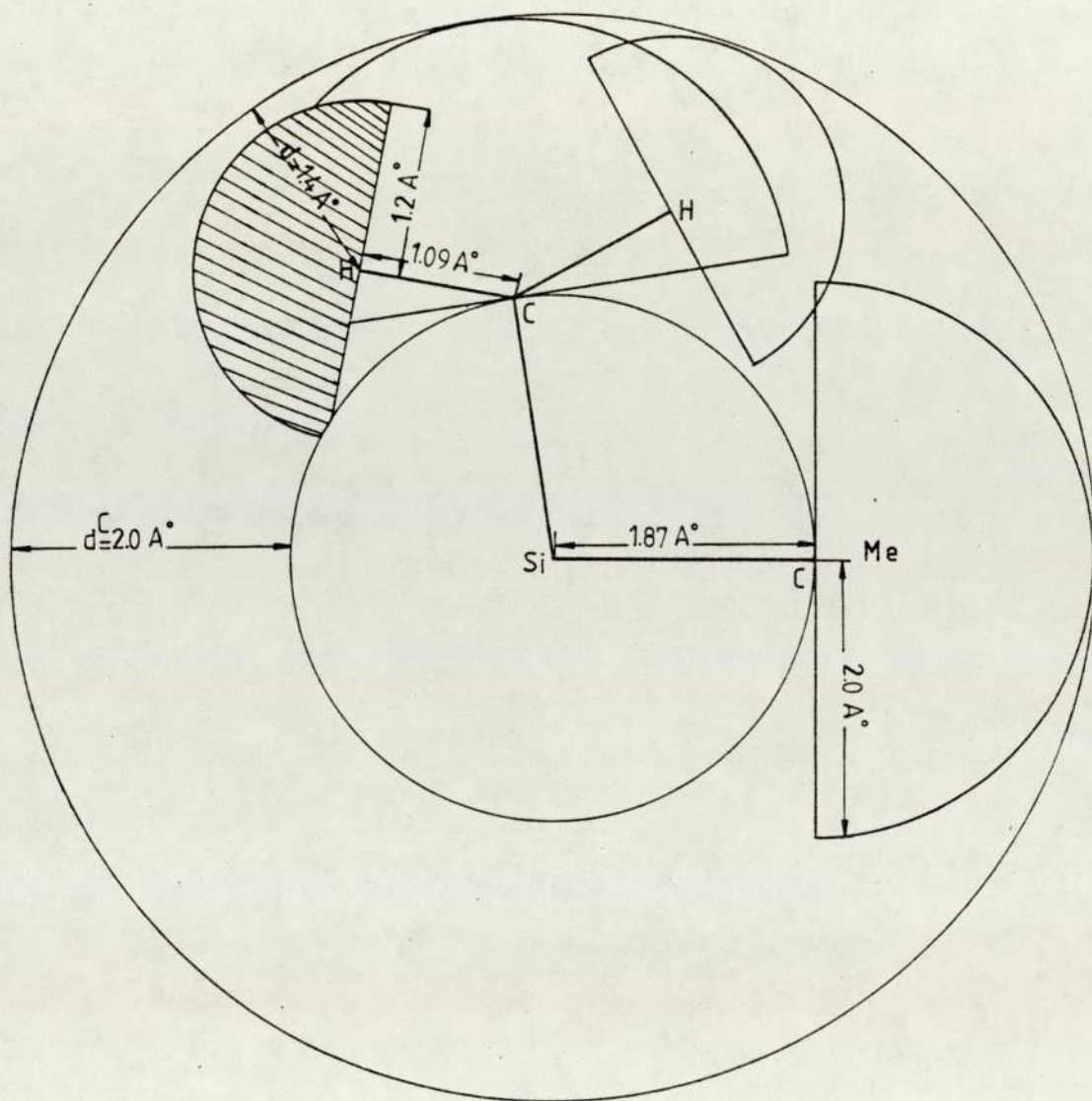
Figure 7.20   Two-dimensional representation of tetramethylsilane
molecule.

258

^1H CH_3 TMS

$d = 0.7\ A°$ $a = r + 0.7$

Solvent	$\left(\dfrac{r}{r+d}\right)^6$	$\langle R_1^2\rangle$	$\langle R_2^2\rangle$	$\langle R_2^2\rangle (r/a)^6$	E_{BI}^2	$\langle R_T^2\rangle$	$(r/a)^6$	$\dfrac{\langle R_1^2\rangle+\langle R_2^2\rangle}{(r/a)^6+E_{BI}^2}$	$\dfrac{\langle R_1^2\rangle+\langle R_2^2\rangle}{\langle R_T^2\rangle+E_{BI}^2}$	δ^1H ppm
TMS	0.387	0.2715	0.543	0.21	0.171	0.8145	0.4815	0.6525	0.986	3.355
CCl_4	0.346	0.40412	2.3097	0.798	0.3	2.7138	1.202	3.014		3.276
C_6H_{12}	0.358	0.3676	1.3214	0.473	0.15	1.689	0.8406	0.991	1.839	3.381
CEt_4	0.409	0.3598	0.6377	0.261	0.178	0.9975	0.6208	1.176	1.176	3.367
C_6H_6	0.335	0.4671	2.7815	0.933	0.143	3.2486	1.4001	1.543	3.392	3.721

Table (7.21) The calculated square fields $\langle R_1^2\rangle$, $\langle R_2^2\rangle$ and the modulated term $\left(\dfrac{r}{a}\right)^6 \langle R_2^2\rangle$ together with the square buffeting field for the proton in TMS.

259

^{1}H TMS

r = − 0.78
m = − 0.043
c = 3.41 ppm.
B = 0.43 × 10^{-18} e.s.u.

δ_+ ppm.

3.5

3.3

1.0

2.0

3.0
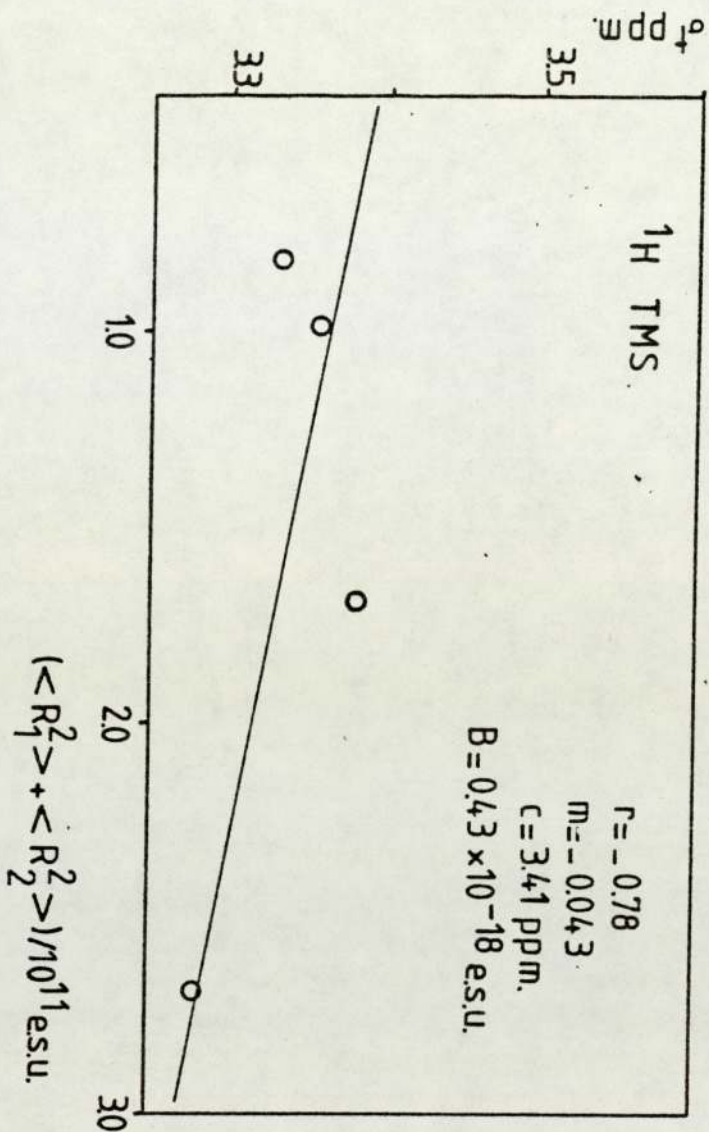
$(\langle R_1^2 \rangle + \langle R_2^2 \rangle)/10^{11}$ e.s.u.

Figure 7.21   Regression of $(\langle R_1^2 \rangle + \langle R_2^2 \rangle)$ on proton shifts of TMS.

260
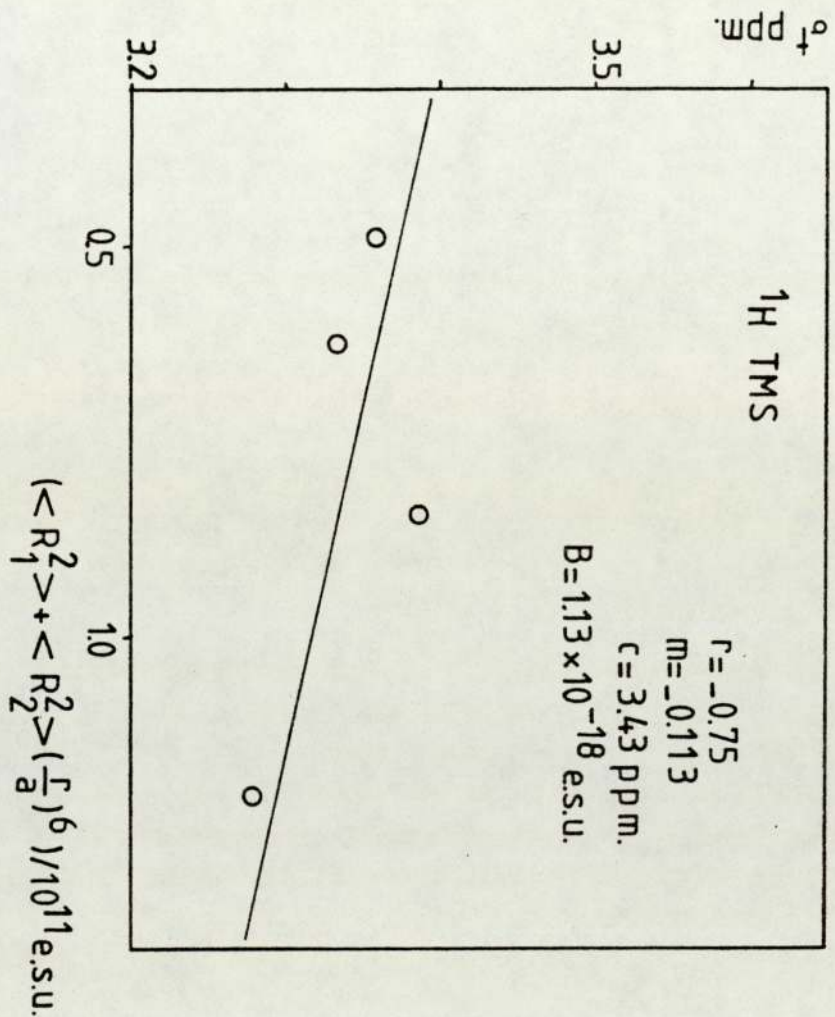
Figure 7.22   Regression of $(<R_1^2> + <R_2^2> (r/a)^6)$ on proton shifts of TMS.

^1H TMS

r = -0.75
m = -0.113
c = 3.43 ppm.
B = 1.13 × 10^{-18} e.s.u.

σ_t ppm.

$(<R_1^2> + <R_2^2>(\frac{r}{a})^6)/10^{11}$ e.s.u.

^{1}H TMS

r = -.08
m = -0.04
c = 3.42 ppm.
B = 04×10^{-18} e.s.u.

$\delta\uparrow$ppm.

3.5

3.2

1.0   2.0   3.0
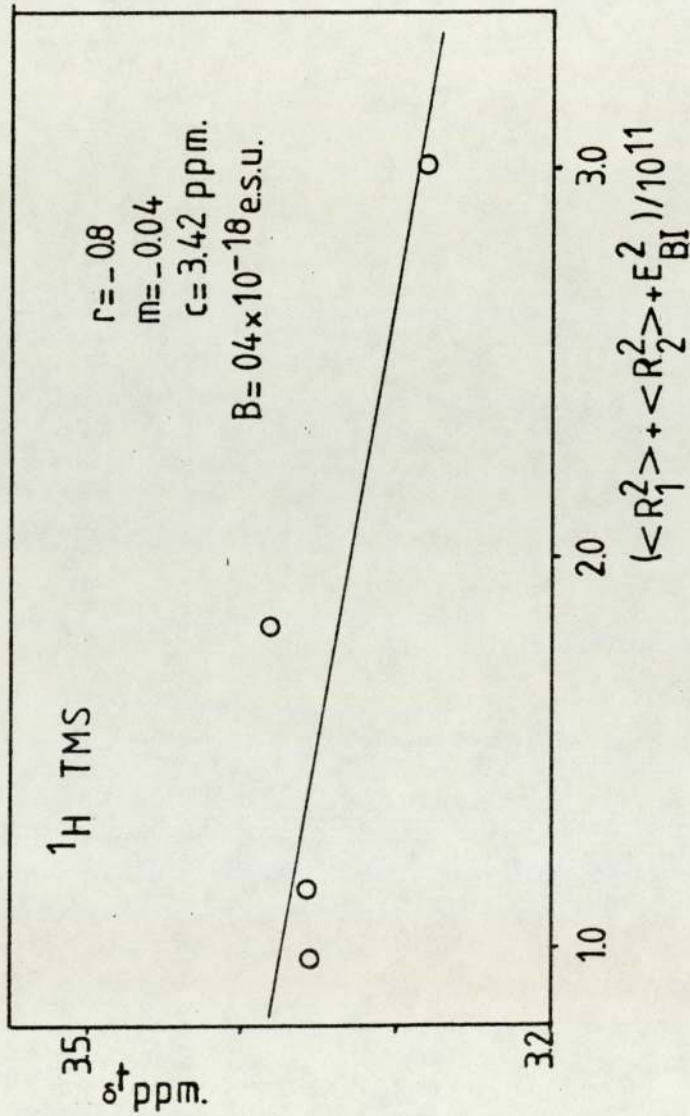
$(\langle R_1^2 \rangle + \langle R_2^2 \rangle + E_{BI}^2)/10^{11}$

Figure 7.23   Regression of $(\langle R_1^2 \rangle + \langle R_2^2 \rangle + E_{BI}^2)$ on proton shifts of TMS.
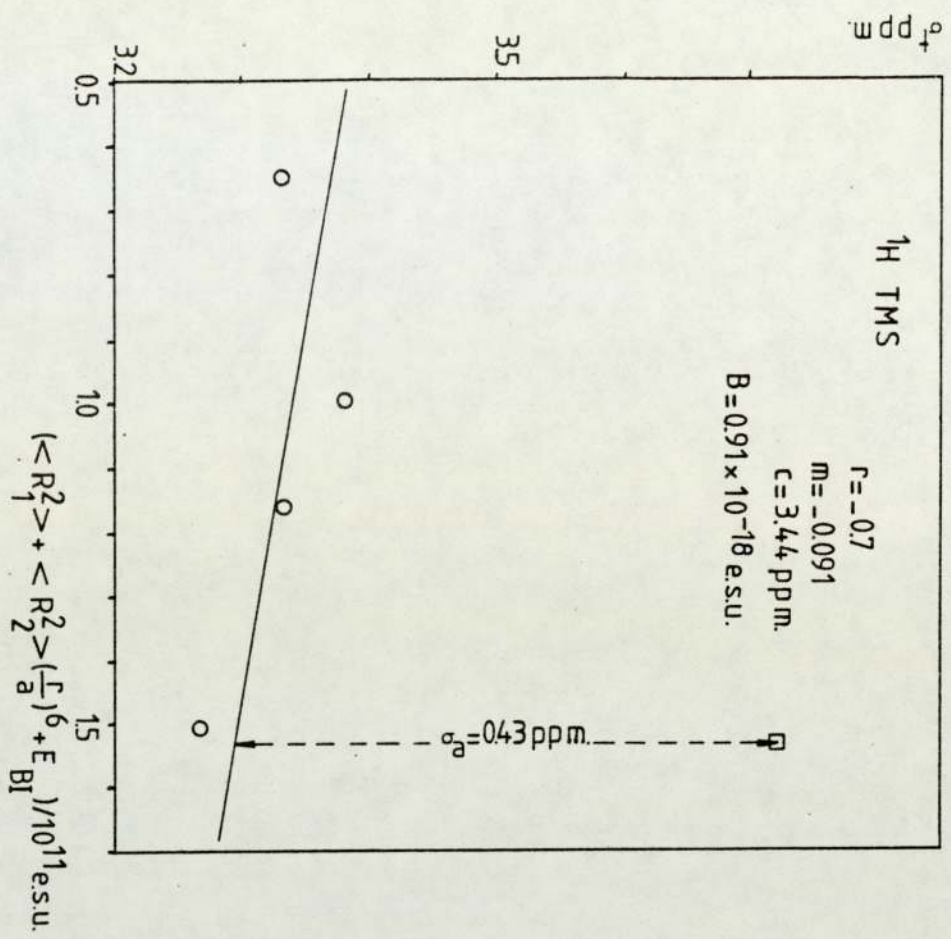
Figure 7.24   Regression of $(<R_1^2> + <R_2^2>)$ $(r/a)^6 + E_{BI}^2)$ on proton shifts of TMS.

^1H TMS

$r = -0.7$
$m = -0.091$
$c = 3.44$ p.p.m.
$B = 0.91 \times 10^{-18}$ e.s.u.

$\sigma_a = 0.43$ ppm.

δ_t ppm

3.5

3.2

0.5

10

15

$(<R_1^2> + <R_2^2>(\frac{r}{a})^6 + E_{BI})/10^{11}$ e.s.u.

Regression of	$B/10^{-18}$ e.s.u.
$<R_1^2> + <R_2^2>$	0.43
$<R_1^2> + <R_2^2>\left(\dfrac{r}{a}\right)^6$	1.13
$<R_1^2> + <R_2^2> + E_{BI}^2$	0.4
$<R_1^2> + <R_2^2>\left(\dfrac{r}{a}\right)^6 + E_{BI}^2$	0.91

Table (7.22)   Collected B values fielded from the various regression on the ^{1}H shifts of TMS.

Figure 7.24, it can be deduced that σ_a for benzene with TMS is 0.43 ppm. This is in good agreement with the value of 0.488 ppm. deduced by Homer and Redhead.[106]

7.4.2   Analysis Of ^{13}C Shifts Of $Si(CH_3)_4$:

The observed and susceptibility corrected shifts of ^{13}C of TMS are given in Table (7.23). Because of the protection from buffeting afforded by the methyl protons, this effect is discounted for ^{13}C nucleus. Table (7.24) shows the calculated $< R^2_1 >$, $< R^2_2 >$, $< R^2_T >$ and the modulated term $< R^2_2 > (r/a)^6$. Figures (7.25, 7.26 and 7.27) show the regressions of $< R^2_1 >$, $< R^2_T >$ and $< R^2_1 > + < R^2_2 > (r/a)^6$ on the corrected shifts; again the gas shift is not used in these regressions. The distance modulation is already given in Table 7.24. It can be seen from Table (7.25) showing the B values obtained from these regressions that the most consistent B value is found from the regression of $< R^2_1 > + < R^2_2 > (r/a)^6$ on the shifts, this is 22.6×10^{-18} e.s.u. The intercept of this regression is 93.29 ppm. that is in reasonable agreement with the gas shift of 96.498 ppm. obtained earlier experimentally. The B value for methyl ^{13}C in TMS is consistent with that of the methyl ^{13}C in CEt_4.

7.4.3   Analysis Of ^{29}Si Shifts of $Si(CH_3)_4$:

The observed and susceptibility corrected shifts of ^{29}Si of TMS in various solvents are presented in Table (7.26). Being at

Solvent	obs. $\delta^{13}C$ Hz	obs. $\delta^{13}C$ ppm	$-2\pi/3 \; X_v$	true $\delta^{13}C$ ppm
None	2174.39	96.498	-	96.498
TMS	2056.88	91.283	1.123	92.406
CCl_4	2030.03	90.091	1.442	91.533
C_6H_{12}	2056.88	91.283	1.327	92.61
CEt_4	2050.77	91.012	1.403	92.415
C_6H_6	2.054.33	91.17	1.296	92.466

Table (7.23) Observed and susceptility corrected ^{13}C shifts of TMS in various solvents. Measurements were made using a JEOL FX 90 Q NMR spectrometer locked at ^2H of D_2O, operating at $30^{o}C$ and an irradiation frequency of 22.533 MHz.

^{13}C TMS   d = 2.0 A°   a = r_2 + d

Solvent	$(r/r+d)^6$	$\langle R_1^2\rangle/_{,o}''$	$\langle R_2^2\rangle/_{,o}''$	$\langle R_2^2\rangle(r/a)^6/_{,o}''$	$\langle R_1^2\rangle+\langle R_2^2\rangle(r/a)^6/_{,o}''$	$(\langle R_1^2\rangle+\langle R_2^2\rangle)/_{,o}''$	$\delta^{13}C$ ppm.
TMS	0.101	0.2715	0.543	0.0548	0.3263	0.8145	92.406
CCl₄	0.071	0.40412	2.3097	0.1643	0.5684	2.7138	91.533
C₆H₁₂	0.077	0.3676	1.3214	0.1014	0.469	1.689	92.61
CEt₄	0.104	0.3598	0.6377	0.0661	0.426	0.9975	92.415
C₆H₆	0.067	0.4671	2.7815	0.18513	0.6524	3.2486	91.98*

Table (7.24) The square fields $\langle R_1^2\rangle$, $\langle R_T^2\rangle$ and the modulated term $\langle R_2^2\rangle\left(\frac{r}{a}\right)^6$ for ^{13}C of TMS. Among the shifts σ_a for bezene with TMS eliminated (as 0.488 ppm) deduced by Homer and Redhead (106).

Figure 7.25   Regression of ($< R^2_1 >$) on ^{13}C of TMS.
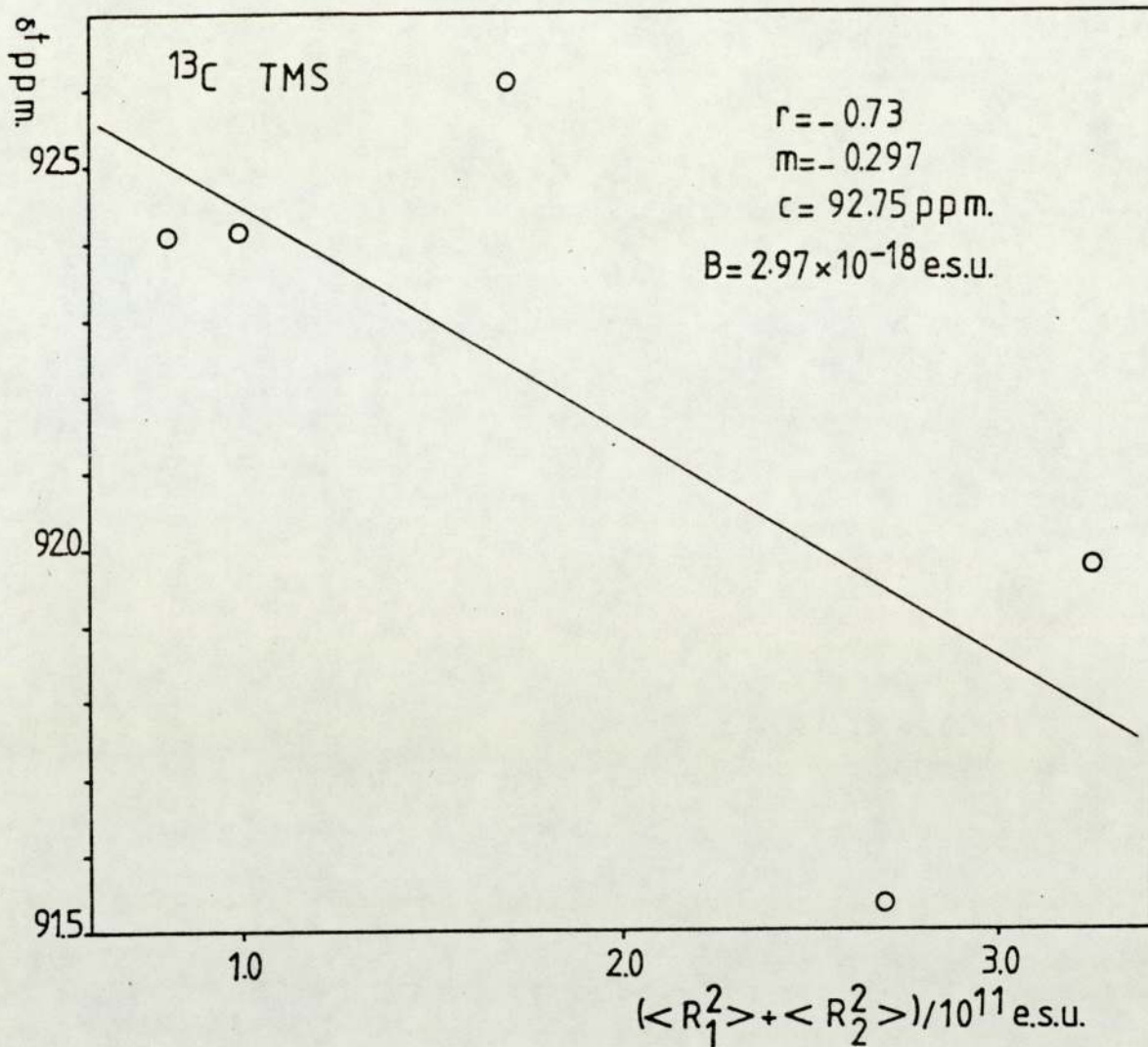
Figure 7.26   Regression of ($<R^2_1>$ + $<R^2_2>$) on ^{13}C shifts of TMS.
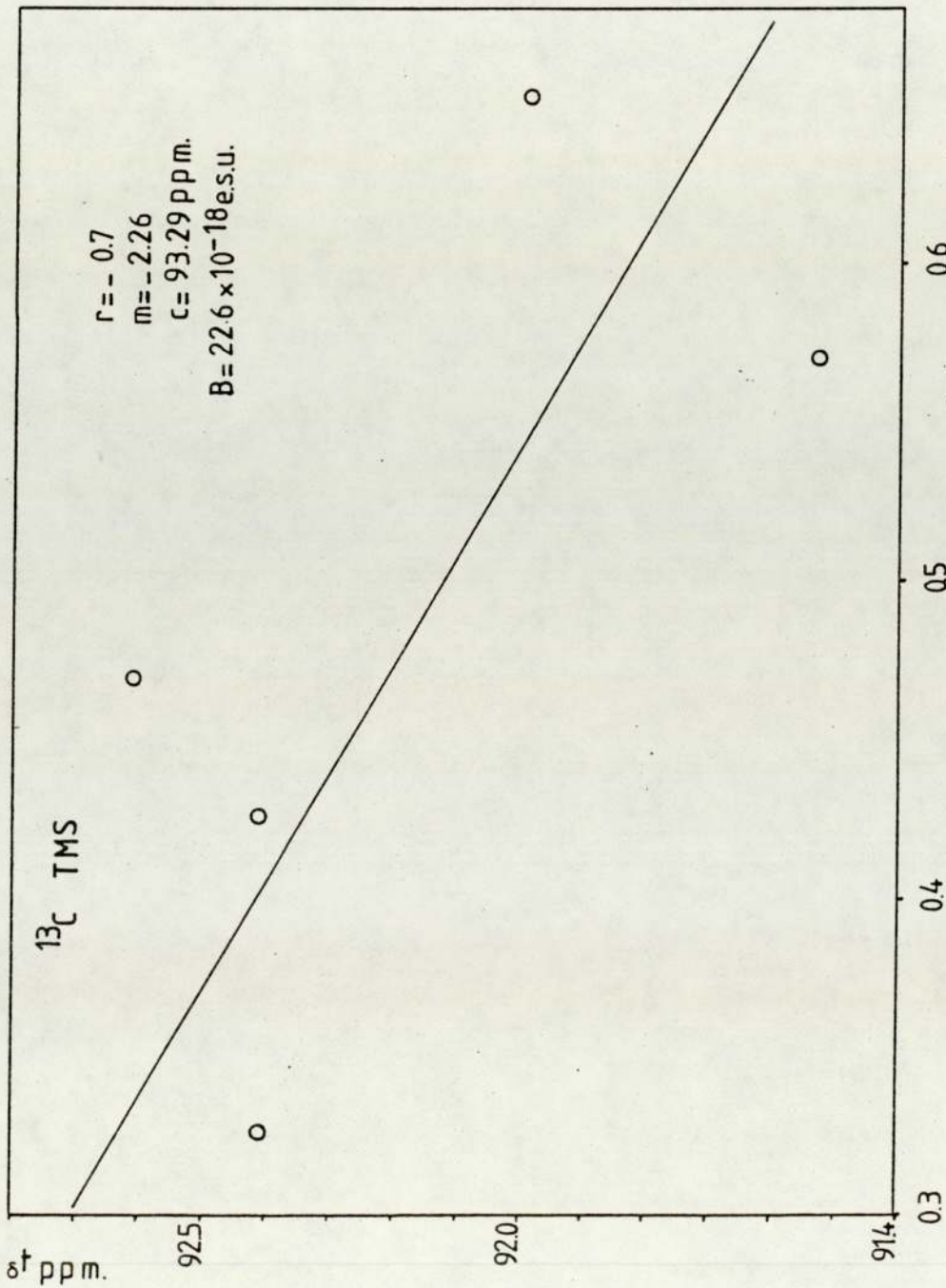
Figure 7.27   Regression of $(<R_1^2> + <R_2^2>(r/a)^6)$ on ^{13}C shifts of TMS.

^{13}C TMS

$r = -0.7$
$m = -2.26$
$c = 93.29$ p.p.m.
$B = 22.6 \times 10^{-18}$ e.s.u.

$\delta^\dagger$ p.p.m.

$<R_1^2> + <R_2^2>(\frac{r}{a})^6)/10^{11}$ e.s.u.

Regression of	B value/10^{-18}
$<R^2>$	33.14
$<R_1^2> + <R_2^2>$	2.97
$<R_1^2> + <R_2^2> \left(\frac{r}{a}\right)^6$	22.6

Table (7.25)   Collected B values for ^{13}C of TMS from the various regressions.

Solvent	obs $\delta\,^{29}$Si Hz	obs $\delta\,^{29}$Si ppm	$-2\pi/_3\,X_v$	true $\delta\,^{29}$Si ppm
TMS	81.05	4.526	1.123	5.649
CCl_4	69.58	3.909	1.442	5.351
C_6H_{12}	76.90	4.320	1.327	5.647
CEt_4	76.9	4.320	1.403	5.723
C_6H_6	86.67	4.869	1.296	6.165

Table (7.26)   The observed and susceptibility corrected ^{29}Si shifts of $SiMe_4$ in various solvents.   Measurements were made using a JEOL FX 90 Q NMR spectrometer locked at ^{2}H of external D_2O, operating at 30°C and irradiation frequency of 17.80188 MHz.
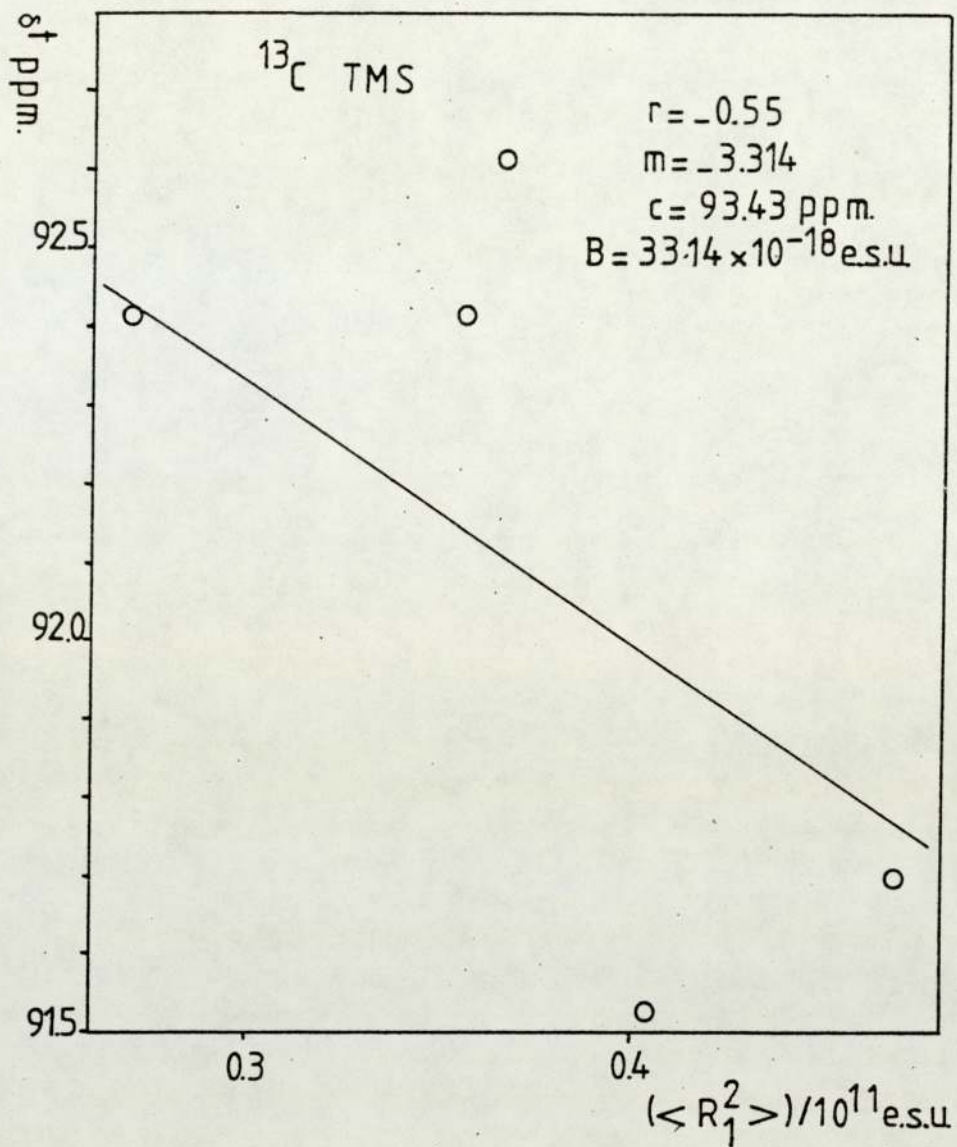
the centre of the molecule, the buffeting effect should certainly not be effective and that the effect of $< R^2_2 >$ should be vanishingly small. Table (7.27) gives the mean square reaction field $< R^2_1 >$ and $< R^2_T >$ together with the corresponding shifts. It is evident that if $< R^2_2 >$ has to be distance modulated then the effect at ^{29}Si nuclide would be vanishingly small. Accordingly regressions of $< R^2_1 >$ and $< R^2_T >$ only have been done on the corrected shifts of ^{29}Si and are shown in Figures (7.28 and 7.29) respectively. The values of B obtained from these regressions are 16.1 x 10^{-18} and 1.74 x 10^{-18} e.s.u. respectively. It can be seen that the value obtained from $< R^2_T >$ regression is exceedingly small, while that obtained from the $< R^2_1 >$ regression is consistent with the similarly sited ^{13}C in the CEt_4.

Additionally, from Figure (7.28) a sensible value of 0.69 ppm. is obtained for σ_a of benzene. This adds further credibility to the foregoing analysis.

7.5 **CONCLUSION**

The analysis presented in this chapter provides the first substantial evidence that whilst $< R^2_1 >$ is operative in all circumstances throughout the Onsager Cavity, $< R^2_2 >$ has to be distance modulated to account for the distance between the periphery of the solute molecule and the resonant nucleus. It is evident also that the buffeting effect is only significant for atoms at the periphery of solute molecules.

Solvent	$< R_1^2 >/10^{11}$ e.s.u.	$< R_T^2 >/10^{11}$	$\delta^{29}Si$ ppm
TMS	0.2715	0.8145	5.649
CCl_4	0.40412	2.7138	5.351
C_6H_{12}	0.3676	1.689	5.647
CEt_4	0.3598	0.9976	5.723
C_6H_6	0.4671	3.2486	6.165 *

Table (7.27)   The mean square reaction field $< R_1^2 >$ and $< R_T^2 >$ together with the ^{19}Si shifts at TMS.
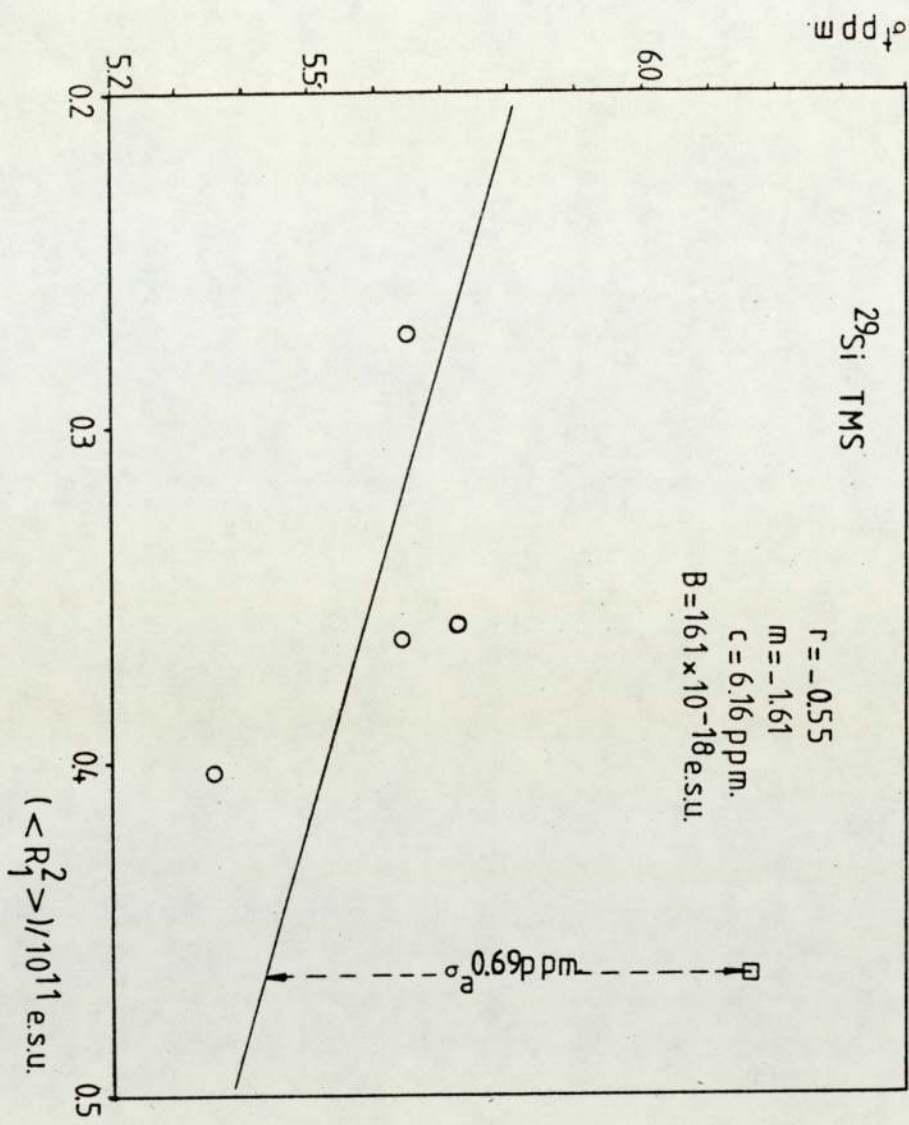
Figure 7.28   Regression of ($<R_1^2>$) on ^{29}Si shifts of TMS.

The plot shows ^{29}Si TMS data with:

$r = -0.55$
$m = -1.61$
$c = 6.16$ p.p.m.
$B = 161 \times 10^{-18}$ e.s.u.

Axes: σ_t p.p.m. (vertical, 5.2 to 6.0) versus $(<R_1^2>)/10^{11}$ e.s.u. (horizontal, 0.2 to 0.5).

σ_a 0.69 p.p.m.
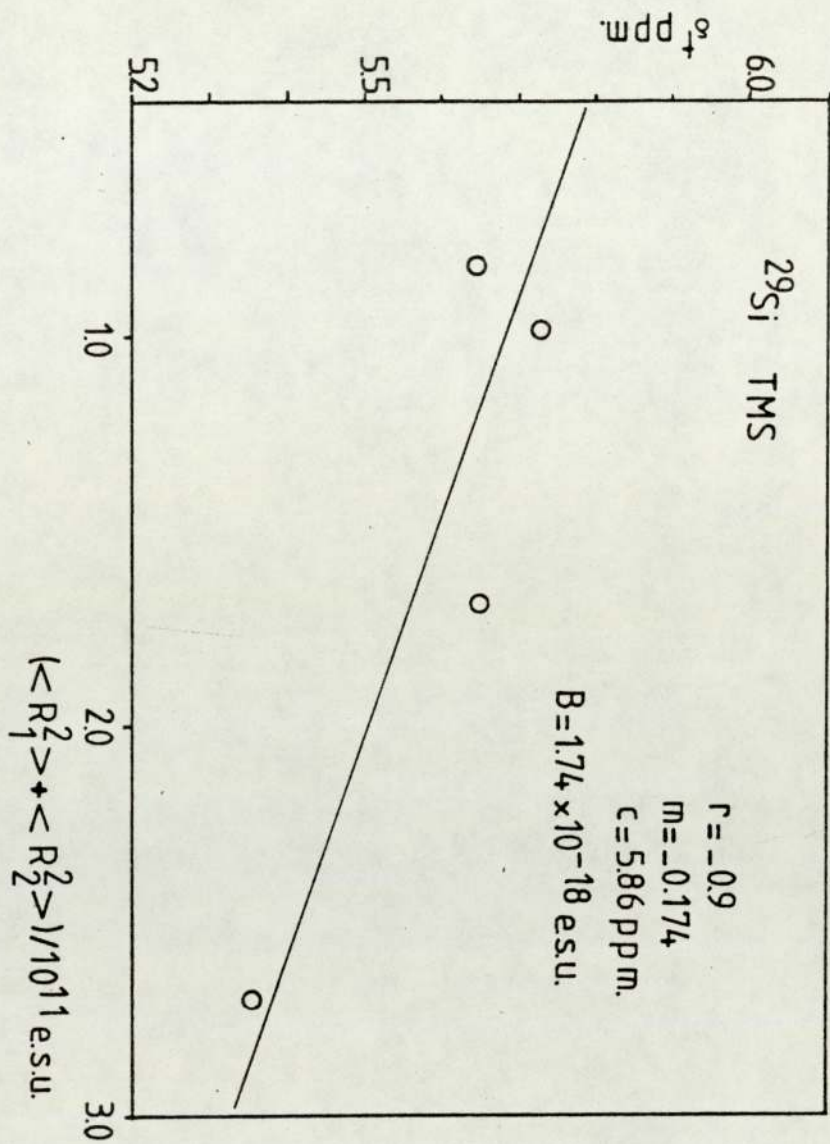
Figure 7.29 Regression of ($<R_1^2>$ + $<R_2^2>$) on ^{29}Si shifts of TMS.

^{29}Si TMS

r = −0.9
m = −0.174
c = 5.86 p.p.m.
B = 1.74 × 10^{-18} e.s.u.

σ ↑ p.p.m.

$(<R_1^2> + <R_2^2>)/10^{11}$ e.s.u.

6.0
5.5
5.2

1.0
2.0
3.0

These conclusions are entirely consistant with the principles involved in the derivation of $\langle R^2_1 \rangle$, $\langle R^2_2 \rangle$ and E^2_{BI}.

$\langle R^2_1 \rangle$, $\langle R^2_2 \rangle$ and E^2_{BI}.

REFERENCES

1.   Pauli, W.; "Naturwiss"; **12**, 741, (1924).

2.   Tolansky; "High Resolution Spectroscopy"; Mathuen, London, (1947).

3.   Stern, O.; "Z. Phys."; 7, 249, (1921).

4.   Gerland, W.; Stern, O; "Ann. Phys. Leipzig"; **74**, 673, (1924).

5.   Rabi, I., Millam, S., Kusch, P., and Zacharias, J.R.; "Phys. Review"; **53**, 526, (1939).

6.   Ramsey, N.F.; "Molecular Beams"; Oxford University Press, (1959).

7.   Bloch, Hansen, W.W., and Packard, M.; "Phys. Review"; **69**, 127, (1946).

8.   Purcell, E.M., Torrey, H.C. and Pound, R.V.; "Phys. Review"; **69**, 37, (1946).

9.   Emsley, J.W., Freeny, J. and Sutcliffe, L.H.; "High Resolution Nuclear Magnetic Resonance Spectroscopy"; Pregamon Press, Oxford, (1965).

10. Pople, J.A., Schneider, W.G. and Bernstein, H.J. "High Resolution Nuclear Magnetic Resonance Spectroscopy"; McCraw Hill, New York, (1959).

11. Jackman, L.M.; "Application of NMR Spectroscopy in Organic Chemistry"; Pergamon Press, London, (1959).

12. Gutoswky, H.S. and McCall, D.W.; "Phys. Review"; 82, 748, (1951).

13. Blombergen, N., Purcell, E.M. and Pound, R.V.; "Phys. Review"; **73**, 679, (1948).

14. Einstein, A.; "Z Phys."; **18**, 121, (1917).

15. Purcell, E.M.; "Phys. Review"; **69**, 681, (1946).

16. Emsley, J.W., Freeny, J. and Sutcliffe, L.H.; "High Resolution Nuclear Magnetic Resonance Spectroscopy"; Volume I, (1965).

17. Bloch, F.; "Phys. Review"; **70**, 460, (1946).

18. Bloch, F.; "Phys. Review"; 102, 104, (1956).

19. Wagsness, R.K. and Bloch, F.; "Phys. Review"; **89**, 728, (1953).

20. Tires, G.V.; "J. Phys. Chem."; **65**, 1916, (1961).

21. Endrew, E.R.; "Nuclear Magnetic Resonance"; Cambridge University Press, (1955).

22. Knight, W.D.; "Phys. Review"; **76**, 1259, (1949).

23. Proctor, W.G. and Yu, F.C.; "Phys. Review"; **77**, 717, (1950).

24. Dickinson, W.C.; "Phys. Review"; **77**, 736, (1950).

25. Tires, G.V.D.; "J. Phys. Chem."; **65**, 1151, (1958).

26. Tires, G.V.D.; "J. Phys. Chem."; **63**, 1379, (1959).

27. Homer, J.; "Tetrahedron"; **23**, 4065, (1967).

28. Lazlo, P., Speert, A., Ottinger, R. and Reisse, J.; "J. Chem. Phys."; **48**, 1732, (1968).

29. Homer, J., Solvent Effect on NMR Spectroscopy, "Applied Spectroscopy Review"; **9**, 1, (1975).

30. Raynes, W.T., Buckingham, A.D. and Bernstein, H.J.; "J. Chem. Phys."; **36**, 3481, (1962).

31. Petrakis, L., and Bernstein, H.J.; "J. Chem. Phys."; **38**, 1562, (1963).

32. Saika, A. and Slichter, C.P.; "J. Chem. Phys."; **22**, 26, (1954).

33. Ramsey, N.F.; "Phys. Review"; **77**, 567, (1950)

                                    78, 699, (1950)

                                    83, 540, (1951)

                                    86, 243, (1952).

34.   Emsley, J.W., Freeny, J. and Sutcliffe, L.H.; "High Resolution of NMR Spectroscopy"; Vol I and II, Pergamon Press, (1965).

35.   Buckingham, A.D., Schaefer, T. and Schneider, W.G.; "J. Chem. Phys."; **32**, 1227, (1960).

36.   Dickinson, W.C.; "Phys. Review"; **81**, 717, (1951).

37.   Lussan, C.; "J. Chem. Phys."; **61**, 462, (1964).

38.   Zimmerman, J.R. and Foster, M.R.; "J. Chem. Phys."; **61**, 282, (1957).

39.   Laszlo, P.; "Progress in NMR Spectroscopy"; **3**, 241, (1967).

40.   Frost, D.J. and Hall, G.E.; "Mol. Phys."; **10**, 191, (1966).

41.   Homer, J., Everdell, M.H., Hartland, E.J. and Jackson, C.J.; "J.C.S."; A, 1111, (1970).

42.   Proctor, W.G. and Yu, F.C.; "Phys. Review"; **81**, 20, (1951).

43.   Gutowsky, H.S. and McCall, D.W.; "Phys. Review"; **82**, 748, (1951).

44.   Dixon, W.T.; Theory and Interpretation of Magnetic Resonance Spectra"; Plenum, (1972).

45.   Bloch, F., Hansen, W.W. and Packard; "Phys. Review"; **70**, 474, (1946).

46.   Bloom, A.L. and Packard; "Science"; **122**, 738, (1955).

47.   Evans, B.A., Richards, R.W.; "J. Sci. Inst."; **37**, 353, (1960).

48.   Primas, H. and Gunthard, "Rev. Sci. Inst."; **28**, 510, (1957).

49.   Williams, R.B.; "Annals. N.Y. Acad. Sci."; 70, 890, (1958).

50.   Packard, M.E.; "Rev. Sci. Inst."; **19**, 435, (1948).

51.   Baker, E.B. and Bard, A.W.; "Rev. Sci. Inst."; **28**, 313, (1957).

52.   McFarland, W. and White, R.F.W.; "Techniques of High Resolution NMR Spectroscopy."; Butterworth, (1973).

53. Arnold, J.J.; "Phys. Review"; **122**, 136, (1956).

54. Varian Associates HA 100 D Model NMR Spectrometer Handbook.

55. Perkin-Elmer R 12 B Model NMR Spectroscopy Handbook, (1968).

56. Clark, W.G.; "Review Sci. Inst."; **35**, 316, (1964).

57. Redfield, A.G. and Gupta, R.K."; Waugh, Academic Press, New York (1971).

58. Lowe, I.J. and Tarr, C.E.; "J. Sci. Inst."; 1, 320, (1968).

59. McKay, R.A. and Woessner, D.E.; "J. Sci. Inst."; **43**, 838, (1966).

60. JEOL F.T NMR Spectrometer FX 90 Q Manual.

61. Rummens, F.A., Raynes, W.T. and Bernstein, J.H.; "J. Phys. Chem."; **72**, 2111, (1968).

62. Onsager, L.; "J. Amer. Chem. Soc."; **58**, 1068, (1936).

63. Rummens, F.H.A.; "Can. J. Chem."; **54**, 254, (1976).

64. Ph.D. Thesis C.C. Percival, (1981). Supervisor Homer, J., Department of Chemistry, University of Aston in Birmingham. "The Effect of Molecular Encounters on NMR Chemical Shifts."

65. Haward, B.B., Linder, B. and Emerson, M.T.; "J. Chem. Phys."; **36**, 485, (1962).

66. Linder, B.; "J. Chem. Phys."; **33**, 668, (1960).

67. Linder, B.; "J. Chem. Phys."; **35**, 371, (1961).

68. Lumbroso, N., Wu, T.K. and Dailey, B.P.; "J. Phys. Chem."; **67**, 2469, (1963).

69. Fontaine, B., Chenon, M.T. and Lumrosa-Bader, N.; "J. Chem. Phys."; **62**, 1075, (1965).

70. De Montgolfier Ph.; "C.R. Acad. Sci. Paris"; **2G3C**, 505, (1966).

71. De Montgolfier Ph.; "J. Chem. Phys."; **64**, 639, (1967).

72. De Montgolfier Ph.; "J. Chem. Phys."; **65**, 1618, (1968).

73. De Montgolfier Ph.; "J. Chem. Phys."; **66**, 685, (1969).

74. Rummens, F.H.A.; "Chem. Phys. Letters"; **31**, 596, (1975).

75. Rummens, F.H.A.; "J. Chem. Phys."; **72**, 448, (1975).

76. Rummens, F.H.A.; "NMR Principles & Progress"; **10**, (1975).

77. Rummens, F.H.A.; "Cana. J. Chem."; **54**, 254, (1976).

78. Rummens, F.H.A. and Bernstein, H.J.; "J. Chem. Phys."; **43**, 2971, (1965).

79. Rummens, F.H.A.; "Mol. Phys."; **19**, 423, (1970).

80. Bottcher, C.J.F.; "Theory of Electric Polarization", Vol I "Dielectric in Static Fields"; 2nd Ed. Elseview Scientific Publishing Co. (1973).

81. Frolich, H.; "Theory of Dielectrics", Oxford University Press, (1958).

82. Yamamoto, T.; "Can. J. Chem."; **44**, 223, (1966).

83. Ph. D. Thesis, A. Coupland, Supervisor, Dr J. Homer (1978), Department of Chemistry, The University of Aston in Birmingham.

84. Handbook of Chemistry and Physics 57th Edition, 1976 - 1977, R. Weast, Chemical Rubber Co Ltd., CRC Press.

85. Eisenshitz and London, F., Z Phys., **60**, 491, (1930).

86. London, F.; "Trans. Faraday Soc."; **33**, 8, (1937).

87. Homer, J.; "J. Mag. Res."; **54**, 1, (1983).

88. Raza, M. and Raynes, W.T.; "Molecular Physics."; **19**, 199, (1970).

89. Williams, D.H., Ronayne, J. and Wilson, R.G.; "Chem. Commun."; P. 1089, (1967).

90. Wilson, R.G. and Williams, D.H.; "J. Chem. Soc. B."; P. 1163, (1968).

91.   Becconsall, J.K.; "Molecular Physics."; **15**, 129, (1968).

92.   Figgis, B.N. and Lewis, J.; "Techniques of Inorganic Chemistry"; Vol 4, (Ecls. H.B. Jonasson and A. Weissberger) Wiley Interscience, New York, (1965).

93.   Reilly, C.A., McConnel, H.M. and Meisenheimer, R.G.; "Phys. Review"; **98**, 264, (1955).

94.   Frei, K. and Bernstein, H.J.; "J. Chem. Phys."; **37**, 1891, (1962).

95.   Homer, J. and Whitney, P.M.; "J.C.S. Chem. Commu."; 153, (1972).

96.   Frost, D.J. and Hall, G.E.; "Mol. Phys."; **10**, 191, (1966).

97.   Timmermans, J. "Physico Chemical Constants of Pure Organic Compounds"; Elsevier, Amsterdam, (1965).

98.   Langley, R.; "Practical Statistics"; (1979), Pan.

99.   Private Communication.

100.   Mislow, K. Korpium, O. and Lewis, R.A. "J. Amer. Society"; **90**, 4847, (1968).

101.   "Ionization Potentials, Appearance Potentials and Heat of Formation of Gaseous Positive Ions."; U.S. Department of Commerce; National Bureau of Standards.

102.   J. Phys. & Chem. Ref. Data, **6**, (1977), Supplement No. 1, Energies of Gaseous Ions.

103.   Gibbons, W.A. and Gill, V.M.S.; "Molecular Phys."; **9**, 163, (1965).

104.   "NMR and Chemistry" By J.W.A. Kitt, 1st Ed. (1973), Chapman and Hall Chemistry Textbook Series, (London).

105.   Rummens, F.H.A. "NMR periodicals"; Vol. **10**, (1960).

106.   Homer, J. and Redhead, D.L.; "J. of Chemical Soc." Faraday Transaction II, **68**, (1972).

107.   Ph.D. Thesis, Whitney, Supervisor Dr J. Homer, Department of
        Chemistry, The University of Aston in Birmingham, (1973).